Solid-phase syntheses and studies of conformationally constrained analogues

of the calcitonin gene peptide superfamily polypeptides calcitonin (Ct)

and islet amyloid polypeptide (IAPP)

Festphasensynthesen und Untersuchungen von konformationell-eingeschränkten

Analoga der Calcitonin-Gen-Peptid-Superfamilien-Polypeptide

Calcitonin (Ct) und Islet Amyloid Polypeptid (IAPP)

DISSERTATION

der Fakultät für Chemie und Pharmazie

der Eberhard-Karls-Universität Tübingen

zur Erlangung des Grades eines Doktors

der Naturwissenschaften

2004

vorgelegt von

Athanasios Kazantzis

Acknowledgments

Finally, I would like to thank my parents and my brother for their patience, support and encouragement.

It should be mentioned that parts of this thesis have been published in:

1.) A. Kazantzis, M. Waldner, J. W. Taylor, & A. Kapurniotu, Eur. J. Biochem., 269, 780-791, 2002.

List of Abbreviations

Ab	Absorbance
Ac	Acetyl
AC	Adenylate cyclase
ACN	Acetonitrile
AcOH	Acetic acid
Ac_2O	Acetic anhydride
ACS	American chemical society
Adoc	1-(1´-adamantyl)-1-methyl-ethoxycarbonyl
Boc	t-Butoxycarbonyl
Bom	π-Benzyloxymethyl
BOP	1-Benzotriazolyloxy-tris-dimethylamino-phosphonium hexafluorophosphate
BSA	Bovine serum albumin
Bzl	Benzyl
cAMP	cyclo-Adenosine monophosphate
CD	Circular dichroism
CNS	Central nervous system
Ct	Calcitonin
ΔG	Gradient change over time
DCC	Dicyclohexylcarbodiimide
DCM	Dichloromethane
DIC	Diisopropylcarbodiimide
DIEA	Diisopropylethylamine
DKP	Diketopiperazine
DMF	Dimethylformamide
DMS	Dimethylsulfide
DMSO	Dimethylsulfoxide
DTT	1,4-Dithio-DL-threitol
DTAB	Dodecyltrimethylammonium bromide
DVB	Divinylbenzene
EC_{50}	Effective concentration at half-maximal response
EDT	1,2-ethanedithiol
EIA	Enzyme immuno assay

Eq	Equivalent
Et	Ethyl
Et$_2$O	Diethylether
FAB	Fast atom bombardment
Fmoc	9-Fluorenylmethoxycarbonyl
FT-IR	Fourier transform infrared spectroscopy
Gdn HCl	Guanidine hydrochloride
GPCR	G-protein coupled receptor
HATU	2-(1H-9Azabenzotriazole-1-yl)-1,1,3,3-tetramethyluronium hexaflurophosphate
HBTU	2-(1-H-benzotriazol-1-yl)-1,1,3,3-tetramethyluronium hexafluorophosphate
HF	Hydrogen fluoride
HFIP	1,1,1,3,3,3-hexafluoro-2-propanol
HPLC	High performance liquid chromatography
HOBt	1-Hydroxybenzotriazole
hrs	hours
IAPP	Islet amyloid polypeptide
IC$_{50}$	Inhibition concentartion at half-maximal response
iPrOH	Isopropyl alcohol
MALDI	Matrix assisted laser desorption ionization
MBHA	p-Methylbenzhydrylamine
Me	Methyl
min	minutes
Mob	4-Methoxybenzyl
MS	Mass spectroscopy
Mtt	4-Methyltrityl
MTT	3-[4,5-dimethylthiazol-1-yl]-2,5-diphenyltetrazolium bromide
NMP	N-methyl pyrrolidinone
NMR	Nuclear magnetic resonance
OBt	1-Benzotriazolyl ester
Oc Hx	Cyclohexyl ester
OD	Optical density
OFm	Formyl ester
p.a	pro analysi
PBS	Phosphate buffer saline

Pip   2-Phenyl isopropyl ester

Pmc   2,2,5,7,8-Pentamethylchroman-6-sufonyl

PyBOP   1-Benzotriazolyloxy-tris-pyrrolidinophosphonium hexafluorophosphate

Rink MBHA   4-(2´, 4´-dimethoxyphenyl-Fmoc-aminomethyl)-phenoxy acetamido-norleucyl

RP   Reversed phase

RPMI   Roswell Park Memorial Institute

RT   Room temperature

SAR   Structure-activity relationship

SD   Standard deviation

SPPS   Solid phase peptide synthesis

TAS   Thioanisole

TBTU   Benzotriazole-1-yl-1,1,3,3,-tetramethyluronium tetrafluoroborate

tBu   tert-Butyl

TFA   Trifluoroacetic acid

TFE   2,2,2-Trifluoroethanol

TIS   Triisopropylsilane

TMB   3,3´, 5, 5´-Tetramethylbenzidine

TMD   Trans membrane domain

Trt   Trityl

UV   Ultraviolet

Z   Benzyloxycarbonyl

Amino-Acids Abbreviations

[Ala, A]	Alanine
[Aib]	2-Aminoisobutyric acid
[Arg, R]	Arginine
[Asn, N]	Asparagine
[Asp, D]	Aspartic acid
[Cys, C]	Cysteine
[Dab]	2,4-Diaminobutyric acid
[Dap]	2,3-Diaminopropionic acid
[Glu, E]	Glutamic acid
[Gln, Q]	Glutamine
[Gly, G]	Glycine
[His, H]	Histidine
[Ile, I]	Isoleucine
[Leu, L]	Leucine
[Lys, K]	Lysine
[Met, M]	Methionine
[Nle, B]	Norleucine
[Orn]	Ornithine
[Phe, F]	Phenylalanine
[Pro, P]	Proline
[Ser, S]	Serine
[Thr, T]	Threonine
[Trp, W]	Tryptophan
[Tyr, Y]	Tyrosine
[Val, V]	Valine
[Xaa]	Unspecified

Table of contents

1 Abstract

Conformationally constrained analogues of natively occuring bioactive polypeptides are valuable tools for the understanding of their structure-function-relationships and for the design and development of lead structures with therapeutic and diagnostic applications. The work described in this thesis focuses on the application of conformational constraints on two polypeptides from the calcitonin gene peptide "superfamily": the calcium- and bone-turnover-regulating hormone calcitonin (Ct) and the carbohydrate metabolism-regulating hormone islet amyloid polypeptide (IAPP). These two, 32 and 37, respectively, residue polypeptides have a common genetic origin and exhibit some primary sequence homology and overlapping biological activities and receptor cross-reactivities.

Ct has been long therapeutically used for the treatment of osteoporosis. The low bioactivity of the human sequence (hCt), however, has been the reason for its limited therapeutic application as compared to the highly potent salmon peptide (sCt). Recent work has shown that introduction of an *i*, *i*+4 side chain lactam bridge between residues 17 and 21 in hCt may lead to analogues with strongly enhanced *in vivo* hypocalcemic activity (Kapurniotu et al., *Eur. J. Biochem.* (1999)). This work has led to the discovery of the hCt analogue cyclo^{17,21}-[Asp^{17}, Orn^{21}]hCt which is the most potent hCt analogue reported todate with regard to *in vivo* hypocalcemic activity. This work has also suggested that a potential β-sheet/β-turn conformation between residues 17 and 21 of hCt might be associated with bioactivity. The first part of the work described here aimed at obtaining detailed information about the effect of the conformational restriction in region 17 to 21 on Ct receptor binding and adenylate cyclase activation and to, possibly, identify structural features that may be directly associated with bioactivity. The specific issues that were addressed included: the effect of the ring size of the lactam bridge and of different types of β-turn-stabilizing residues at positions 18 and 19 on receptor binding and AC activation, a role for a putative "Asx-turn" in region 17 to 21, for the H-bonding ability of the amino group of Phe^{19}, and for the side chain of residue 17 in receptor binding and adenylate cyclase (AC) activation, the importance of the integrity of the backbone in region 17 to 21 for bioactivity, and, finally, the effect on bioactivity of the introduction of hydrophobic residues that are present in the α-helical region of the sCt sequence into the respective region of the potent hCt analogue cyclo^{17,21}-[Asp^{17}, Orn^{21}]hCt. Towards this goal, twenty five hCt analogues bearing a cyclic conformational constraint and/or several substitutes for residues in region 17 to 21 that was postulated to be important for bioactivity were designed. The analogues were synthesized in good yields and purity by solid phase (SPPS) synthetic protocols using the Boc- and/or the Fmoc- strategy in

combination with special side chain protection strategies for the side chain-to-side chain cyclization on the resin. Following purification by RP-HPLC and characterization by mass spectrometry, their binding affinities to the Ct-receptor and their AC activation potencies were investigated using the T47D cell line. The studies with the ring size analogues showed that the 19-membered analogues cyclo[17,21]-[Asp[17], Orn[21]]hCt and cyclo[17,21]-[Glu[17], Dab[21]]hCt together with the 20-membered ring cyclo[17,21]-[Asp[17], Lys[21]]hCt had the highest receptor binding affinities as compared to all other analogues. In the AC activation assay, cyclo[17,21]-[Asp[17], Orn[21]]hCt was found to be the strongest hCt agonist, whereas cyclo[17,21]-[Asp[17], Lys[21]]hCt was similarily potent to hCt and cyclo[17,21]-[Glu[17], Dab[21]]hCt was less potent than hCt. Receptor binding affinities and AC activation potencies were significantly reduced in the 18-membered ring containing cyclo[17,21]-[Asp[17], Dab[21]]hCt and very weak in the 17-membered ring analogue cyclo[17,21]-[Asp[17], Dap[21]]hCt. No receptor binding and a very weak AC activation potential was found for [Asp[17], Orn[21]]hCt which strongly suggested that the Asp[17] to Orn[21] bridge-induced conformational restriction in cyclo[17,21]-[Asp[17], Orn[21]]hCt is directly associated with both increased receptor binding affinity and stronger AC activation potential. The studies with a series of substitution analogues of cyclo[17,21]-[Asp[17], Lys[21]]hCt and respective control peptides showed that inversing the chirality of residues at positions 18 and 19 or replacing Lys[18] by a type I β-turn-stabilizing residue (Aib) was compatible with the receptor binding requirements of the cyclic analogue, while these substitutions led to reduction of AC activitation potency. In the hCt sequence, inversement of chirality of residues 18 and 19 led to a strong reduction of both receptor binding affinity and AC activation ability. Furthermore, the studies with a series of analogues of cyclo[17,21]-[Asp[17], Orn[21]]hCt where residues 18 and 19 have been replaced by the "Asx-turn"-inducing residues Pro and Ser showed that residues Lys[18] and Phe[19] are very important for both receptor binding and AC activation. In fact, it was shown that these substitutions led to analogues with strongly reduced receptor binding affinities and AC activation potencies. The studies with N-methylated Phe[19] analogues of cyclo[17,21]-[Asp[17], Orn[21]]hCt clearly suggested that the H-bonding ability of Phe[19] is very important for receptor binding affinity and AC activation, while the studies with the βeta-analogues of cyclo[17,21]-[Asp[17], Orn[21]]hCt showed that the integrity of the backbone between residues 17 and 21 is a necessary requirement for receptor binding and AC activation. The results of the studies with hCt analogues bearing a Dab or a Dap residue instead of Asn[17] suggested an immediate association of both the carbonyl and the amino function of the Asn side chain with receptor binding affinity and AC activation potency. Finally, the studies on the effect of introducing hydrophobic residues from the potential helical region of sCt into

cyclo[17,21]-[Asp[17], Orn[21]]hCt or [Asp[17], Orn[21]]hCt indicated that the presence of Nle[8], Leu[12,16,19] and Tyr[22] results in a strong enhancement of AC potency. Importantly, these substitutes alone were able to strongly enhance the receptor binding affinity of [Asp[17], Orn[21]]hCt, whereas they had no effect on the affinity of cyclo[17,21]-[Asp[17], Orn[21]]hCt. Taken together, the results of the studies with all hCt analogues have demonstrated that region 17 to 21 of hCt plays a very important role in bioactivity and that small structural variations in this region can strongly affect both the receptor binding affinity and the AC activation potential. This result suggested that rationally introduced structural variations in the region 17 to 21 of hCt may result in highly potent and thus therapeutically interesting hCt agonists.

The second member of the calcitonin gene peptide family IAPP is believed to play a crucial role in the pathogenesis of type II diabetes. One reason for this is that IAPP amyloid aggregates are found in the pancreata of more than 95% of type II diabetes patients and that these aggregates are cytotoxic. Understanding the molecular mechanism underlying the strong β-sheet-forming and the related amyloidogenic and cytotoxic potentials of the human IAPP sequence is the basis for the understanding the molecular basis of this disease and the development of therapeutic strategies. Conformational restriction via a rational introduction of N-methyl rests in amide bonds of short, β-sheet-forming, amyloidogenic sequences has been very recently suggested to be a reasonable strategy to delineate the structure-amyloidogenicity-cytotoxicity relationships of such sequences and convert amyloid-forming sequences into non-amyloidogenic and non-cytotoxic ones. The second part of the thesis describes in detail the SPPS of the (human) IAPP sequence, of the strongly amyloidogenic IAPP mutant S20G-IAPP, and of five IAPP analogues that have been conformationally constrained via N-methylation of amide bonds. In addition, first studies on the effect of the selective introduction of N-methyl rests on the β-sheet-forming potential and the cytotoxic properties of one representative N-methylated IAPP analogue as compared to the natively occuring IAPP sequence are presented.

The SPPS of IAPP, S20G-IAPP, and the N-methylated analogues proved to be a demanding task. This was due to the presence of several sterically hindered and aggregation-prone residues in the IAPP sequence and also due to synthetic problems related to steric hindrance of couplings and peptide bond lability in sequences containing N-methylated residues. Due to the low yield of the synthesis of IAPP, an optimized synthetic protocol was applied to the synthesis of S20G-IAPP and resulted in a reasonable yield and HPLC profile for crude S20G-IAPP. During the syntheses of the N-methylated analogues [(N-Me) Phe[23], (N-Me) Ala[25]] IAPP [1], [(N-Me) Gly[24], (N-Me) Ile[26]] IAPP [2], [(N-Me) Ala[25], (N-Me) Leu[27]] IAPP [3],

and [(N-Me) Ile[26], (N-Me) Leu[27]] IAPP [4] several couplings involving N-methyl residues were incomplete. Unreacted amino groups of the N-methyl residues were subsequently capped by acetylation which resulted in a number of TFA-mediated amide bond cleavages: these included cleavages between an Ac-(N-Me) Ile and Leu, or (N-Me) Leu, between Ac-(N-Me) Phe and Gly, and between Ac-(N-Me) Leu and Ser. The byproducts of these syntheses were completely characterized and the side reactions were thus understood. Importantly, the studies showed that the above peptide bonds were susceptible to hydrolysis under the TFA peptide resin cleavage conditions only when the N-methylated residues were in an acetylated form. Thus, this side reaction occurred mainly in the capped, partial sequences and only at the final TFA deprotection step at the end of the synthesis, while the full sequence N-methylated IAPP analogues *per se* were stable under the conditions of the Fmoc-synthetic strategy. Due to the very low coupling yield of (N-Me) Ala[25] on (N-Me) Ile[26], the synthesis of the fifth IAPP analogue ([(N-Me) Ala[25], (N-Me) Ile[26], (N-Me) Leu[27]] IAPP [5]) bearing three consecutive N-methylated residues was only performed up to residue 25. Although the overall yields of the syntheses of the full sequence containing, N-methylated IAPP analogues [1] to [4] were low due to the incomplete couplings, overall, less by-products as compared to the IAPP synthesis formed, which led to higher yields in the RP-HPLC purification process than in IAPP.

Finally, analogue [(N-Me) Gly[24], (N-Me) Ile[26]] IAPP [2] was selected as a first analogue to study the effect of the rational introduction of N-methyl rests on the β-sheet and cytotoxicity potential of IAPP. These studies clearly showed that the two N-methyl groups at Gly[24] and Ile[26] led to a strong reduction of the β-sheet-forming potential and an abolishment of cytotoxicity of IAPP towards the pancreatic β-cell line RIN5fm. These results suggested that there is a direct association of the conformational restriction induced by the rational N-methylation of amide bonds with IAPP amyloidogenicity and cytotoxicity.

Taken together, the results of this work showed that restriction of conformational flexibility of medium-sized bioactive polypeptides can yield valuable information about the structure-activity-relationships and contribute to the design of potent agonists (hCt analogues) or analogues with an altered or completely different biophysical profile as compared to the natively occuring polypeptides (IAPP analogues). In addition, the results of this work suggest that the conformational restriction strategy may be applicable to other polypeptides sequences too, including longer sequences or other amyloidogenic ones. This work also showed that the SPPS of N-methylated and aggregation prone polypeptide sequences is still a formidable synthetic task.

2 Objective

Restricting the conformational flexibility of medium-sized polypeptides has proven a valuable approach towards understanding the structural and conformational features of bioactivity. Thus, in the case of peptide hormones, a number of studies in the past 20 years have shown that this approach can lead to the discovery of analogues with potent agonistic or antagonistic properties. In the case of polypeptides with specific biophysical properties, such as for example a β-sheet, self-assembly and a with self-assembly related cytotoxic potential, conformational restriction may lead to the design of novel analogues that have an altered or completely different biophysical profile as compared to the natively occuring peptide sequence. The rationally designed conformationally constrained analogues are in both cases tools for the understanding of the structure-activity-relationships of the natively occuring polypeptides and lead structures for the development of novel compounds with therapeutic and diagnostic applications.

The work described in this thesis focuses on the application of conformational constraints on one representative for each one of the above mentioned two "categories" of polypeptides, i.e. the two polypeptides calcitonin (Ct) and islet amyloid polypeptide (IAPP). These two 32 and 37, respectively, residue polypeptides belong together with the 37 residue calcitonin gene-related peptide (CGRP) and the 52 residue polypeptide adrenomedullin, to the so-called calcitonin gene peptide "superfamily". These four polypeptides have a common genetic origin, exhibit some primary sequence homology, and also exhibit overlapping biological activities and cross-reactivities between receptors.

The calcium- and bone-turnover-regulating hormone calcitonin, which has been discovered 40 years ago, has been therapeutically used since many years for the treatment of osteoporosis and other bone disorder diseases. Thereby, the low bioactivity of the human sequence (hCt) has led to its limited therapeutic application as compared to the highly potent salmon Ct (sCt). Recent work, however, has shown that introduction of conformational constraints in form of i, i+4 side chain lactam bridges in the sequence of human Ct (hCt) can strongly affect conformation and bioactivity and lead to potent agonists of the *in vivo* hypocalcemic activity of hCt. Based on the above findings, the first part of the work described here aimed at obtaining information about the molecular mechanism of Ct bioactivity and thus at contributing to the development of novel Ct-based drugs via the design, synthesis, and study of receptor binding and adenylate cyclase activity of a series of conformationally constrained Ct analogues.

Other than in the case of Ct, the biological role of IAPP, which has been discovered as the major component of pancreatic amyloid deposits in type II diabetes in 1987, has been yet not well described. IAPP is secreted together with insulin from the β-cells of pancreas and is believed to play an important role in carbohydrate metabolism as an insulin counterregulatory hormone, while it also exhibits an overlapping hypocalcemic activity and bone-turnover effect with Ct. Most importantly, the IAPP molecule appears to play a crucial role in the pathogenesis of noninsulin-dependent or type II diabetes that is a progressive, pancreatic cell-degenerative disease that affects more than 150 million people worldwide. An important role of IAPP on the pathogenesis of this disease has been suggested based on the findings that a) more than 95% of type II diabetes patients contain extracellular fibrillar IAPP amyloid aggregates in their pancreata which colocalize with degenerated cells, b) IAPP oligomeric and multimeric proto- and fibrillar aggregates are cytotoxic, c) the sequence of human (h) IAPP *per se* has an extremely strong intermolecular β-sheet-forming, aggregation and amyloidogenic potential whereas the sequence of animal species that do not develop amyloid deposits and type II diabetes (i.e. rats) is devoid of β-sheet and amyloidogenic properties. Both the molecular "rules" for the strong β-sheet and amyloidogenic potential of the IAPP sequence and the conformation and self-assembly state of the cytotoxicity-mediating IAPP "molecular forms" are yet unknown. Therefore, understanding the structural and conformational requirements that confer on the hIAPP sequence its β-sheet-forming, amyloidogenic, and cytotoxic properties is an important step in the process of understanding and developing ways to delay or inhibit the disease progress. Furthermore, to date there are more than 25 other than IAPP polypeptides/proteins that exhibit an amyloid-forming propensity that has been associated with the pathogenesis of various cell-degenerative and fatal diseases that are known as protein aggregation diseases. The most prominent representatives of these polypeptide/protein sequences are the β-amyloid peptide of the Alzheimer's disease and the prion protein of the spongiform encephalopathies. According to a number of studies that have been performed mainly in the past 10 years, a common molecular mechanism may underly the β-sheet-forming, amyloid formation and cytotoxicity potentials of all these various polypeptide sequences. Hence, understanding the structural and conformational "requirements" for amyloidogenicity and cytotoxicity of the IAPP sequence would also assist in elucidating the molecular mechanism of other protein aggregation diseases pathogenesis.

One approach to understanding the molecular basis of the β-sheet and amyloid formation potential of polypeptides is via the selective introduction of N-methyl rests in amide bonds of

the native sequence that are believed, based on structural models, to be crucial for β-sheet formation. In fact, very recent work has demonstrated that N-methylation of the amide bonds at G24 and I26 in short sequences of the amyloid core of hIAPP, i.e. sequences between residues 23-27, 22-27, 20-27, and 20-29 that are capable of forming β-sheet and amyloid aggregates by themselves, could completely abolish their β-sheet- and amyloid forming potentials. Similar results have been recently found when short amyloid core sequences of β-amyloid polypeptide were selectively N-methylated. The effect, however, of selective N-methylation on the amyloidogenic and cytotoxic potential of the full sequence of an amyloidogenic polypeptide has not yet been investigated. This can be due to the difficulties that one often encounters during the solid phase peptide synthesis (SPPS) of an amyloidogenic and/or N-methylated peptide sequence. These are due to the presence of several hydrophobic and aggregation-prone residues in the amyloid sequences and also due to synthetic problems related to steric hindrance and peptide bond lability, which are often caused by the presence of N-methylated residues. Hence, the SPPS of both amyloid-forming sequences such as full sequence hIAPP and of their N-methylated analogues is a demanding task.

The 2nd part of the thesis aimed at performing and investigating SPPS of full sequence (h)IAPP, of the strongly amyloidogenic (h)IAPP mutant S20G-IAPP, and of a series of specifically N-methylated analogues of full sequence (h)IAPP. The work should mainly focus on the investigation of side reactions and the optimization of synthetic protocols that should allow for obtaining mg amounts of the above polypeptides in pure form to be used for future structure-amyloidogenicity-cytotoxicity studies. Finally, the effect of the selective introduction of N-methyl rests on the β-sheet-forming potential and the cytotoxic properties of one representative N-methylated IAPP analogue as compared to the natively occuring IAPP sequence should be examined.

3 Introduction

3.1 Solid Phase Peptide Synthesis (SPPS)

Solid phase peptide synthesis (SPPS) is based on the sequential coupling of α-amino and side chain protected amino acid residues to an insoluble support (Scheme 1). The acid-labile tert-butyloxycarbonyl (Boc) group or the base-labile 9-fluorenylmethoxycarbonyl (Fmoc) group can be used for protection of the α-amino group. Cleavage of the Boc-protecting group is achieved with trifluoroacetic acid (TFA), whereas the Fmoc protecting group is cleaved with piperidine. After removal of the N^{α}-protecting groups, the subsequent protected amino acid is added using either a coupling reagent or a pre-activated amino acid derivative. The resulting peptide, which is attached to the resin through its C-terminus via a linker can be cleaved to yield a peptide-acid or peptide-amide, depending on the linker used. Side chain protecting groups are chosen to be cleaved simultaneously with the detachment of the peptide from the resin. Final cleavage of the peptide from the resin and removal of the side chain protecting groups requires strong acid, such as hydrogen fluoride (HF) in Boc-chemistry, and TFA in Fmoc-chemistry (Figure 1). Dichloromethane (DCM) and N, N′-dimethylformamide (DMF) are solvents that are usually applied throughout the SPPS [1].

Solid phase peptide synthesis has several advantages over solution synthesis:

   a) reactions can be driven nearly to completion through the use of excess reagents
   b) excess reagents and soluble by-products can be simply removed by washing of the resin
   c) since the peptide assembly occurs on the polymer, there is no loss of peptide throughout the synthesis
   d) the synthetic process has been automatized.

For the synthesis the use of small particle-sized resins of low cross-linking is preferred. Such resins allow for rapid diffusion of reagents inside the beads and their high swelling ability enables for them to better accommodate the growing peptide chain [2]. Polystyrene (PS) based supports are usually employed cross-linked with divinylbenzene (DVB) (1-2%). Effective solvation of the resin is one of the most crucial issues for efficient chain assembly during SPPS. Under proper solvation conditions the linear polystyrene chains are nearly as accessible to reagents as if they were free in solution [3]. When the support is well-solvated diffusion of reagents is not a rate-limiting factor of the coupling reaction. Obtaining proper solvation conditions of resins and peptide resins is not always straightforward. Peptide resins are

expected to have physicochemical properties that differ considerably from the initial resin because of the addition of the polar peptide backbone. The peptide backbone would require a polar solvent (such as DMF) to ensure optimum solvation and, hence, accessibility to the reagents [4].

In addition, the use of low-substitution resins (0.1-0.4 mmole / gr) may increase the α-amino group accessibility by decreasing steric interactions as well as aggregation of the peptide chains [5]. Activation of the carboxyl group is a requisite for the chemical formation of a peptide bond. Since the reactivity of the activated species strongly affects the coupling yield several activation procedures have been developed. One of the most common peptide bond formation procedures is the use of dicyclohexylcarbodiimide (DCC). DCC can be replaced by N,N´-diisopropylcarbodiimide (DIC) which results in the formation of diisopropylurea that is more readily soluble than the dicyclohexylurea formed with DCC use. Addition of 1-hydroxybenzotriazole (HOBt) to DCC–mediated couplings improves coupling reactions [6]. The activation procedure takes place *in situ*. *In situ* activation of the carboxyl function is also achieved with the phosphonium 1-benzotriazolyloxy-tris-dimethylamino-phosphonium hexafluorophosphate (BOP), 1-benzotriazolyloxy-tris-pyrrolidinophosphonium hexafluorophosphate (PyBOP) and the uronium benzotriazole-1-yl-1,1,3,3,-tetramethyluronium tetrafluoroborate (TBTU), and 2-(1-H-benzotriazol-1-yl)-1,1,3,3-tetramethyluronium hexafluorophosphate (HBTU) type activators [7].

Despite the general utility and efficiency of SPPS, the synthesis of 'difficult sequences' is still a problem. Ideally, the coupling reaction of a deprotected amino group and an activated carboxyl group should proceed to nearly 100% completion. However, coupling yields of less than 99% are occasionally observed, which are not acceptable for the synthesis of long peptides [8]. This is due to 'the arithmetic demon'[9] according to which the overall yield in a multistep process depends on the yield per step (Figure 2). Couplings are also sequence- and residue-dependent. Difficulties often arise as peptides are elongated through residues 12-20 of their sequences. It has been demonstrated that difficult sequences originate from secondary structure formation such as intermolecular β-sheet formation. The aggregation of the resin bound peptide chains makes the deprotected N^{α}-amino group of the growing peptide only partially accessible to the incoming activated amino acid [10].
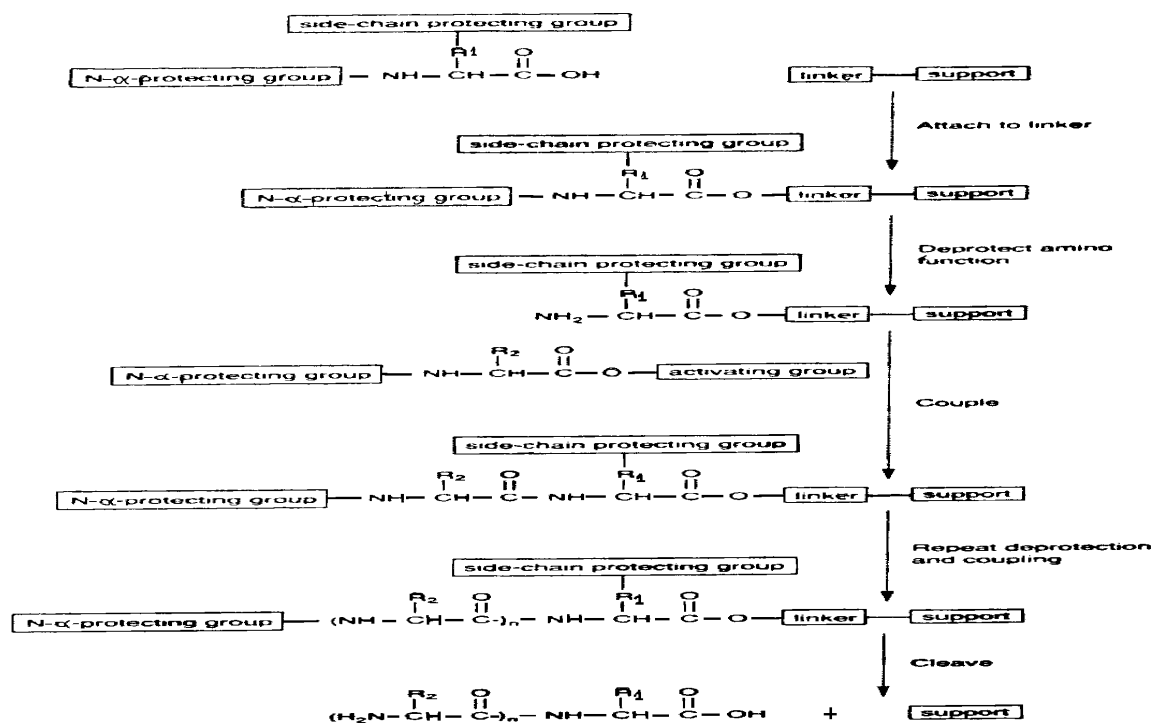
Scheme 1. General scheme of SPPS from synthesis notes [1].
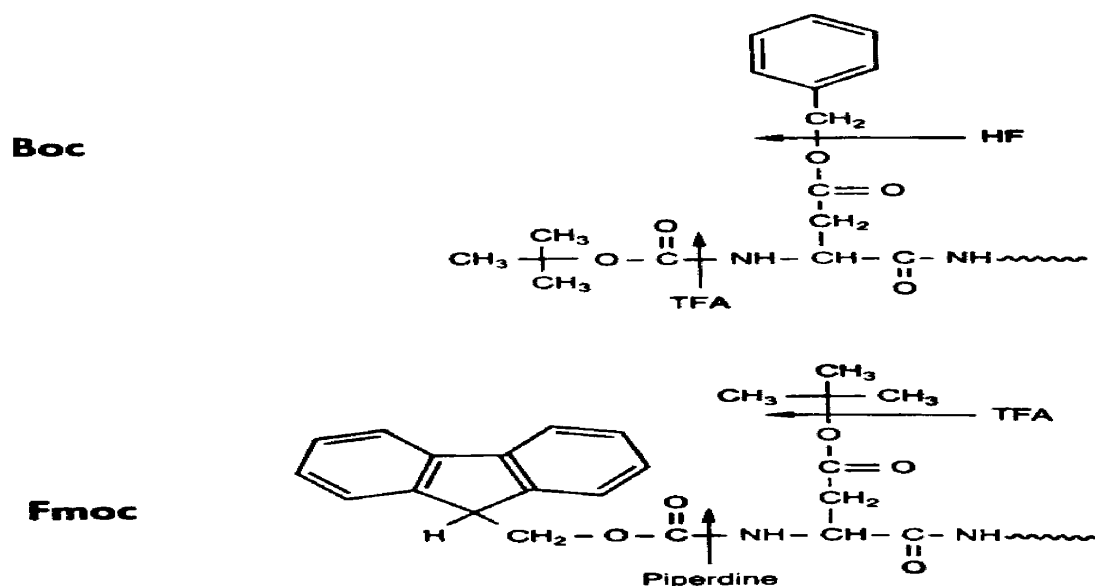
Figure 1. Protecting group strategies in SPPS (Boc- and Fmoc-chemistry) from synthesis notes [1].

Several attempts have been undertaken for the prediction of difficult couplings and improvement of their yields. Sequences that are difficult to synthesize by the one chemistry, are often difficult to be synthesized with another chemistry. The main reasons are the aggregation of the peptide on the resin and steric hindrance due to bulky side chain and/or protectings groups. In the case of N-methylated peptides, the presence of a methyl group in the N^α amino group introduces an additional steric interference that greatly reduces the accessibility of the peptide chain resulting in reduced coupling efficiencies [11].
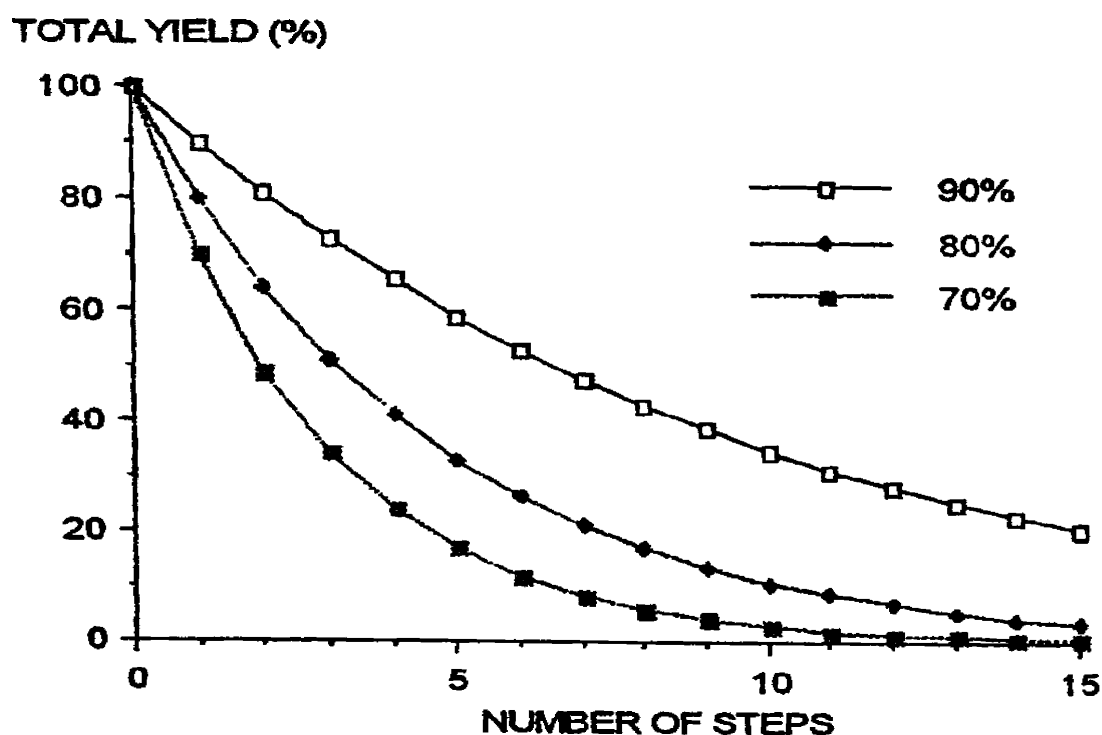
Figure 2. Effect of coupling yield per coupling step on the overall yield of a synthesis (the 'arithmetic demon') from Andersson et al. [9].

3.1.1 Diketopiperazine formation

Alkyl esters of dipeptides bearing a free amino group can undergo spontaneous cyclization and produce 2,5-diketopiperazines (DKP). The mechanism involved is the nucleophilic attack of a carbonyl group by an a amine group (Figure 3):
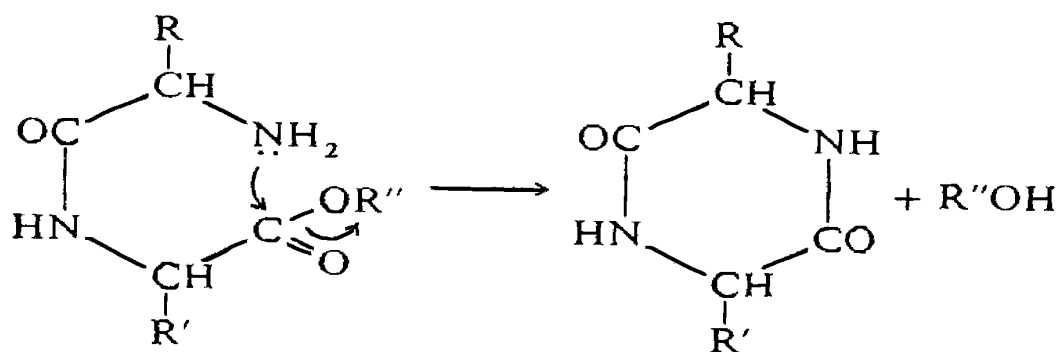
Figure 3. Mechanism of DKP formation adapted from Bodansky [12].

DKP formation can be either acid- or base-catalysed and is strongly dependent on the nature and sequence of the amino acids. In DKP both amide bonds are *cis*, that is the carbonyl oxygen atom and the amide hydrogen are on the same side of the C-N partial double bond. Ring formation is particularly pronounced in glycine and proline containing peptides: in the former because of the absence of an interfering side-chain, in the latter because the cyclic side-chain lies in the plane of the DKP molecule and is out of the way during ring closure. Similarly, DKP are readily formed when one of the residues belongs to the L and the other to the D family of amino acids as well as with N-methylated amino acids [13].

The formation of DKPs leads to lower overall yield of the final peptide, but also results in the presence in the crude peptide of deletion sequences missing the two residues that formed the cyclic dipeptide and cleaved away from the resin [14].

3.1.2 Acidic hydrolysis of N-methylated peptides

Synthetic peptides containing an N-methylated amino acid residue that have the general structure R^1- (N-Alkyl) X_1-X_2-R^2 have been reported to undergo facile TFA catalyzed hydrolysis under standard TFA cleavage / deprotection conditions of SPPS. The peptide bond cleaved is the bond C-terminal to the N-alkylated amino acid. The N-terminal fragment is believed to undergo equilibration of the C^α-chiral center of the N-alkylated residue. The mechanism that explains this equilibration includes formation of the oxazolone-like intermediates α, α' and b (Figure 4), which are formed via the cleavage of a species that is generated by protonation at the N-methyl residue and subsequent nucleophilic attack of an

adjacent carbonyl group. Direct hydrolysis of intermediates α and α´ to give an N-terminal fragment is found to be much slower than tautomerization to the enol b [15].
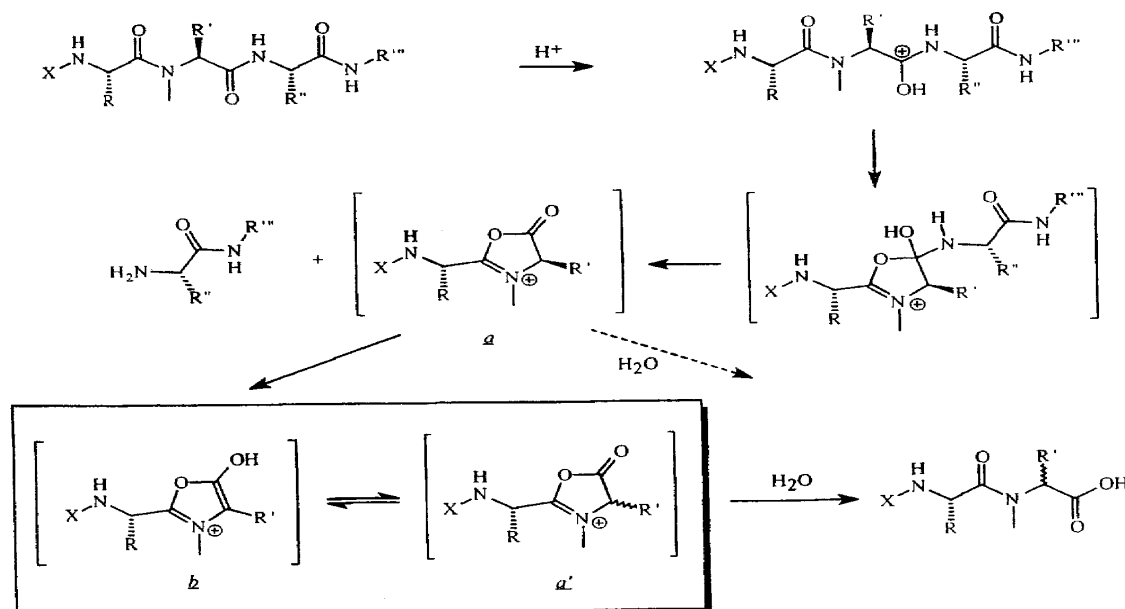
Figure 4. Proposed mechanism of the acidic hydrolysis of N-methyl containing peptide sequences according to Urban *et al.* [15].

3.2 Constrained peptides

Knowledge of the active conformation of a bioactive polypeptide is a major step towards understanding the mechanism underlying its biological function. Although a variety of biophysical techniques exist to study polypeptide conformation, a major obstacle in the study of short peptide sequences is their intrinsic flexibility. In solution short linear peptides are usually adopting a large number of conformation states that are almost equivalent energetically and, although slightly preferred conformations may be more populated in some cases, overall peptide conformation is generally highly dependent on the environment. The number of conformational 'possibilities' in peptides and proteins can be reduced by introducing constraints. Indeed, nature uses several such constraints to reduce the flexibility of polypeptide chains, including the incorporation of cyclic amino acid residues (proline) and the formation of macrocycles through disulfide bonds. In these ways, particular conformations of peptides and proteins are stabilized [16].

Model constrained peptides are used to study in detail the conformational preferences of natural and modified amino acid residues and assist to gain insight into their tendencies to adopt particular secondary structure. Constrained analogues of biologically active peptides have been generated to induce specific structural features and to understand the conformational requirements for receptor binding and signal transduction, leading to the development of potent agonists and/or antagonists [17].

α-Helices, β-sheets, and turns are the three main classes of secondary structure in peptides and proteins that one may want to stabilize through the use of constraints. The constraints can be classified into two broad categories: local and global constraints. Various different chemical modifications of the peptide backbone or the side-chains have been used to modulate local conformational properties of peptides. These include peptide bond surrogates and cyclic as well as conformationally constrained amino acid residues. Perhaps the simplest way to modify the local stereochemical properties of the peptide backbone is to introduce D-amino acids. Heterochiral (LD or DL) dyads have an increased tendency to form β-turns because of the stabilizing effect of a D-amino acid on a β-turn conformation. The amide bond surrogates (such as CO-O, CS-TH, CH_2-NH) are modifications that directly affect the conformation of the novel backbone. In addition, such modifications can result in improved enzymatic stability, novel solubility properties and can significantly affect the *in vivo* transport characteristics of the analogues [18].

One of the steric constraint that have been used to limit the conformational space available to a polypeptide chain are alkylations in the N and C_α positions [19]. N-methylation restricts the conformations of both the residue bearing the modification and the preceding residue and studies carried out on model peptides have shown the tendency of N-methylated residues to participate in different turn conformations, depending on the chirality of the sequence and the *trans* or *cis* conformation of the tertiary amide bond [20].

The most general way to introduce a global constraint into a peptide chain and to affect drastically its overall conformation is the formation of a covalent bond between distant parts in the sequence. These constraints affect all the degrees of freedom of the peptide sequence in the ring that has been generated that should thus be able to adopt a more rigid conformation than in the parent linear form. The increased rigidity of the ring structure can also induce 'preferred' conformations in the previously linear parts of the molecule. Cyclization can be performed by linking the two backbone termini, or two side chains, or one of the termini and a side chain, etc and formation of amide or disulfide bonds is thus the simplest method to achieve this. Side chain-to-side chain cyclization between residues *i, (i+4)* has been applied

for the stabilization of the α-helical conformation [21]. However, not only α-helices can be stabilized by *i, (i+4)* lactam bridges but also β-turn conformations, although there have been no reports of the effect of the chain length of this type of cyclic structure on β-turn stabilization [22]. In contrast, *i, (i+3)* lactam bridges model tetrapeptides have been demonstrated to stabilize β-turns [23].

In general, changes in the overall direction of the peptide chain are necessarily introduced by cyclic constraints and, hence, cyclic peptides are ideal models to study reverse-turn preferences of different amino acid residues and interactions that stabilize turns in peptides and proteins [24].

3.2.1 Rational design of drugs: constrained peptides

Many short linear peptides (usually up to 50 residues) are key factors in the regulation of a wide variety of biological processes acting as hormones, neurotransmitters, or inhibitors of protein interactions. Major efforts have thus been dedicated to the development of agonists or antagonists of these peptides that could be used as drugs with high specificity and low toxicity. Much of the research in the field of peptide drugs has been based on the synthesis of a large number of analogues with different substitutions / or deletions, on determining the steric and hydrophobicity / hydrophilicity characteristics of a particular peptide sequence, as well as the minimum number of residues that are necessary for biological activity [25]. Although such approaches are very informative, it is often difficult to find reasonable correlations between the experimentally obtained data. The reason for this is that various biological activities of the analogues can be due to changes in the conformational properties of the analogues, rather than due to changes in amino acid polarity and/or bulkiness which is what was intended to occur. However, different conformations may result in similar side-chain orientations, and various binding modes to receptors may also exist. Moreover, the conformational analysis of the analogues and the native short or medium-sized peptide is usually hampered by their high flexibility. The synthesis and study of constrained analogues has thus emerged as a very powerful approach in peptide drug design [26]. Ideally, a conformational constraint that stabilizes the bioactive conformation of a peptide should result in an increased receptor binding affinity, as there is little conformational entropy lost upon binding to the receptor. Furthermore, several biologically active peptides are believed to interact with different receptors, and constraining particular features can lead to drugs with high receptor specificity and free from undesired side effects [27]. Structural features that may

be important for the biological activity of a given peptide sequence can be predicted / or suspected based on a conformational study of the peptide, from results obtained with deletion / substitution studies, and from known conformational propensities of residues in the sequence. An iterative process can then be started by using conformational constraints to test and refine the structural conformational hypotheses. The conformational and topological requirements for agonist or antagonist activity and for receptor specificity can be studied by modifying the constraints and using various biological assays [28].

3.3 Calcitonin gene peptide superfamily

The calcitonin gene peptide superfamily consists of calcitonin (Ct), calcitonin gene-related peptide (CGRP), islet amyloid polypeptide (IAPP) and adrenomedullin. Ct and CGRP derive from the Ct / CGRP gene, which is located on chromosome 11. Alternative splicing of the primary RNA transcipt leads to translation of CGRP and Ct peptides in tissue-specific manner [for example, in the central nervous system (CNS), splicing of the CT/CGRP gene produces CGRP, whereas in the C cells of the thyroid gland Ct is formed]. The gene encoding for IAPP is located on chromosome 12, which is believed to be derived from evolutionary duplication of chromosome 11. This peptide superfamily share common structural features that are responsible for the overlapping biological effects and also for the cross-reactivity between receptors [29].

3.3.1 Calcitonins

Calcitonin (Ct) is a polypeptide hormone secreted by the C-cells of the thyroid gland in mammals and the ultimobranchial body in birds, reptiles and fish. Calcitonin is mainly kwown for its hypocalcemic effect and the inhibition of bone resorption, and is used therapeutically for the treatment of osteoporosis, Paget's disease and other hypercalcemia-related diseases. The observed antinociceptive effect of calcitonin on animals and patients suffering from Paget's disease are also suggestive of potential new applications in the treatment of pain [30].

Calcitonins from at least ten different species have been isolated and their primary sequences were determined. All of them consist of 32 amino acid residues with a disulfide bond between Cys^1 and Cys^7 and a prolinamide at their C-terminal (Figure 5). The two Cys residues, the C-terminal Pro and the following residues Leu^4, Ser^5, Thr^6, Leu^9, Gly^{28} are highly conserved

among these ten calcitonins. The salmon and eel calcitonins (sCt and eCt) differ in their sequence in only three positions (26,27 and 29), whereas sCt and human calcitonin (hCt) differ in 17 positions (~50% homology). The homology between hCt and rat calcitonin (rCt) is very high (they differ in only two positions: 16 and 26) [31].

CSNLSTCVLG[10]	KLSQELHKLQ[20]	TYPRTNTGSG[30]	TP	**sCt**
CSNLSTCVLG[10]	KLSQELHKLQ[20]	TYPRTDVGAG[30]	TP	**eCt**
CGNLSTCMLG[10]	TYTQDFNKFH[20]	TFPQTAIGVG[30]	AP	**hCt**
CGNLSTCMLG[10]	TYTQDLNKFH[20]	TFPQTSIGVG[30]	AP	**rCt**
CSNLSTCVLS[10]	AYWRNLNNFH[20]	RFSGMGFGPE[30]	AP	**pCt**
CASLSTCVLG[10]	KLSQELHKLQ[20]	TYPRTDVGAG[30]	AP	**chCt**

Figure 5. Primary structures of Calcitonins (s: salmon, e: eel, h: human, r: rat, p: porcine, ch: chicken).

sCt and eCt are about 50 times more potent than hCt and other mammalian calcitonins *in vivo*. Therefore, sCt is the mainly therapeutically used calcitonin. hCt is also used but to a lesser degree. It has been long proposed that the propensity of the Cts to form an α-helix in the region [8-22] might correlate with their bioactivities [32]. sCt and hCt have regurlarly spaced hydrophobic amino acids at each third or fourth residue in the region [8-22] of the polypeptide chain. This regular spacing of hydrophobic amino acids would allow the peptide to fold into an amphiphilic α-helix in which one face of the helix is hydrophobic and the other hydrophilic [33]. Nuclear magnetic resonance (NMR) studies in mixed solvents such as methanol-water, or trifluoroethanol (TFE)-water, suggested the presence of a central helix in sCt that extends from residue 8 to 22, and similar results have been reported for hCt in TFE solutions [34]. The higher biological potency of sCt compared to hCt has been associated with a higher helix forming propensity in the region [8-22] for the sCt. However, for hCt there is no direct link between helicity and bioactivity. In contrast, other factors such as a β-turn/β-sheet conformation in the central region of hCt, overall conformationally flexibility, tertiary structure interactions and interactions of specific residues may be related to bioactivity [35]. NMR studies in non-helix-inducing media (such as in neat dimethylsulfoxide (DMSO) or

DMSO / water) indicated a type I β-turn centered around residues 18 and 19 connecting two short antiparallel β-sheets to be present in the central region of hCt [36, 37]. Interestingly, hCt has three aromatic residues in position 12, 16 and 19, whereas these positions are occupied by leucine residues in sCt [38].

Receptors for several peptide hormones belong to the superfamily of seven trans-membrane domain G-protein-coupled receptors (7 TMD-GPCRs). Based on primary structure homology, this superfamily can be divided into several subfamilies. The most recently identified subfamily comprises receptors for the peptide hormones calcitonin, parathyroid hormone, glucagon, glucagon-like peptide, secretin and vasoactive intestinal peptide. The diversity of intracellular effects mediated by members of the 7 TMD-GPCR superfamily is generated by coupling of the receptors to various G-proteins. An additional source of diversity results from the existence of receptor subtypes (or isoforms) that recognize the same ligand. These subtypes may be discrete gene products or the result of alternative splicing of primary messenger RNA transcripts to yield different protein products [39].

Ct receptors are localized in bone and kidney and also in the CNS, i.e. the brain. Human and rat Ct receptors are the best characterized in terms of their ligand interactions and these receptors are known to be expressed in multiple isoforms as a result of alternative gene splicing. The major isoforms of the human Ct receptor, $hCTR_{I1-}$ and $hCTR_{I1+}$ differ in the absence and presence, respectively, of a 16-residue insert in the proposed first intracellular loop region [40]. The insert-negative isoform of the human receptor appears to be the dominant isoform in most tissues, including the CNS. Both hCTR isoforms bind sCt with identical affinities, but the insert-positive isoform exhibits impaired signal transduction via the adenylyl cyclase (AC) and phospholipase C second-messenger systems [41].

Structure-activity relationships studies (SAR) have indicated that region [1-7] of the Cts is important for AC activation, while binding to the Ct receptor is believed to be mediated by region [8-32] [42]. Salmon calcitonin binds to human calcitonin receptors with a higher affinity as compared to hCt.

According to one hypothetical model [43] (Figure 6), the structural feature that is responsible for the hormone binding has been mapped to the amphiphilic α-helical region, which has been proposed to interact primarily with the extracellular N-terminal domain of the Ct receptor. Hormone binding to the Ct receptor has been proposed to occur via two possible pathways: in pathway 1 binding occurs through the amphiphilic helix to the N-terminal domain of the Ct receptor and in pathway 2 by direct interactions of the hormone ligand with binding sites in the transmembrane domain of the Ct receptor. Pathway 1 may be more prominent for sCt

binding than for hCt binding. A tight, 'closed' complex (3) is then postulated to be a prerequisite for efficient receptor activation and signal transduction.
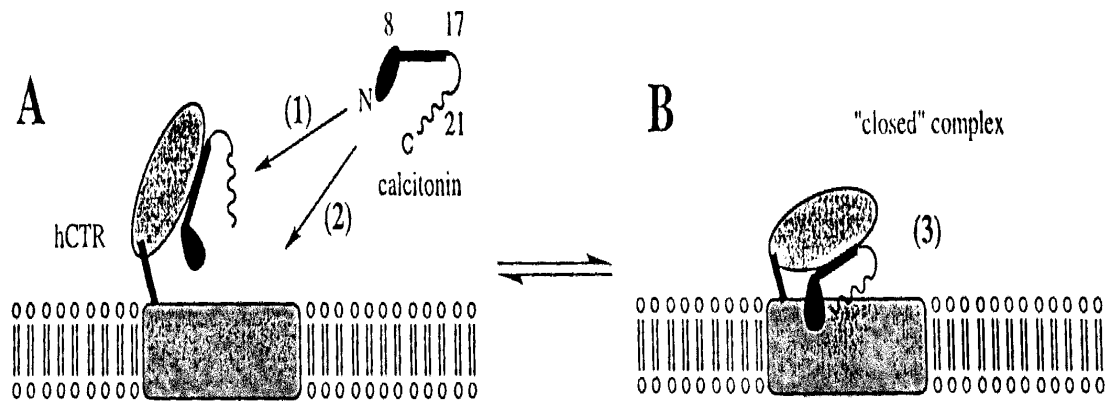
Figure 6. Hypothetical model for receptor binding by the Cts [43]. The structural domains of Ct are depicted: the N-terminal disulfide-bridge (N), the amphiphilic α-helix [8-17], a β-turn in region [17-21] and the C-teminal domain [21-32]. (A): in pathway 1 binding of the calcitonin to the Ct receptor occurs through binding of the amphiphilic α-helix of the hormone to the N-terminal domain of the receptor, where in pathway 2 binding of the calcitonin to the Ct receptor occurs through direct interactions of the hormone ligand with binding sites in the transmembrane domain of the Ct receptor. (B): a tight, 'closed' complex (3) between the receptor and the hormone ligand is required for efficient receptor activation and signal transduction.

3.3.2 Islet Amyloid Polypeptide (IAPP)

IAPP is expressed mainly in the islets of Langerhans of pancreas and is believed to be genetically, structurally and functionally related to both Ct and CGRP [29]. hCt and hCGRP exhibit a primary sequence homology of 15 and 46% respectively, to the hIAPP sequence. The conserved amino acids between hIAPP and hCGRP are located in the regions between residues 1 and 20 and between 29 and 37. More than 80% of the hIAPP sequence is broadly conserved in the mammalian species suggesting a significant biological function for this polypeptide [44].

hIAPP is expressed as a 89-residue containing pre-propeptide and is stored in form of the 67-residue human ProIAPP (hProIAPP) in secretory vesicles of the β-cells together with insulin (and proinsulin). hIAPP is secreted together with insulin (in a ratio of insulin to hIAPP of 100 to 1) following proteolytic processing of the pro-region in response to insulin secretagogues and the basal blood concentration of IAPP in humans has been reported to be between 1 and 10 pM [45]. The most well-studied biological effects of IAPP include its effect on carbohydrate metabolism and on bone metabolism [46]. IAPP is believed to play a role as an insulin counter-regulator in skeletal muscle by inhibiting glycogen synthesis and promoting glycolysis. IAPP has been also reported to inhibit insulin secretion by the β-cells [47]. In addition, IAPP excerts hCt-like effects on bone turnover that include the inhibition of bone resorption most likely by inhibition of the osteoclastic activity and the reduction of plasma calcium. The biological activities of IAPP are believed to be mediated by G-protein coupled receptors, while a specific IAPP receptor has not been yet identified and characterized [48]. It is possible that IAPP can interact with CGRP receptors in target tissues such as in the brain, lung, stomach, spleen and liver [49].

Although more than 80% of the hIAPP sequence is conserved in the mammalian species besides humans and human primates, only a few animal species including cats, dogs, monkeys and raccoons develop IAPP-derived islet amyloid. There is a clear species- and sequence-specificity of the amyloidogenic potential of the IAPP sequence [50]. *In vitro* studies have shown that hIAPP easily forms amyloid fibrils, whereas synthetic rat IAPP (rIAPP) is not able to form amyloid [51]. The sequence of rIAPP differs from the one of the hIAPP in 6 out of 37 amino acids with 5 out of these 6 amino acids located in the region between 20 and 29 (Figure 7). Two to three of the five different amino acids in the rat sequence are proline, which is a known β-sheet-breaking residue [52]. The amino acid constitution of sequence IAPP [20-29] has been, therefore, suggested to define and modulate the amyloidogenic propensities of complete sequence IAPP from different species [53].

```
   |‾‾‾‾|
   |      |
KCNTATCATQ¹⁰     RLANFLVVHS²⁰     NNFGAILSST³⁰     NVGSNTY     hIAPP
   |‾‾‾‾|
   |      |
KCNTATCATQ¹⁰     RLANFLVRSS²⁰     NNLGPVLPPT³⁰     NVGSNTY     rIAPP
   |‾‾‾‾|
   |      |
KCNTATCATQ¹⁰     RLANFLVRSS²⁰     NNFGTILSST³⁰     NVGSDTY     mIAPP
   |‾‾‾‾|
   |      |
KCNTATCATQ¹⁰     RLANFLVRTS²⁰     NNLGAILSPT³⁰     NVGSNTY     dIAPP
   |‾‾‾‾|
   |      |
KCNTATCATQ¹⁰     RLANFLIRSS²⁰     NNLGAILSPT³⁰     NVGSNTY     cIAPP
```

Figure 7. Primary structures of IAPP (h: human, r: rat, m: monkey, d: dog, c: cat).

Type II diabetes mellitus (NIDDM) is a cell degenerative disease that belongs to the family of protein aggregation diseases (such as Alzeimer's, Huntington's or Parkinson's disease). More than 90% of patients with type II diabetes have amyloid deposits in the β-cells of the pancreas [54]. Pancreatic amyloid fibrils consists of IAPP and contain the polypeptide chains organized in a 'cross-β-sheet' structure [55]. In the past ten years evidence has been gathered that there is a common mechanism of amyloid formation for various polypeptides (such as IAPP, and the AD β-amyloid peptide) that include a conformational transition of mainly random coil or α-helical polypeptides into β-sheet aggregates. In addition, there is increasing evidence that fibrillar / or protofibrillar species formed by ordered aggregation of these polypeptides are cytotoxic and that their formation process is directly associated with the pathologic onset of the corresponding disease [56].

The conversion of monomeric and soluble polypeptides into insoluble amyloid fibrils is a multistep process, which has been yet not understood. This is also due to the fact that the detailed biophysical characterization of various different structural and assembly states of one polypeptide sequence is necessary, which in turn requires the complementary use of several independent biophysical methods for its elucidation [57].

The mechanism speculated for the amyloidogenic pathway of hIAPP is consistent with a nucleation-dependent polymerisation mechanism [58]. In Figure 8, a proposed model of possible molecular events in the hIAPP amyloid formation pathway via a partially folded intermediate state (I) (2) is shown [59]. According to the model during folding [from the unfolded state (U) (3) to folded state (N) (1)] or unfolding, this partly folded state and its self-associated forms [(2) and (4), respectively in Figure 8] are in a concentration-dependent equilibrium with native nonamyloidogenic hIAPP (1). The intermediate folded state (I) is not stable as a monomer but can be stabilized by self-association into an oligomeric species (x-

mer). The monomer and the oligomer species of the intermediate state (I) are early, soluble, α-helix and β-sheet-containing precursors of amyloid fibrils, with the potential to further associate in an enviroment- and concentration-depedent manner into β-sheet-rich protofibrillar (5) and fibrillar assemblies (6). Question marks (?) indicate that the intermediate steps in the amyloid forming pathway have not yet been characterized. Also, the exact structure, the assembly state, and the biophysical properties of the partly folded states (2) and (4) have not yet been characterized.
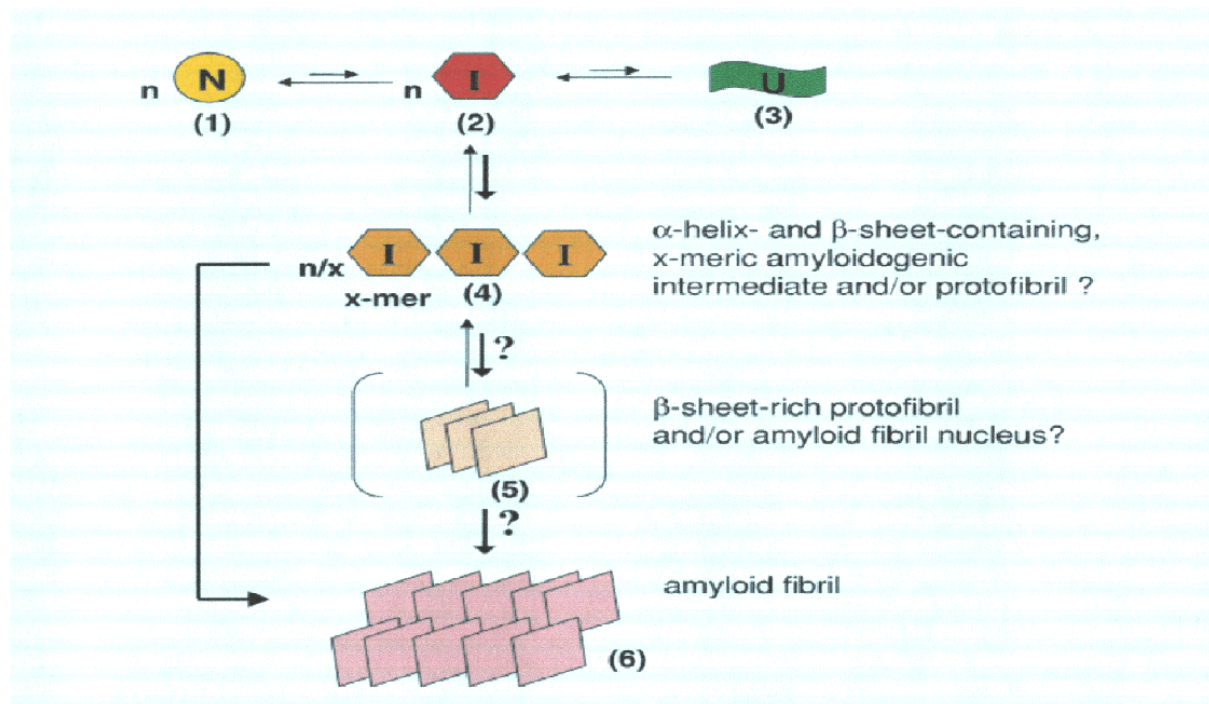
Figure 8. Model of possible molecular events in the hIAPP amyloid formation pathway via a partially folded intermediate state(s) [59]. [(N) or (1): native or folded state, (U) or (3): unfolded state, (I) or (2): intermediate folded state, (4): multimer formed through self-association of intermediate folded state(s), (5): protofibril species rich in β-sheet structure, (6): amyloid fibril].
Question marks (?) indicate that the intermediate steps in the amyloid forming pathway have not yet been characterized.

4 Materials and Methods

4.1 Materials

Resins for solid phase synthesis were purchased by Bachem (Heidelberg, Germany) and Novabiochem (Laüfelfingen, Switzerland). Boc-protected amino acids were supplied by Bachem (Heidelberg, Germany), and Fmoc-protected amino acids were purchased by Rapp Polymere (Tübingen, Germany), except for the following: Fmoc-Asp(OPip)-OH, Fmoc-Dab(Adoc)-OH, Fmoc-Dap(Boc)-OH, Fmoc-Dap(Adoc)-OH, Fmoc-Glu(OPip)-OH, Fmoc-Orn(Mtt)-OH which were supplied by Bachem. Fmoc N-methylated amino acids were purchased by Novabiochem. Solvents required for synthesis such as DMF (lab grade), DCM (p.a grade) which was distilled prior to use, and NMP (synthesis grade) were acquired by Merck (Darmstadt, Germany). Additional solvents such as: MeOH (p.a grade), EtOH (p.a grade), Et_2O (p.a grade), AcOH (100%) and iPrOH (p.a grade) were also purchased by Merck (Darmstadt, Germany). Coupling reagents were obtained by the following sources: TBTU (synthesis grade) by Rapp Polymere, HOBt (purum ≥ 98%) by Fluka (Buchs, Switzerland), DIC (purum ≥ 99%) by Sigma-Aldrich (Steinheim, Germany), DIEA (≥ 98%) by Fluka (Buchs, Switzerland), piperidine (synthesis grade) by Merck-Schuchardt (Hohenbrunn, Germany). Additional chemicals used during the synthesis were the following: acetic anhydride by Sigma-Aldrich (Steinheim, Germany), ninhydrin (~99%) by Fluka, triisopropylsilane (TIS) (99%) by Sigma-Aldrich, 4 M HCl in dioxane (synthesis grade) by Sigma-Aldrich. Reagents used for cleavage of the peptides from the resin were: TFA (peptide synthesis grade) by Biosolve (Valkenswaard, Netherland), phenol (99%) by Sigma-Aldrich, where the scavengers thioanisole (TAS) (≥ 99%), 1,2-ethanedithiol (EDT) (≥ 98%), dimethylsulfide (DMS) (≥ 99%) were supplied by Fluka. Solvents for the HPLC purifications were: acetonitrile (ACN) (liquid chromatography grade) by Merck and TFA (protein sequencing grade) by Fluka. NH_4HCO_3 (≥ 99%) was from Fluka, and HCl (37%), guanidine hydrochloride (Gdn HCl) (99%) and urea (99%) were provided by Sigma-Aldrich. Synthetic analogues (hCt and sCt) for the bioactivity assays were from Novabiochem. Medium (RPMI 1640), fetal bovine serum and cell culture antibiotics and hormones (hydrocortisone, insulin) were from Invitrogen (Karlsruhe, Germany). Salmon [125]I- labelled Ct and the EIA kit for cAMP determination (Biotrak) were both from Amersham Pharmacia Biotech (Freiburg, Germany). For the *in vitro* toxicity assays of IAPP and IAPP analogue [2], 1,1,1,3,3,3-hexafluoro-2-propanol (HFIP) and 3-[4,5-dimethylthiazol-2-yl]-2,5-diphenyltetrazolium bromide (MTT) were from Sigma-Aldrich.

4.2 Methods

4.2.1 SPPS using the Boc-strategy

Boc-chemistry SPPS was performed using Boc-protected amino acids on p-methyl-benzhydrylamine (MBHA) polystyrene resin (crosslinked with 1% DVB). Peptide assembly was carried out manually using a glass reaction vessel equipped with filter unit. Removal of the N^α-Boc group (except for Gln) was performed by 50% TFA in DCM, followed by neutralization of the resin with 5% DIEA in DCM and subsequent washings with DCM, iPrOH and DMF. Thereafter, a solution of the Boc-amino acid, TBTU, DIEA (in a molar ratio of 4/4/6) was added. Couplings were performed for 60 to 90 min and their completeness was checked by Kaiser test (see 4.2.5). When not satisfactory, either a second coupling or capping of the peptide resin with Ac_2O (10-fold molar excess) in the presence of DIEA (10-fold molar excess) in DMF for 45 min was carried out. In the calcitonin analogues after the coupling of Met^8 the subsequent cleavages of the Boc-group were achieved with 50% TFA in DCM plus 1% DMS as scavenger of the tert-butyl. The above steps were repeated for each amino acid and are summarized in table 1.

All Boc-amino acids were of L-configuration unless otherwise specified and the side chain protecting groups were the following: Asp(OcHx), Cys(Mob), His(π-Bom), Lys(2-Cl-Z), Ser(Bzl), Thr(Bzl), Tyr(2-Br-Z).

4.2.1.1 Cleavage of the N^α-Boc-group of glutamine

The calcitonin sequence has two glutamine residues that may form pyroglutamine during TFA-mediated Boc-cleavage [60]. Therefore, a special protocol was applied for the cleavage of the Boc-group of Gln. According to it, 4 M HCl in dioxane was used and short washing steps were applied. After cleavage of the Boc-group and neutralization a positive Kaiser test indicated the presence of free amino groups. The next amino acid was then coupled using 6-fold molar excess instead of 4-fold molar excess that was applied in the standard coupling protocol.

The procedure is shown in table 2.

Table 1. Protocol for SPPS using Boc-chemistry.

Synthesis cycle:	Reagent:	Time:
Wash	DMF	2 x 1 min
Wash	DCM	2 x 1 min
Deprotect	50% TFA / DCM [§]	1 x 2 min
Deprotect	50% TFA / DCM [§]	1 x 28 min
Wash	DCM	2 x 1 min
Neutralize	5% DIEA / DCM	2 x 2 min
Wash	DCM	2 x 1 min
Wash	iPrOH	1 x 1 min
Wash	DCM	1 x 1 min
Wash	DMF	2 x 1 min
Coupling	Boc-AA / TBTU / DIEA (Eq: 4 / 4 / 6)	60-90 min
Wash	DMF	3 x 1 min
Acetylation	Ac_2O / DIEA (Eq: 10 / 10)	45 min
Wash	DMF	3 x 1 min

[§]: after Met^8 in Ct analogues plus 1% DMS as scavenger.

Table 2. Cleavage of the N^α-Boc-group of Gln.

Synthesis cycle:	Reagent:	Time:
Wash	dioxane	1 x 10 sec
Deprotect	4 M HCl / dioxane	1 x 2 min
Deprotect	4 M HCl / dioxane	1 x 28 min
Wash	dioxane	1 x 10 sec
Wash	DCM	2 x 10 sec
Neutralize	5% DIEA / DCM	2 x 1 min
Wash	DCM	1 x 1 min
Wash	DMF	1 x 1 min

4.2.1.2 Cyclization strategy in synthesis by Boc-chemistry

The synthesis of the side chain-to-side chain lactam bridged analogues of calcitonin was accomplished using a previously established side chain-to-side chain cyclization strategy on

the resin [21]. The use of Asp & Orn / Lys amino acids derivatives at positions 17 & 21 that

beared base labile side chain protecting groups (Fmoc- and OFm respectively) enabled for the

selective cleavage of these groups in the presence of Boc- and Bzl- based groups. After

incorporation of the residue at position 17, the peptide resin was treated with piperidine in

DMF (25% v/v) to remove the side-chain groups of residues 17 & 21. A small aliquot of resin

was tested with Kaiser test and following washes of the resin, BOP (4-fold molar excess) and

DIEA (4-fold molar excess) in DMF were added. Completeness of the cyclization was

checked with the Kaiser test (after 4 hrs reaction time) and in most of the cyclizations a

second coupling was performed overnight (16-18 hrs). Finally, unreacted groups were

acetylated by Ac_2O and DIEA in DMF (10-fold molar excess each) for 45 min. The protocol

is summarized in table 3.

Table 3. Cleavage of Fmoc- and OFm- side chain protecting groups and side chain-to-side

chain cyclization protocol in Boc-SPPS.

Synthesis cycle:	Reagent:	Time:
Wash	DMF	2 x 1 min
Deprotect	25% piperidine / DMF	1 x 2 min
Deprotect	25% piperidine / DMF	1 x 28 min
Wash	DMF	3 x 1 min
Wash	10% DIEA / DMF	1 x 1 min
Wash	10% DIEA / DMF	1 x 3 min
Wash	DMF	3 x 1 min
Cyclization	BOP / DIEA (Eq: 4 / 4)	1 x 4 hrs 1 x 16 hrs
Wash	DMF	3 x 1 min
Acetylation	Ac_2O / DIEA (Eq: 10 / 10)	45 min
Wash	DMF	3 x 1 min

4.2.2 SPPS using the Fmoc-strategy

For the Fmoc-strategy an orthogonal protection scheme was applied with the Fmoc- group as

a temporary protection of the N^α group and tBu- and Trt-based side chain protecting groups.

The 4-(2´, 4´-dimethoxyphenyl-Fmoc-aminomethyl)-phenoxy acetamido-norleucyl resin

(Rink amide MBHA) was used in the case of peptide amides (such as Ct and IAPP

analogues). Fmoc-cleavage was achieved by 25% piperidine in DMF. Couplings were

performed using Fmoc-AA and TBTU (4-fold molar excess) in the presence of DIEA (6-fold

molar excess). Couplings of N-methylated amino acids, as well as couplings on N-methylated amino acids were performed as described under sections 4.2.3 and 4.2.4. The following Fmoc-protected amino acid derivatives were applied: Asp(OtBu), Glu(OtBu), Gln(Trt), Cys(Trt), His(Trt), Lys(Boc), Thr(tBu), Ser(tBu), Arg(Pmc), and Tyr(tBu). The side chain protecting groups of the residues that were to be covalently linked via side chain-to-side chain were: 2-phenyl-isopropyl ester (OPip) for Asp[17], 4-methyl-trityl (Mtt) for Orn[21] & Lys[21] and adamantyl-1-methyl-ethoxy-carbonyl (Adoc) for Dap[21] & Dab[21]. Coupling efficiencies were checked by the Kaiser test and/or reversed-phase high performance liquid chromatography (RP-HPLC) and mass spectroscopic (MS) analysis of a small sample of peptide resin following treatment with TFA to cleave the peptide from the resin (see 4.2.7.3). The protocol is summarized in table 4.

Table 4. Protocol for SPPS using Fmoc-chemistry.

Synthesis cycle:	Reagent:	Time:
Wash	DMF	2 x 1 min
Deprotect	25% piperidine / DMF	1 x 5 min
Deprotect	25% piperidine / DMF	1 x 20 min
Wash	DMF	4 x 1 min
Coupling	Fmoc-AA / TBTU / DIEA (Eq: 4 / 4 / 6)	60-90 min
Wash	DMF	3 x 1 min
Acetylation	Ac$_2$O / DIEA (Eq: 10 / 10)	45 min
Wash	DMF	3 x 1 min

4.2.2.1 Cyclization strategy in Fmoc-chemistry

Cyclizations in calcitonins were performed between the side chains of residues 17 and 21. After incorporation of residue 17, the peptide resin was washed with distilled DCM. A mixture of triisopropylsilane (TIS) (5%) (v/v) and TFA (1%) (v/v) in distilled DCM was added to cleave the side chain groups OPip, Mtt and / or Adoc. At this point, the positive Kaiser test indicated the presence of free side chain amino groups. The peptide resin was further washed with distilled DCM and with DMF and was then neutralized with 1% DIEA in DMF and finally washed with DMF. The cyclization reaction was performed by the addition of BOP (4-fold molar excess) and DIEA (4-fold molar excess) in DMF. The progress of the reaction (after 4-5 hrs) was checked by Kaiser test. Thereafter, the cyclization reaction was

repeated for another 16-20 hrs. Upon completeness of the 2nd cyclization reaction, capping of the peptide resin was carried out with acetic anhydride and DIEA in DMF (10-fold molar excess each) for 45 min. The protocol is summarized in table 5.

Table 5. Cleavage protocol of special side chains groups and side chain-to-side chain cyclization protocol in Fmoc-SPPS.

Synthesis cycle:	Reagent:	Time:
Wash	DCM	3 x 1 min
Deprotect	TIS / TFA (5% / 1%) in DCM	2 x 2 min
Deprotect	TIS / TFA (5% / 1%) in DCM	6 x 10 min
Wash	DCM	3 x 1 min
Wash	DMF	3 x 1 min
Neutralize	1% DIEA / DMF	2 x 2 min
Wash	DMF	3 x 1 min
Cyclization	BOP / DIEA (Eq: 4 / 4)	1 x 4 hrs 1 x 16 hrs
Wash	DMF	3 x 1 min
Acetylation	Ac$_2$O / DIEA (Eq: 10 / 10)	45 min
Wash	DMF	3 x 1 min

4.2.2.2 Coupling of Cys residues in Fmoc-SPPS

Coupling of Fmoc-Cys(Trt)-OH was performed by a different method than the coupling of the other amino acids. This is due to the fact that the activation of Fmoc-Cys(Trt) when performed with TBTU in the presence of base as normally performed in Fmoc-strategy can cause significant racemization of Cys [61]. Therefore, Cys couplings were performed using an *in situ* activation protocol via 1-hydroxybenzotriazole (HOBt) and diisopropylcarbodiimide (DIC). For this activation no addition of base was necessary [62]. Specifically, equimolar amounts of Fmoc-Cys(Trt)-OH , HOBt, and DIC (4-fold molar excess each with regard to the amino groups) were dissolved in DMF (concentration 0.15 M each). Following stirring of the reaction mixture at 4 °C for 45 min, the solution containing the OBt-ester of Fmoc-Cys(Trt) was added to the N$^{\alpha}$-deprotected peptide resin. Coupling was performed for 60-90 min. A second activation / coupling cycle was also performed using the same methodology. Coupling

efficiency was estimated by the Kaiser test and prior to proceeding with the synthesis a capping step (Ac$_2$O / DIEA in DMF, 10-fold molar excess each) was usually performed.

4.2.3 Coupling of N-methyl residues

For the coupling of N-methyl (N-Me) residues the standard TBTU coupling as described under 4.2.1 and 4.2.2 was applied. In the Ct analogues (such as QCcyclo, QClinear), that were synthesized by both chemistries (Boc- and Fmoc-), the single N-methyl residue (N-Me) Phe[19] was coupled twice using 4-fold molar excess of protected amino acid in the presence of 4-fold molar excess TBTU and 6-fold molar excess DIEA. However, in the IAPP analogues, the N-methylated residues (N-Me) Phe, (N-Me) Gly, (N-Me) Ala, (N-Me) Ile, (N-Me) Leu were coupled using up to 10-fold excess of the protected amino acid with the corresponding amounts of TBTU and DIEA. Coupling times were often longer than the ones used for non-N-methylated amino acids, whereas use of mixture of solvents or coupling at elevated temperatures were usually employed. These procedures depending on the particular sequence to be synthesized are described (in detail) in the results part. The following tables (tables 6, 7, 8, 9, 10) provide an overview of the conditions used for the coupling of N-methylated amino acids.

Table 6. Coupling conditions for the TBTU-coupling of (N-Me) Phe[23] residue in IAPP analogue [1].

IAPP analogue	Synthesis	No. of Couplings	AA & TBTU[#] Excess	Time	Temp	Solvent	Acetylation after coupling
1	1st	2	6-fold	90 min 15 hrs	RT	Magic mix[1]	Yes

[#] ratio of AA / TBTU / DIEA was: 1 / 1 / 1.5

[1] magic mix was DMF / DCM / NMP: 1 / 1 / 1 (v/v/v) with 1% Triton X100

Table 7. Coupling conditions for the TBTU-coupling of (N-Me) Gly[24] residue in IAPP analogue [2].

IAPP analogue	Synthesis	No. of Couplings	AA & TBTU[#] Excess	Time	Temp	Solvent	Acetylation after coupling
2	1st	2	4-fold	90 min 135 min	RT	DMF	Yes

[#] ratio of AA / TBTU / DIEA was: 1 / 1 / 1.5

Table 8. Coupling conditions for the TBTU-coupling of (N-Me) Ile[26] residue in IAPP analogues [2], [4], and [5].

IAPP analogue	Synthesis	No. of Couplings	AA & TBTU[#] Excess	Time	Temp	Solvent	Acetylation after coupling
2	1st	3	4-fold	90 min 90 min 110 min	RT	DMF	Yes
4	1st	2	6-fold	17 hrs 4/17 hrs	RT 50 °C/RT	DMF	Yes
4	2nd	4	5-fold 5-fold 5-fold 7-fold	100 min 16 hrs 3 hrs 16/4/20 hrs	RT RT RT RT/40 °C/RT	DMF	Yes
5	1st	2	8-fold	17 hrs 4/17 hrs	RT 50 °C/RT	DMF	Yes
5	2nd	4	4-fold 4-fold 8-fold 4-fold	80 min 85 min 7/15 hrs 4 hrs	RT RT 50 °C/RT 60 °C	DMF	Yes

[#] ratio of AA / TBTU / DIEA was: 1 / 1 / 1.5

Table 9. Coupling conditions for the TBTU-coupling of (N-Me) Leu[27] residue in IAPP analogues [3], [4], and [5].

IAPP analogue	Synthesis	No. of Couplings	AA & TBTU[#] Excess	Time	Temp	Solvent	Acetylation after coupling
3	1st	1	2-fold	90 min	RT	DMF	No
3	2nd	2	4-fold	70 min 75 min	RT	DMF NMP	Yes
3	3rd	2	4-fold	70 min 75 min	RT	DMF	No
4	1st	2	4-fold	75 min 75 min	RT	DMF	No
4	2nd	2	4-fold	75 min 75 min	RT	DMF	No
5	1st	2	6-fold	75 min 75 min	RT	DMF	No
5	2nd	2	4-fold	70 min 90 min	RT	DMF	No

[#] ratio of AA / TBTU / DIEA was: 1 / 1 / 1.5

Table 10. Coupling conditions for the TBTU-coupling of (N-Me) Ala[25] residue in IAPP analogues [1], [3], and [5].

IAPP analogue	Synthesis	No. of Couplings	AA & TBTU[#] Excess	Time	Temp	Solvent	Acetylation after coupling
1	1st	2	5-fold	90 min	RT	DMF	No
3	1st	1	2-fold	110 min	RT	DMF	No
3	2nd	2	4-fold	70 min 60 min	RT	DMF NMP	Yes
5	1st	1	10-fold[§]	24 hrs	RT	Magic mix[1]	No
5	2nd	2	8-fold 4-fold	1.3/5 hrs 18 hrs	50 °C/ RT RT	DMF	No

[#] ratio of AA / TBTU / DIEA was: 1 / 1 / 1.5
[§] no DIEA was used
[1] magic mix was DMF / DCM / NMP: 1 / 1 / 1 (v/v/v) with 1% Triton X100

4.2.4 Coupling on N-methyl residues

Coupling of amino acids on N-methyl residues was as difficult as the coupling of N-methyl amino acids. The coupling efficiency could only be evaluated by a small-scale cleavage of peptide resin, chromatographic separation of peptides and characterization by mass spectroscopy, because the Kaiser test could not be applied (see 4.2.5). The following tables (tables 11, 12, 13, 14, 15, 16, 17, 18) provide a summary of the coupling conditions in the region [19-27] of the IAPP analogues.

Table 11. Synthesis summary in region [19-27)] for IAPP analogue [1].

AA residue	Excess	No. couplings	Conditions	Cleavage	Acetylation
Leu[27]	4-fold	2	DMF: 1 x 70 min DMF: 1 x 70 min		
Ile[26]	4-fold	2	DMF: 1 x 60 min DMF: 1 x 80 min	x	
(N-Me) Ala[25]	5-fold	2	DMF: 1 x 90 min DMF: 1 x 90 min		
Gly[24]	5-fold	2	DMF: 1 x 75 min DMF: 1 x 15 hrs	x	x
(N-Me) Phe[23]	6-fold	2	DMF: 1 x 90 min Magic mix[1]: 1 x 15 hrs	x	x
Asn[22]	6-fold 10-fold 6-fold	3	DMF: 1 x 90 min DMF: 1 x 14 hrs Magic mix[1]: 1 x 90 min	x	x
Asn[21]	6-fold 10-fold	2	DMF: 1 x 145 min DMF: 1 x 16 hrs		x
Ser[20]	6-fold	2	DMF: 1 x 60 min DMF: 1 x 55 min		
Ser[19]	6-fold	2	DMF: 1 x 65 min DMF: 1 x 60 min	x	

[1] magic mix was DMF / DCM / NMP: 1 / 1 / 1 (v/v/v) with 1% Triton X100

Table 12. Synthesis summary in region [19-27] for IAPP analogue [2].

AA residue	Excess	No. couplings	Conditions	Cleavage	Acetylation
Leu[27]	4-fold	2	DMF: 1 x 90 min DMF: 1 x 90 min		
(N-Me) Ile[26]	4-fold	3	DMF: 1 x 90 min DMF: 1 x 90 min DMF: 1 x 110 min	x	x
Ala[25]	4-fold 4-fold 6-fold 6-fold 6-fold	5	DMF: 1 x 90 min DMF: 1 x 90 min DMF: 1 x 90 min DMF: 1 x 90 min NMP: 1 x 150 min	x	x
(N-Me) Gly[24]	4-fold	2	DMF: 1 x 90 min DMF: 1x 135 min	x	x
Phe[23]	6-fold	3	DMF: 1 x 90 min DMF: 1 x 150 min	x	x
Asn[22]	6-fold	2	DMF: 1x 100 min DMF: 1 x 100 min		
Asn[21]	6-fold	2	DMF: 1 x 90 min DMF: 1 x 120 min		
Ser[20]	6-fold	2	DMF: 1 x 80 min DMF: 1 x 60 min		
Ser[19]	6-fold	2	DMF: 1 x 90 min DMF: 1 x 80 min	x	

Table 13. Synthesis summary in region [19-27] for IAPP analogue [3] / (1st synthesis).

A.A residue	Excess	No. couplings	Conditions	Cleavage	Acetylation
(N-Me) Leu[27]	2-fold	1	DMF: 1 x 90 min		
Ile[26]	2-fold	2	DMF: 1 x 75 min DMF: 1 x 75 min		x
(N-Me) Ala[25]	2-fold	1	DMF: 1 x 110 min		
Gly[24]	2-fold	2	DMF: 1 x 80 min DMF: 1 x 95 min	x	x
Phe[23]	2-fold	2	DMF: 1 x 60 min DMF: 1 x 60 min		
Asn[22]	2-fold	2	DMF: 1 x 80 min DMF: 1 x 90 min		
Asn[21]	2-fold	2	DMF: 1 x 75 min DMF: 1 x 80 min		
Ser[20]	2-fold	2	DMF: 1 x 60 min DMF: 1 x 60 min		
Ser[19]	2-fold	2	DMF: 1 x 70 min DMF: 1 x 80 min	x	

Table 14. Synthesis summary in region [19-27] for IAPP analogue [3] / (2nd synthesis).

A.A residue	Excess	No. couplings	Conditions	Cleavage	Acetylation
(N-Me) Leu^{27}	4-fold	2	DMF: 1 x 70 min NMP: 1 x 75 min		x
Ile^{26}	4-fold	2	DMF: 1 x 75 min NMP: 1 x 85 min		x
(N-Me) Ala^{25}	4-fold	2	DMF: 1 x 70 min NMP: 1 x 60 min		x
Gly^{24}	4-fold	2	DMF: 1 x 70 min NMP: 1 x 80 min	x	x
Phe^{23}	4-fold	2	DMF: 1 x 60 min DMF: 1 x 70 min		
Asn^{22}	4-fold	2	DMF: 1 x 100 min DMF: 1 x 75 min		
Asn^{21}	4-fold	2	DMF: 1 x 60 min DMF: 1 x 70 min		
Ser^{20}	4-fold	2	DMF: 1 x 65 min DMF: 1 x 75 min		
Ser^{19}	4-fold	2	DMF: 1 x 65 min DMF: 1 x 80 min	x	

Table 15. Synthesis summary in region [19-27] for IAPP analogue [4] / (1st synthesis).

A.A residue	Excess	No. couplings	Conditions	Cleavage	Acetylation
(N-Me) Leu^{27}	4-fold	2	DMF: 1 x 75 min DMF: 1 x 75 min		
(N-Me) Ile^{26}	6-fold	2	DMF: 1 x 17 hrs DMF: WB* 4 hrs/17 hrs	x	x
Ala^{25}	5-fold	3	DMF: 1 x 6 hrs DMF: 1 x 18 hrs DMF: 1 x 150 min	x	x
Gly^{24}	5-fold	2	DMF: 1 x 100 min DMF: 1 x 3 hrs		
Phe^{23}	5-fold	3	DMF: 1 x 100 min DMF: 1 x 11 hrs DMF: 1 x 18 hrs	x	x
Asn^{22}	5-fold	2	DMF: 1 x 120 min DMF: 1 x 140 min		
Asn^{21}	5-fold	2	DMF: 1 x 2 hrs DMF: 1 x 18 hrs		x
Ser^{20}	5-fold	2	DMF: 1 x 70 min DMF: 1 x 80 min		
Ser^{19}	5-fold	2	DMF: 1 x 70 min DMF: 1 x 80 min	x	

* Water Bath

Table 16. Synthesis summary in region [19-27] for IAPP analogue [4] / (2nd synthesis).

A.A residue	Excess	No. couplings	Conditions	Cleavage	Acetylation
(N-Me) Leu[27]	4-fold	2	DMF: 1 x 95 min DMF: 1 x 150 min		
(N-Me) Ile[26]	5-fold 5-fold 5-fold 7-fold	4	DMF: 1 x 100 min DMF: 1 x 16 hrs DMF: 1 x 3 hrs DMF: 16 hrs / WB* 4hrs / 20 hrs	x	x
Ala[25]	6-fold	3	DMF: WB 2 hrs / 23hrs DMF: WB 3hrs / 19hrs DMF: WB 3 hrs / 14hrs	x	x
Gly[24]	5-fold	2	DMF: 1 x 75 min DMF: 1 x 140 min		
Phe[23]	5-fold	2	DMF: 1 x 85 min DMF: 1 x 80 min		
Asn[22]	5-fold	2	DMF: 1 x 120 min DMF: 1 x 80 min		
Asn[21]	5-fold	2	DMF: 1 x 75 min DMF: 1 x 60 min		
Ser[20]	5-fold	2	DMF: 1 x 75 min DMF: 1 x 85 min		
Ser[19]	5-fold	2	DMF: 1 x 105 min DMF: 1 x 110 min	x	

* Water Bath

Table 17. Synthesis summary in region [25-27] for IAPP analogue [5] / (1st synthesis)

A.A residue	Excess	No. couplings	Conditions	Cleavage	Acetylation
(N-Me) Leu[27]	6-fold	2	DMF: 1 x 75 min DMF: 1 x 75 min	x	
(N-Me) Ile[26]	8-fold	2	DMF: 1 x 17 hrs DMF: WB* 4 hrs / 17 hrs	x	x
(N-Me) Ala[25]	10-fold	1	Magic mix[1] : 1 x 24 hrs	x	

* Water Bath
[1] Magic mix was DMF / DCM / NMP: 1 / 1 / 1 (v/v/v) with 1% Triton X100

Table 18. Synthesis summary in region [25-27] for IAPP analogue [5] / (2nd synthesis)

A.A residue	Excess	No. couplings	Conditions	Cleavage	Acetylation
(N-Me) Leu27	4-fold	2	DMF: 1 x 70 min DMF: 1 x 90 min		
(N-Me) Ile26	4-fold 4-fold 8-fold 4-fold	4	DMF: 1 x 80 min DMF: 1 x 85 min DMF: WB* 7 hrs / 15 hrs DMF: WB* 4 hrs	x	x
(N-Me) Ala25	4-fold 8-fold	2	DMF: 1 x 18 hrs DMF: WB* 90 min / 5hrs	x	

* Water Bath

4.2.5 Kaiser test

The most widely used test for the presence or absence of free amino groups on a peptide resin (deprotection / coupling steps) was devised by E.T.Kaiser [63]. The test is simple and quick. However some amino groups (such as in Ser, Asn) do no show the expected dark blue colour that is typical for more than 95% free primary amino groups. Additionally, the test could not be applied in the case of the imino-acid Pro or N-methylated amino acids because the test could detect only primary amino groups and not secondary. Occasionally, also false negative tests are observed (as in the case of a sterically hindered N^α amino group) [64].

For the Kaiser test the following three solutions are prepared:

- Ninhydrin in ethanol (5 gr in 100 ml ethanol)
- Phenol in ethanol (40 gr in 10 ml ethanol)
- An aqueous solution of potassium cyanide in pyridine (2 ml of aqueous 0.001 M KCN in 100 ml pyridine)

A small sample of resin is placed into a glass test tube and washed three times with ethanol. Two drops of each of the above solutions is then added to the resin and the mixture is mixed thoroughly and heated at 110 °C for 5 min. Blue beads and blue solution indicate the presence of more than 95% free amino groups while a yellow solution and yellow beads indicate that the coupling is more than 99% complete.

4.2.6 Attachment of the C-terminal amino acid to the resin

There are several linkers and derivatized resins for Boc- and Fmoc-SPPS available. For the synthesis of peptide amides (as in the case of Ct, IAPP and analogues), resins with linkers containing a free amino group were selected (MBHA for Boc- and Rink Amide MBHA for Fmoc-chemistry).

4.2.6.1 Attachment of the C-terminal amino acid for the synthesis of Ct analogues using Boc-strategy

Attachment of the C-terminal residue (Boc-Pro) was achieved using the following synthetic protocol: in 1gr of resin, Boc-protected amino acid (10-fold molar excess with regard to the substitution level of the resin) was coupled using TBTU (10-fold excess) and DIEA (15-fold excess). After 2 hrs coupling time Kaiser test indicated the completeness of the reaction. The resin was acetylated (Ac$_2$O / DIEA 10-fold molar excess each in DCM) for 1 hr before proceeding with the synthesis.

4.2.6.2 Attachment of the C-terminal amino acid for the synthesis of Ct analogues using Fmoc-strategy

Attachment of the C-terminal residue (Fmoc-Pro) was achieved using the following protocol: in 1gr of resin, Fmoc-protected amino acid (5-fold molar excess with regard to the substitution level of the resin) was coupled using TBTU (5-fold excess) and DIEA (7.5-fold excess). After 2 hrs coupling time, Kaiser test or determination of the substitution level of the resin was performed as follows.

4.2.6.3 Attachment of the C-terminal amino acid for the synthesis of IAPP analogues

The C-terminal residue [Fmoc-Tyr(tBu)] was attached to the resin taking into consideration the intended 'dilution' of the substitution level of the resin (substitution level of resin usually was 0.5-0.7 mmole / gr, the intended substitution level between 0.2-0.3 mmole / gr). The protected amino acid (80% with regard to the total amount of NH$_2$ groups of the resin) was coupled using TBTU and DIEA (ratio of AA / TBTU / DIEA: 1 / 1 / 1.5). After 4 hrs coupling

time, determination of the substitution level was estimated as below (4.2.6.4). Depending on the determined substitution level, the coupling was repeated or capping of unreacted amino groups (Ac_2O / DIEA in DMF, 10-fold molar excess each with regard to the total NH_2-groups of the resin) for 1 hr was performed.

4.2.6.4 Determination of the substitution level of resin in Fmoc-strategy

Estimation of the substitution level of Fmoc-protected peptide resin was performed by measuring the absorbance of the piperidine-dibenzofulvene adduct that is generated after Fmoc-cleavage as follows: two aliquots of the dry peptide resin (3-4 mg) were weighted in a volumetric flask (10 ml), which was then filled with 25% piperidine in DMF and left to stand for 15 min. Thereafter, the absorbance at 290 nm was measured and the substitution level of the peptide resin was estimated by the formula:

Substitution level: $(Ab_{290nm} \times 10) / (\varepsilon \times w \times 10^{-3})$ in mmole / gr

where Ab_{290nm} : absorbance of sample at 290 nm

ε : molecular coefficient of piperidine-dibenzofulvene at 290 nm = 5800

w : weight of peptide resin (in mg)

The resin was acetylated (Ac_2O / DIEA 10-fold molar excess each in DMF) for 1 hr before proceeding with the synthesis.

4.2.7 Final deprotection of side-chains and cleavage from the resin

4.2.7.1 Final deprotection of side chains and cleavage of full length sequences from the resin in Boc-chemistry

The most popular reagent for cleavage of peptides synthesized by Boc-chemistry is anhydrous HF. This procedure appears to be the most versatile and least harmful to the peptides attached to the resin [65]. The major disadvantage of the procedure remains its highly toxic and reactive nature, which requires the use of an HF resistant cleavage apparatus. Before HF cleavage the N-terminal Boc-group was removed from the peptide resin, followed by proper washes (DCM, DMF, Et_2O) and drying in dessicator. The HF cleavage was performed for 30 min at –

20 °C, and 1 hr at 0 °C. The crude Ct peptides were obtained by treatment of the peptide resin (200 mg) with 10 ml of a mixture of (HF / TAS / DMS / p-thiocresol) (10 / 1 / 1 / 2, v/v/v/w). Cysteine (500 mg) was added to the cleavage mixture in order to suppress a possible N-terminal thiazolidine formation, which is likely to occur during HF cleavage of peptides with N-terminal Cys and the Bom-group for the side chain protection of His [66]. Following accomplishment of the cleavage reaction, HF and DMS were evaporated and cold diethylether was added to the peptide resin. The precipitated crude peptide was filtered together with the resin and washed with cold diethylether (3 times) to remove the scavengers. Thereafter, 10% aqueous AcOH was used to extract (3 times) the product from the peptide resin mixture and the extracts were collected and lyophilised.

4.2.7.2 Final deprotection of side chains and cleavage of full length sequences from the resin in Fmoc-chemistry

The N-terminal Fmoc-group was first removed (with 25% piperidine in DMF) and the peptide resin was dried. Thereafter, the cleavage of side chain protecting groups and the peptide from the resin was carried out by treatment of the resin with TFA and scavengers. A widely used cleavage mixture is a slight modification of reagent K [TFA / water / TAS / EDT / phenol: 83 / 4.5 / 4.5 / 2 / 6 (v/v/v/v/w)] [67]. Cleavage of the peptide resins were carried out at a concentration of 50-100 mg resin per 12 ml reagent K for 3 hrs at room temperature. After filtering the reaction mixture through a fritted funnel and washing with TFA (three times), the filtrate was evaporated (at ~ 30-33 °C). The resulting crude peptide was dissolved in 10% AcOH and the AcOH solution was then extracted with cold diethylether (three times at 4 °C). Extraction was performed as follows: following addition of diethylether and mixing, the solution was centrifuged (2000g, 3 min) and the ether layer was discarded. Thereafter, the aqueous layer was lyophilised.

In the case of the IAPP analogue [6] [S20G-IAPP], the post cleavage work up procedure was as follows: the TFA solution (after filtering out the resin) was evaporated in a rotary evaporator till a small volume (~2 ml) and was transferred to a centrifuge containing cold diethylether. The peptide was left to precipitate (~10-15 min), was centrifuged (2000g, 2 min) and the ether layer was removed. The precipitate was then washed with cold ether twice (as above) and after the final removal of the ether, the precipitated peptide was dissolved in10% AcOH (~5 ml) plus some drops of 50% AcOH, and lyophilised.

4.2.7.3 Deprotection of side chains and cleavage of partial peptide sequences from the resin in Fmoc-chemistry

Partial peptide sequences (mostly in IAPP analogues) with 10 to 15 residues were cleaved from the resin after treatment of the resin with TFA / H_2O (95 / 5 v/v) for 2 hrs at RT. The absence of residues such as Cys, Arg, Met enabled the cleavage without the addition of scavengers in the cleavage mixture [68]. Again, the N-terminal Fmoc-group was first removed (with 25% piperidine in DMF) and the peptide resin was dried. After 2 hrs treatment with TFA / H_2O the peptide / resin mixture was transferred with a pasteur pipette to a fritted eppendorf tube, washed with neat TFA and centrifuged (2000g, 2 min). The TFA / peptide solution was diluted 10-fold in H_2O and extracted with cold diethylether (as described under 4.2.7.2). The aqueous layer was then analysed by RP-HPLC and eluting peptide peaks were collected and lyophilised. MALDI-MS of the peptide peaks provided valuable information concerning the difficulties (incomplete couplings, deletion sequences) encountered during the peptide chain assembly.

4.2.8 Disulfide bridge formation

4.2.8.1 Disulfide bridge formation for the Ct analogues

Crude peptides in their reduced form were subjected to air oxidation (in the dark) for disulfide bridge formation (Cys^1 to Cys^7). This was achieved by dissolving crude material (~1 mg / ml) in aqueous 0.1 M NH_4HCO_3 containing 1.5 M Gdn HCl. Gdn HCl was included to improve solubilities of the peptides and oxidation yields. The completion of the oxidation was monitored by RP-HPLC and for Ct sequences 2 hrs were usually sufficient time for the oxidation to be accomplished.

4.2.8.2 Disulfide bridge formation for the IAPP analogues

The IAPP analogues were also subjected to air oxidation (in the dark) for disulfide bridge formation (Cys^2 to Cys^7). Oxidations (1 mg crude material / ml solution) were performed in aqueous 0.1 M NH_4HCO_3, containing 3 M Gdn HCl to improve solubilities of the peptides and oxidation yields [except for IAPP and S20G-IAPP in which 6 M Gdn HCl was used]. The

completion of the oxidation was monitored by RP-HPLC and for IAPP analogues 2-4 hrs were usually required for the oxidation to be accomplished.

4.2.9 RP-HPLC purification of the products

Purification of the products (Ct and IAPP analogues) was carried out by RP-HPLC on a C_{18} Nucleosil column with a length of 25 cm, internal diameter of 8 mm and 7 μm particle size. The device consisted of a Biotronic (Maintal, Germany) BT-8100 HPLC pump, a Biotronic BT-8200 uv-vis detector and a Shimadzu (Kyoto, Japan) C-R6A integrator. The flow rate was 2 ml / min and eluting buffers were: A, 0.058% (v/v) TFA in water and B, 0.05% (v/v) TFA in 90% ACN / water. Peptides were detected at 214 nm and the gradients that were applied are shown in the tables 19, 20 and 21. Eluates containing peptide peaks were immediately frozen in dry ice, and lyophilised.

Table 19. HPLC gradient 1 [Change of gradient over time (ΔG): 1% / min)].

Step	Time (min)	Buffer A (%)	Buffer B (%)
1	0	70	30
2	7	70	30
3	37	40	60

Table 20. HPLC gradient 2 (ΔG: 2.66% / min).

Step	Time (min)	Buffer A (%)	Buffer B (%)
1	0	90	10
2	1	90	10
3	31	10	90

Table 21. HPLC gradient 3 (ΔG: 0.74% / min).

Step	Time (min)	Buffer A (%)	Buffer B (%)
1	0	65	35
2	7	65	35
3	34	45	55

4.2.10 Characterization of the peptides

4.2.10.1 Matrix Assisted Laser Desorption Ionisation Mass Spectroscopy (MALDI-MS)

Characterization of the oxidized and HPLC purified peptides was performed by MALDI-MS with a Kompact MALDI Kratos Analytical system (Duisburg, Germany). Peptides were dissolved in a (1:1) mixture of 5% TFA and 70% ACN / 0.01% TFA. Thereafter, 1.5 µl of α-cyano-4-hydroxycinnamic acid (matrix) was placed on the slide, air dried and then 1.5 µl of the peptide sample were added. The mass was recorded on the positive ion mode and average mass was determined as $[M+H]^+$. The average expected mass of the peptides was calculated using the Peptide Companion software (WindowChem Software, North Fairfield, USA).

4.2.10.2 Fast Atom Bombardment Mass Spectroscopy (FAB-MS)

Partial sequences of peptides (Ct and IAPP sequences) with a mass smaller than 2000 Dalton, were also measured by FAB using a MAT 711A Finnigan mass system (Bremen, Germany). Peptides were dissolved in liquid matrix (glycerol). The mass was recorded on the positive ion mode and average mass was determined as $[M+H]^+$.

4.2.10.3 Amino acid analysis

Peptides (0.5 mg) were hydrolysed for 24 hrs in 6 M HCl at 110 °C. Samples were loaded into an Eppendorf (Hamburg, Germany) LC3000 amino acid analyser equipped with a cation exchange resin column. Sample concentration was 100 µM and ninhydrin post column derivatisation with detection at 570 nm was used for the determination of the amino acids [69].

4.2.11 Concentration determination of Ct and IAPP solutions with UV spectroscopy

HPLC purified peptides were stored in lyophilised form at –20 °C. Peptide stock solutions were made by dissolving the peptide in 1 mM HCl to a final concentration of about 500 µM. An exact concentration determination was necessary and was performed using UV-spectroscopy with a Kontron Uvicon (Watford, UK) spectrophotometer. UV absorbance of

the peptide solution was measured between 330 and 240 nm and the absorbance at 274.5 nm was used to determine the exact peptide concentration (a representative example is shown in Figure 9). At this wavelength, the extinction coefficient of the Tyr residue (ε=1370 M^{-1} cm^{-1}) and the disulfide bridge of Cys^{1} and Cys^{7} (ε=70 M^{-1} cm^{-1}) was 1440 M^{-1} cm^{-1}. Peptide concentrations were calculated according to the formula:

$$[C] = Ab_{274.5nm} / (\varepsilon \times l)$$

where
ε= molecular extinction coefficient of peptides at 274.5nm

l= the length of the cuvette (1 cm)
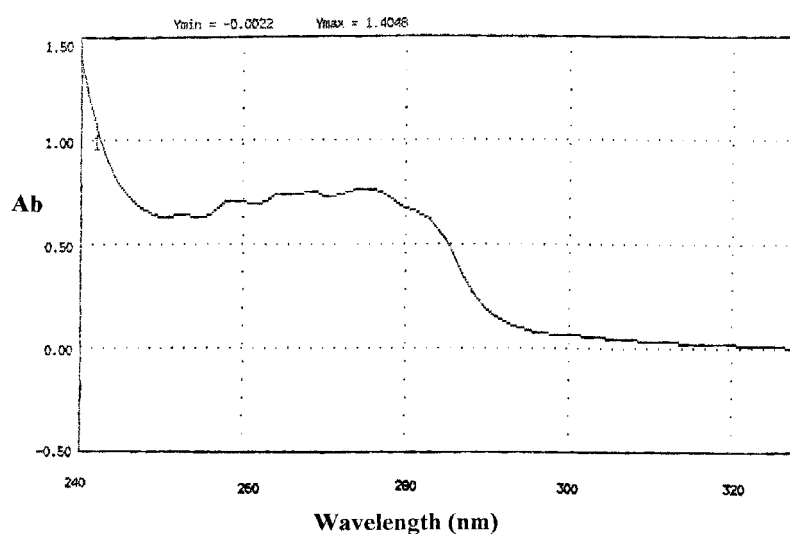
Figure 9. UV spectrum of a 0.52 mM stock solution of GCcyclo (in 1 mM HCl).

4.2.11.1 Secondary structure of IAPP with FT-IR spectroscopy

Fibrillar IAPP was prepared under strong amyloidogenic conditions as follows: 10% acetic acid was added to peptide solutions to give a concentration of 2.14 mM. Following incubation at RT for 4 days, the solution was neutralized with 10% NH$_4$OH. Insoluble aggregates were collected and dried over KOH platlets. They were resuspended in ^{2}H$_2$O at an apparent concentration of 5 mM, applied onto a CaF$_2$ plate and air-dried. Spectra were measured in a Perkin-Elmer spectrophotometer (Spectrum 1000).

4.2.12 Biological Assays

4.2.12.1 Cell culture

The biological activity of the synthetic Ct analogues were tested using the human breast cancer cell line T47D that was obtained from the American Tissue Culture Collection. Cells were cultured in RPMI 1640 medium supplemented with 10% heat inactivated fetal bovine serum, 1% streptomycin / penicillin, 0.1 µM insulin and 0.1 µM hydrocortisone. Cells were grown at 37 °C in a humidified atmosphere containing 5% CO_2. The hormones were removed from the medium when subculturing the cells 2-3 days prior to the binding assays. Cells were subcultured in 12-well plates for the receptor binding experiments or in 96-well plates for the EIA experiments and were used when reached a confluence of 90%.

4.2.12.2 Calcitonin receptor binding assay

The receptor binding assay was performed based on the following protocol: cells in the 12-well plates (1ml / well or 0.2×10^6 cells / well) were washed with phosphate buffered saline (PBS) (1 x 1 ml) at ambient temperature and then prewarmed (at 37 °C) assay buffer that consisted of RPMI 1640 with 0.1% bovine serum albumin (BSA) (w/v) was added to each well (930µl). [125]Iodine-labelled sCt (5 µCi, specific activity 2000 Ci per mmole, labelled at Tyr[22]) in its lyophilised form was reconstituted in 0.1 M HCl (200 µl) and aliquoted in eppendorf tubes (15 µl each), that were kept at –20 °C). For each 12-well plate, one aliquot containing 0.38 µCi was thawed at RT, diluted with assay buffer (245 µl) and used immediately. Twenty microliters of this solution of the tracer (0.03 µCi) were added to each well at room temperature and the plate was mixed by gentle shaking. Thereafter, solutions (50 µl) of different peptide concentrations in assay buffer were added to the cells and following gentle mixing, cells were incubated for 1 hr at RT. Peptide solutions were freshly made prior to each experiment by diluting peptide stocks (~500 µM in 1mM HCl) in assay buffer. Binding to the calcitonin receptor was terminated by aspiration of the medium and washings of the cells with PBS (3 x 3 ml each time). Cells were scraped from the wells by short treatment (1 min) with 0.5 M NaOH (2 x 0.5 ml each time) and placed into plastic vials. Bound radioactivity was then measured using a γ-counter LKB Wallac 1282 CompuGamma

(Stockholm, Sweden). Specific binding was calculated as the difference between total binding (tracer alone) and non-specific binding (100 nM unlabelled sCt).

4.2.12.3 Adenylate cyclase activation assay

T47D cells were subcultured in 96-well plates two days prior the experiment (as described under 4.2.12.1). At the day of the experiment ($\sim 10^4$ cells per 100 µl culture medium) the medium was removed. The cells were washed with PBS (200 µl) and then assay medium that consisted of RPMI 1640 with 0.1% BSA (w/v) was added (100 µl). Peptide solutions of different concentrations (freshly made and kept on ice) were added (100 µl) to the cells and incubations were performed for 15 min at 37 °C. Thereafter, the medium was removed and 200 µl of cell lysis buffer 1B that consisted of 0.25% dodecyltrimethylammonium bromide (DTAB) in 0.05 M acetate buffer pH 5.8 with 0.02% w/v BSA were added to each well. An aliquot of the cell lysate containing solution (20 µl) was then diluted 25-fold with lysis buffer 1B and then a sample (100 µl) was transferred to the EIA plate. In each well of the plate, rabbit antiserum (reconstituted with 11 ml lysis buffer 2B) was added (100 µl) and the solution was incubated for 2 hrs at 4 °C. Thereafter, the cAMP horseradish peroxidase-conjugate was reconstituted in 11 ml assay buffer and 50 µl were added to each well and the plate was incubated for 1 hr at 4 °C. The solution was then removed from the wells, and the plate was thoroughly washed with 0.01 M phosphate buffer (pH 7.5) containing 0.05 w/v Tween 20. Residual liquid was removed by blotting the plate on tissue paper. Immediately thereafter 150 µl of the solution containing the enzyme substrate (solution consisted of 3,3´, 5,5´-tetramethylbenzidine (TMB) / hydrogen peroxide in 20% v/v DMF) was added to all wells (a blue colour started to develop). The plate was mixed using a Rocky shaker (LTF Labortechnik, Wasserburg, Germany) for 20 min at RT, and the reaction was stopped (at 20 min) by adding 1 M H_2SO_4 to all wells (100 µl). Thereafter the plate was placed in the Biorad 3550 EIA reader (München, Germany) and the optical density at 450 nm was measured.

4.2.12.4 Cytotoxicity assay for IAPP and IAPP analogue [2]

The HTB14 human glioblastoma/astrocytoma cell line (American Type Culture Collection) was cultured in Dulbecco's modified Eagle's medium containing 10% heat-inactivated fetal bovine serum, 2 mM glutamine, and 0.1 mg / ml penicillin / streptomycin. Exponentially

growing cells were plated at a density of 1 x 10^5 cells / ml (100 µl / well). Following incubation for 24 hrs (37 °C, humidified atmosphere with 5 % CO_2), serial dilutions of the peptide were made in cell culture medium and 11 µl added to the culture wells. The original peptide solution were 5 µM IAPP in 10 mM sodium phosphate buffer (pH 7.4) containing 1% 1,1,1,3,3,3-hexafluro-2-propanol (HFIP). These solutions were incubated for 1 day at RT. Final concentrations of peptide in the wells were 50 and 5 nM. Cell viability was assessed 24 hrs later by measuring the cellular reduction of 3-[4,5-dimethylthiazol-2-yl]-2,5-diphenyltetrazolium bromide (MTT) by measuring the absorbance at 595 nm.

Complete inhibition of cell function (0% viability) was defined as the absorbance value obtained in wells containing 0.1% Triton X-100; 100% MTT reduction was defined as the absorbance value obtained upon the addition of the vehicle alone. For the calculation of cell viability (% of control) the following formula was used:

$$\% \text{ MTT reduction} = [(Ab_{sample} - Ab_{0.1\%\ Triton}) / (Ab_{medium} - Ab_{0.1\%\ Triton}) \times 100$$

5 Results

5.1 Design of calcitonin analogues

The calcitonins from different species (i.e. human, salmon, eel, porcine) have a number of common structural features. These include a N-terminal disulfide loop linking cysteine residues 1 and 7, a potential amphiphilic α-helix between 8 and 22, and a C-terminal amide. In 1995, Kapurniotu and Taylor [22] designed, synthesized and studied three hCt analogues with lactam bridges joining the side-chains of residues 17 and 21 or the side-chains of residues 10 and 14. For these syntheses, residues Asn[17] and Thr[21] were replaced by Lys[17] and Asp[21], Asp[17] and Lys[21] and residues Gly[10] and Gln[14] by Lys[10] and Asp[14] resulting in the analogues: cyclo[17,21]-[Lys[17], Asp[21]]hCt (1), cyclo[17,21]-[Asp[17], Lys[21]]hCt (2) and cyclo[10,14]-[Lys[10], Asp[14]]hCt (3). These types of lactam-bridged structures were chosen on the basis of their α-helix potential as previously found for several peptide hormones and model amphiphilic α-helical peptides [70]. The analogues incorporated the lactam bridge in positions corresponding to the hydrophilic face of the helix, leaving the hydrophobic face intact and charged residues were not selected for substitution in order to keep the overall charge of the molecule unchanged. Peptide 2 showed an 80-fold higher potency than hCt in the [^{125}I] sCt radioreceptor binding assay in rat brain membranes and a 10-fold increase in potency in the *in vivo* hypocalcemic assay in mice whereas the other two peptides (1) and (3) showed no significant increase in potency compared to hCt in either of these assays. However, correlations of the bioactivities with the solution conformations of the analogues as determined by circular dichroism (CD) indicated that a non-helical conformation might be important for bioactivity. The results indicated that a β-sheet / β-turn conformation that had been previously suggested by Motta *et al.* [37] for hCt residues 17-20 might correspond to the bioactive conformation of hCt.

To further study the role of a potential β-turn structure for hCt bioactivity, Kapurniotu *et al.* [71] have recently devised the following hCt analogues: cyclo[17,21]-[Asp[17], Orn[21]]hCt (CCcyclo), [Asp[17], Orn[21]]hCt (CClinear), cyclo[17,21]-[Asp[17], Dab[21]]hCt (DCcyclo), cyclo[17,21]-[Asp[17], Dap[21]]hCt (FCcyclo) and cyclo[17,21]-[Glu[17], Dab[21]]hCt (GCcyclo) (Scheme 2, group 1). These analogues were designed to study the effect of ring-size of the lactam-bridge of residues 17 and 21 on hCt conformation and bioactivity. These analogues contained shorter rings than the 20-membered ring of cyclo[17,21]-[Asp[17], Lys[21]]hCt (analog 1). This was achieved by replacing residue 21 by α,ω-diamino acid residues bearing side chains of various lengths. The results of the hypocalcemic assays showed dramatic effects of the various bridges on *in*

vivo hypocalcemic activity: CCcyclo was found to be ~ 400 times more potent than hCt and 4 times more potent than sCt. By contrast, no increased potency was found for the control peptide CClinear indicating that the enhanced *in vivo* bioactivity was due to the conformational restriction introduced by the lactam-bridge of the side-chains. The 18-membered ring containing DCcyclo was 30 times more potent than hCt, while the 17-membered ring containing FCcyclo showed a similar bioactivity to hCt. In spite of having the same ring size as CCcyclo, GCcyclo was 74 times less potent than CCcyclo. These findings would argue for local conformational feature that is strongly related to the position of the βCO of Asn^{17} and that may play an important role for hCt bioactivity, whereas the low activity of GCcyclo could be due to the incapability of the γCO of Glu^{17} to involve into the same hydrogen bonding as Asn or Asp in a so called 'Asx turn' [72]. These data together with the results of the conformational analyses indicated that a stabilized type I β-turn/antiparallel β-sheet conformation in region [17-21] might be associated with hCt bioactivity (Figure 10).
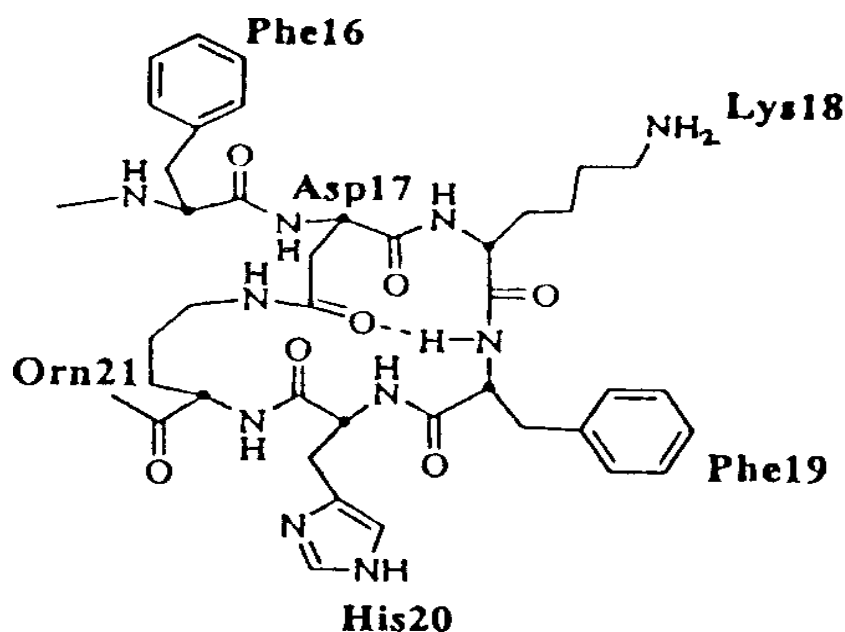
Figure 10. Schematic representation of the postulated lactam bridge-stabilized bioactive conformation in hCt between residues 17 and 21. The hydrogen bond, which might form between the side chain carbonyl of Asp^{17} and the αNH of Phe^{19}, is indicated by the dashed line.

To study the importance of the topological features of the region between residues 17 and 21 for bioactivity, and to test the hypothesis that a type I β-turn/β-sheet conformation in this region might be stabilized by the lactam bridge, several analogues of cyclo[17,21]-[Asp[17], Lys[21]] hCt having type I and type II β-turn-stabilizing substitutions for residues 18 and 19, as well as non-bridged control peptides were designed [73] (Scheme 3, group 2). Based on previously reported NMR data [37], this postulated β-turn might be centered at residues 18 and 19.

To study the effect of substituting residues in region [18-19] with amino acids that favor 'Asx-turn' (such as Pro at position (i+1) / Ser at position (i+2) of the turn) [74] the following analogues of cyclo[17,21]-[Asp[17], Orn[21]]hCt were designed: cyclo[17,21]-[Asp[17], Pro[18], Ser[19], Orn[21]] hCt (HCcyclo) and cyclo[17,21]-[Asp[17], Pro[18], Orn[21]]hCt (ICcyclo) as well as the linear control peptides [Asp[17], Pro[18], Ser[19], Orn[21]]hCt (HClinear) and [Asp[17], Pro[18], Orn[21]]hCt (IClinear) (Scheme 4, group 3).

To study the role of the hydrogen bond forming ability of the N^α-H of Phe[19], analogues cyclo[17,21]-[Asp[17], (N-Me) Phe[19], Orn[21]]hCt (QCcyclo) and [Asp[17], (N-Me) Phe[19], Orn[21]]hCt (QClinear) were designed (Scheme 5, group 4). These analogues incorporated a N^α-Me substitution at residue 19, that should abolish the potential hydrogen bond formation between the N^α-H of Phe[19] and the side chain CO of residue 17 which has been also proposed by Kapurniotu et al. [71] to be related to in vivo bioactivity (Figure 10).
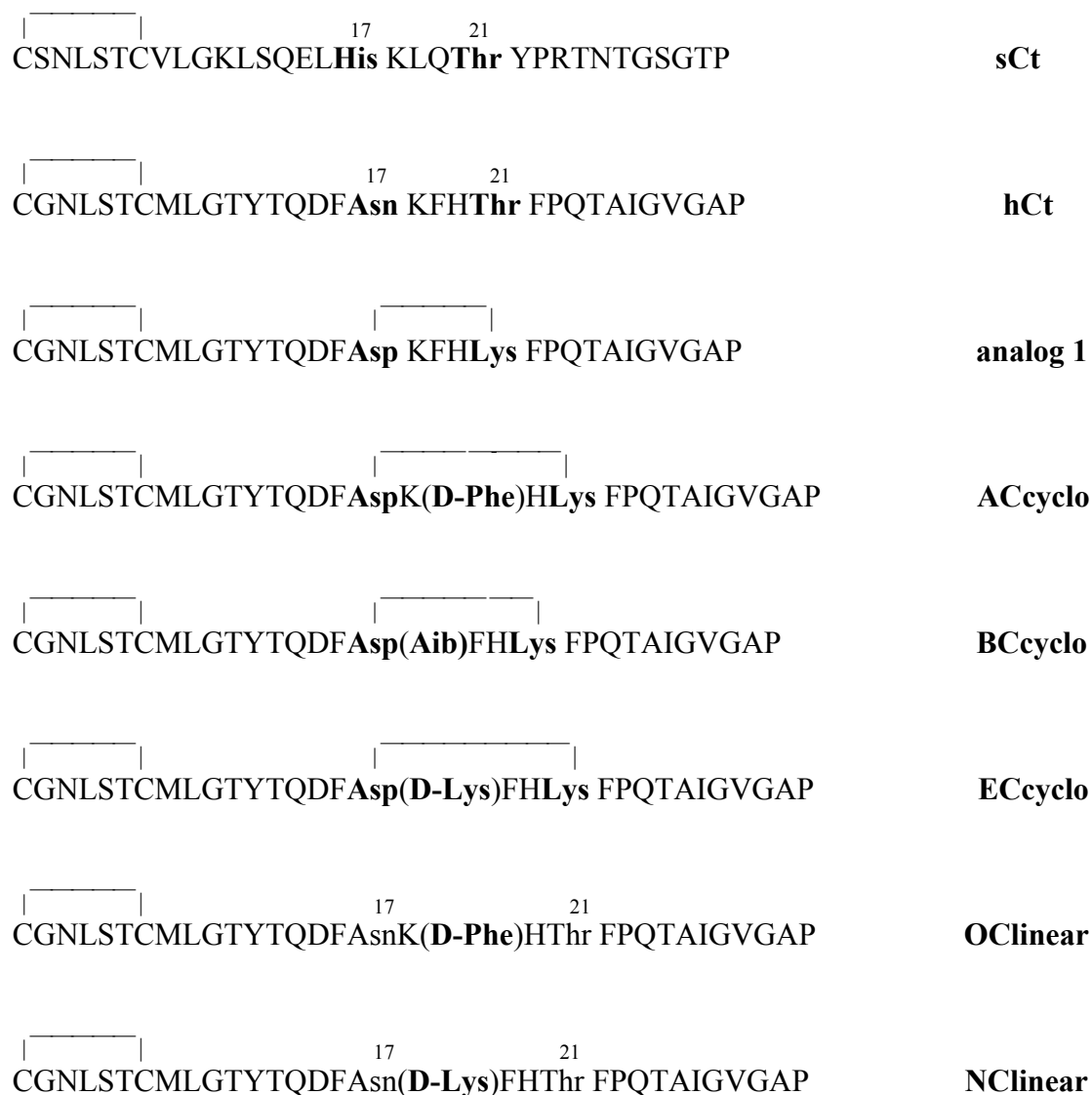
To study the effect of distorting the backbone on bioactivity the βeta-peptides: cyclo[17,21]-[βeta-Asp[17], Orn[21]]hCt (βeta-CCcyclo) and cyclo[17,21]-[βeta-Asp[17], (N-Me) Phe[19], Orn[21]]hCt (βeta-QCcyclo) as well as their linear control peptides [βeta-Asp[17], Orn[21]]hCt (βeta-CClinear) and [βeta-Asp[17], (N-Me) Phe[19], Orn[21]] (βeta-QClinear) were designed (Scheme 6, group 5). Also, hCt analogues [Dap[17]]hCt and [Dab[17]]hCt having Dap and Dab at position 17, respectively, were designed to provide additional insight into the importance of the side chain CO at position 17 for hCt bioactivity (Scheme 7, group 6).

Finally, two peptides were designed that combined the presence of substituents that have been previously found by others to be important for bioactivity and the Asp / Orn lactam bridge of CCcyclo. These peptides were cyclo[17,21]-[Nle[8], Leu[12,16,19], Asp[17], Orn[21], Tyr[22]]hCt (TCcyclo) and [Nle[8], Leu[12,16,19], Asp[17], Orn[21], Tyr[22]]hCt (TClinear) (Scheme 8, group 7) that carried a Nle[8] for Met[8] substitution, that eliminates the possibility of oxidation of Met[8], a Tyr[22] for Phe[22] substitution (since Tyr[22] is present in the sCt sequence it has been suggested to be important for bioactivity), and Leu substitutents for the residues 12,16, and 19 that might occupy the hydrophobic face of the potential amphiphilic helix of hCt (because Leu[12,16,19] are also present in sCt and have been linked to bioactivity) [75].
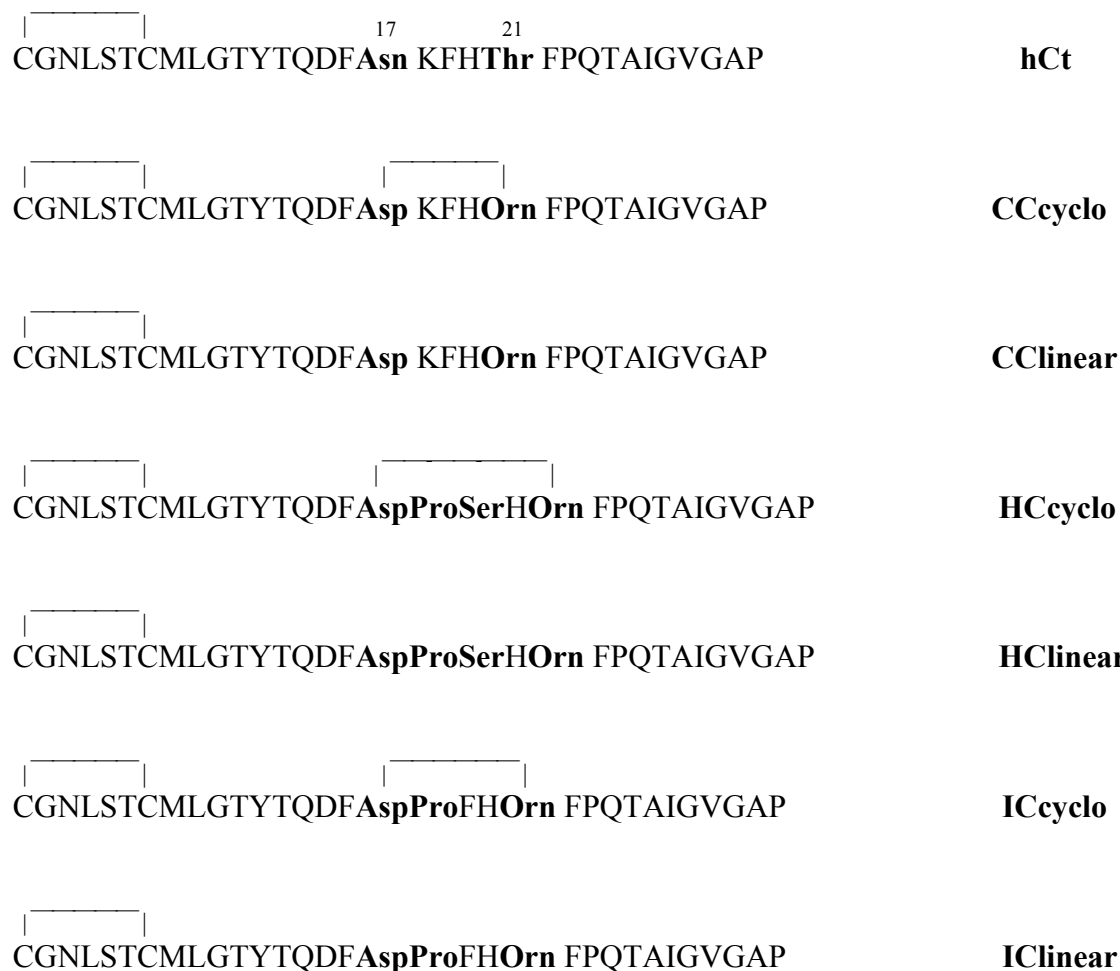
Scheme 2. Primary structures of sCt, hCt and analogues of group 1 to study the effect of ring size on Ct bioactivity.
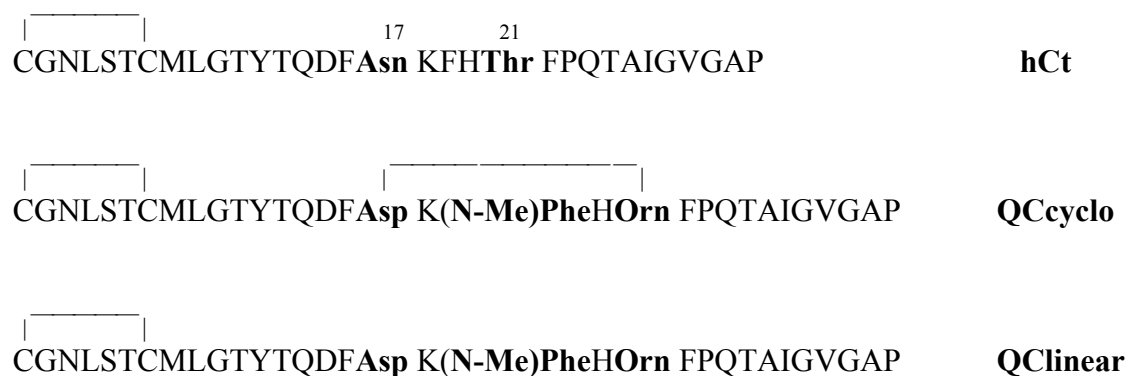
```
 |‾‾‾‾‾‾|              17      21
CSNLSTCVLGKLSQEL**His** KLQ**Thr** YPRTNTGSGTP                    **sCt**
```

```
 |‾‾‾‾‾‾|              17      21
CGNLSTCMLGTYTQDF**Asn** KFH**Thr** FPQTAIGVGAP                    **hCt**
```

```
 |‾‾‾‾‾‾|           |‾‾‾‾‾‾|
CGNLSTCMLGTYTQDF**Asp** KFH**Lys** FPQTAIGVGAP        **analog 1** (20-member ring)
```

```
 |‾‾‾‾‾‾|           |‾‾‾‾‾‾|
CGNLSTCMLGTYTQDF**Asp** KFH**Orn** FPQTAIGVGAP        **CCcyclo** (19-member ring)
```

```
 |‾‾‾‾‾‾|           |‾‾‾‾‾‾|
CGNLSTCMLGTYTQDF**Asp** KFH**Dab** FPQTAIGVGAP        **DCcyclo** (18-member ring)
```

```
 |‾‾‾‾‾‾|           |‾‾‾‾‾‾|
CGNLSTCMLGTYTQDF**Asp** KFH**Dap** FPQTAIGVGAP        **FCcyclo** (17-member ring)
```

```
 |‾‾‾‾‾‾|           |‾‾‾‾‾‾|
CGNLSTCMLGTYTQDF**Glu** KFH**Dab** FPQTAIGVGAP        **GCcyclo** (19-member ring)
```

```
 |‾‾‾‾‾‾|              17      21
CGNLSTCMLGTYTQDF**Asp** KFH**Orn** FPQTAIGVGAP        **CClinear**
```

Scheme 3. Primary structures of sCt, hCt, analog 1 and analogues of group 2 to study the importance of β-turn stabilizing residues at positions 18,19 (substituents are shown in bold).

```
          ┌────────┐            17      21
CSNLSTCVLGKLSQEL**His** KLQ**Thr** YPRTNTGSGTP                    **sCt**
```

```
          ┌────────┐            17      21
CGNLSTCMLGTYTQDF**Asn** KFH**Thr** FPQTAIGVGAP                    **hCt**
```

```
          ┌────────┐                  ┌────────┐
CGNLSTCMLGTYTQDF**Asp** KFH**Lys** FPQTAIGVGAP                    **analog 1**
```

```
          ┌────────┐                  ┌─────────────┐
CGNLSTCMLGTYTQDF**Asp**K(**D-Phe**)H**Lys** FPQTAIGVGAP           **ACcyclo**
```

```
          ┌────────┐                  ┌─────────────┐
CGNLSTCMLGTYTQDF**Asp(Aib)**FH**Lys** FPQTAIGVGAP                 **BCcyclo**
```

```
          ┌────────┐                  ┌─────────────┐
CGNLSTCMLGTYTQDF**Asp(D-Lys)**FH**Lys** FPQTAIGVGAP              **ECcyclo**
```

```
          ┌────────┐            17      21
CGNLSTCMLGTYTQDFAsnK(**D-Phe**)HThr FPQTAIGVGAP                  **OClinear**
```

```
          ┌────────┐            17      21
CGNLSTCMLGTYTQDFAsn(**D-Lys**)FHThr FPQTAIGVGAP                  **NClinear**
```

Scheme 4. Primary structures of hCt, CCcyclo, CClinear, and analogues of group 3 designed to study the importance of an 'Asx-turn' in region 17-21.

```
 |‾‾‾‾‾‾‾|              17      21
CGNLSTCMLGTYTQDFAsn KFHThr FPQTAIGVGAP                    hCt
```

```
 |‾‾‾‾‾‾‾|           |‾‾‾‾‾‾‾|
CGNLSTCMLGTYTQDFAsp KFHOrn FPQTAIGVGAP                    CCcyclo
```

```
 |‾‾‾‾|
CGNLSTCMLGTYTQDFAsp KFHOrn FPQTAIGVGAP                    CClinear
```

```
 |‾‾‾‾‾‾‾|                |‾‾‾‾‾‾‾‾‾|
CGNLSTCMLGTYTQDFAspProSerHOrn FPQTAIGVGAP                 HCcyclo
```

```
 |‾‾‾‾‾‾|
CGNLSTCMLGTYTQDFAspProSerHOrn FPQTAIGVGAP                 HClinear
```

```
 |‾‾‾‾‾‾‾|              |‾‾‾‾‾‾‾|
CGNLSTCMLGTYTQDFAspProFHOrn FPQTAIGVGAP                   ICcyclo
```

```
 |‾‾‾‾‾‾|
CGNLSTCMLGTYTQDFAspProFHOrn FPQTAIGVGAP                   IClinear
```

Scheme 5. Primary structures of hCt and analogues of group 4 designed to study the importance of the H-bonding ability of the NH of Phe[19].

```
 |‾‾‾‾‾‾|              17      21
CGNLSTCMLGTYTQDFAsn KFHThr FPQTAIGVGAP                    hCt
```

```
 |‾‾‾‾‾‾‾|           |‾‾‾‾‾‾‾‾‾‾‾‾‾‾|
CGNLSTCMLGTYTQDFAsp K(N-Me)PheHOrn FPQTAIGVGAP            QCcyclo
```

```
 |‾‾‾‾‾‾|
CGNLSTCMLGTYTQDFAsp K(N-Me)PheHOrn FPQTAIGVGAP            QClinear
```

Scheme 6. Primary structures of hCt and βeta-analogues of group 5 designed to study the effect of moving the side chain CO at position 17 / or distorting the backbone of CCcyclo on bioactivity.

```
     |⎯⎯⎯⎯|                   17        21
CGNLSTCMLGTYTQDF**Asn** KFH**Thr** FPQTAIGVGAP                            **hCt**
```

```
     |⎯⎯⎯⎯|                        |⎯⎯⎯|
CGNLSTCMLGTYTQDF**(βeta)Asp**KFH**Orn** FPQTAIGVGAP                  **βeta-CCcyclo**
```

```
     |⎯⎯⎯⎯|
CGNLSTCMLGTYTQDF**(βeta)Asp** KFH**Orn** FPQTAIGVGAP                 **βeta-CClinear**
```

```
     |⎯⎯⎯⎯|                        |⎯⎯⎯⎯⎯⎯|
CGNLSTCMLGTYTQDF**(βeta)Asp**K**(N-Me)Phe**H**Orn** FPQTAIGVGAP     **βeta-QCcyclo**
```

```
     |⎯⎯⎯⎯|
CGNLSTCMLGTYTQDF**(βeta)Asp**K**(N-Me)Phe**H**Orn** FPQTAIGVGAP     **βeta-QClinear**
```
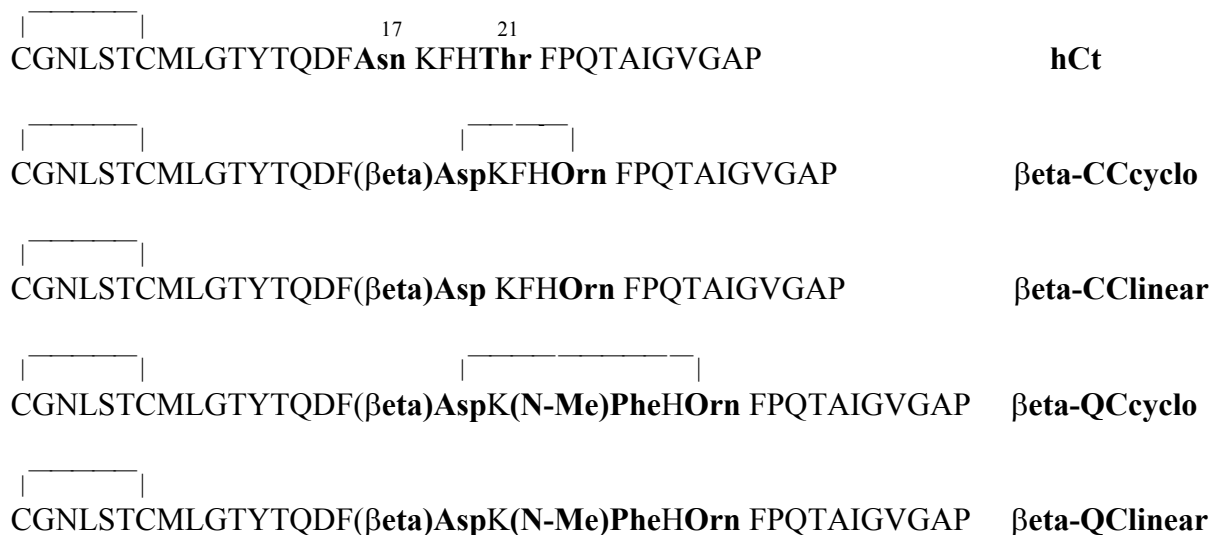
Scheme 7. Primary structures of hCt and hCt analogues of group 6 to study the importance of the presence of the side chain CO at residue17.

```
     |⎯⎯⎯⎯|                   17        21
CGNLSTCMLGTYTQDF**Asn** KFH**Thr**FPQTAIGVGAP                             **hCt**
```

```
     |⎯⎯⎯⎯|                   17        21
CGNLSTCMLGTYTQDF**Dap** KFH**Thr**FPQTAIGVGAP                         **Dap[17] hCt**
```

```
     |⎯⎯⎯⎯|                   17        21
CGNLSTCMLGTYTQDF**Dab** KFH**Thr**FPQTAIGVGAP                         **Dab[17] hCt**
```
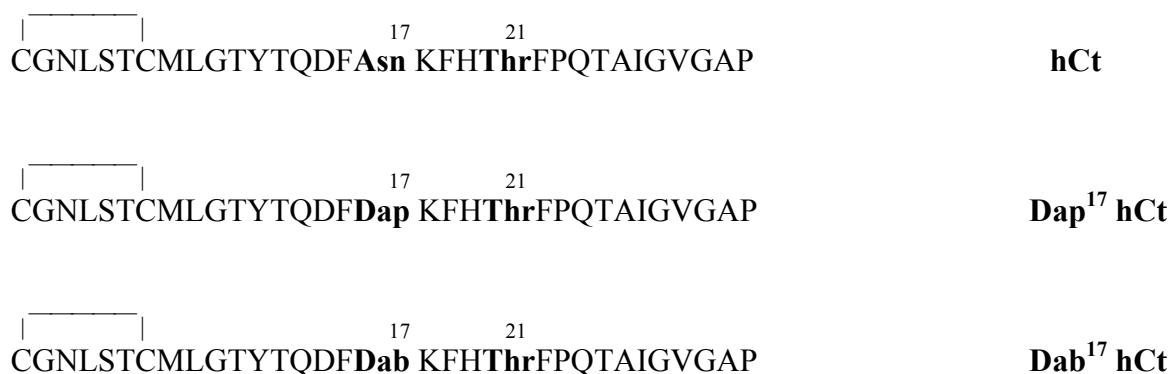
Scheme 8. Primary structures of analogues of group 7 that were designed to study the importance of combined substitutions in the hydrophobic face of the potential α-helix; Nle[8] for Met[8], Leu[12,16,19] for Y[12], F[16], F[19] and Y[22] for F[22].

```
     |⎯⎯⎯|                        |⎯⎯⎯⎯⎯|
CGNLSTC**Nle**LGT**Leu**TQD**LeuAsp** K**Leu**H**OrnTyr**PQTAIGVGAP            **TCcyclo**
```

```
     |⎯⎯⎯⎯|
CGNLSTC**Nle**LGT**Leu**TQD**LeuAsp**K**Leu**H**OrnTyr**PQTAIGVGAP              **TClinear**
```
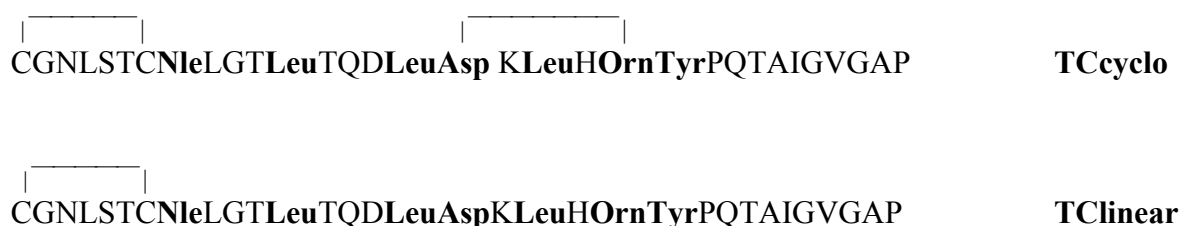
5.1.1 Peptide synthesis using Boc-SPPS for calcitonins

All peptides of Table 22 were synthesized using p-methylbenzhydrylamine (MBHA) resin having a substitution level 0.57 mmole / gr. Residues [23-32] of hCt were single coupled (4-fold excess for the protected amino acid and TBTU, 6-fold excess for DIEA) for 80 min, and the completeness of each coupling was checked by the Kaiser test. Cleavage of the N^{α}-Boc group was performed with 50% TFA in DCM, with the exception of Gln^{24} and Gln^{14} where 4 N HCl in dioxane was employed. Intramolecular cyclization of N-terminal Gln to pyroglutamate is a frequent cause of chain termination in SPPS [76]. This side reaction is catalysed by weak acids such as Boc- amino acids and the TFA that is used for deprotection in Boc-SPPS. Ring closure has been found to be suppressed by the use of 4 N HCl in dioxane [77]. Following coupling of Met^8, the cleavage mixture for Boc-group (50% TFA in DCM) contained 1% dimethylsulfide (DMS) as scavenger to prevent attachment of the tert-butyl cations to $Met^{8\ [78]}$.

The side-chain lactam bridge formation between residues 17 and 21 was performed by the side chain-to-side chain cyclization strategy on the resin based on the method of Felix *et.al.* [21]. The base-labile side-chain protecting groups Fmoc / OFm were selectively cleaved by 25% piperidine in DMF and cyclization was performed using BOP with DIEA (4-fold excess). The completeness of the cyclization was checked by the Kaiser test and subsequent capping of unreacted functional groups with Ac_2O (10-fold excess) with DIEA (10-fold excess) was performed.

The coupling of (N-Me) Phe^{19} (in QCcyclo) was performed once, using 3-fold excess of amino acid and TBTU and 4.5-fold excess for DIEA, but extensive coupling time (100 min) was employed. Residues [1-22] of the Ct sequences were single coupled (4-fold excess for the protected amino acid and TBTU, 6-fold excess for DIEA) for 90 min with Kaiser test performed after each coupling.

The final cleavage of the peptides from the resin was achieved with anhydrous HF and the following scavengers were used: thioanisole (TAS), dimethylsulfide (DMS) and p-thiocresol. Peptides were obtained in their reduced form and the crude material was dissolved in 10% AcOH and analysed by RP-HPLC. Some of HPLC profiles of the products appeared to be quite broad. The reason for this could be the high aggregation potential of the peptides, the heterogeneous nature of the mixture, or formation of intermolecular S-S bond formation leading to covalently linked multimers. The crude material was oxidized (in the dark) under dilute conditions (3×10^{-4} M) in 0.5 M Gdn HCl in aqueous 0.1 M NH_4HCO_3. Oxidations

were usually complete after 1-2 hrs as indicated by RP-HPLC. The two forms of the peptides (reduced / oxidized) were separated by RP-HPLC on the basis of their different retention times (a shift of 1-1.5 min towards longer times for the oxidized form). A representative example of the two forms (reduced / oxidized) of peptide CCcyclo is shown: In Figure 11, the peak at 23.1 min is the reduced form of the peptide, and in Figure 12, the peak at 24.4 min is the oxidized form. In the case of peptide βeta-CCcyclo the two forms (reduced / oxidized) are shown: In Figure 13, the peak at 21.7 min is the reduced form of the peptide, and in Figure 14, the peak at 23.1 min is the oxidized form. Pure oxidized peptide was obtained usually in a yield of 5-10% with respect to the crude reduced material.

The only difficulty that was encountered in the Boc-syntheses was the one during the synthesis of βeta-QCcyclo: the RP-HPLC trace (Figure 15) of the crude material dissolved in 10% AcOH revealed the presence of two peaks: a peak at 21.7 min and another at 24.5 min. Upon oxidation under dilute conditions, both peaks were shifted towards longer times: 22.9 min and 25.7 min respectively (Figure 16). According to MALDI-MS, the peak at 22.9 min was the correct product (expected $[M+H]^+$: 3429.9, found $[M+H]^+$: 3429.1), whereas the other peak was a deletion sequence (found $[M+H]^+$: 3300.2). The missing residue (-129) was most probably Lys[18], due to incomplete coupling of this residue to (N-Me) Phe[19] (expected: 3301.8).

Table 22. Peptides synthesized by Boc-chemistry (in their oxidized form) and their mass (as determined by MALDI-MS).

Short Name	Sequence	$[M+H]^+$ expected:	$[M+H]^+$ found:
CCcyclo	cyclo[17,21]-[Asp[17], Orn[21]]hCt	3414,9	3414,0
ACcyclo	cyclo[17,21]-[Asp[17], D-Phe[19], Lys[21]]hCt	3428,9	3448,2[§]
QCcyclo	cyclo[17,21]-[Asp[17], (N-Me) Phe[19], Orn[21]]hCt	3429,9	3433,9
βeta-QCcyclo	cyclo[17,21]-[βeta-Asp[17], (N-Me) Phe[19], Orn[21]]hCt	3429,9	3429,1
βeta-CCcyclo	cyclo[17,21]-[βeta-Asp[17], Orn[21]]hCt	3414,9	3420,3

[§]: $[M+Na]^+$ adduct 3450,9
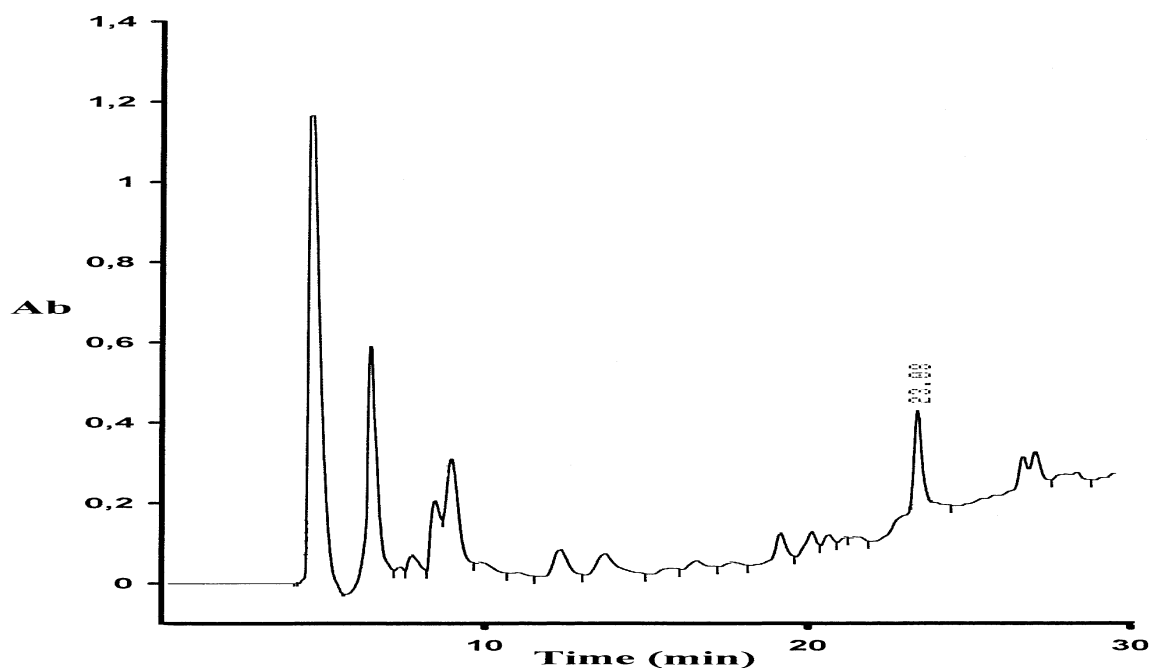
Figure 11. RP-HPLC analysis of crude CCcyclo (in reduced form) using gradient 1 on a C_{18} column, flow rate 2 ml / min and detection at 214 nm. Injection of 0.5 mg crude peptide in 600 µl aqueous 10 mM HCl solution.
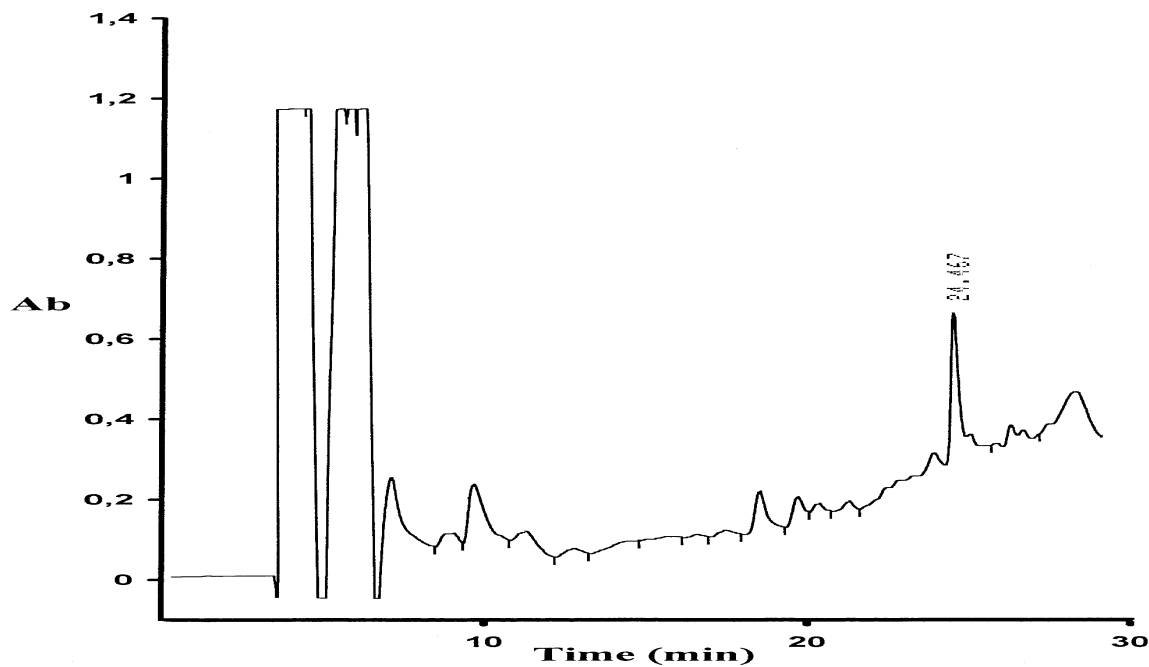
Figure 12. RP-HPLC analysis of crude CCcyclo (in oxidized form) using gradient 1 on a C_{18} column, flow rate 2 ml / min and detection at 214 nm. Injection of 0.3 mg crude peptide in 400 µl 0.5 M Gdn HCl in aqueous 0.1 M NH_4HCO_3 solution.
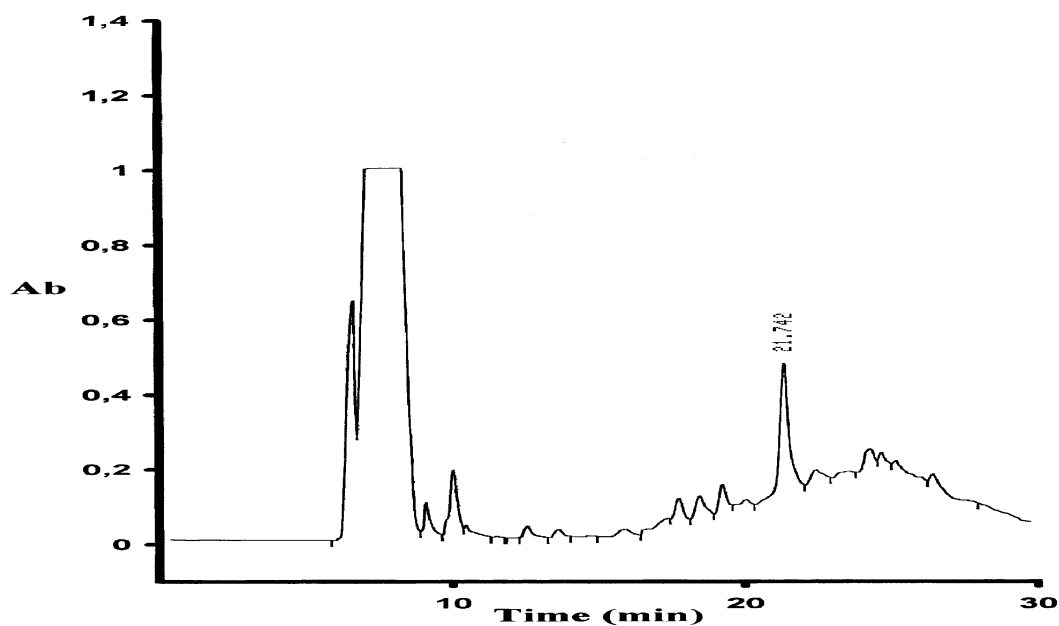
Figure 13. RP-HPLC analysis of crude βeta-CCcyclo (in reduced form) using gradient 1 on a C_{18} column, flow rate 2 ml / min and detection at 214 nm. Injection of 1.1 mg crude peptide in 1 ml aqueous 10% AcOH solution.
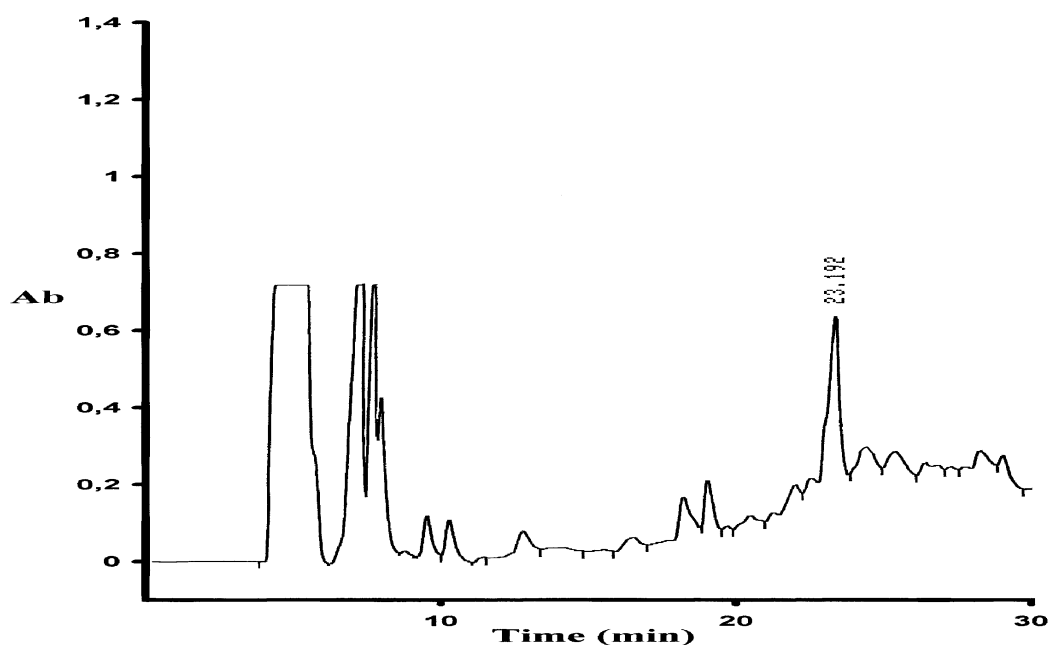
Figure 14. RP-HPLC analysis of crude βeta-CCcyclo (in oxidized form) using gradient 1 on a C_{18} column, flow rate 2 ml / min and detection at 214 nm. Injection of 0.8 mg crude peptide in 1.4 ml 0.5 M Gdn HCl in aqueous 0.1 M NH_4HCO_3 solution.
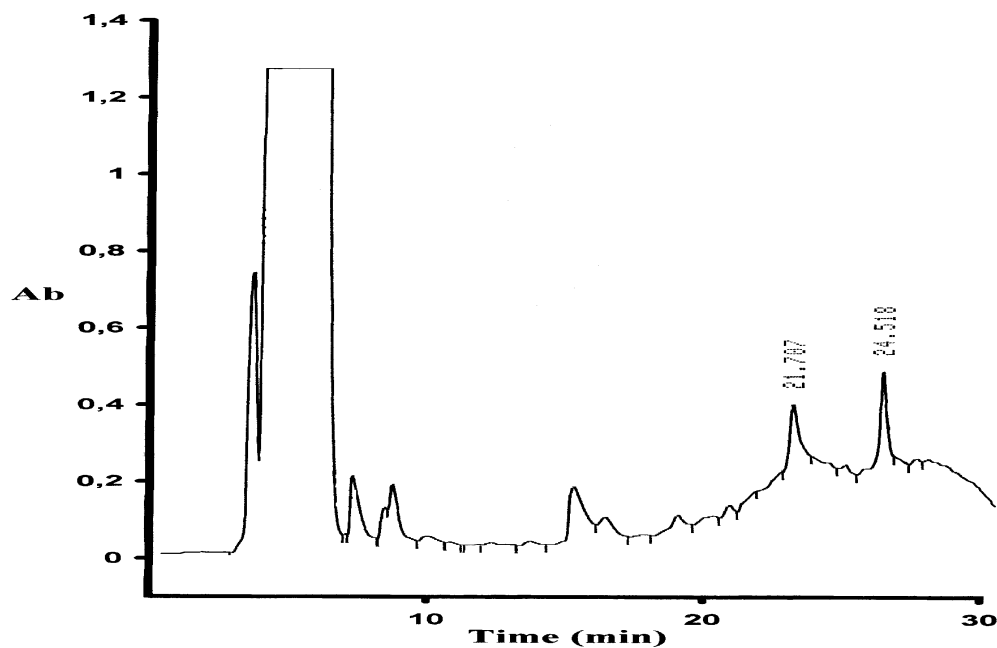
Figure 15. RP-HPLC analysis of crude βeta-QCcyclo (in reduced form) using gradient 1 on a C$_{18}$ column, flow rate 2 ml / min and detection at 214 nm. Injection of 1 mg crude peptide in 1 ml aqueous 10% AcOH solution.
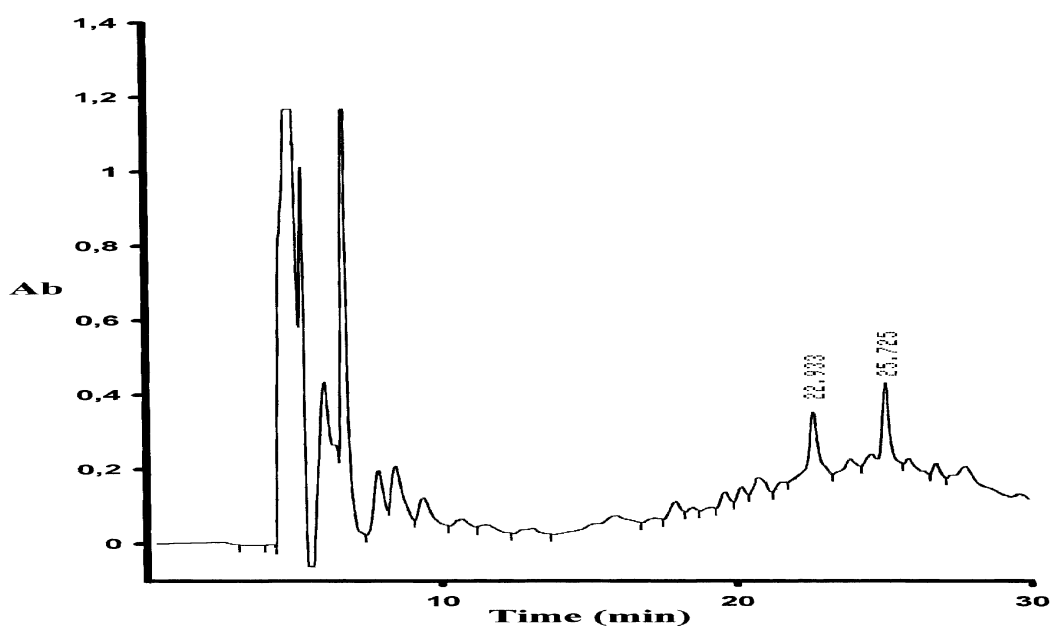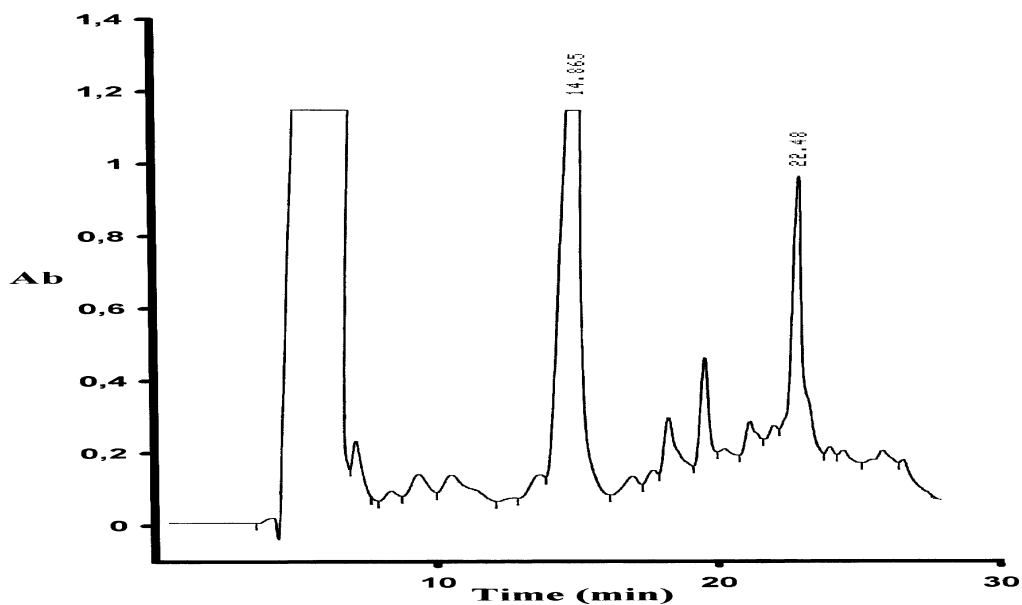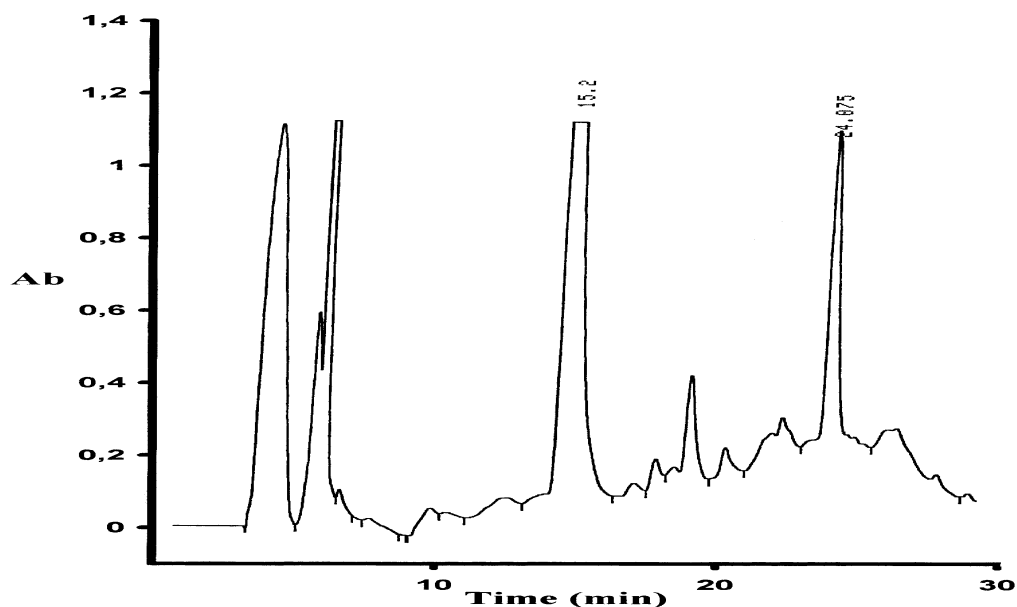

Figure 16. RP-HPLC analysis of crude βeta-QCcyclo (in oxidized form) using gradient 1 on a C$_{18}$ column, flow rate 2 ml / min and detection at 214 nm. Injection of 0.2 mg crude peptide in 300 µl 0.5 M Gdn HCl in aqueous 0.1 M NH$_4$HCO$_3$ solution.

5.1.2 Peptide synthesis using Fmoc-SPPS for calcitonins

The peptides synthesized by Fmoc-chemistry are summarized in Table 23. Fmoc-SPPS was performed using the Rink amide MBHA resin (substitution level: 0.49 mmole / gr). Fmoc-protected amino acids (4-fold excess) were coupled using 4-fold excess TBTU and 6-fold excess DIEA for 45 min with the exception for the C-terminal amino acid. Couplings were done twice. The side chain-to-side-chain cyclization between residues 17 and 21 was performed on the resin support [21]. The very acid labile side-chain protecting groups 4-methyltrityl (Mtt) / 1-(1´-adamantyl)-1-methyl-ethoxycarbonyl (Adoc) were used for residue 21 and 2-phenyl isopropyl ester (Opip) for residue 17 and were selectively cleaved with TFA (1% v/v) in DCM. Under these conditions the other side-chain protecting groups remained intact. 5% TIS was included in the mixture to quench the trityl cations. The cyclization was performed using 4-fold excess of BOP in the presence of 4-fold excess of DIEA in DMF. Cyclization reactions were complete according to Kaiser test after 1 x 4 hrs; 1 x 15 hrs and acetylation (10-fold excess for Ac_2O / DIEA) of the unreacted amino groups was carried out as standard part of the methodology.

Cys residues were coupled using a different coupling method from the method used for the other residues. The reason for this is that DIEA catalyzed coupling methods can lead to considerable amounts of racemization of Fmoc-Cys(Trt) residues during the activation / coupling process [61]. Therefore, the activation of Cys was carried out under neutral conditions in a medium free of base, using 4-fold excess of HOBt and 4-fold excess of DIC in DMF (45 min at 4 °C). The solution was then added to the N^α-deprotected peptide resin and left to react for 1 hr (second coupling followed according to the same method). Acetylation after incorporation of Cys^7 was carried out in the syntheses of CCcyclo, HCcyclo, HClinear, ICcyclo, IC linear, TCcyclo and TClinear.

Cleavage of the peptides from the resin was achieved using a slight modidication of reagent K [67] for 3 hrs at RT. The elution profiles of the crude products were of good purity with regard to the main product. Depending on the sequence that was constructed several deletion sequences were also detected. In several syntheses (e.g. DCcyclo, ECcyclo, QCcyclo, CClinear, HClinear) the main product (reduced form) co-eluted with a by-product missing 100 mass units (as was determined by MALDI-MS). Upon air oxidation (as described under 5.1.1) of the crude material the two products were resovled (the main product shifted to longer retention times, where the by-product eluted at the initial retention time). This chromatographic behaviour in combination with the mass difference detected by the MALDI-

MS suggested that the missing residue was a cysteine (most probably Cys[1]). In other synteses (such as BCcyclo, [Dap[17]]hCt, TCcyclo, TClinear) the missing cysteine residue was also a problem and additionally a second by-product that corresponded to a peptide missing 57 mass units was detected (probably Gly[2]). This indicated that the couplings in this region of the polypeptide were difficult as compared to the other residues in the sequence. RP-HPLC purification was usually sufficient to isolate the main product in yields between 5-10% with regard to the crude peptide. Characterization was performed by MALDI-MS and retention times in RP-HPLC.

In Figure 17, the RP-HPLC profile of crude CCcyclo (reduced form, peak at 22.5 min) after cleavage and lyophilization is shown. In Figure 18, the RP-HPLC trace of CCcyclo (oxidized form, peak at 24.0 min) is shown.

Both chemistries (Fmoc- and Boc-) proved to be reliable methods for the solid phase synthesis of the analogues. Fmoc-chemistry was preferred since it is easier by this method to remove peptide / and side-chain protecting groups than by Boc-chemistry. In Figure 19 an analytical run of RP-HPLC purified CCcyclo synthesized by Boc-chemistry is shown. In Figure 20 an analytical run of the same peptide synthesized by Fmoc-chemistry is shown.

Table 23. Peptides synthesized by Fmoc-chemistry (in their oxidized form) and their mass (as determined by MALDI-MS).

Short Name	Sequence	[M+H]$^+$ expected:	[M+H]$^+$ found:
analog 1	cyclo^{17,21}-[Asp^{17}, Lys^{21}]hCt	3428,9	3437,2
CCcyclo	cyclo^{17,21}-[Asp^{17}, Orn^{21}]hCt	3414,9	3413,7
DCcyclo	cyclo^{17,21}-[Asp^{17}, Dab^{21}]hCt	3400,9	3399,2
FCcyclo	cyclo^{17,21}-[Asp^{17}, Dap^{21}]hCt	3386,9	3388,1
GCcyclo	cyclo^{17,21}-[Glu^{17}, Dab^{21}]hCt	3414,9	3434,4[#]
CClinear	[Asp^{17}, Orn^{21}]hCt	3432,9	3431,2
ACcyclo	cyclo^{17,21}-[Asp^{17}, D-Phe^{19}, Lys^{21}]hCt	3428,9	3448,2[§]
BCcyclo	cyclo^{17,21}-[Asp^{17}, Aib^{18}, Lys^{21}]hCt	3386,9	3386,5
ECcyclo	cyclo^{17,21}-[Asp^{17}, D-Lys^{18}, Lys^{21}]hCt	3428,9	3449,3[§]
OClinear	[D-Phe^{19}]hCt	3418,9	3418,9
NClinear	[D-Lys^{18}]hCt	3418,9	3417,9
HCcyclo	cyclo^{17,21}-[Asp^{17}, Pro^{18}, Ser^{19}, Orn^{21}]hCt	3323,9	3322,2
HClinear	[Asp^{17}, Pro^{18}, Ser^{19}, Orn^{21}]hCt	3341,9	3339,7
ICcyclo	cyclo^{17,21}-[Asp^{17}, Pro^{18}, Orn^{21}]hCt	3383,9	3382,9
IClinear	[Asp^{17}, Pro^{18}, Orn^{21}]hCt	3401,9	3405,3
QCcyclo	cyclo^{17,21}-[Asp^{17}, (N-Me) Phe^{19}, Orn^{21}]hCt	3429,9	3433,9
QClinear	[Asp^{17}, (N-Me) Phe^{19}, Orn^{21}]hCt	3447,9	3445,6
βeta-CClinear	[βeta-Asp^{17}, Orn^{21}]hCt	3432,9	3438,1
βeta-QClinear	[βeta-Asp^{17}, (N-Me) Phe^{19}, Orn^{21}]hCt	3447,9	3446,5
Dap^{17} linear	[Dap^{17}]hCt	3389,9	3389,4
Dab^{17} linear	[Dab^{17}]hCt	3403,9	3403,5
TCcyclo	cyclo^{17,21}-[Nle^8, Leu^{12,16,19}, Asp^{17}, Orn^{21}]hCt	3294,9	3297,7
TClinear	[Nle^8, Leu^{12,16,19}, Asp^{17}, Orn^{21}]hCt	3312,9	3316,9

[#]: [M+Na]$^+$ adduct 3436,9

[§]: [M+Na]$^+$ adduct 3450,9

Figure 17. RP-HPLC analysis of crude CCcyclo (in reduced form) using gradient 1 on a C_{18} column, flow rate 2 ml / min and detection at 214 nm. Injection of 0.9 mg crude peptide in 1 ml aqueous 10% AcOH solution (the peak at 14.8 min is due to scavenger phenol form the cleavage mixture).

Figure 18. RP-HPLC analysis of crude CCcyclo (in oxidized form) using gradient 1 on a C_{18} column, flow rate 2 ml / min and detection at 214 nm. Injection of 1 mg crude peptide in 1 ml 1.5 M Gdn HCl in aqueous 0.1 M NH_4HCO_3 solution (the peak at 15.2 min is due to scavenger phenol form the cleavage mixture).
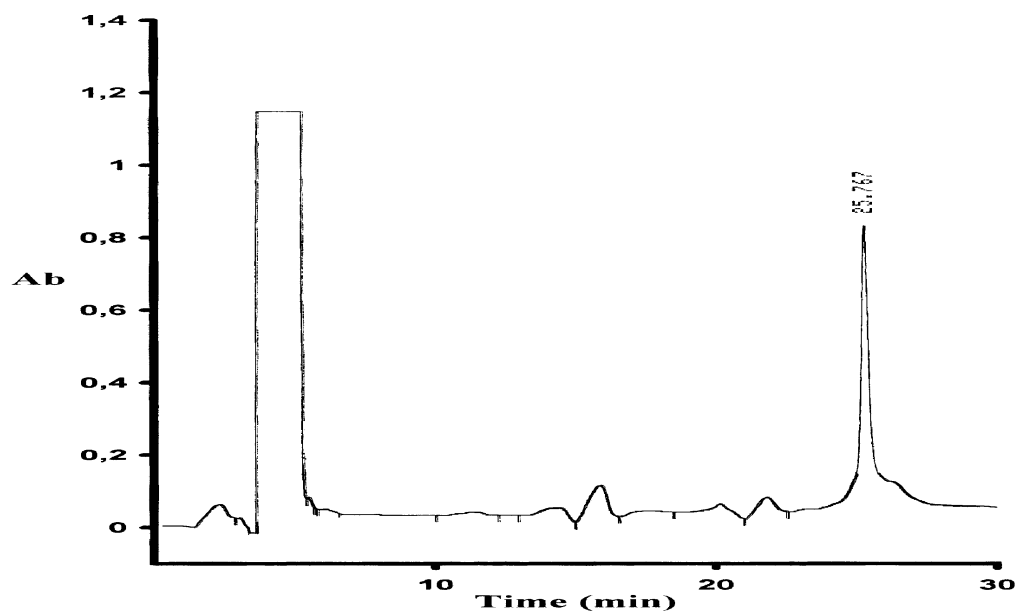
Figure 19. Analytical run of HPLC purified and oxidized CCcyclo (synthesized by Boc-chemistry) using gradient 1 on a C_{18} column, flow rate 2 ml / min and detection at 214 nm. Injection of 30 µg pure peptide in 300 µl aqueous 10% AcOH solution.
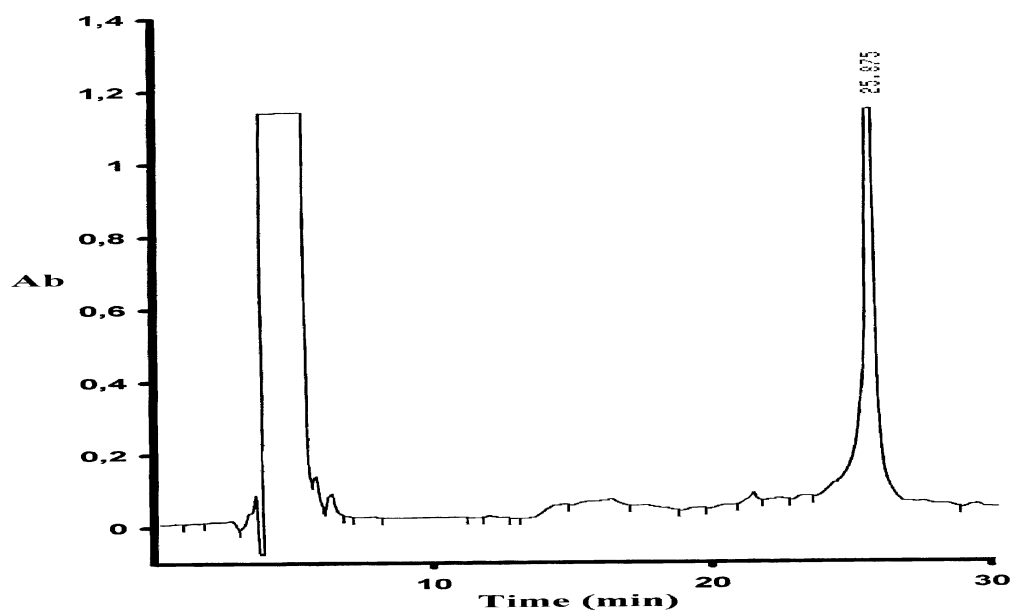
Figure 20. Analytical run of HPLC purified and oxidized CCcyclo (synthesized by Fmoc-chemistry) using gradient 1 on a C_{18} column, flow rate 2 ml / min and detection at 214 nm. Injection of 30 µg pure peptide in 300 µl aqueous 10% AcOH solution.

5.1.3 Binding to the calcitonin receptor

Several of the biological activities of the Cts are thought to be mediated via binding to a receptor that belongs to the family of G-protein coupled receptors [79]. Ct-receptors are localized in bone and kidney as well as in the central nervous system, i.e. the brain. High affinity receptors for Cts exist in some cell lines including the human breast cancer cell line T47D. Peptide receptor binding affinities were assayed in the T47D cell line and compared to the affinity of sCt which is the strongest known naturally occurring ligand and hCt which is a weak ligand. The assay was based on the competitive inhibition of ^{125}I-sCt (15 nM) by the analogues. All analogues were assayed in the range 0.01-100 nM in at least two independent experiments and in each experiment each concentration was assayed in duplicate. The specific binding of the peptides was the difference between total binding (radioligand alone) and non-specific binding. The latter was determined as the binding of 10 nM sCt and was assessed from 13 independent experiments to be 12.94% ($\pm$ 3.59).

Receptor binding affinities were calculated as IC_{50} values (concentration of Ct analogue that displaces 50% of bound radioligand from the receptor). Binding of the analogues was compared to sCt-binding ($IC_{50} = 0.8$ nM) and hCt-binding ($IC_{50} = 4.46$ nM), which showed an affinity that was six-fold lower than the sCt affinity. As shown in Figure 21, analog 1 with an $IC_{50} = 2.45$ nM and CCcyclo with an $IC_{50} = 1.73$ nM had three-fold and two-fold respectively lower binding affinities than sCt. However, both peptides bound better to the receptor as hCt. The 18-membered ring containing analogue DCcyclo ($IC_{50} = 9.57$ nM) bound weaker than hCt, while the 17-membered ring containing analogue FCcyclo nearly did not bind at all. These results indicated that further constraining the lactam bridge than in CCcyclo had a negative effect on the binding affinity of the peptides. CClinear did not bind at all. This result indicated that the exchanging of residues Asn^{17} and Thr^{21} by Asp^{17} and Orn^{21} results in a complete abolishment of receptor binding. On the other hand the introduction of a lactam bridge between the side chains of these residues (in CCcyclo) leads to a strongly enhanced binding. Of interest, the peptide GCcyclo ($IC_{50} = 2.18$ nM) was as potent as CCcyclo. Since both peptides had the same ring size (19-membered ring) but different residues constituted the lactam bridge (Glu^{17} / Dab^{21} instead of Asp^{17} / Orn^{21}), this result suggested that these substitutions are compatible with receptor binding affinity.
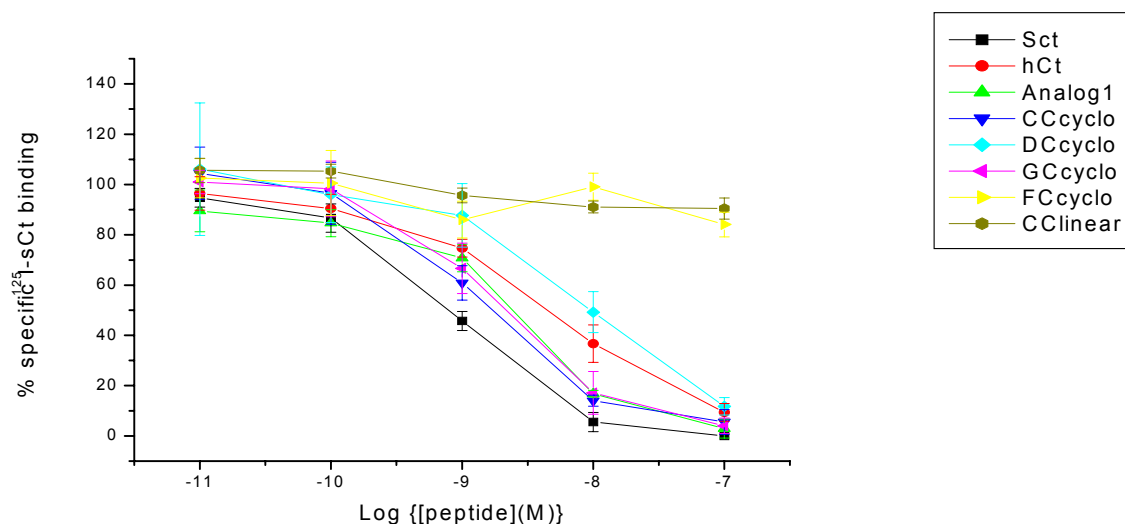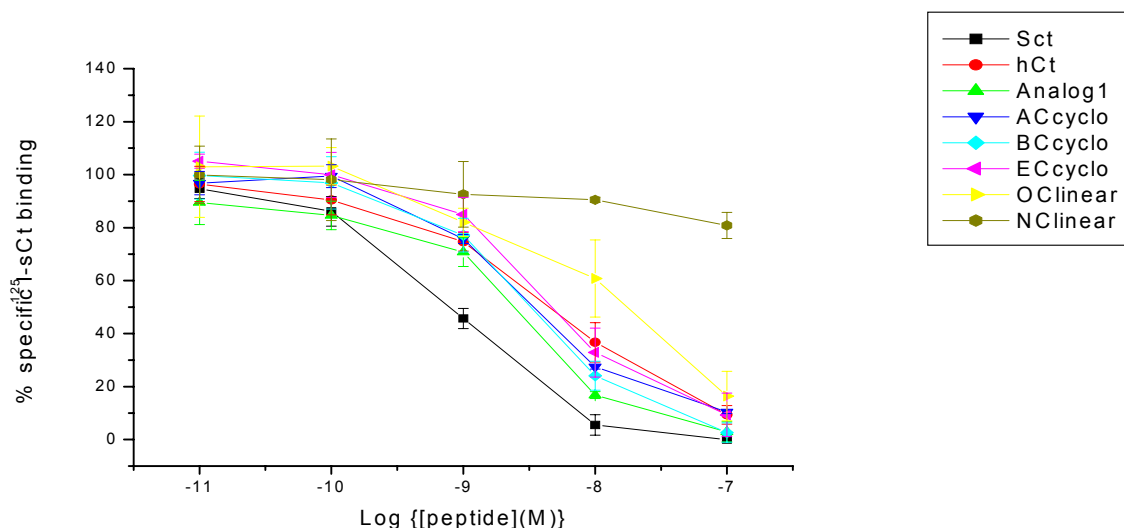
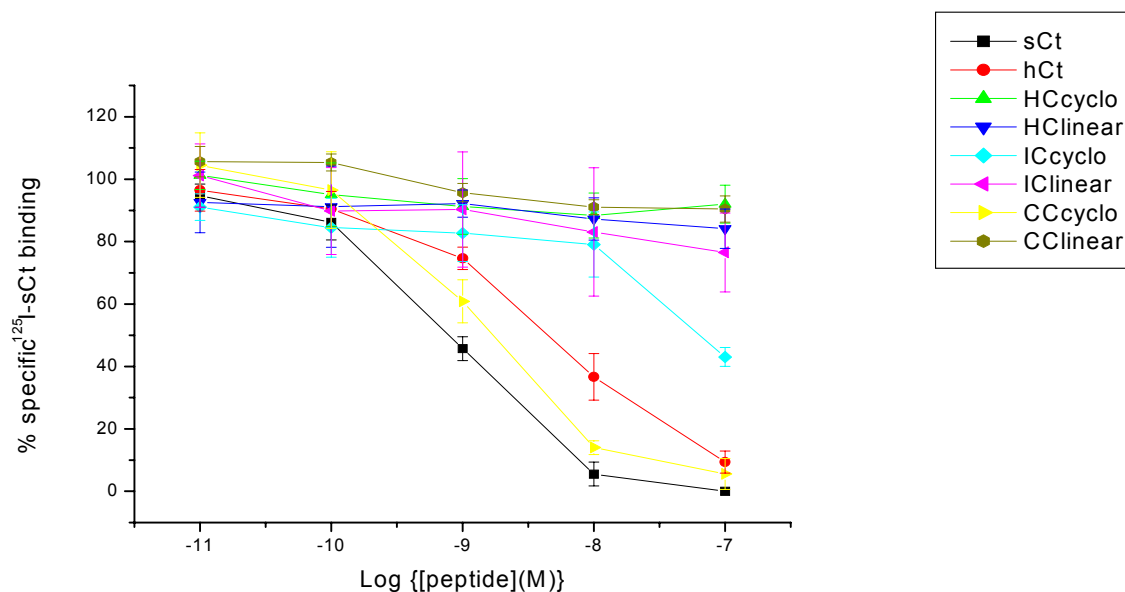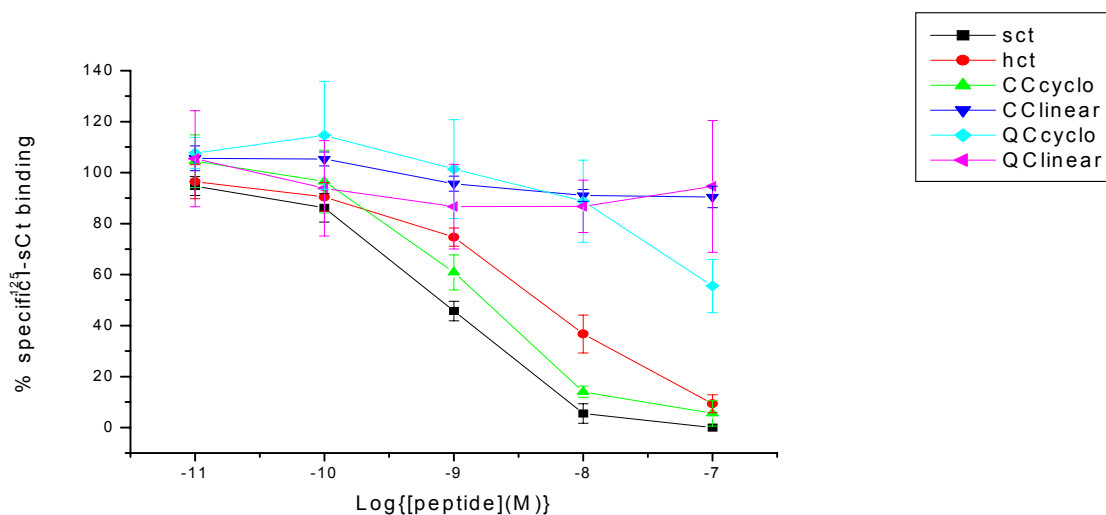**Figure 21.** Human Ct receptor binding of hCt, sCt and bridged analogues of group 1 to T47D cells assessed *via* displacement of bound ^{125}I-labelled sCt. Specific radioligand binding is plotted vs. the concentration of competing hCt, sCt and analogues as indicated. Binding isotherms are mean ± SD for two to three independent experiments (each of them performed in duplicate) and the data for sCt and hCt are the mean of 14, respectively, 13 experiments.

The second group of peptides consisted of bridged and non-bridged substitution analogues of analog 1. The aims of the receptor binding studies with these analogues was to identify the topologically important features of residues in region 18 to 20 of the Ct sequence, including the role of chirality of residues 18 and 19, for bioactivity. According to the obtained results (Figure 22), peptides ACcyclo (IC_{50} = 3.46 nM), BCcyclo (IC_{50} = 3.31 nM) and ECcyclo (IC_{50} = 4.67 nM) had slightly lower binding affinities as compared to analog 1 (IC_{50} = 2.45 nM). The significance of the chirality for L-Lys[18] for receptor binding was further confirmed by the comparison of the binding activities of the non-bridged analogues OClinear and NClinear. Those analogues had one substitution as compared to hCt. OClinear (IC_{50} = 17.78 nM) had significantly less binding affinity than hCt, while NClinear showed nearly no binding. These data indicated that the D-Phe[19] substitution for L-Phe[19] (in OClinear) was only partially compatible with hCt activity whereas the D-Lys[18] substitution for L-Lys[18] (in NClinear) strongly affected receptor binding affinity.
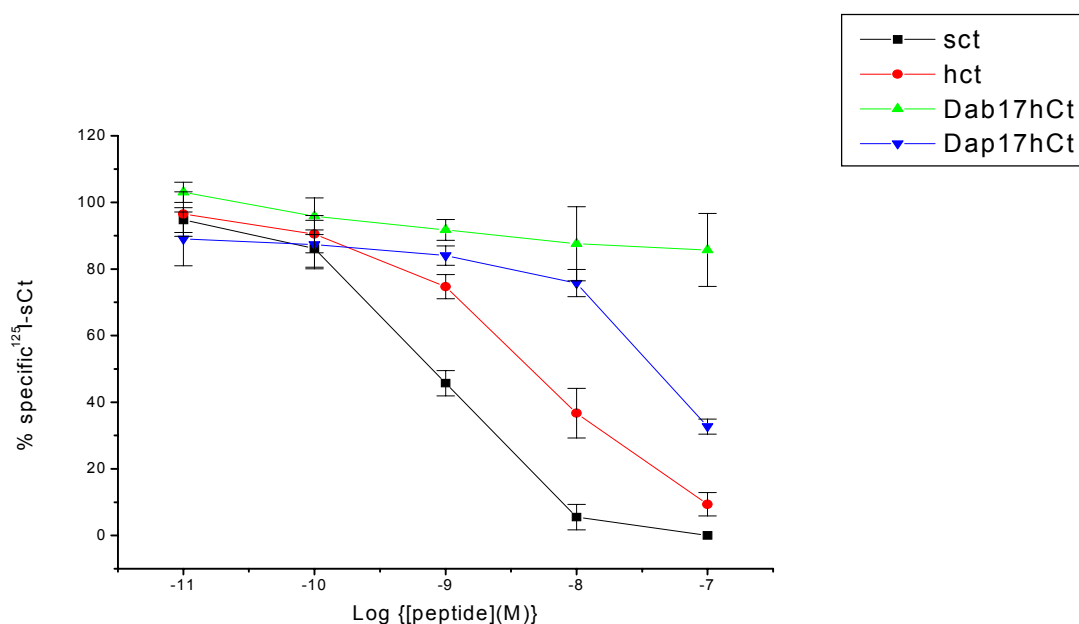
Figure 22. Human Ct receptor binding of hCt, sCt and analogues of group 2 to T47D cells assessed *via* displacement of bound ^{125}I-labelled sCt. Specific radioligand binding is plotted vs. the concentration of competing hCt, sCt and analogues as indicated. Binding isotherms are mean ± SD for two to three independent experiments (each of them performed in duplicate) and the data for sCt and hCt are the mean of 14, respectively, 13 experiments.

The third group of peptides consisted of substitution analogues of CCcyclo and CClinear and provided additional insight in the structural features of bioactivity of the agonist CCcyclo. These peptides had one substitution (Pro^{18} for Lys^{18} in ICcyclo / IClinear) or two substitutions (Pro^{18} for Lys^{18} and Ser^{19} for Phe^{19} in HCcyclo / HClinear) as compared to CCcyclo. With the exception of ICcyclo (IC$_{50}$ = 64.56 nM), which showed an extremely weak binding behaviour, the other three peptides showed almost no binding (Figure 23). The results showed that exchanging of Lys^{18} and Phe^{19} by the 'Asx-turn' compatible residues Pro^{18} and Ser^{19}, strongly affected the binding affinity of CCcyclo.

Figure 23. Human Ct receptor binding of hCt, sCt, CCcyclo, CClinear and analogues of group 3 to T47D cells assessed *via* displacement of bound ^{125}I-labelled sCt. Specific radioligand binding is plotted vs. the concentration of competing hCt, sCt and analogues as indicated. Binding isotherms are mean ± SD for two to three independent experiments (each of them performed in duplicate) and the data for sCt and hCt are the mean of 14, respectively, 13 experiments.

Next, the binding affinities of peptides QCcyclo and QClinear (group 4) were studied and compared with the ones of CCcyclo and CClinear (Figure 24). Both QCcyclo and QClinear showed nearly no binding. The results suggested that the N^{α}-H of Phe[19] is very important for receptor binding and/or that the presence of the methyl group was not compatible with receptor binding. The group of βeta-peptides (group 5), βeta-CCcyclo / βeta-CClinear and βeta-QCcyclo / βeta-QClinear was then studied and compared to CCcyclo / CClinear (Figure 25). In this group, the backbone of the peptides was distorted by the extra methylene group present and the bridge between the side-chains in the cyclo analogues was also shorter by one methylene (-CH$_2$-) than in the previous normal peptides. Again, all βeta-peptides showed no binding, which indicated a very important role for the region [17-21] in receptor binding.

Figure 24. Human Ct receptor binding of hCt, sCt, CCcyclo, CClinear and analogues of group 4 to T47D cells assessed *via* displacement of bound ^{125}I-labelled sCt. Specific radioligand binding is plotted vs. the concentration of competing hCt, sCt and analogues as indicated. Binding isotherms are mean ± SD for two to three independent experiments (each of them performed in duplicate) and the data for sCt and hCt are the mean of 14, respectively, 13 experiments.
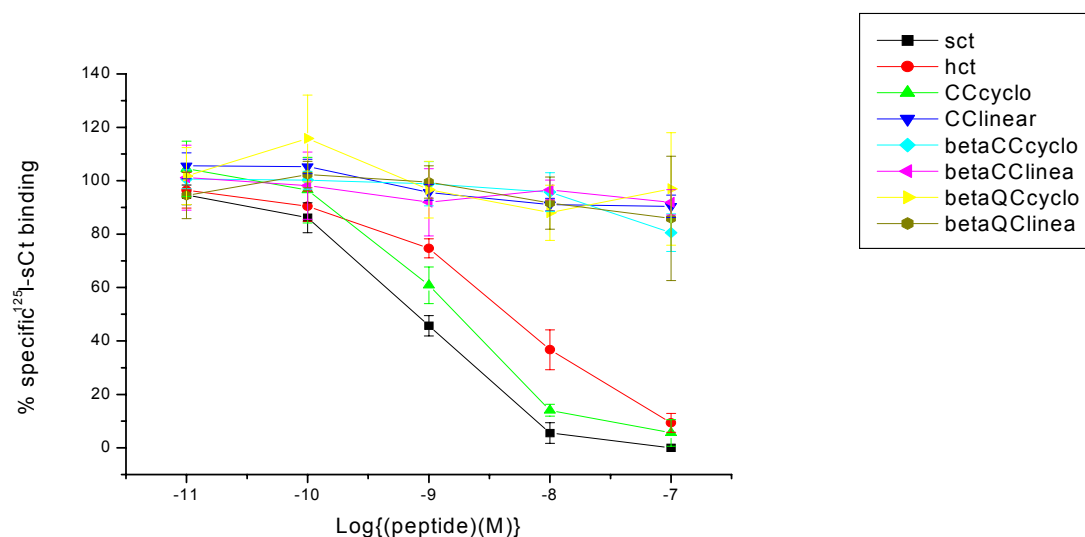
Figure 25. Human Ct receptor binding of hCt, sCt, CCcyclo, CClinear and analogues of group 5 to T47D cells assessed *via* displacement of bound ^{125}I-labelled sCt. Specific radioligand binding is plotted vs. the concentration of competing hCt, sCt and analogues as indicated. Binding isotherms are mean ± SD for two to three independent experiments (each of them performed in duplicate) and the data for sCt and hCt are the mean of 14, respectively, 13 experiments.

Next, receptor binding of the non-bridged hCt analogues Dap^{17} and Dab^{17} (group 6) was determined in order to study the importance of the carbonyl group at position 17 (Figure 26). Thereby, peptide $[Dab^{17}]hCt$ had almost no receptor binding, while $[Dap^{17}]hCt$ showed a weak (IC_{50} = 39.8 nM) binding to the receptor. These results indicated that: a) the CO function of the side-chain of residue Asn^{17} is very important for binding and b) also the amino group of the side-chain of residue 17 and its topology may play a role in binding. Peptides TCcyclo and TClinear (group 7) were designed to study the collective effect of the lactam bridge of CCcyclo and the exchange of aromatic residues Tyr^{12}, Phe^{16}, Phe^{19} by Leu, which are the residues present at these positions in the sCt sequence. TCcyclo (IC_{50} = 2.63 nM) exhibited a somewhat reduced affinity as compared to CCcyclo. Similarly, TClinear (IC_{50} = 6.76 nM) was slightly less potent than hCt (Figure 27).

Figure 26. Human Ct receptor binding of hCt, sCt, and analogues of group 6 to T47D cells assessed *via* displacement of bound ^{125}I-labelled sCt. Specific radioligand binding is plotted vs. the concentration of competing hCt, sCt and analogues as indicated. Binding isotherms are mean ± SD for two to three independent experiments (each of them performed in duplicate) and the data for sCt and hCt are the mean of 14, respectively, 13 experiments.
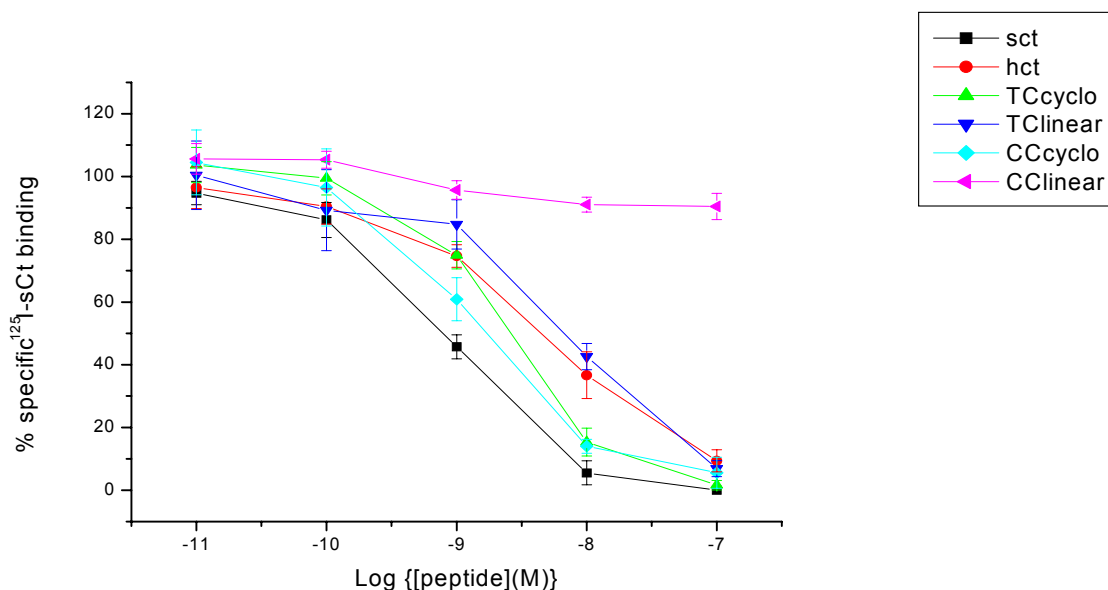
Figure 27. Human Ct receptor binding of hCt, sCt, CCcyclo, CClinear and analogues of group 7 to T47D cells assessed *via* displacement of bound ^{125}I-labelled sCt. Specific radioligand binding is plotted vs. the concentration of competing hCt, sCt and analogues as indicated. Binding isotherms are mean ± SD for two to three independent experiments (each of them performed in duplicate) and the data for sCt and hCt are the mean of 14, respectively, 13 experiments.

5.1.4 Activation of the adenylate cyclase (AC)

hCt binding to receptors of T47D cells results in activation of the adenylate cyclase (AC) [80]. Thus the initial event following binding of Cts to their T47D cell receptors is the increase in intracellular cAMP levels. cAMP acts as a signal transducer (second messenger) by modifying the rates of various enzyme-catalyzed reactions [81]. The increase in the level of cAMP is due to an activation of the adenylate cyclase. The ability of a receptor ligand to regulate adenylate cyclase and increase cAMP production is closely associated with its receptor agonist potential [82]. Therefore, the synthetic analogues were next tested with regard to the activation of AC.

The EIA assay that was applied selectively measures intracellular cAMP levels following peptide binding to the membrane receptors. The assay is based on the competition between unlabelled cAMP and a fixed quantity of peroxidase-labelled cAMP for a limited number of binding sites of a cAMP specific antibody which is coated on the ELISA plates (Scheme 9).

The studies aimed at determining the concentration of peptides that caused the half maximal elevation of cAMP (EC_{50}) as compared to the maximal activation, which would be a measure of agonist potency of the synthesized analogues. Thereby, the weakest agonist was expected to cause only a weak increase in the cAMP levels resulting in more bound peroxidase-labelled cAMP. This, in turn, would upon treatment with the TMB substrate give blue colour and enhanced absorbance at 450 nm. The basal concentration of cAMP was estimated by treatment of the cells in cell assay medium without peptide. The maximum level of cAMP was determined by treatment with 100 nM hCt. The percentage of maximum adenylate cyclase (AC) activation was estimated using the formula:

$$\% \text{ maximum AC activation} = [(Ab_{sample} - Ab_{basal}) / (Ab_{100 \text{ nM hCt}} - Ab_{basal})] \times 100$$

All analogues were tested in a concentration range between 0.01 and 100 nM in two independent experiments (each time in duplicate), with the exception for the standards sCt and hCt which were tested three times.

Scheme 9. EIA assay based on the competition between unlabelled cAMP (induced by peptide treatment) and a fixed quantity of peroxidase-labelled cAMP for a limited number of binding sites of a cAMP specific antibody [83].
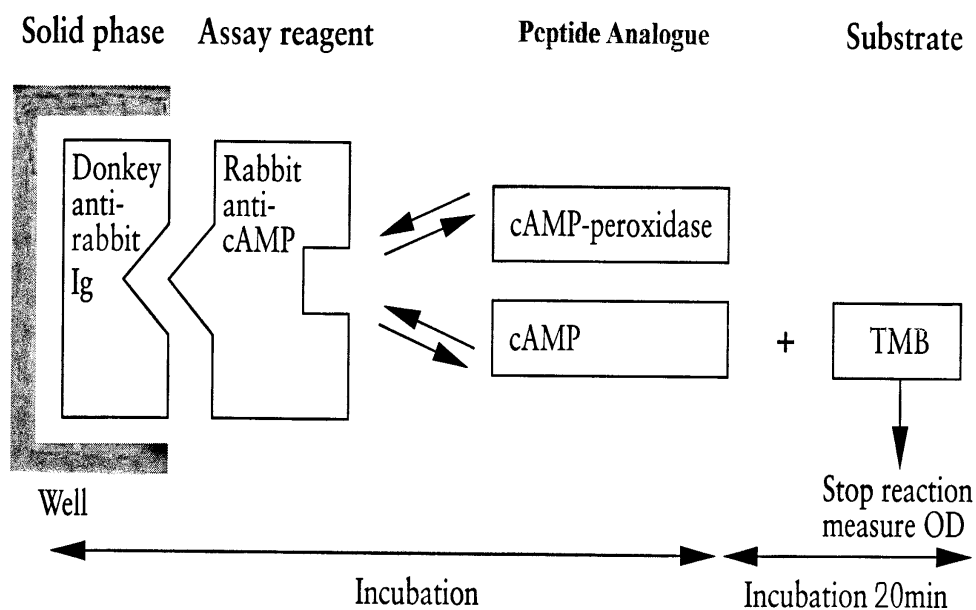
All analogues were compared to sCt which was the most potent ligand (EC_{50} = 0.03 nM) and hCt which had two-fold lower potency than sCt (EC_{50} = 0.072 nM). In the first group of peptides (Figure 28), the most active was CCcyclo (EC_{50} = 0.048 nM) followed by the other analogues in the order of: hCt = analog 1 (EC_{50} = 0.075 nM) > GCcyclo (EC_{50} = 0.154 nM) $\geq$ DCcyclo (EC_{50} = 0.177 nM) >>> FCcyclo (EC_{50} = 7.07 nM) >> CClinear (EC_{50} = 37.32 nM). Interestingly, CCcyclo was three times more potent than GCcyclo, though both peptides had 19-membered ring size. CClinear only weakly activated AC, which suggested that the lactam bridge is very important for both binding of the peptide to the receptor and the subsequent activation of the AC.
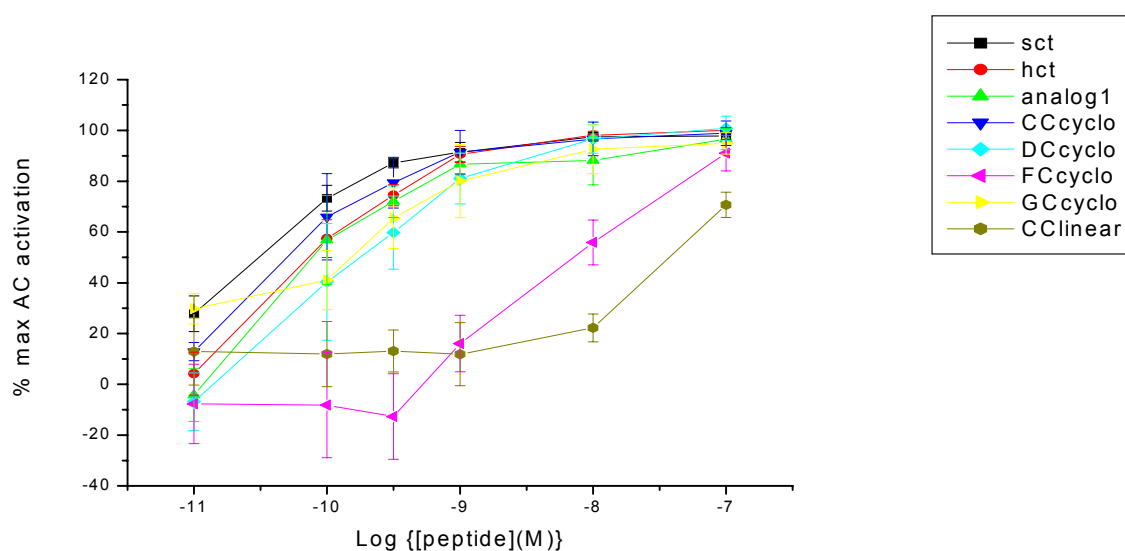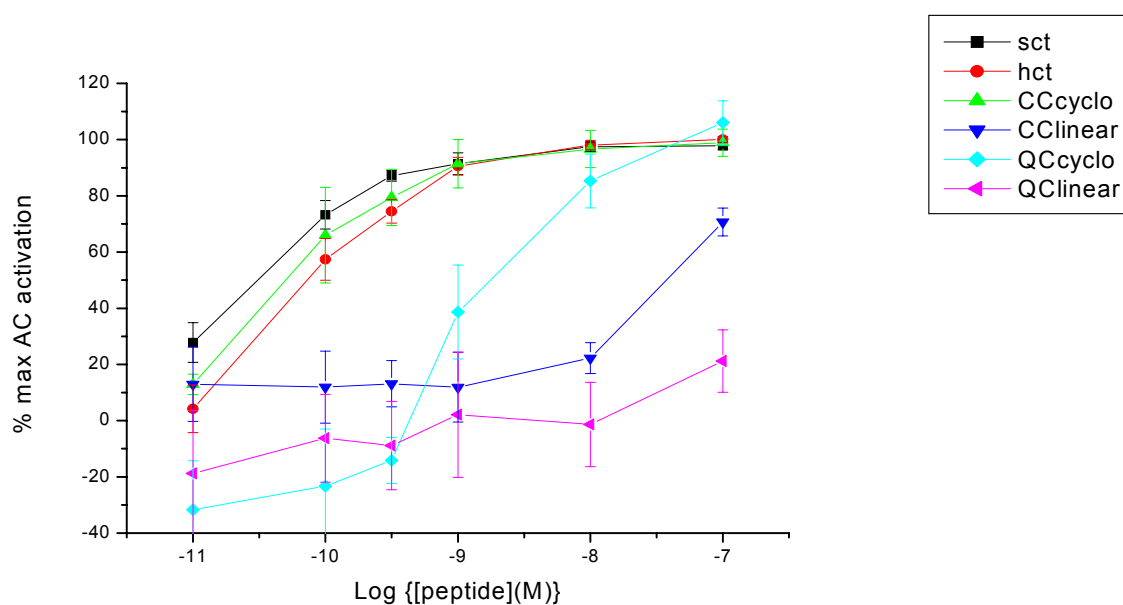

Figure 28. Activation of adenylate cyclase in T47D cells by analogues of group 1. Adenylyl cyclase activation above basal levels is plotted as a function of peptide concentration (on a log scale). Each point is the mean ± SD of two independent assays (performed in duplicate).

All analogues of the second group were less potent than analog 1 and native hCt (Figure 29). The order of the potencies was the following: hCt (EC_{50} = 0.072 nM) = analog 1 (EC_{50} = 0.075 nM) $\geq$ ACcyclo (EC_{50} = 0.095 nM) $\geq$ ECcyclo (EC_{50} = 0.177 nM) $\geq$ BCcyclo (EC_{50} = 0.234 nM) > OClinear (EC_{50} = 0.478 nM) >>> NClinear (EC_{50} = 10 nM). Thus, the presence of D-residues in the analogues affected the activation of the AC with the substitution D-Phe[19] for L-Phe[19] being better tolerated than the substitution of D-Lys[18] for L-Lys[18]. The non-bridged analogues OClinear and NClinear only weakly induced AC activation.
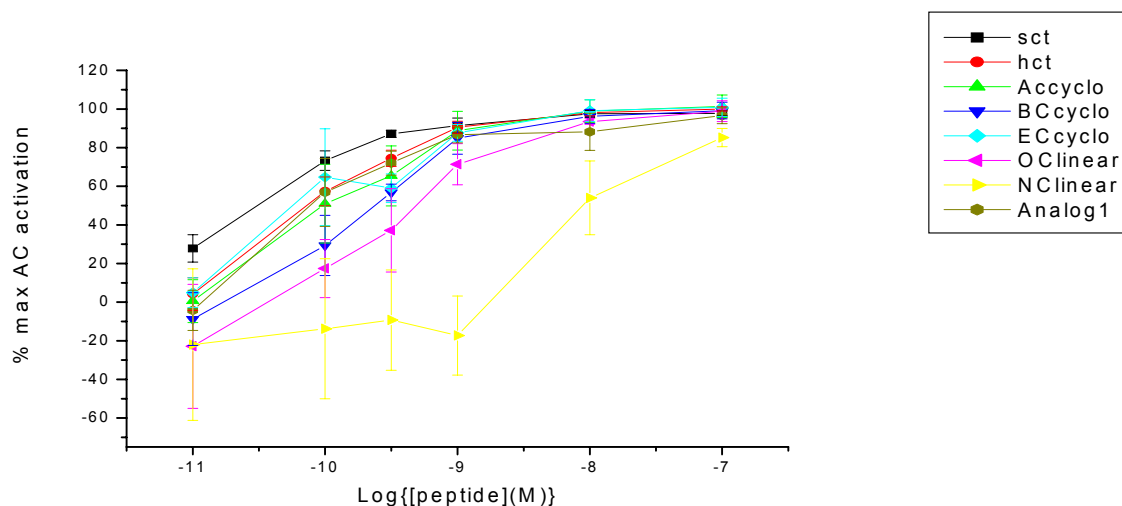
Figure 29. Activation of adenylate cyclase in T47D cells by analogues of group 2. Adenylyl cyclase activation above basal levels is plotted as a function of peptide concentration (on a log scale). Each point is the mean ± SD of two independent assays (performed in duplicate).

The third group of peptides with 'Asx-turn' compatible residues at positions 18, 19 (Pro[18], Ser[19]), exhibited extremely low potencies. Moreover, only the cyclo analogues: ICcyclo (EC_{50} = 3.71 nM) and HCcyclo (EC_{50} = 27.5 nM) activated AC, whereas the linear anlogues were completely devoid of activity (Figure 30). This was in agreement with the previously found lack of receptor binding (see 5.1.3).
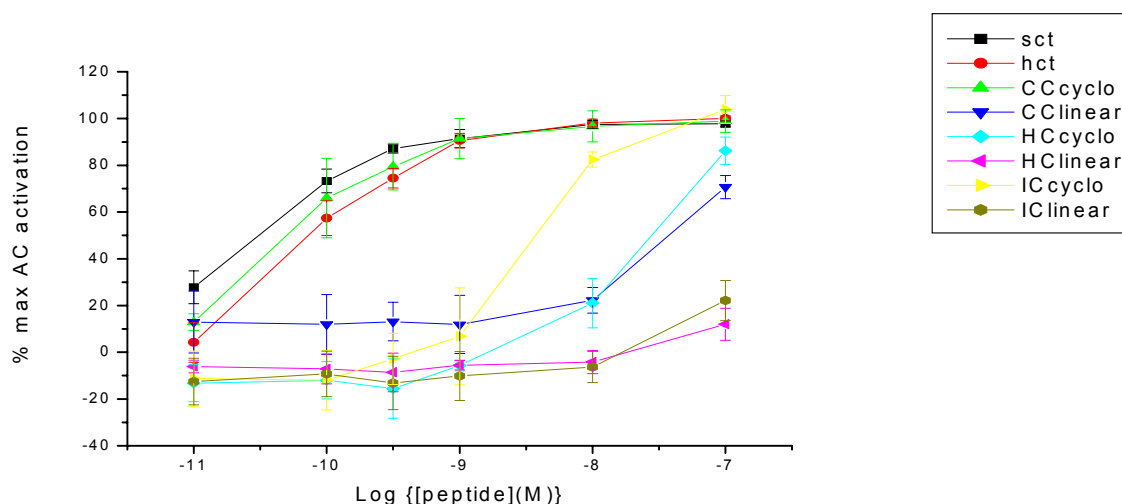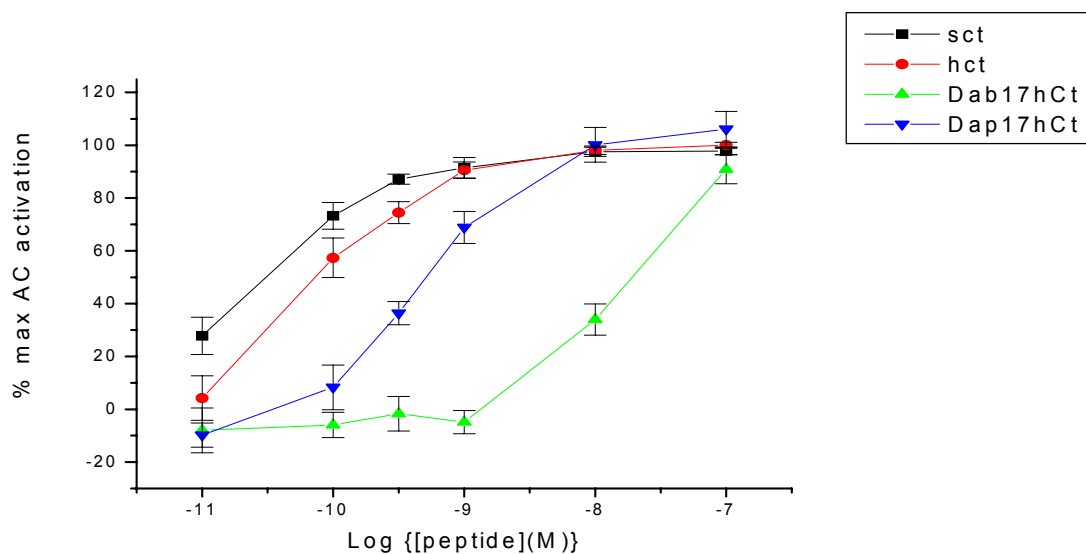

Figure 30. Activation of adenylate cyclase in T47D cells by analogues of group 3. Adenylyl cyclase activation above basal levels is plotted as a function of peptide concentration (on a log scale). Each point is the mean ± SD of two independent assays (performed in duplicate).

In the fourth group of peptides, only QCcyclo (EC_{50} = 1.73 nM) showed AC activation potency. By contrast, QClinear was extremely (as CClinear) low in activity (Figure 31). In QCcyclo the presence of (N-Me) Phe[19] residue, which is postulated to destroy a potential hydrogen bond between residues 17 and 19, was the main cause for the reduced activity compared to CCcyclo (see 5.1.3).

The same low potency was observed for analogues of the fifth group of peptides. In this group all the βeta-peptides (cyclo / linear analogues) exhibited low AC potencies (Figure 32). These results indicated that the extra methylene group (-CH_2-) in the backbone of these analogues was related to their extremely low potency.

Figure 31. Activation of adenylate cyclase in T47D cells by analogues of group 4. Adenylyl cyclase activation above basal levels is plotted as a function of peptide concentration (on a log scale). Each point is the mean ± SD of two independent assays (performed in duplicate).
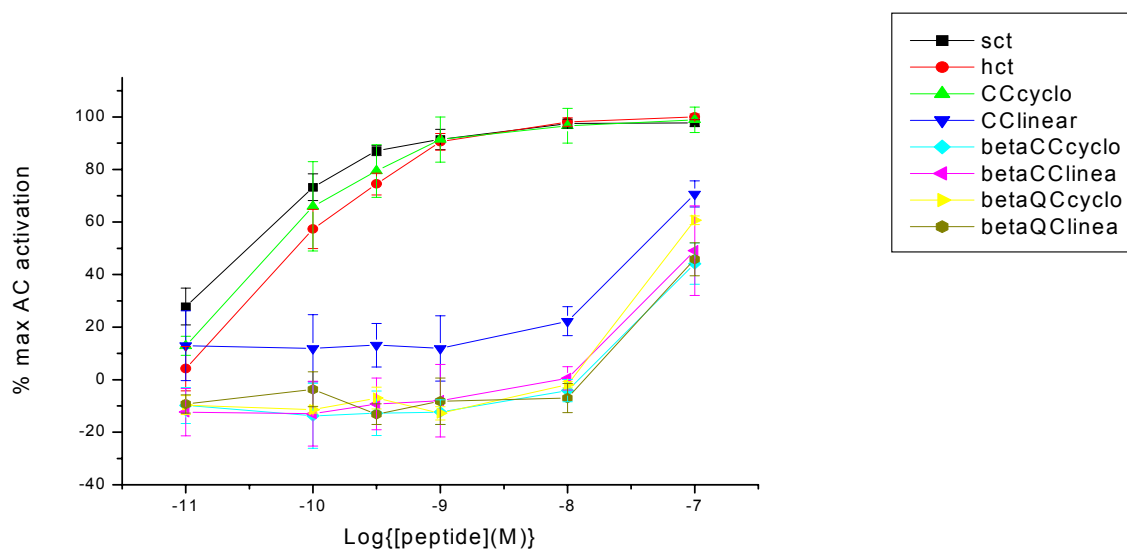
Figure 32. Activation of adenylate cyclase in T47D cells by analogues of group 5. Adenylyl cyclase activation above basal levels is plotted as a function of peptide concentration (on a log scale). Each point is the mean ± SD of two independent assays (performed in duplicate).

Next, the hCt analogues with the substitution Dap^{17} / Dab^{17} for Asn^{17} (group 6) were tested and found to exhibit significantly lower AC activation potency than hCt (Figure 33). Peptide $[Dap^{17}]$hCt (EC_{50} = 0.512 nM) was seven-fold less potent than hCt, where $[Dab^{17}]$hCt (EC_{50} = 19 nM) was thirty seven times less potent than $[Dap^{17}]$hCt. The results confirmed again that: a) the CO function of the side-chain of residue 17 is very important for AC activation and b) also the amino group of the side-chain of residue 17 and its topology play a role in AC activation.

The two peptides of group 7 bearing hydrophobic substitutions ($Leu^{12,16,19}$) for the aromatic amino acids and Tyr^{22} for Phe^{22} and Nle^{8} for Met^{8} were then examined (Figure 34). TCcyclo (EC_{50} = 0.038 nM) was almost as active as sCt, whereas the unbridged TClinear (EC_{50} = 0.275 nM) was seven times less active than sCt and almost four times less active than hCt. However, TClinear was hundred thirty five times more active than CClinear. The findings showed that: a) the decreased receptor binding affinity of TCcyclo as compared to sCt did not affect its AC activation and b) the hydrophobic residues and Tyr^{22} were important for the AC activation.

Figure 33. Activation of adenylate cyclase in T47D cells by analogues of group 6. Adenylyl cyclase activation above basal levels is plotted as a function of peptide concentration (on a log scale). Each point is the mean ± SD of two independent assays (performed in duplicate).
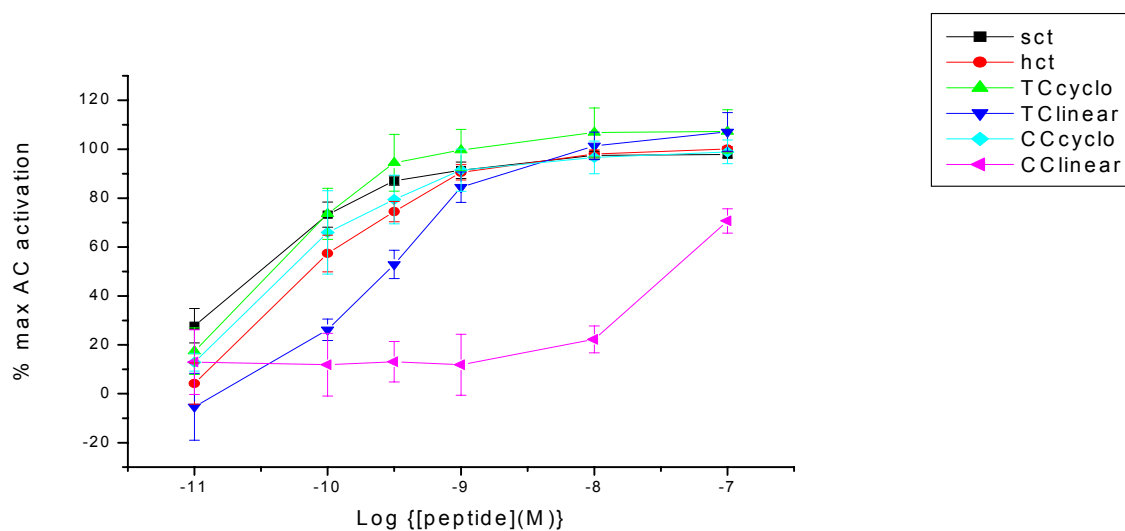
Figure 34. Activation of adenylate cyclase in T47D cells by analogues of group 7. Adenylyl cyclase activation above basal levels is plotted as a function of peptide concentration (on a log scale). Each point is the mean ± SD of two independent assays (performed in duplicate).

5.2 Design of IAPP analogues

To date there is yet no experimental structural model of amyloid fibrils of complete sequence IAPP available. IAPP [20-29] or SNNFGAILSS is a partial IAPP fragment that is able to form amyloid fibrils. This partial IAPP sequence has been broadly applied as a model IAPP sequence to identify the molecular determinants of IAPP amyloidogenicity at the level of primary and secondary structure [84].

According to studies by Griffiths and Lansbury [85], IAPP [20-29] fibrils have a highly pleated β-sheet structure between Gly^{24} and Ile^{26}. According to this model (Scheme 10), the β-sheet core of the amyloid fibrils consists of two antiparallel β-sheet strands each of them containing residues IAPP [23-27]. The β-sheet places the side chains of Gly^{24}, Ile^{26} and Ser^{28} on one face of the sheet and the side chains of Phe^{23}, Ala^{25}, Leu^{27} and Ser^{29} on the other side. This model has been confirmed by studies of Tenidis *et al.* [86], who showed that the short fragment IAPP [23-27] or FGAIL is able to form amyloid fibrils.
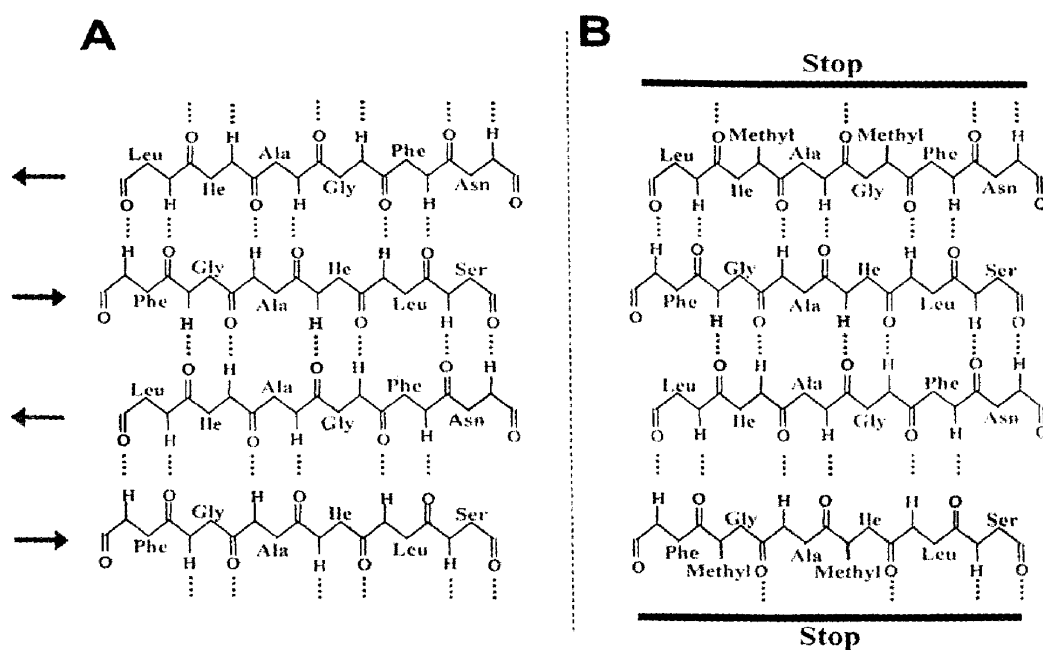
Scheme 10. (A) Proposed model of the Asn^{22}-Ser^{28} region of the intermolecular, antiparallel β-sheet of the amyloid core. The arrows on the left indicate the direction of the β-strands. (B) Hypothetical mechanism of inhibition of the lateral extension of the β-sheet model in (A) *via* selective N-methylation of Gly^{24} and Ile^{26} [87].

Based on the above model of IAPP fibril, FGAIL and other short amyloid forming fragments of IAPP were N-methylated at Gly^{24} and Ile^{26} [87]. The approach aimed at transforming these β-sheet prone, amyloidogenic and cytotoxic sequences into non-amyloidogenic and non-cytotoxic ones. In fact, the selective N-methylation of residues Gly^{24} and Ile^{26} in the short amyloid core IAPP sequences resulted in a complete abolishment of β-sheet, amyloid forming and cytotoxic properties of the native sequences.

Based on these results, the strategy of selective N-methylation of amide bonds was next applied to full sequence IAPP (in this work IAPP refers to hIAPP sequence) (Scheme 11). From the synthetic point of view, however, incorporation of N-methyl residues in peptide sequences has proven often to be a very difficult test due to insufficient coupling yields [88], or cleavage of amide bonds [89]. In addition, as the N-methyl residues were to be incorporated into amyloid core sequences, it was expected that the synthetic problems would increase. Therefore, a detailed study of the synthesis of 5 novel N-methylated IAPP analogues was undertaken. The N-methyl residues were designed to 'occupy' the one side of the potential β-strand of the IAPP [23-27] amyloid core sequence in analogues: [(N-Me) Phe^{23}, (N-Me) Ala^{25}] IAPP [1], [(N-Me) Gly^{24}, (N-Me) Ile^{26}] IAPP [2], and [(N-Me) Ala^{25}, (N-Me) Leu^{27}] IAPP [3]. In analogue [(N-Me) Ile^{26}, (N-Me) Leu^{27}] IAPP [4] it was attempted to introduce two consequent and in analogue [(N-Me) Ala^{25}, (N-Me) Ile^{26}, (N-Me) Leu^{27}] IAPP [5] three consequent N-methyl residues. Full sequence IAPP which is due to its exceptionally high amyloid-forming potential a very difficult synthetic task was also synthesized. In addition, an IAPP mutant S20G-IAPP [6] that has been associated with the early appearance of Type II diabetes in Japanese and has been reported to have even stronger amyloidogenic properties than IAPP [90] was synthesized. The structures of the synthesized analogues are shown in Scheme 11.

Scheme 11. Primary structures of IAPP, the N-methylated IAPP analogues [1] – [5] that were synthesized in this work, and analogue [6] with the S20G mutation. IAPP has a C-terminal amide which is not shown. The introduced substituents are shown in bold and the (N-Me) amino acids are shown using the three letter code.

```
  |‾‾‾‾|        10          20          30
KCNTATCATQ RLANFLVHSS NNFGAILSST NVGSNTY
```

IAPP

```
  |‾‾‾|                           23          25
KCNTATCATQRLANFLVHSSNN(NMe)PheG(NMe)AlaILSSTNVGSNTY
```

$[(\text{N-Me}) \text{ Phe}^{23}, (\text{N-Me}) \text{ Ala}^{25}]$ **IAPP [1]**

```
  |‾‾‾|                              24          26
KCNTATCATQRLANFLVHSSNNF(NMe)GlyA(NMe)IleLSSTNVGSNTY
```

$[(\text{N-Me}) \text{ Gly}^{24}, (\text{N-Me}) \text{ Ile}^{26}]$ **IAPP [2]**

```
  |‾‾‾|                               25          27
KCNTATCATQRLANFLVHSSNNFG(NMe)AlaI(NMe)LeuSSTNVGSNTY
```

$[(\text{N-Me}) \text{ Ala}^{25}, (\text{N-Me}) \text{ Leu}^{27}]$ **IAPP [3]**

```
  |‾‾‾|                                26          27
KCNTATCATQRLANFLVHSSNNFGA(NMe)Ile(NMe)LeuSSTNVGSNTY
```

$[(\text{N-Me}) \text{ Ile}^{26}, (\text{N-Me}) \text{ Leu}^{27}]$ **IAPP [4]**

```
  |‾‾‾|                             25          26          27
KCNTATCATQRLANFLVHSSNNFG(NMe)Ala(NMe)Ile(NMe)LeuSSTNVGSNTY
```

$[(\text{N-Me}) \text{ Ala}^{25}, (\text{N-Me}) \text{ Ile}^{26}, (\text{N-Me}) \text{ Leu}^{27}]$ **IAPP [5]**

```
  |‾‾‾|        10          20          30
KCNTATCATQ RLANFLVHSGly NNFGAILSST NVGSNTY
```

S20G-IAPP [6]

5.2.1 Synthesis of IAPP

As IAPP contains a C-terminal amide function, the synthesis was performed on Rink Amide MBHA resin (substitution level: 0.28 mmole / gr with regard to the C-terminal amino acid Tyr). The intended 'dilution' of the resin (0.2-0.3 mmole total amino groups) was achieved during the loading of the C-terminal Tyr. The synthesis was performed manually using DMF for washings and couplings, whereas a 25% solution of piperidine in DMF was used for the deprotection of the Fmoc-group. All couplings were performed twice, with an *in situ* activation protocol: briefly, Fmoc-amino acid (4-fold excess with regard to the mmoles of C-terminal Tyr) and TBTU (4-fold excess) were dissolved in DMF followed by the addition of DIEA (6-fold excess) in this activation mixture. The mixture was then added to the N^α-deprotected resin. Each coupling cycle was 60-90 min and completeness of the couplings was checked by the Kaiser test (for residues in the region IAPP [17-37]). The C-terminal ten residues IAPP [28-37] or SSTNVGSNTY were coupled without any difficulty and the identity of the correct decapeptide on the resin was confirmed by cleavage of a small amount of the peptide resin and characterization of the product by RP-HPLC (retention time) and MALDI-MS. Cys^2 and Cys^7 were coupled by the HOBt-ester coupling method as described for the Ct sequences. Accordingly, AA activation was performed by HOBt / DIC (in equimolar amounts to the amino acid) at 4 °C for 45 min as described. The activation mixture was added to the N^α-deprotected peptide resin and left to react for 90 min, followed by a second coupling using the same method. No acetylations were performed throughout the synthesis.

The progress of the synthesis was evaluated by cleavage at position 19. After incorporation of residue Ser^{19}, a small sample of peptide resin was subjected first to Fmoc-cleavage and then to a mixture of TFA / H_2O (95/5 v/v) (2 hrs, RT). Following filtration of the resin, the solution was subjected to RP-HPLC analysis (Figure 35). MALDI-MS showed that the peak at 16.9 min had the expected mass for IAPP [19-37] (Figure 36): ($[M+H]^+$ expected: 1933.1, found: 1935.2). The RP-HPLC profile of IAPP [19-37] also indicated that the synthesis proceeded in good yields up to residue 19.
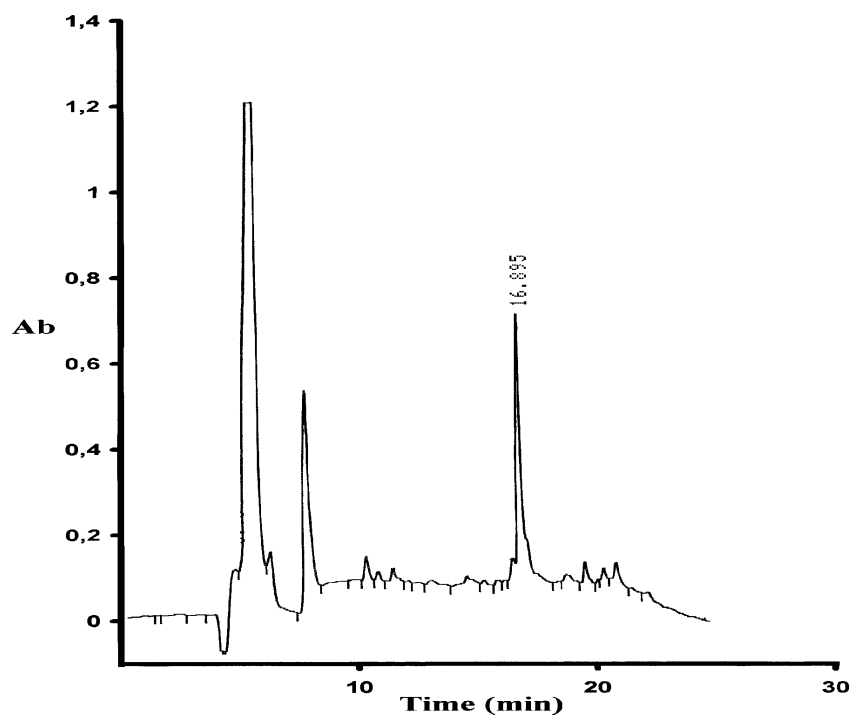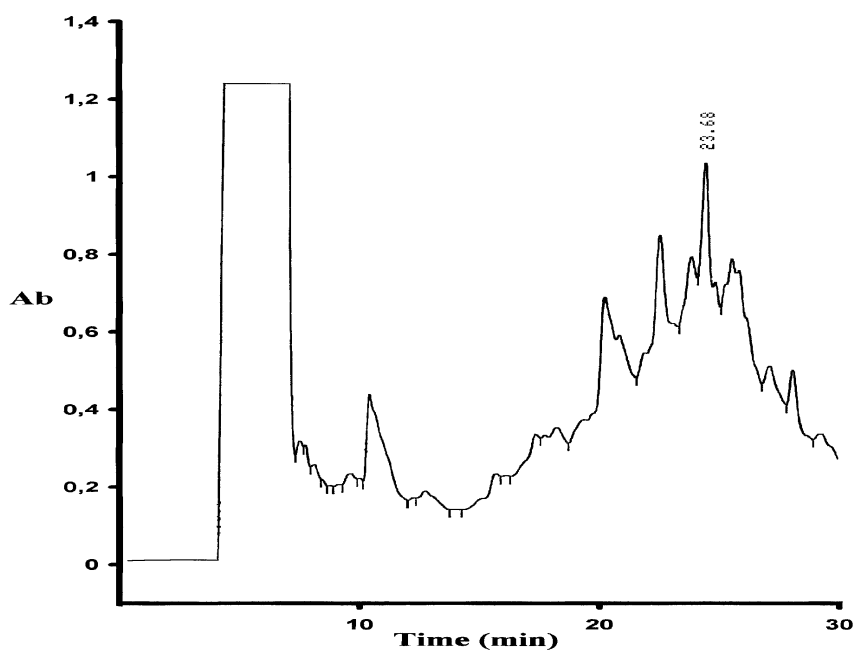
Figure 35. RP-HPLC analysis of crude IAPP [19-37] using gradient 2 on C_{18} column, flow rate 2 ml / min and detection at 214 nm. Injection of 0.2 mg crude peptide in 100 µl aqueous 10% TFA solution.
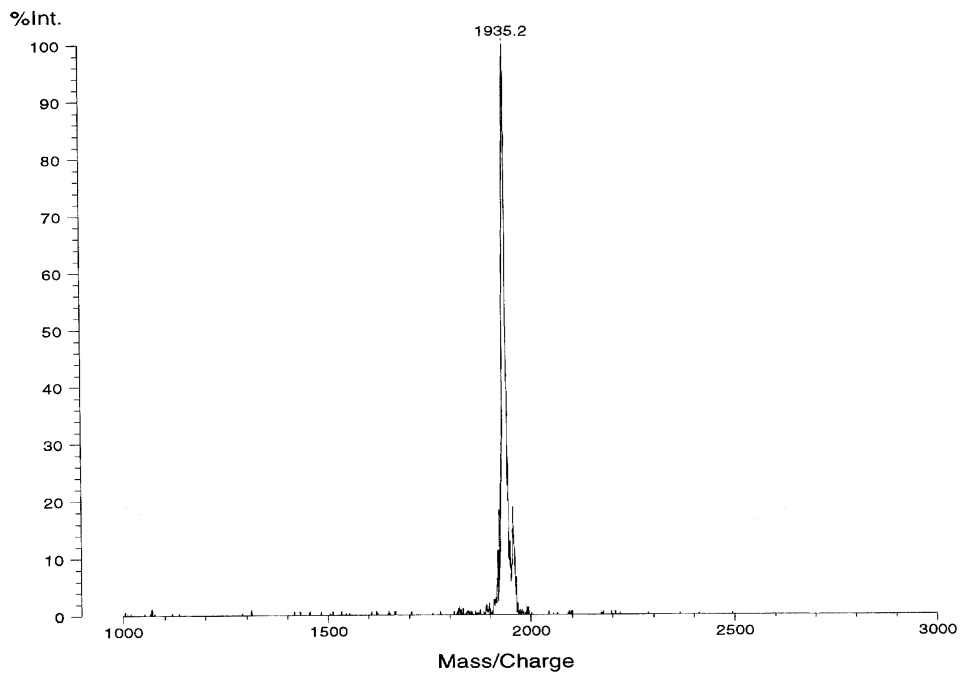

Figure 36. MALDI-MS of HPLC-purified peak at 16.9 min (see Figure 35) from crude IAPP [19-37].

Residues 18 to1 were coupled using the same protocol as above. There was no Kaiser test after the coupling / deprotection step; only before and after the coupling of the Cys^2 and Cys^7 a Kaiser test was performed. At the end of the synthesis aliquots of dry peptide resin were treated with reagent K (3 hrs, RT). Following evaporation of TFA the crude peptide was suspended in 10% AcOH, washed with Et_2O three times and the aqueous phase lyophilised overnight and analysed by RP-HPLC. Crude IAPP was not soluble in 10% AcOH, (even at 0.3 mg / ml), probably due to aggregation. Crude IAPP was however good soluble in aqueous 8 M urea. The chromatographic separation was however difficult (Figure 37). The profile of the crude material (dissolved in aqueous 8 M urea solution) indicated either the presence of several by-products of the synthesis or that the peptide aggregated on the column. The peak at 23.7 min corresponded according to MALDI-MS to the reduced product IAPP ($[M+H]^+$ expected 3906.4, found 3905.0). The reduced form of the peptide was collected by preparative RP-HPLC, lyophilised and subjected to air oxidation for the formation of the intramolecular disulfide bond between the two cysteines. The oxidation (1 mg / ml) was performed in 6 M Gdn HCl in aqueous 0.1 M NH_4HCO_3 (in the dark) and required ~ 4 hrs for completion. Oxidized products were separated by HPLC retention time (Figure 38). A deletion sequence was identified during the purification of the peptide, which coeluted with reduced IAPP. The mass of the deletion product (peak at 23.7 min) was found to be 3156 and could correspond to fragment IAPP [9-37] ($[M+K]^+$ expected: 3151.5), due to incomplete coupling at this region (incomplete coupling of Ala^8 to Thr^9). The peak at 24.8 min corresponded according to MALDI-MS to the oxidized product IAPP (Figure 39) ($[M+H]^+$ expected 3904.4, found 3901.7). An analytical RP-HPLC of pure, oxidized IAPP is shown in Figure 40. The overall yield of oxidized peptide with regard to the crude peptide was 3%.

Figure 37. RP-HPLC analysis of crude IAPP (in reduced form) using gradient 1 on C_{18} column, flow rate 2 ml / min and detection at 214 nm. Injection of 1 mg crude peptide in 1 ml aqueous 8 M urea solution.
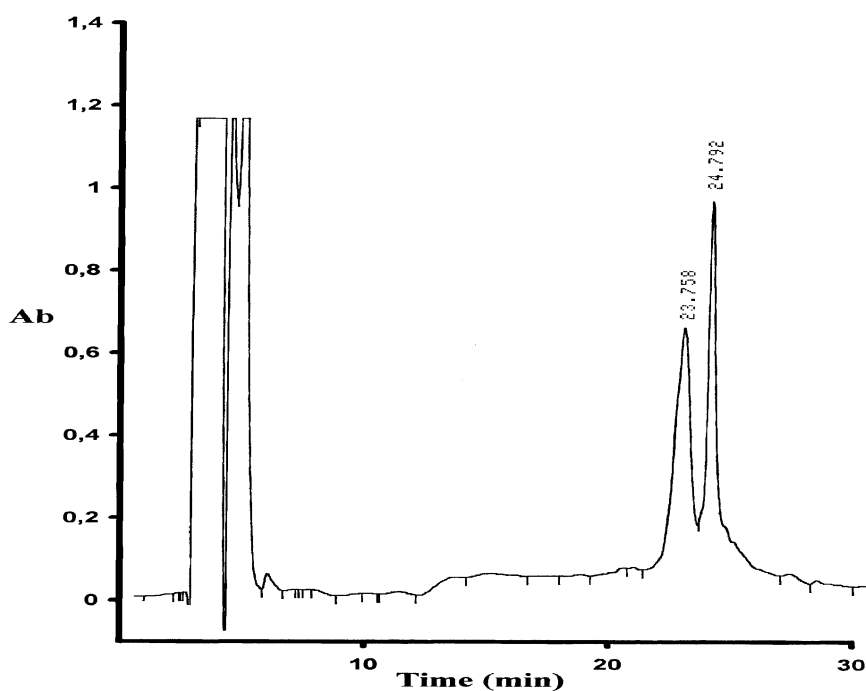
Figure 38. RP-HPLC analysis of crude IAPP (in oxidized form) using gradient 1 on C_{18} column, flow rate 2 ml / min and detection at 214 nm. Injection of 100 µg crude peptide in 250 µl in aqueous 0.1 M NH_4HCO_3 solution containing 6 M Gdn HCl.
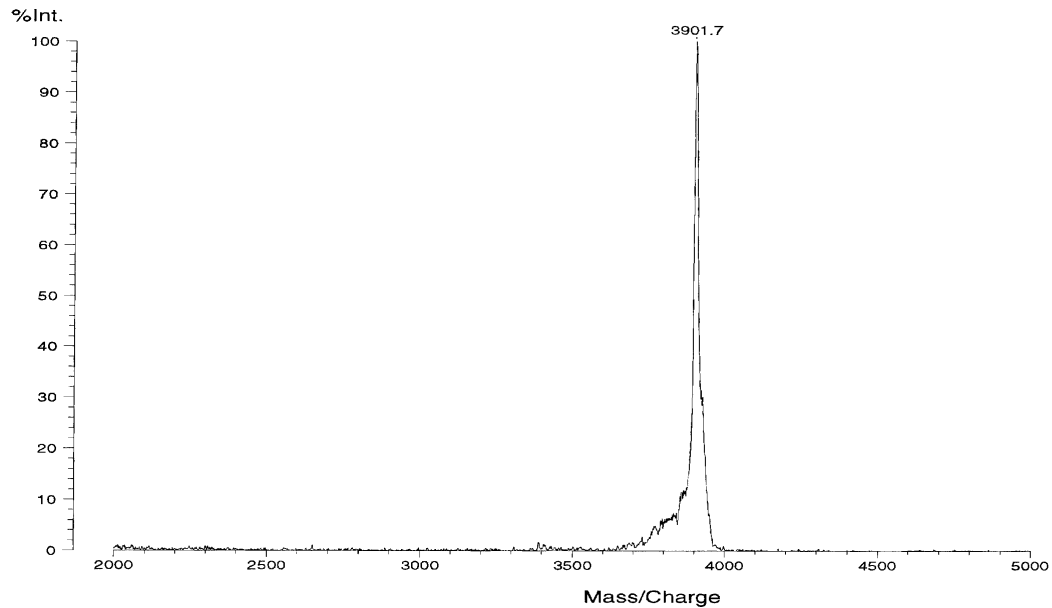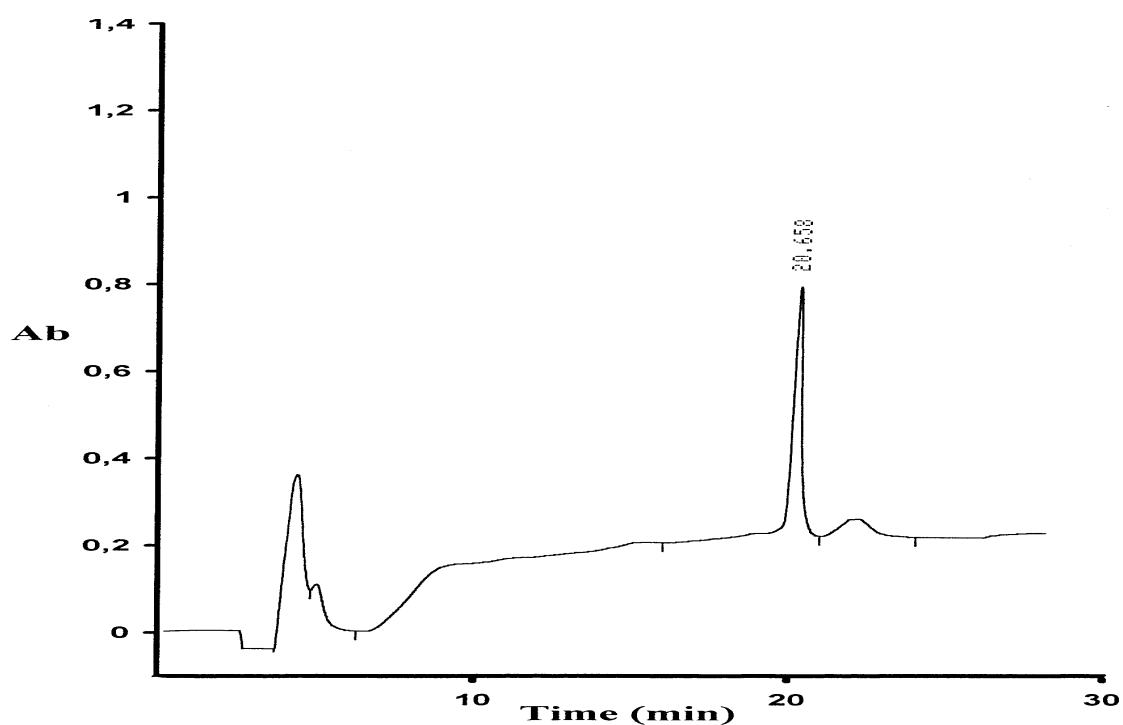
Figure 39. MALDI-MS of HPLC purified peak at 24.8 min (see Figure 38) from crude IAPP (oxidized form).

Figure 40. RP-HPLC analysis of pure IAPP (in oxidized form) using gradient 2 on C_{18} column, flow rate 2 ml / min and detection at 214 nm. Injection of 10 µg pure peptide in 100 µl aqueous 100 mM HCl.

5.2.2 Synthesis of [(N-Me) Phe²³, (N-Me) Ala²⁵] IAPP [1]

Synthesis was performed manually by the Fmoc-strategy on Rink MBHA resin (substitution level: 0.25 mmole / gr with regard to C-terminal Tyr residue). Amino acids were coupled twice using 4-fold excess (with regard to Tyr) of the Fmoc-protected AA and TBTU in DMF and 6-fold excess DIEA for the activation mixture. The synthesis was performed as described for IAPP (see 5.2.1). A different coupling procedure was used for region [19-25]: (N-Me) Ala²⁵ was coupled twice using 5-fold excess (2 x 90 min), and the next residue Gly²⁴ was coupled also twice using 5-fold excess (1 x 75 min, 1 x 15 hrs). Following cleavage of a small amount of [(N-Me) Ala²⁵] IAPP [24-37] resin and subsequent RP-HPLC purification (Figure 41), the main peak at 15.1 min was identified as the expected product [(N-Me) Ala²⁵] IAPP [24-37] ([M+H]⁺ expected: 1398.5, found: 1397.0). The Fmoc-protected peptide resin [(N-Me) Ala²⁵] IAPP [24-37] was then acetylated before proceeding with the couplings.

The couplings of the next two residues were more difficult: in the case of (N-Me) Phe²³ a 6-fold excess of amino acid was used and a solvent mixture of DCM / DMF / NMP (1:1:1 v/v/v) was applied (1 x 90 min, 1 x 15 hrs). Before proceeding with the next residue, the peptide resin Fmoc-[(N-Me) Phe²³, (N-Me) Ala²⁵] IAPP [23-37] was acetylated. The coupling of Asn²² to (N-Me) Phe²³ required three attempts: two with 6-fold excess (2 x 90 min) and a third one with 10-fold excess (1 x 14 hrs). In addition the above mentioned solvent mixture (equal volumes of DCM / DMF / NMP) was applied for the couplings. Cleavage of a small amount of [(N-Me) Phe²³, (N-Me) Ala²⁵] IAPP [22-37] resin (before acetylation of non-reacted groups of (N-Me) Phe²³) and subsequent RP-HPLC purification (Figure 42) showed that the peak at 18.0 min was the expected product [(N-Me) Phe²³, (N-Me) Ala²⁵] IAPP [22-37] ([M+H]⁺ expected: 1674.8, found: 1674.2) according to MALDI-MS (Figure 43). The shoulder at 17.4 min was [(N-Me) Phe²³, (N-Me) Ala²⁵] IAPP [23-37] ([M+H]⁺ expected: 1560.7, found: 1559.2) and indicated that the coupling of Asn²² to (N-Me) Phe²³ was 60 to 70% complete. The peptide resin Fmoc-[(N-Me) Phe²³, (N-Me) Ala²⁵] IAPP [22-37] was acetylated, where the next residue Asn²¹ was coupled twice: one with 6-fold excess (1 x 145 min) and a second one with 10-fold excess (1 x 16 hrs). The Fmoc-protected peptide resin [(N-Me) Phe²³, (N-Me) Ala²⁵] IAPP [21-37] was acetylated.

Taken together, in the region [21-25] couplings were found to be more difficult than the previous ones, as evaluated by small cleavages of resin and RP-HPLC profiling, which might has been due to the presence of bulky side chains protecting groups (Trt) in combination with the N-methyl groups of Ala²⁵ and Phe²³. Therefore, to enhance the coupling efficiencies we

increased the amount of the reagents (up to 10-fold excess), the time of the reactions (up to 16 hrs) and utilized a mixture of solvents as detailed above. The next two residues (Ser[20] and Ser[19]) were coupled twice using 6-fold excess of amino acid (2 x 60 min). At this point, a small cleavage of peptide resin and RP-HPLC separation of the mixture (Figure 44) showed the presence of two products: one peak at 15.3 min with a mass of 1397, corresponding to [(N-Me) Ala[25]] IAPP [24-37] ([M+H]$^+$ expected: 1398.5) and the main fraction at 17.1 min with the correct mass for [(N-Me) Phe[23], (N-Me) Ala[25]] IAPP [19-37] ([M+Na]$^+$ expected: 1985.1, found: 1982.2) (Figure 45). The formation of the product at 15.3 min could be explained as follows: incomplete coupling of Asn[22] on (N-Me) Phe[23] (see Figure 42) and the subsequent acetylation of the peptide resin. The truncated peptide Ac-[(N-Me) Phe[23], (N-Me) Ala[25]] IAPP [23-37] would have been then still attached to the resin during the subsequent synthetic steps. However, during the TFA cleavage of the [(N-Me) Phe[23], (N-Me) Ala[25]] IAPP [19-37] peptide resin, the peptide bond between Ac-(N-Me) Phe[23] and Gly[24] might have been cleaved leading to the formation of the partial fragment [(N-Me) Ala[25]] IAPP [24-37] which was eluting at 15.3 min (Figure 44). This mechanism could be in accordance with the mechanism of acidic hydrolysis of N-alkylated peptides during TFA deprotection conditions proposed by Urban *et al.* [15] (see also 3.1.2, Figure 4).
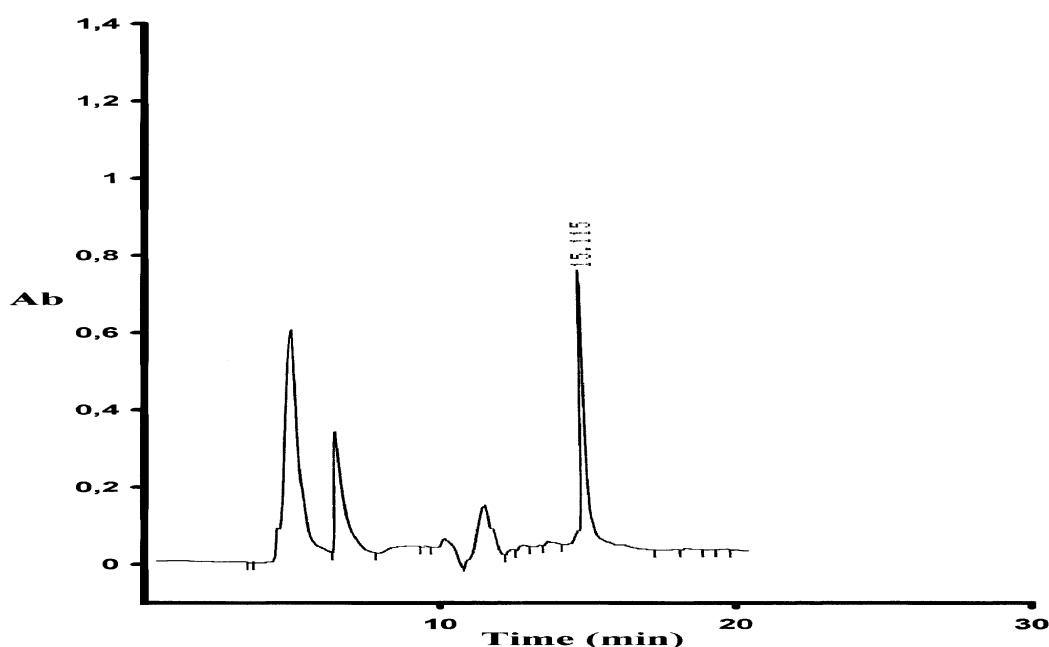
Figure 41. RP-HPLC analysis of crude [(N-Me) Ala[25]] IAPP [24-37] using gradient 2 on C$_{18}$ column, flow rate 2 ml / min and detection at 214 nm. Injection of 40 µg of crude peptide in 100 µl aqueous 10% TFA solution.
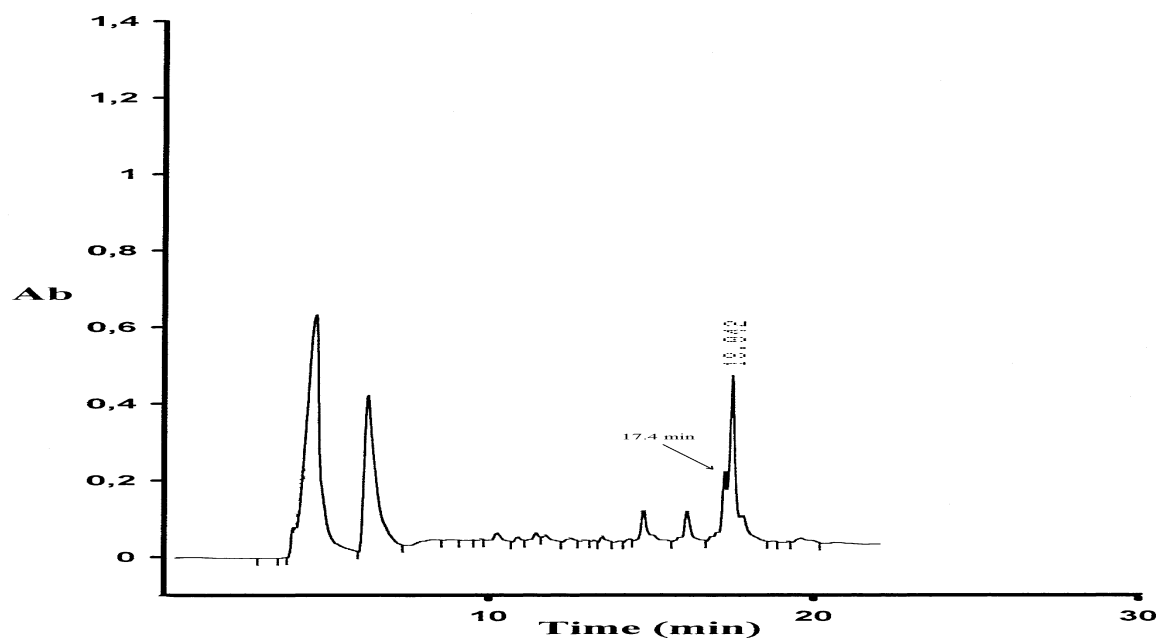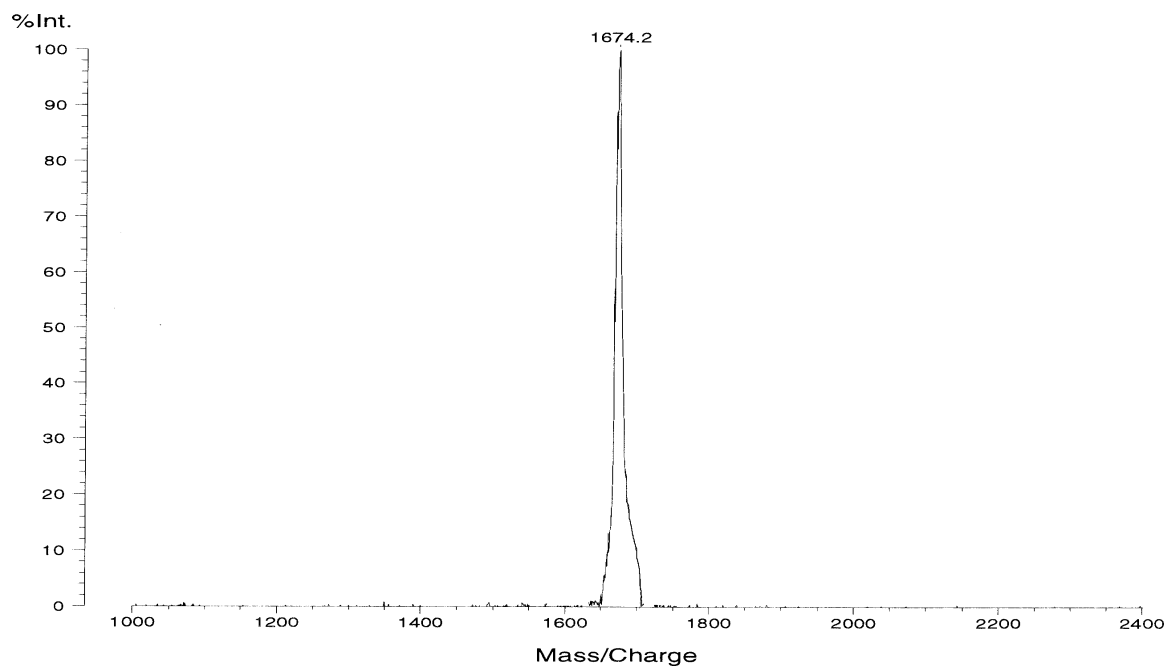
Figure 42. RP-HPLC analysis of crude [(N-Me) Phe[23], (N-Me) Ala[25]] IAPP [22-37] using gradient 2 on C_{18} column, flow rate 2 ml / min and detection at 214 nm. Injection of 50 µg of crude peptide in 100 µl aqueous 10% TFA solution.

Figure 43. MALDI-MS of HPLC purified peak at 18.0 min (see Figure 42) from crude [(N-Me) Phe[23], (N-Me) Ala[25]] IAPP [22-37].
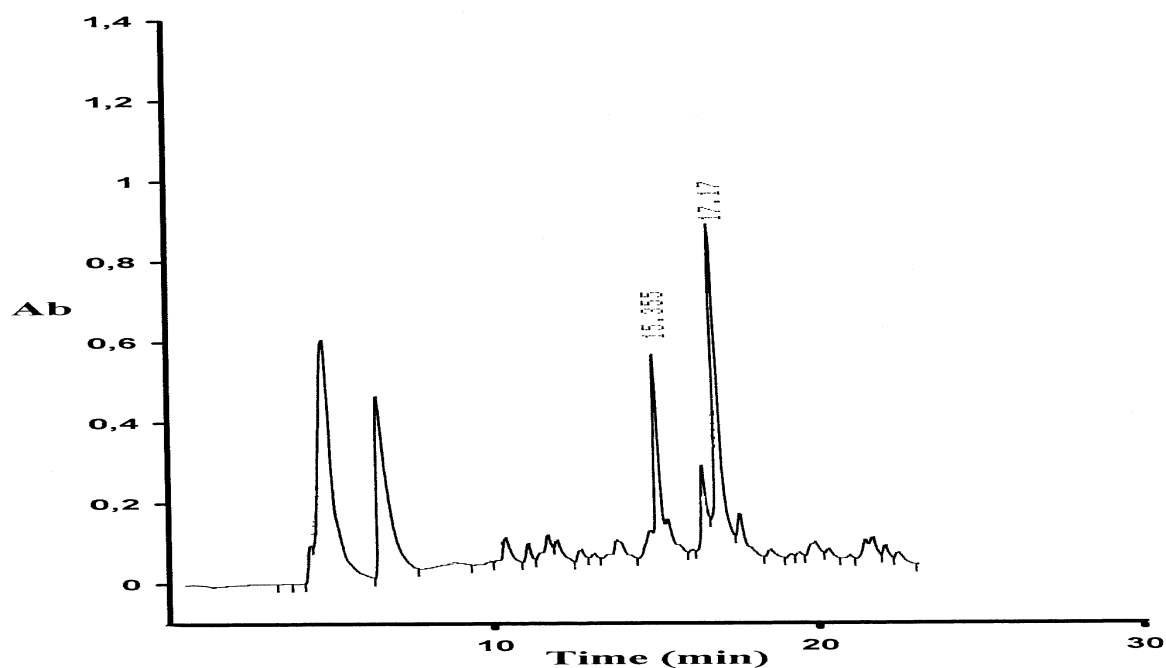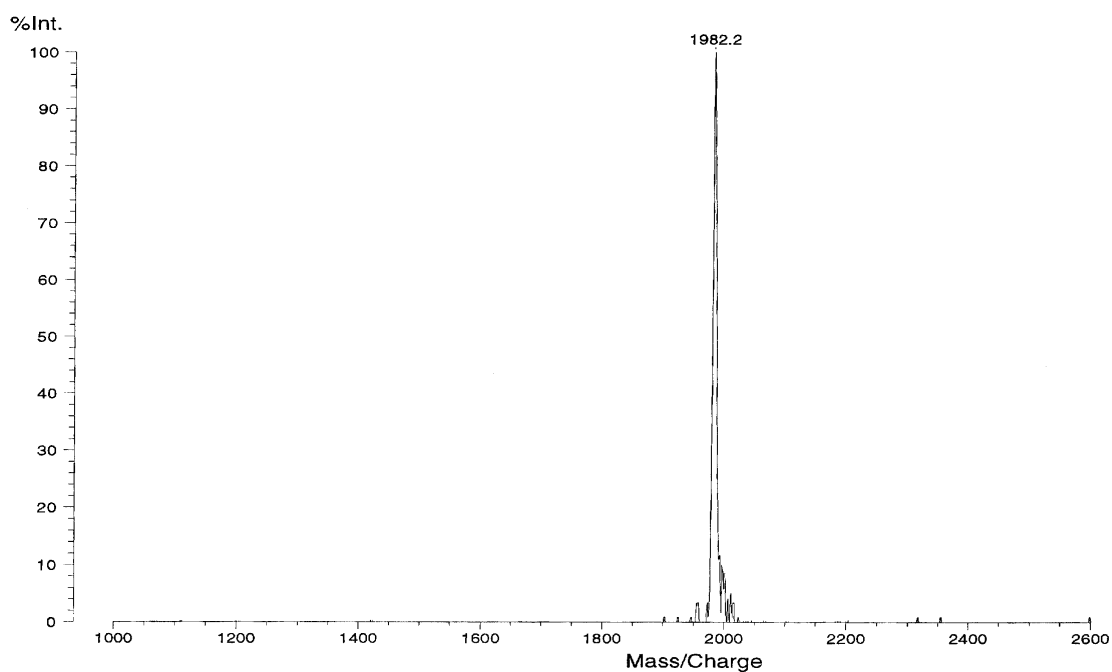
Figure 44. RP-HPLC analysis of crude [(N-Me) Phe^{23}, (N-Me) Ala^{25}] IAPP [19-37] using gradient 2 on C$_{18}$ column, flow rate 2 ml / min and detection at 214 nm. Injection of 60 µg of crude peptide in 100 µl aqueous 10% TFA solution.

Figure 45. MALDI-MS of HPLC purified peak at 17.1 min (see Figure 44) from crude [(N-Me) Phe^{23}, (N-Me) Ala^{25}] IAPP [19-37].

The remaining eighteen residues (His[18] till Lys[1]) were coupled twice, using 4-fold excess for the amino acids and TBTU and 6-fold excess for DIEA. Each coupling cycle was about 60 to 80 min, with a Kaiser test done after the couplings of His[18], Val[17], Leu[16], Thr[9], and Cys[7]. Cys[7] and Cys[2] were doubly coupled using the HOBt-ester coupling method as described (see 5.2.1) (1 x 80 min, 1 x 75 min). No acetylations were performed in the region [1-18].

At the end of the synthesis, the peptide resin was cleaved with reagent K (3 hrs, RT). Crude product was dissolved in 10% AcOH, followed by Et_2O washes (3 times) and lyophilised overnight. The crude lyophilised peptide was then dissolved in 50% AcOH, a small amount of dithiothreitol (DTT) was added and the solution (after warming at 45 °C for 45 min) was analysed by RP-HPLC (Figure 46). The main peak at 22.5 min was identified by MALDI-MS to correspond to the expected product [(N-Me) Phe[23], (N-Me) Ala[25]] IAPP ($[M+H]^+$ expected: 3936.4, found: 3934.3), where the adjacent peaks were deletion products of the synthesis: the peak at 22.0 min had a mass of 3833.4 and corresponded to a deletion peptide missing one Cys residue ($[M+H]^+$ expected: 3833.3), and the peak at 23.5 min most probably corresponded to [(N-Me) Phe[23], (N-Me) Ala[25]] IAPP [8-37] as was indicated by MALDI-MS. During the air oxidation of the crude peptide (1 mg / ml) in aqueous 0.1 M NH_4HCO_3 containing 3 M Gdn HCl (Figure 47), the main peak was shifted one minute later (at 23.6 min) overlapping with one of the two deletion products. Therefore, it was necessary to search for alternative chromatographic conditions to purify the crude product. This was achieved by changing the gradient of buffer B in A from 35% to 55% in 27 min (gradient 3). The oxidation procedure (in the dark) required at least four hours and at these chromatographic conditions (Figure 48), the peak eluting at 19.1 min corresponded according to MALDI-MS to [(N-Me) Phe[23], (N-Me) Ala[25]] IAPP (Figure 49) ($[M+H]^+$ expected: 3934.4, found: 3931.9), where the peak eluting at 18.4 min corresponded according to MALDI-MS to the truncated peptide [(N-Me) Phe[23], (N-Me) Ala[25]] IAPP [8-37] due to incomplete coupling of Cys[7] to Ala[8] ($[M+K]^+$ expected: 3252.7, found: 3251.2) (Figure 50).

An analytical RP-HPLC of pure, oxidized [(N-Me) Phe[23], (N-Me) Ala[25]] IAPP is shown in Figure 51. The overall yield of oxidized peptide with regard to the crude peptide was 3%.
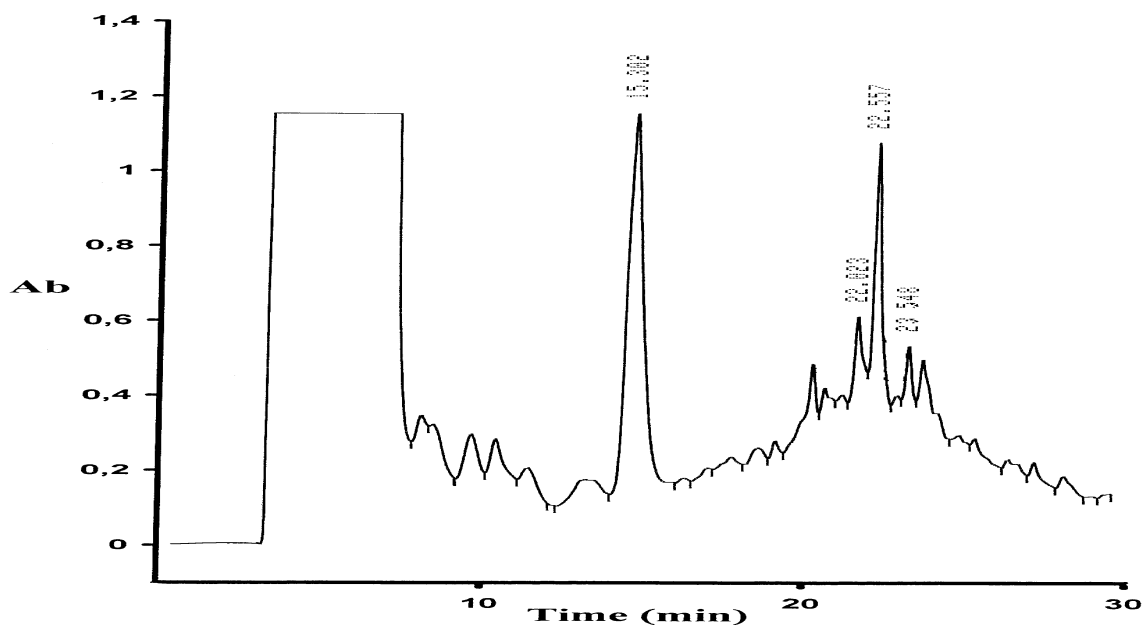
Figure 46. RP-HPLC analysis of crude [(N-Me) Phe[23], (N-Me) Ala[25]] IAPP (in reduced form) using gradient 1 on C_{18} column, flow rate 2 ml / min and detection at 214 nm. Injection of 200 μg of crude peptide in 300 μl aqueous 50% AcOH solution (the peak at 15.3 min is due to scavenger phenol from the cleavage mixture).
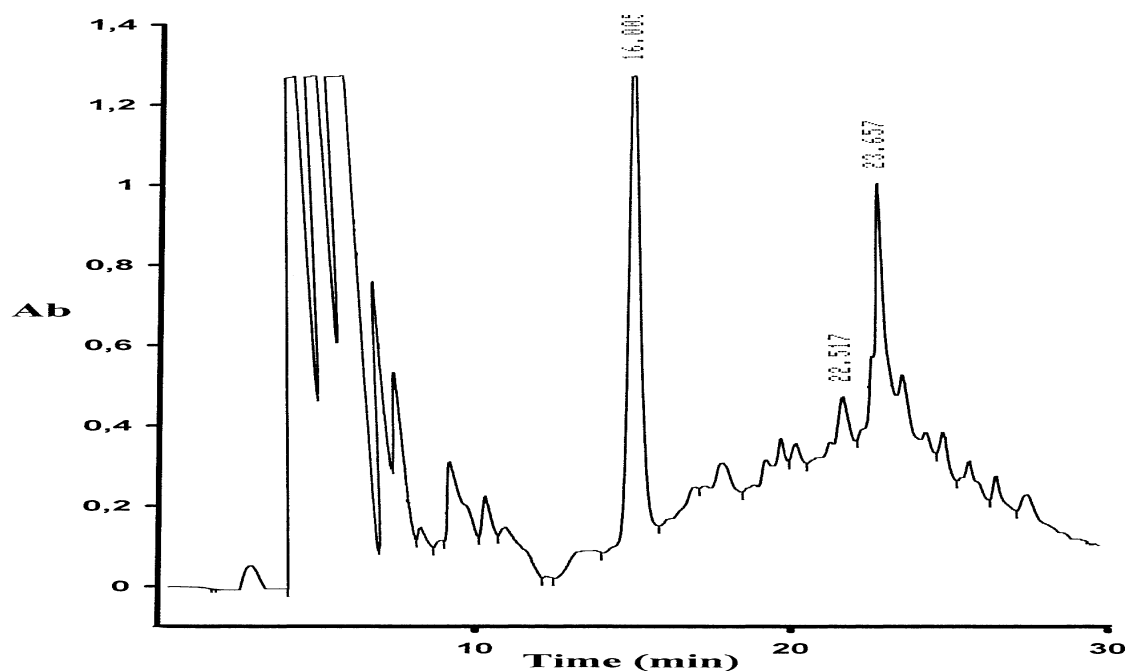

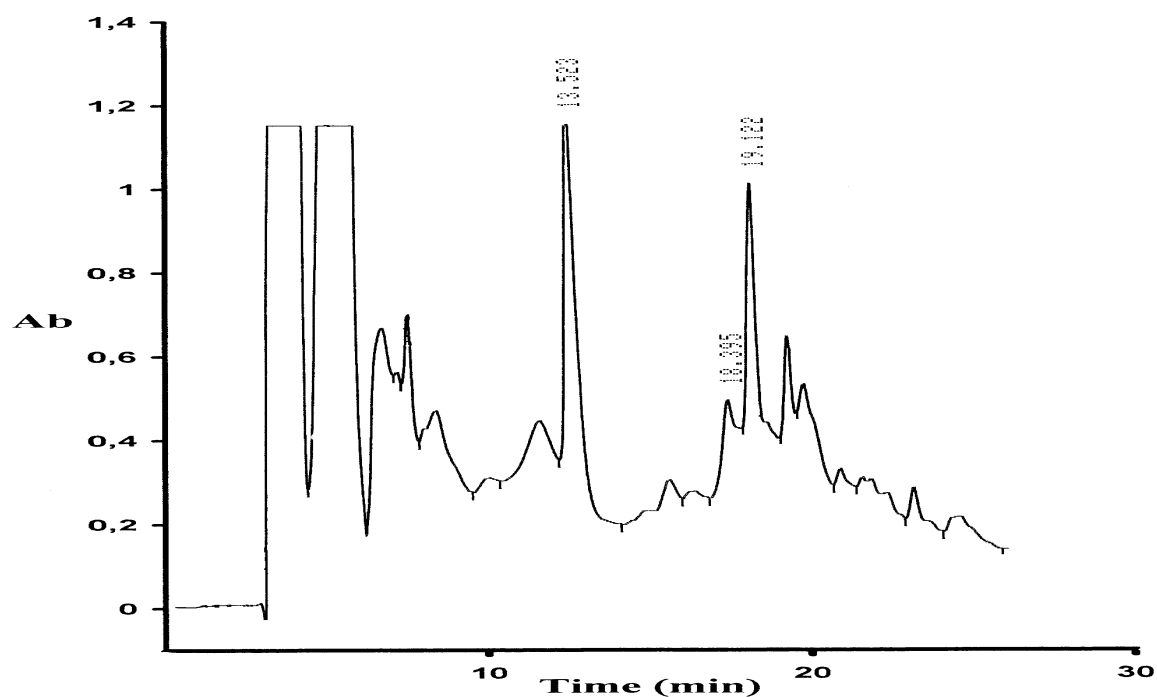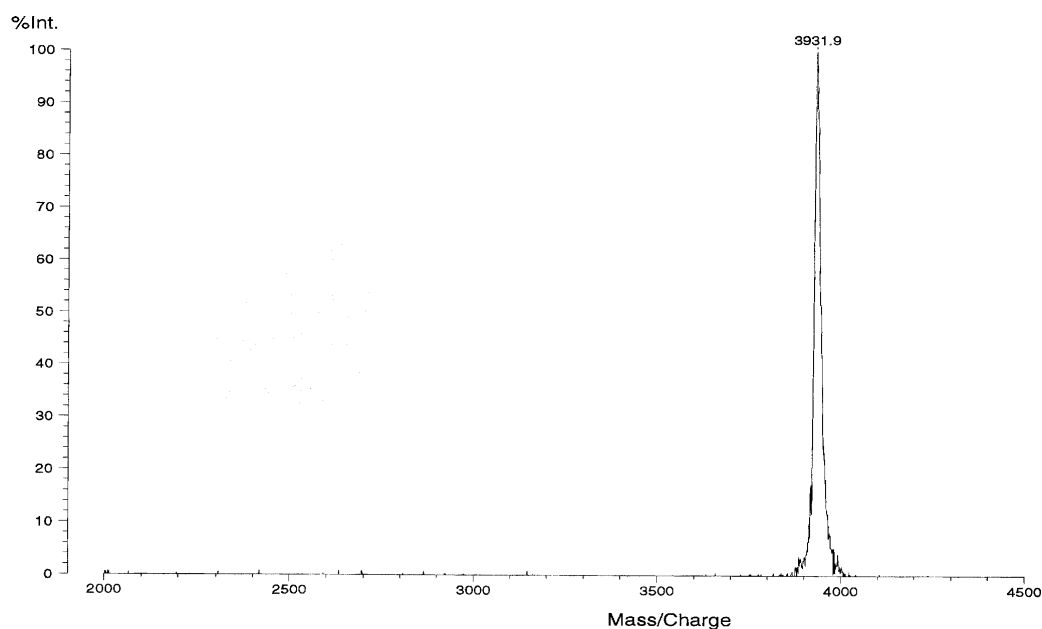**Figure 47.** RP-HPLC analysis of crude [(N-Me) Phe[23], (N-Me) Ala[25]] IAPP (in oxidized form) using gradient 1 on C_{18} column, flow rate 2 ml / min and detection at 214 nm. Injection of 200 μg of crude peptide in 400 μl 3 M Gdn HCl in aqueous 0.1 M NH_4HCO_3 solution (the peak at 16.0 min is due to scavenger phenol from the cleavage mixture).

Figure 48. RP-HPLC analysis of crude [(N-Me) Phe^{23}, (N-Me) Ala^{25}] IAPP (in oxidized form) using gradient 3 on C$_{18}$ column, flow rate 2 ml / min and detection at 214 nm. Injection of 1 mg crude peptide in 1 ml 3 M Gdn HCl in aqueous 0.1 M NH$_4$HCO$_3$ solution (the peak at 13.5 min is due to scavenger phenol from the cleavage mixture).

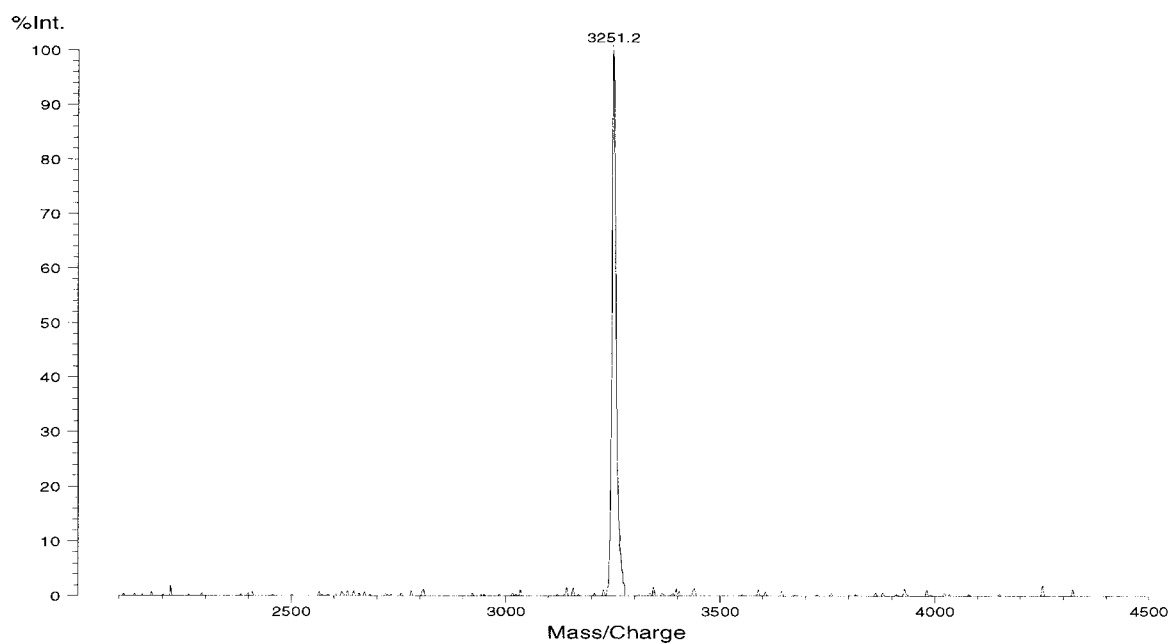**Figure 49.** MALDI-MS of oxidized, HPLC purified peak at 19.1 min (see Figure 48) corresponding to [(N-Me) Phe^{23}, (N-Me) Ala^{25}] IAPP.

Figure 50. MALDI-MS of HPLC purified peak at 18.4 min (see Figure 48) most probably corresponding to [(N-Me) Phe^{23}, (N-Me) Ala^{25}] IAPP [8-37].
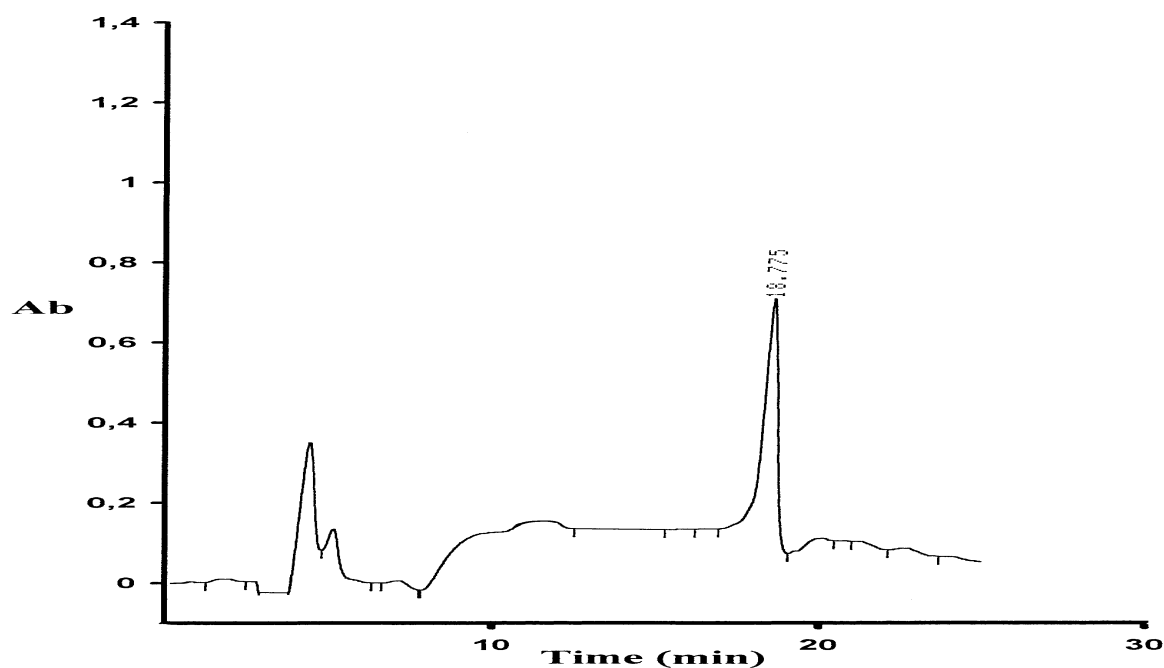
Figure 51. RP-HPLC analysis of pure [(N-Me) Phe^{23}, (N-Me) Ala^{25}] IAPP (in oxidized form) using gradient 2 on C$_{18}$ column, flow rate 2 ml / min and detection at 214 nm. Injection of 12 μg pure peptide in 100 μl aqueous 100 mM HCl.

5.2.3 Synthesis of [(N-Me) Gly^{24}, (N-Me) Ile^{26}] IAPP [2]

The standard Fmoc-protocol was applied on Rink MBHA resin (substitution level: 0.21 mmole Tyr / gr). Each residue was coupled twice (4-fold excess) with TBTU (4-fold excess) and DIEA (6-fold excess) (2 x 90 min). (N-Me) Ile^{26} was coupled three times (4-fold excess, 2 x 90 min, 1 x 110 min). However, the cleavage of a small amount of resin and subsequent RP-HPLC analysis indicated that the coupling of (N-Me) Ile^{26} to Leu^{27} had proceeded almost to 70-80% completion. The peptide resin Fmoc-[(N-Me) Ile^{26}] IAPP [26-37] was acetylated before proceeding with the synthesis. The next amino acid Ala^{25} required two couplings with 4-fold excess (2 x 90 min) and three with 6-fold excess (2 x 90 min, 1 x 150 min in NMP) to achieve an overall coupling yield close to 60-70% according to HPLC analysis of the coupling. Acetylation was performed again before coupling (N-Me) Gly^{24} (4-fold excess (1 x 90 min, 1 x 135 min)), which was followed by acetylation of the Fmoc-protected [(N-Me) Gly^{24}, (N-Me) Ile^{26}] IAPP [24-37] peptide resin. For the coupling of Phe^{23}, the amount of amino acid was slightly increased (5-fold excess, (1 x 90 min, 1 x 150 min, 1 x 120 min)) and the peptide resin Fmoc-[(N-Me) Gly^{24}, (N-Me) Ile^{26}] IAPP [23-37] was acetylated after the coupling. The RP-HPLC trace (Figure 52) of the cleavage mixture at this point (before acetylation of non-reacted groups of (N-Me) Gly^{24}) revealed a main peak at 16.9 min which corresponded to [(N-Me) Gly^{24}, (N-Me) Ile^{26}] IAPP [23-37] according to MALDI-MS ([M+H]$^{+}$ expected: 1560.7, found: 1560.0). The following amino acids were then double coupled as follows: Asn^{22} (5-fold excess, (2 x 100 min)), Asn^{21} (5-fold excess, (1 x 90 min, 1 x 120 min)), Ser^{20} (4-fold excess, (1 x 80 min, 1 x 60 min)) and Ser^{19} (4-fold excess, (1 x 90 min, 1 x 80 min)). HPLC analysis following cleavage from the resin at the stage of [(N-Me) Gly^{24}, (N-Me) Ile^{26}] IAPP [19-37] (Figure 53) and MALDI-MS (Figure 54) showed that the main fraction at 16.1 min corresponded to the expected product [(N-Me) Gly^{24}, (N-Me) Ile^{26}] IAPP [19-37] ([M+H]$^{+}$ expected: 1963.1, found: 1963.7).

Residues 18 to 1 were coupled twice using 4-fold excess for the amino acid each time, TBTU (4-fold excess) and DIEA (6-fold excess) for more than an hour. Acetylation was performed after the couplings of residues Val$^{18}$, Thr^{9}, Cys^{7} and Cys^{2}. At the end of the synthesis, the resin was cleaved with reagent K (3 hrs, RT). The crude peptide was dissolved in 10% AcOH and analysed by HPLC. According to the RP-HPLC separation (Figure 55), the fraction at 22.8 min was identified as the expected reduced product [(N-Me) Gly^{24}, (N-Me) Ile^{26}] IAPP. Oxidation (in the dark) of the crude material (1 mg / ml) was performed in 3 M Gdn HCl in aqueous 0.1M NH$_4$HCO$_3$ for 120 min. RP-HPLC purification (Figure 56) and MALDI-MS

(Figure 57**)** showed that the peak at 23.9 min was the oxidized form of the peptide ([M+H]$^+$ expected: 3934.4, found: 3933.0). The other fraction resolved by RP-HPLC (at 24.5 min) had according to MALDI-MS a mass of 3855.6, most probably a deletion sequence with a missing Ala residue (possibly Ala^8 or Ala^5) (expected: 3863.3, found: 3855.6).

An analytical RP-HPLC of pure, oxidized [(N-Me) Gly^{24}, (N-Me) Ile^{26}] IAPP is shown in Figure 58**.** The overall yield of oxidized peptide with regard to the crude peptide was 5%.
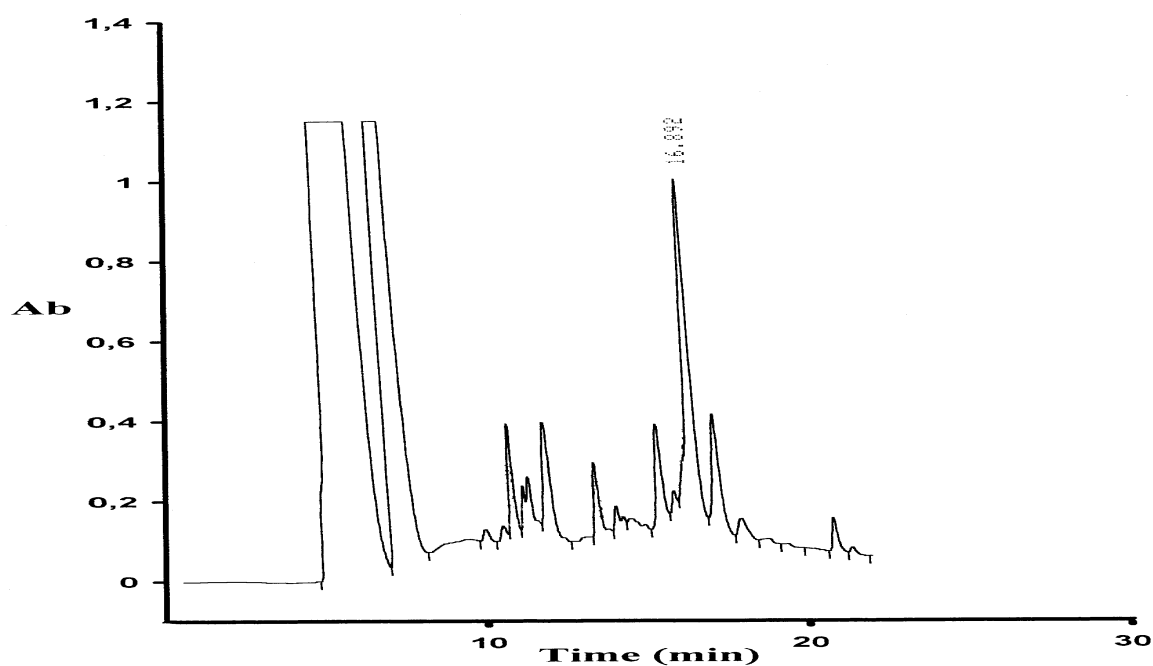
Figure 52. RP-HPLC analysis of crude [(N-Me) Gly^{24}, (N-Me) Ile^{26}] IAPP [23-37] using gradient 2 on C$_{18}$ column, flow rate 2 ml / min and detection at 214 nm. Injection of 40 µg crude peptide in 100 µl aqueous 10% TFA solution.
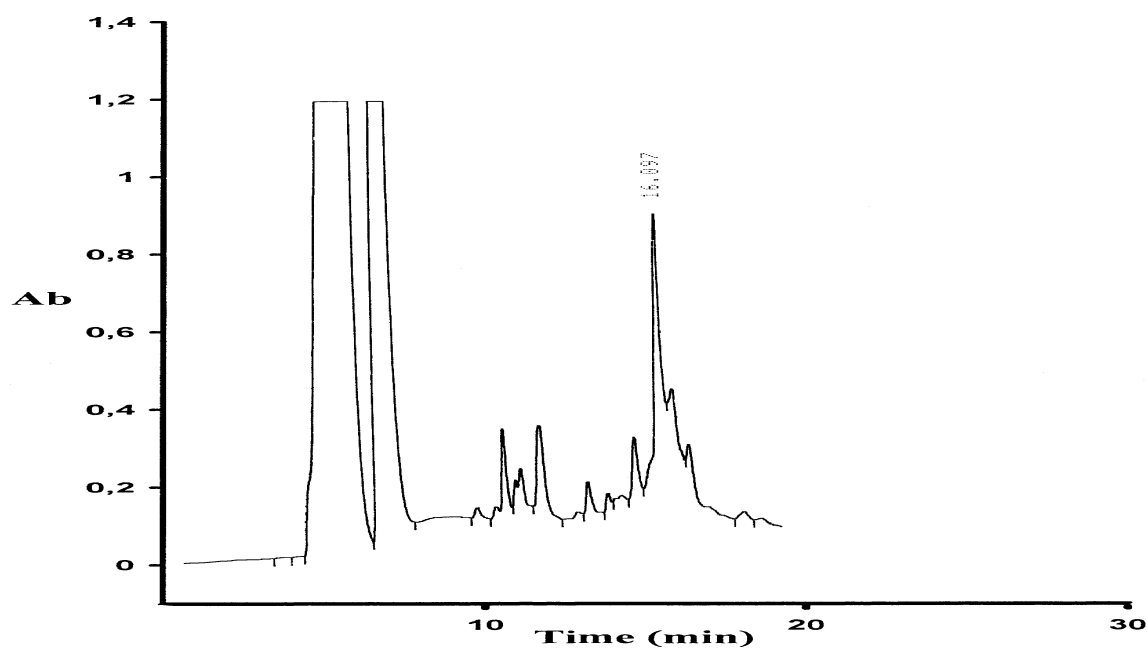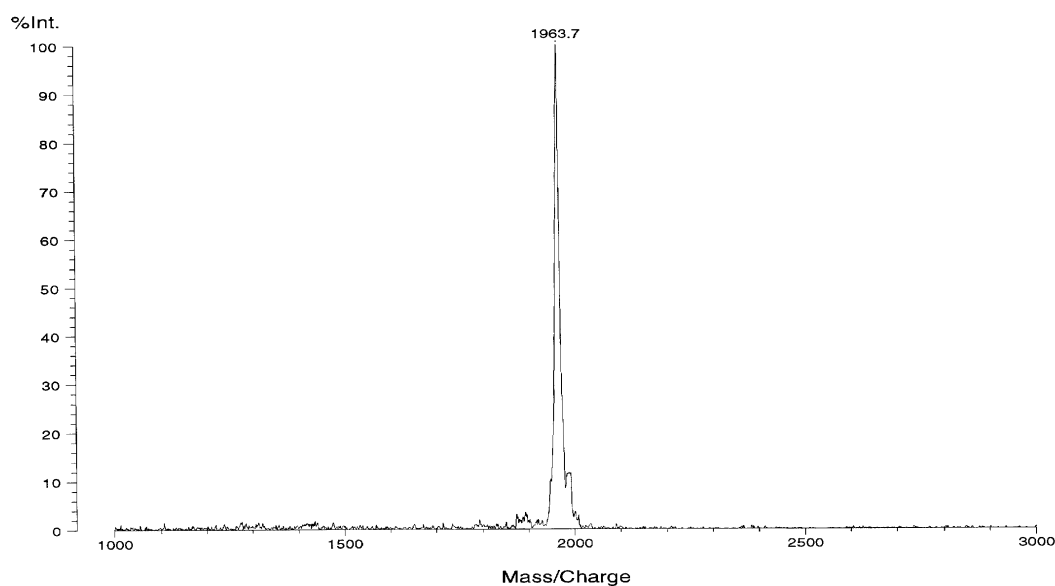
Figure 53. RP-HPLC analysis of crude [(N-Me) Gly^{24}, (N-Me) Ile^{26}] IAPP [19-37] using gradient 2 on C$_{18}$ column, flow rate 2 ml / min and detection at 214 nm. Injection of 40 µg crude peptide in 100 µl aqueous 10% TFA solution.

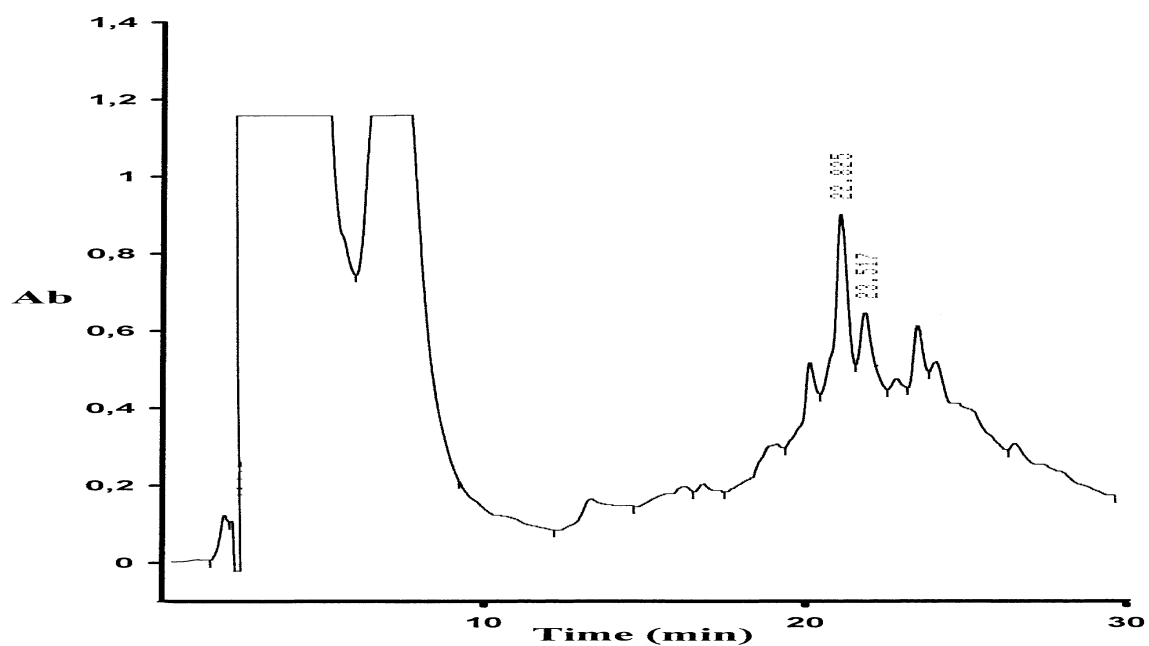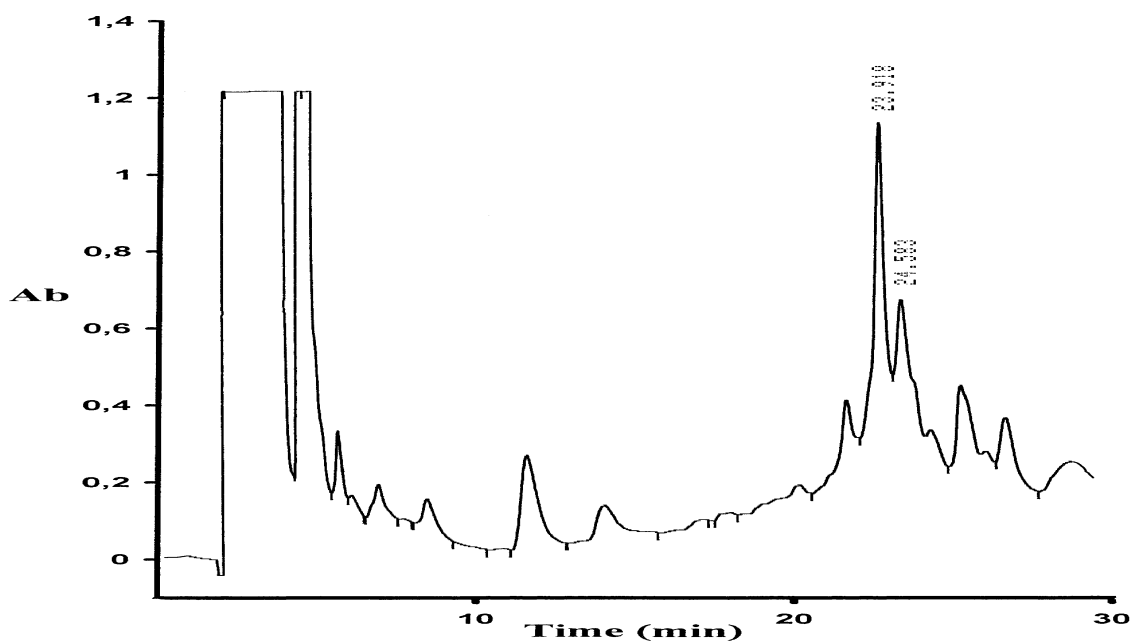**Figure 54.** MALDI-MS of HPLC purified peak at 16.1 min (see Figure 53) from crude [(N-Me) Gly^{24}, (N-Me) Ile^{26}] IAPP [19-37].

Figure 55. RP-HPLC analysis of crude [(N-Me) Gly^{24}, (N-Me) Ile^{26}] IAPP (in reduced form) using gradient 1 on C$_{18}$ column, flow rate 2 ml / min and detection at 214 nm. Injection of 300 µg crude peptide in 500 µl aqueous 10% AcOH solution.

Figure 56. RP-HPLC analysis of crude [(N-Me) Gly^{24}, (N-Me) Ile^{26}] IAPP (in oxidized form) using gradient 1 on C$_{18}$ column, flow rate 2 ml / min and detection at 214 nm. Injection of 600 µg crude peptide in 600 µl 3 M Gdn HCl in aqueous 0.1 M NH$_4$HCO$_3$.
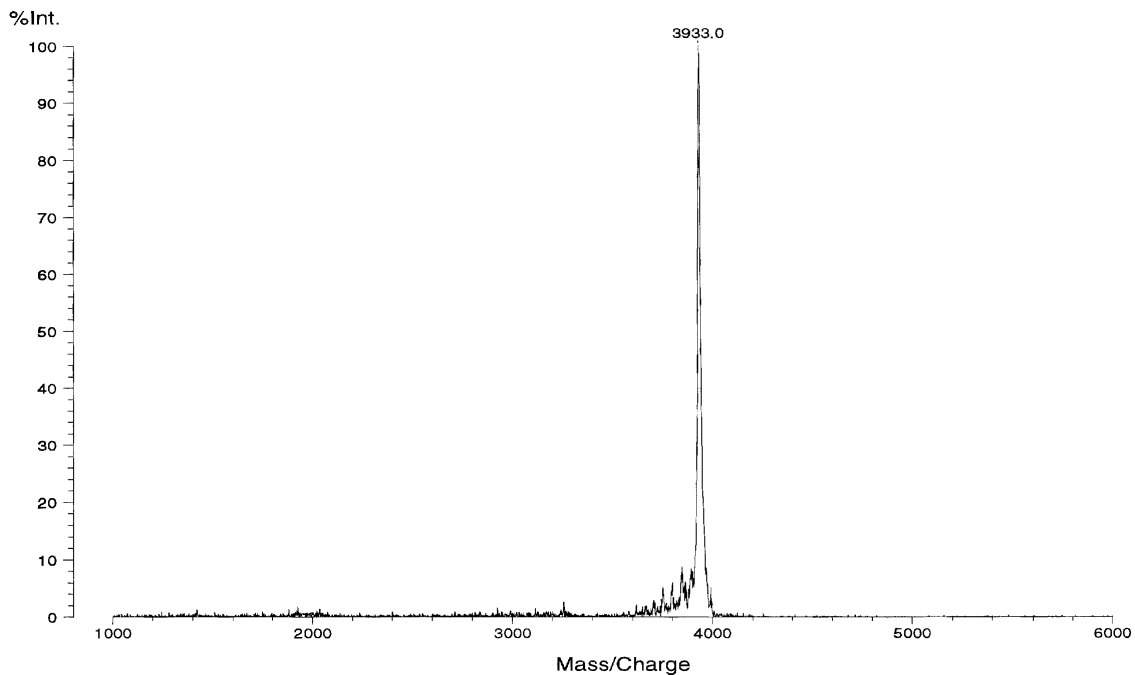
Figure 57. MALDI-MS of HPLC purified peak at 23.9 min (see Figure 56) from oxidized crude [(N-Me) Gly^{24}, (N-Me) Ile^{26}] IAPP.
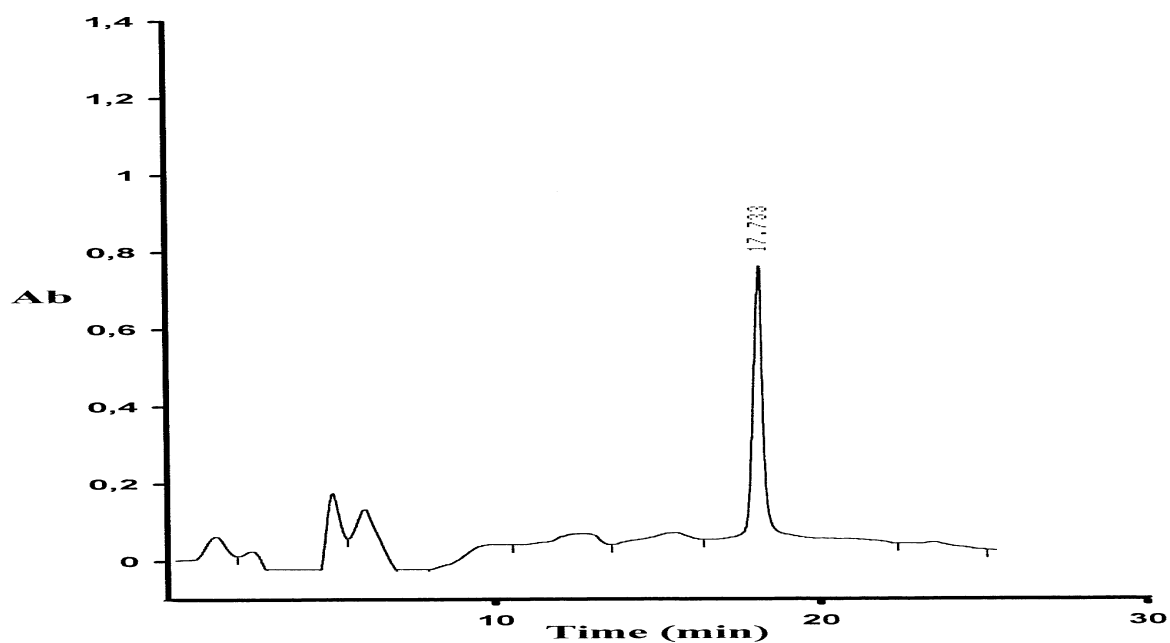

Figure 58. RP-HPLC of pure [(N-Me) Gly^{24}, (N-Me) Ile^{26}] IAPP (in oxidized form) using gradient 2 on C$_{18}$ column, flow rate 2 ml / min and detection at 214 nm. Injection of 10 µg pure peptide in 100 µl aqueous 100 mM HCl.

5.2.4 Synthesis of [(N-Me) Ala[25], (N-Me) Leu[27]] IAPP [3]

The Fmoc-strategy was followed also for this synthesis on Rink Amide MBHA resin (substitution level: 0.5 mmole Tyr / gr) and coupling protocols were as described (see 5.2.1-5.2.3). The following residues were coupled by variation of these protocols: (N-Me) Leu[27] was coupled once in DMF (2-fold excess, 1 x 90 min). Kaiser test indicated that the coupling proceeded to completion. Ile[26] was coupled twice (2-fold excess, 2 x 75 min) followed by acetylation of the Fmoc-[(N-Me) Leu[27]] IAPP [26-37] peptide resin. (N-Me) Ala[25] was coupled once (2-fold excess, 1 x 110 min). No acetylation was performed only Kaiser test which was negative. The following residue Gly[24] was double coupled (2-fold excess, 1 x 80 min, 1 x 95 min). A small amount of [(N-Me) Ala[25], (N-Me) Leu[27]] IAPP [24-37] resin was used for cleavage with a mixture of TFA / water (95/5) (2 hrs, RT). The cleavage mixture was analysed by RP-HPLC (Figure 59) that showed two main products: one at 11.3 min which according to MALDI-MS had a mass of 1029.8 and a second at 15.5 min with a mass of 1412.8, that corresponded to [(N-Me) Ala[25], (N-Me) Leu[27]] IAPP [24-37] ([M+H]+ expected: 1413.5, found: 1412.8). The product with a mass of 1029.8 corresponded to fragment IAPP [28-37], as confirmed also by amino acid analysis: Asn (2) 1.9, Thr (2) 1.8, Ser (3) 2.3, Gly (1) 1.0, Val (1) 1.0 and Tyr (1) 1.0. The resin was acetylated after the coupling of Gly[24] to (N-Me) Ala[25] and the following amino acids were coupled twice (2-fold excess each time): Phe[23] (2 x 60 min), Asn[22] (1 x 80, 1 x 90 min), Asn[21] (1 x 75, 1 x 80 min), Ser[20] (2 x 60 min) and Ser[19] (1 x 70, 1 x 80 min). No acetylations were performed in the region [19-24]. A small amount of [(N-Me) Ala[25], (N-Me) Leu[27]] IAPP [19-37] resin was treated by a mixture of TFA / water (95/5) (2 hrs, RT) and subjected to RP-HPLC analysis. The RP-HPLC profile (Figure 60) revealed three main fractions: one at 11.4 min which according to MALDI-MS had a mass of 1029.2 corresponding to IAPP [28-37] (see above), one at 15.6 min with a mass of 1412.8 corresponding to [(N-Me) Ala[25], (N-Me) Leu[27]] IAPP [24-37] and one at 17.1 min with a mass of 1995.3, corresponding to the expected product [(N-Me) Ala[25], (N-Me) Leu[27]] IAPP [19-37] ([M+Na]+ expected: 1985.1, found: 1995.3) (Figure 61). These results indicated that elongation of the fragment [24-37] was only partially possible (70 to 80% with regard to amino groups of Gly[24]) under the applied coupling conditions.

Due to the low yield with regard to the expected product the synthesis was repeated. For the second attempt, double couplings (4-fold excess) were employed for the residues in the region [24-27]: (N-Me) Leu[27] (1 x 70, 1 x 75 min), Ile[26] (1 x 75, 1 x 85 min), (N-Me) Ala[25] (1 x 70, 1 x 60 min) and Gly[24] (1 x 70, 1 x 80 min). The second coupling was performed in NMP and

after each coupling the peptide resin was acetylated. A small cleavage of [(N-Me) Ala[25], (N-Me) Leu[27]] IAPP [24-37] resin yielded the same RP-HPLC profile as in the first attempt. The synthesis was continued with the following residues (double couplings, 4-fold excess): Phe[23] (1 x 70, 1 x 60 min), Asn[22] (1 x 100, 1 x 75 min), Asn[21] (1 x 70, 1 x 60 min), Ser[20] (1 x 65, 1 x 75 min) and Ser[19] (1 x 65, 1 x 80 min). Kaiser test after each coupling was negative. At this point cleavage of [(N-Me) Ala[25], (N-Me) Leu[27]] IAPP [19-37] resin and RP-HPLC analysis (Figure 62) showed that the same three major fractions were present: one at 11.5 min, another at 15.6 min and a last one at 17.1 min, which was the expected product [(N-Me) Ala[25], (N-Me) Leu[27]] IAPP [19-37]. The question that needed to be addressed was why IAPP [28-37] formed during the synthesis. The possible explanations were that:

a) an incomplete coupling of (N-Me) Leu[27] to Ser[28] occurred, although the Kaiser test after the coupling was negative. However, in this case the peptide IAPP [28-37] should be acetylated, which is not what is found b) the coupling of Ile[26] to (N-Me) Leu[27] was incomplete since the coupling was not checked by Kaiser test due to the (N-Me) amino acid. Since the peptide resin was then acetylated we suspected that an amide bond cleavage between Ac-(N-Me) Leu[27] and Ser[28] might have occurred during the TFA cleavage of the peptide from the resin.

The synthesis was therefore repeated to investigate this issue: (N-Me) Leu[27] was coupled twice (4-fold excess, 1 x 70, 1 x 75 min) and the coupling was complete as judged by cleavage and RP-HPLC analysis of a small aliquot of peptide resin (Figure 63). The main peak at 12.7 min corresponded to the expected peptide [(N-Me) Leu[27]] IAPP [27-37], as shown by MALDI-MS ([M+H]$^+$ expected: 1157.2, found: 1161.5). However, coupling of Fmoc-Ile[26] to (N-Me) Leu[27] proved to be extremely difficult even after three consecutive couplings (4-fold excess), two of them performed in DMF (1 x 75, 1 x 85 min) and the third one in NMP (1 x 85 min). The RP-HPLC trace of the crude product (Figure 64) revealed the presence of two main products: one at 12.7 min corresponding to [(N-Me) Leu[27]] IAPP [27-37] ([M+H]$^+$ expected: 1157.2, found: 1156.6), and a second one at 15.4 min with a mass of 1271.6, corresponding to [(N-Me) Leu[27]] IAPP [26-37] ([M+H]$^+$ expected: 1270.4). The conclusions that were drawn from the results of this synthetic attempt as compared to the previous two ones were the following: a) incorporation of (N-Me) Leu[27] was complete and b) the coupling of Ile[26] to (N-Me) Leu[27] was a very difficult one (30 to 40% completion) and could not be completed by the coupling methods applied in this work.

In an additional experiment (N-Me) Leu[27] was coupled twice (4-fold excess, 2 x 60 min) and the coupling was close to completion as judged by cleavage and RP-HPLC analysis of a small

aliquot of peptide resin (Figure 65): the main peak at 13.3 min was the expected peptide [(N-Me) Leu^{27}] IAPP [27-37] ([M+H]$^+$ expected: 1157.2, found: 1156.0). The peptide resin after deprotection of the Fmoc-group of (N-Me) Leu^{27} was acetylated, practically leading to peptide chain termination at this point. A small amount of Ac-[(N-Me) Leu^{27}] IAPP [27-37] resin was treated by a mixture of TFA / water (95/5) (2 hrs, RT) and subjected to RP-HPLC analysis. The RP-HPLC (Figure 66) showed that the main peak was eluting at 11.8 min and corresponded to IAPP [28-37] ([M+H]$^+$ expected: 1029.0, found: 1028.9). This finding indicated that the acetylated form of the peptide [(N-Me) Leu^{27}] IAPP [27-37] was indeed unstable and that during TFA deprotection conditions the peptide bond between Ac-(N-Me) Leu^{27} and Ser^{28} was cleaved. This result was in agreement with the previous finding of peptide bond cleavage of Ac-(N-Me) Phe^{23} and Gly^{24} in analogue IAPP [1] (see 5.2.2) and previous literature report [15].

The peptide resins [(N-Me) Ala^{25}, (N-Me) Leu^{27}] IAPP [19-37] from the first two synthetic attempts, were used for the coupling of the remaining residues till Lys^1. Residues 18 to 1 were coupled twice (4-fold excess, 2 x 60-75 min) with Kaiser test done after the couplings of His^{18}, Phe^{15}, Thr^9, Thr^5. Again, for the couplings of Cys^7 and Cys^2 instead of activation with TBTU / DIEA, the HOBt-ester protocol was used (AA in 6-fold excess, 2 x 90 min) (see 5.2.1-5.2.3). At the end of the synthesis, the peptide resins were treated with reagent K (3 hrs, RT). The crude peptide was subjected to RP-HPLC analysis. The analytical profile of the reduced form of the crude peptide (Figure 67) with one main peak at 23.7 min ([M+H]$^+$ expected: 3936.4, found: 3934.9) indicated that the peptide was obtained in good purity although the yield due to the low coupling efficiency of Ile^{26} to (N-Me) Leu^{27} was low. The peptide was purified following oxidation (in the dark) that was performed by dissolving crude material (1 mg /ml) in aqueous 0.1 M NH$_4$HCO$_3$ containing 3 M Gdn HCl. The oxidation (Figure 68) required almost two hours for completion and the peak at 24.9 min was the expected product [(N-Me) Ala^{25}, (N-Me) Leu^{27}] IAPP ([M+H]$^+$ expected: 3932.4, found: 3934.1) (Figure 69).

An analytical RP-HPLC of pure, oxidized [(N-Me) Ala^{25}, (N-Me) Leu^{27}] IAPP is shown in Figure 70. The overall yield of the oxidized peptide with regard to the crude peptide was 5%.
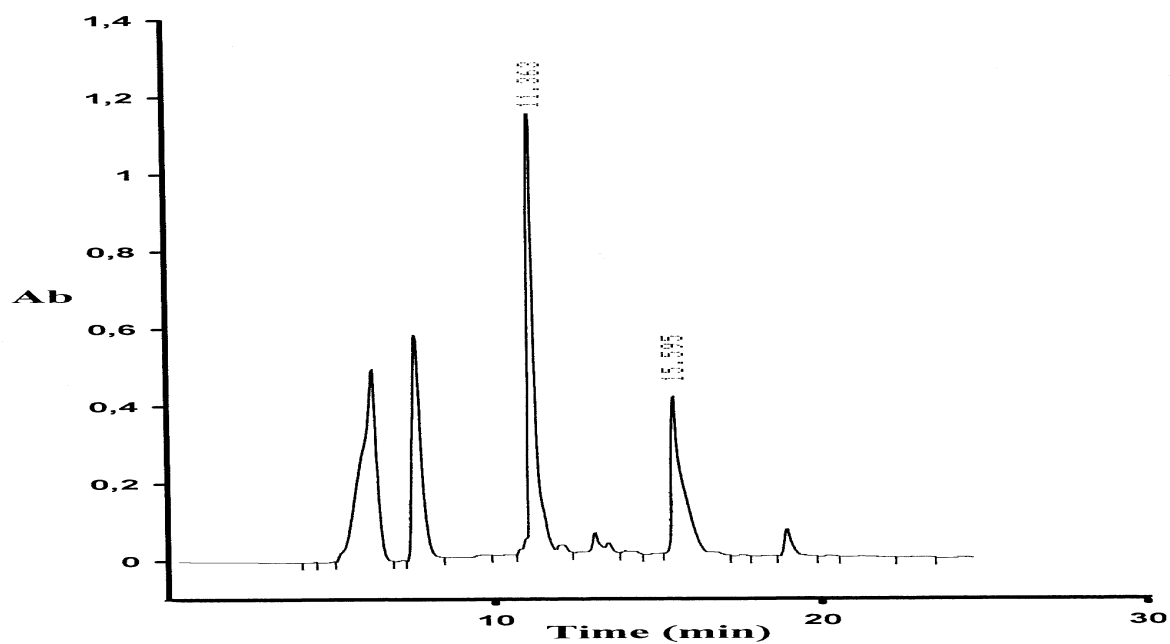
Figure 59. RP-HPLC analysis of crude [(N-Me) Ala[25], (N-Me) Leu[27]] IAPP [24-37] (1st synthesis) using gradient 2 on C_{18} column, flow rate 2 ml /min and detection at 214 nm. Injection of 100 µg crude peptide in 100 µl aqueous 10% TFA solution.
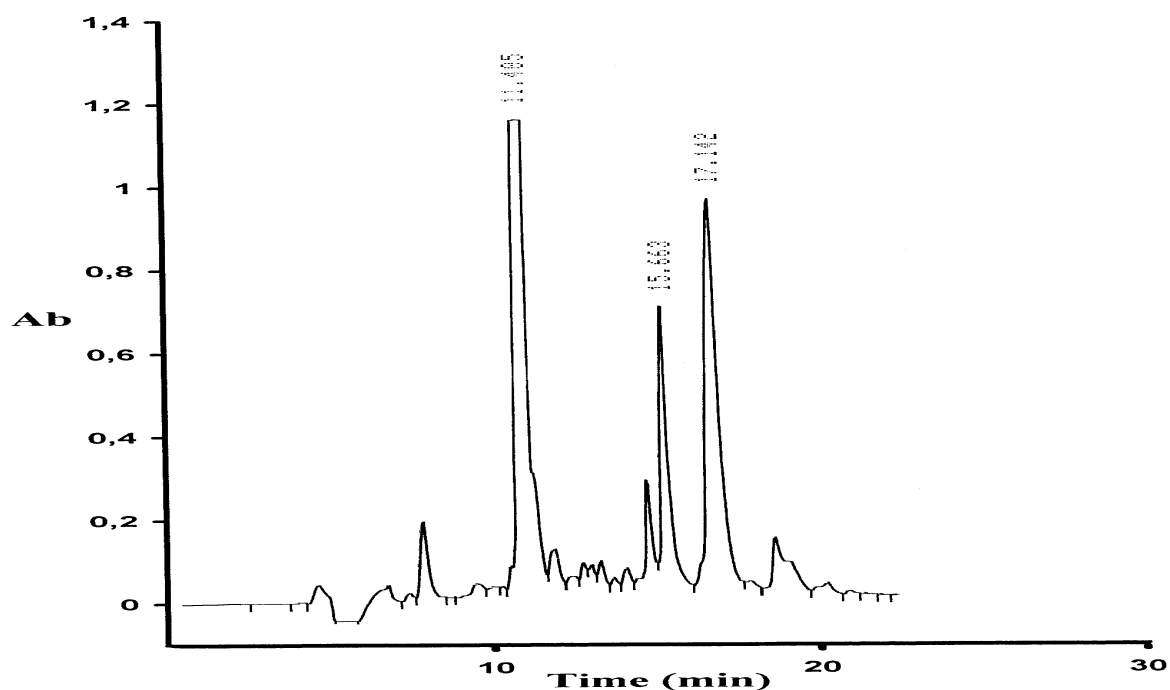

Figure 60. RP-HPLC analysis of crude [(N-Me) Ala[25], (N-Me) Leu[27]] IAPP [19-37] (1st synthesis) using gradient 2 on C_{18} column, flow rate 2 ml /min and detection at 214 nm. Injection of 800 µg crude peptide in 1 ml aqueous solution.
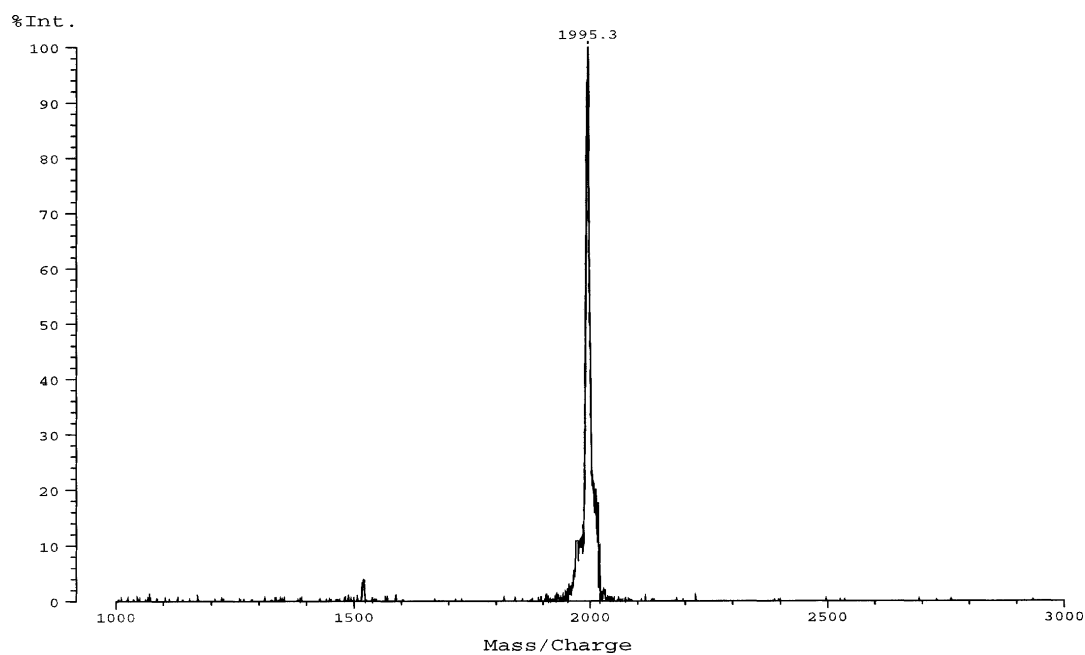
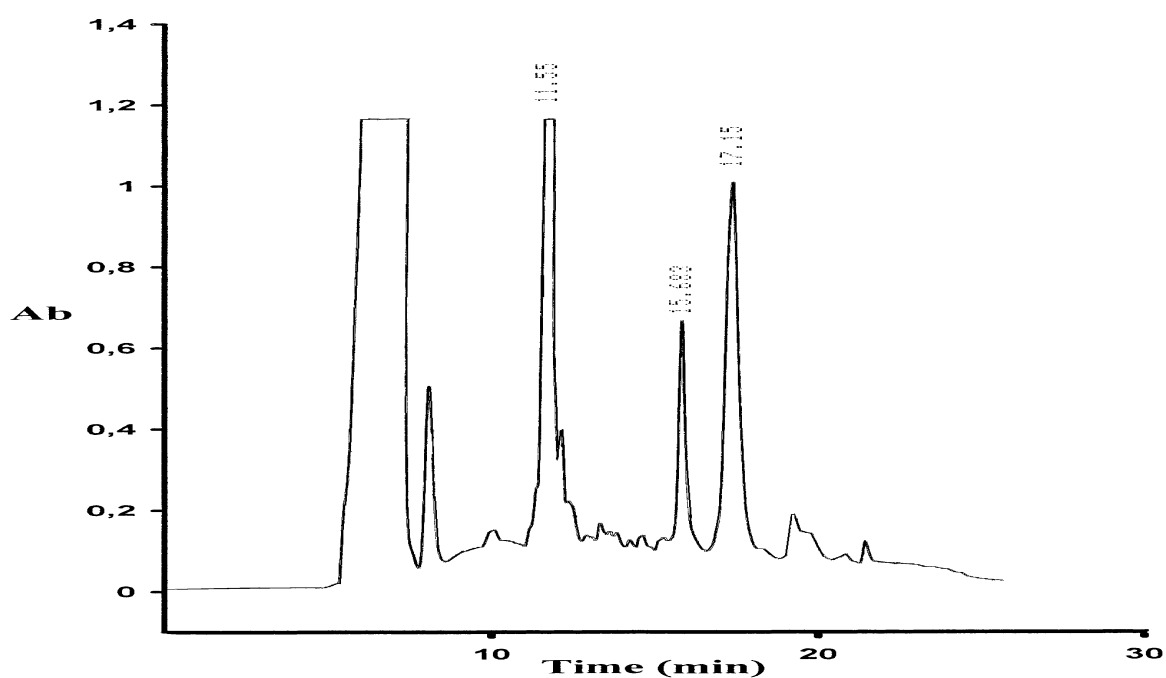**Figure 61.** MALDI-MS of HPLC purified peak at 17.1 min (see Figure 60) from crude [(N-Me) Ala^{25}, (N-Me) Leu^{27}] IAPP [19-37].

Figure 62. RP-HPLC analysis of crude [(N-Me) Ala^{25}, (N-Me) Leu^{27}] IAPP [19-37] (2nd synthesis) using gradient 2 on C$_{18}$ column, flow rate 2 ml /min and detection at 214 nm. Injection of 50 μg crude peptide in 50 μl aqueous 10% AcOH solution.
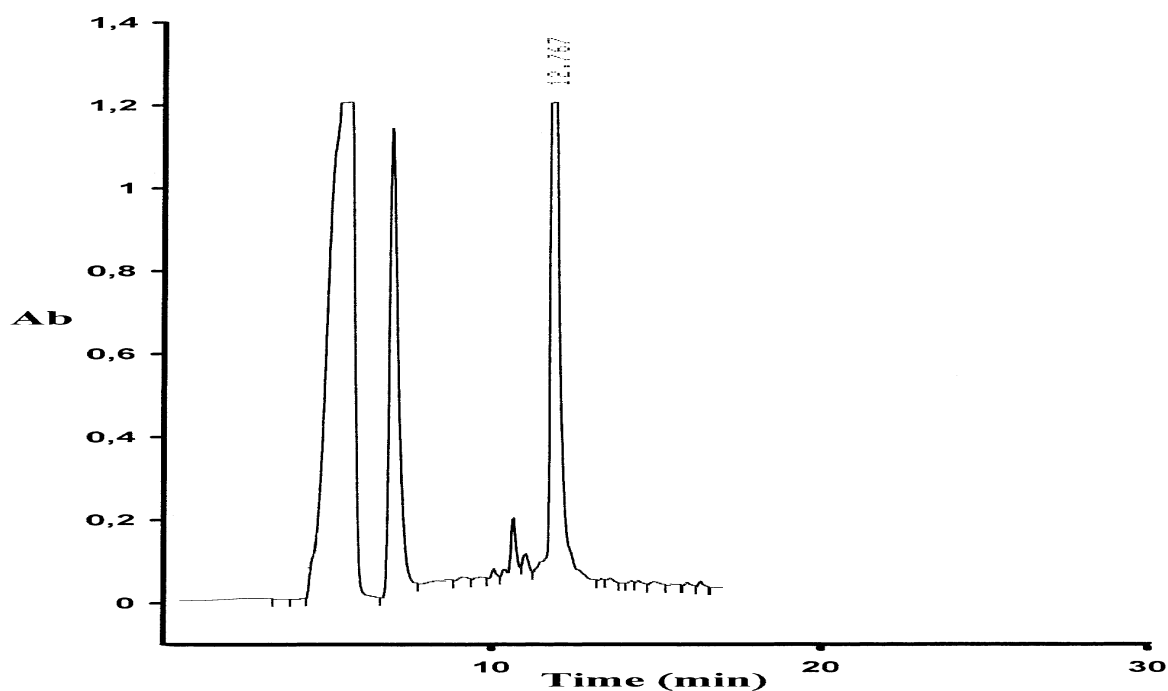
Figure 63. RP-HPLC analysis of crude [(N-Me) Leu[27]] IAPP [27-37] (3rd synthesis) using gradient 2 on C_{18} column, flow rate 2 ml / min and detection at 214 nm. Injection of 100 μg crude peptide in 150 μl aqueous 10% TFA solution.

Figure 64. RP-HPLC analysis of crude [(N-Me) Leu[27]] IAPP [26-37] (3rd synthesis) using gradient 2 on C_{18} column, flow rate 2 ml / min and detection at 214 nm. Injection of 50 μg crude peptide in 150 μl aqueous 10% TFA solution.
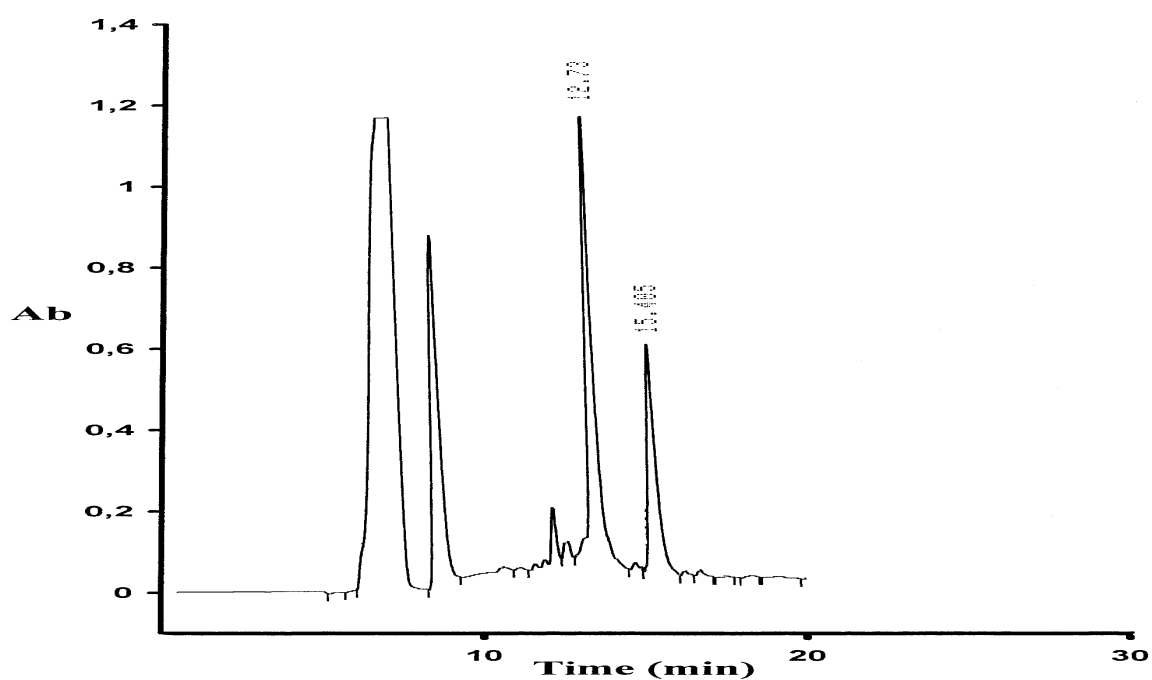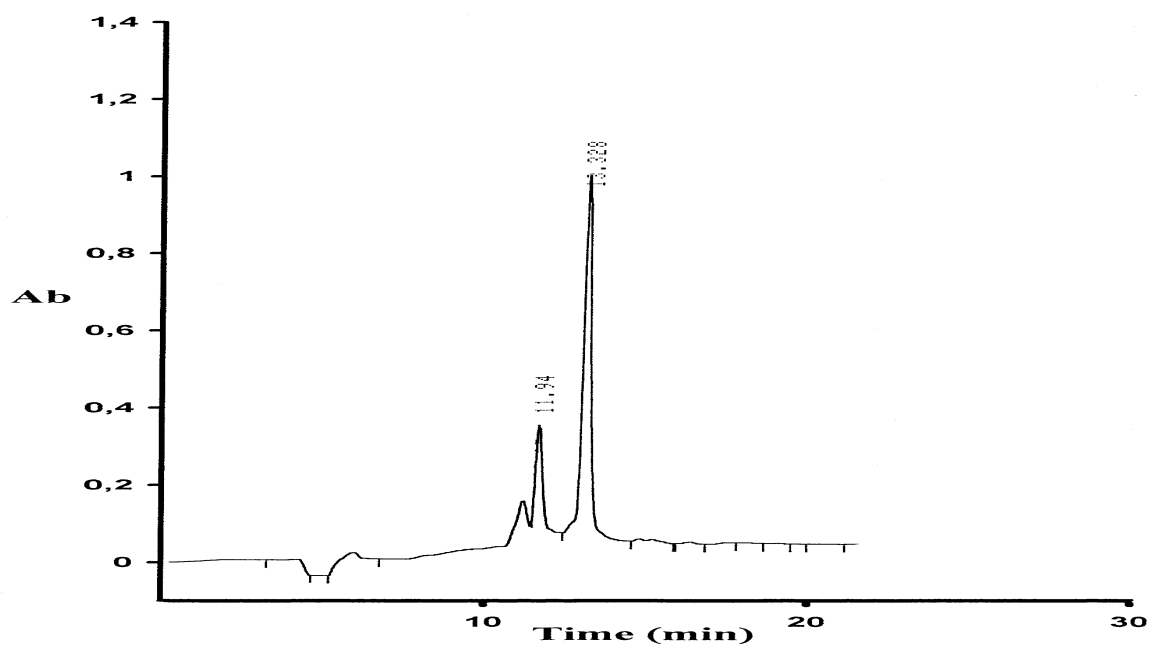
Figure 65. RP-HPLC analysis of crude [(N-Me) Leu[27]] IAPP [27-37] (4th synthesis) using gradient 2 on C_{18} column, flow rate 2 ml / min and detection at 214 nm. Injection of 250 μg crude peptide in 400 μl water.

Figure 66. RP-HPLC analysis of crude Ac-[(N-Me) Leu[27]] IAPP [27-37] (4th synthesis) using gradient 2 on C_{18} column, flow rate 2 ml / min and detection at 214 nm. Injection of 200 μg crude peptide in 200 μl water.

Figure 67. RP-HPLC analysis of crude [(N-Me) Ala^{25}, (N-Me) Leu^{27}] IAPP (in reduced form) using gradient 1 on C$_{18}$ column, flow rate 2 ml / min and detection at 214 nm. Injection o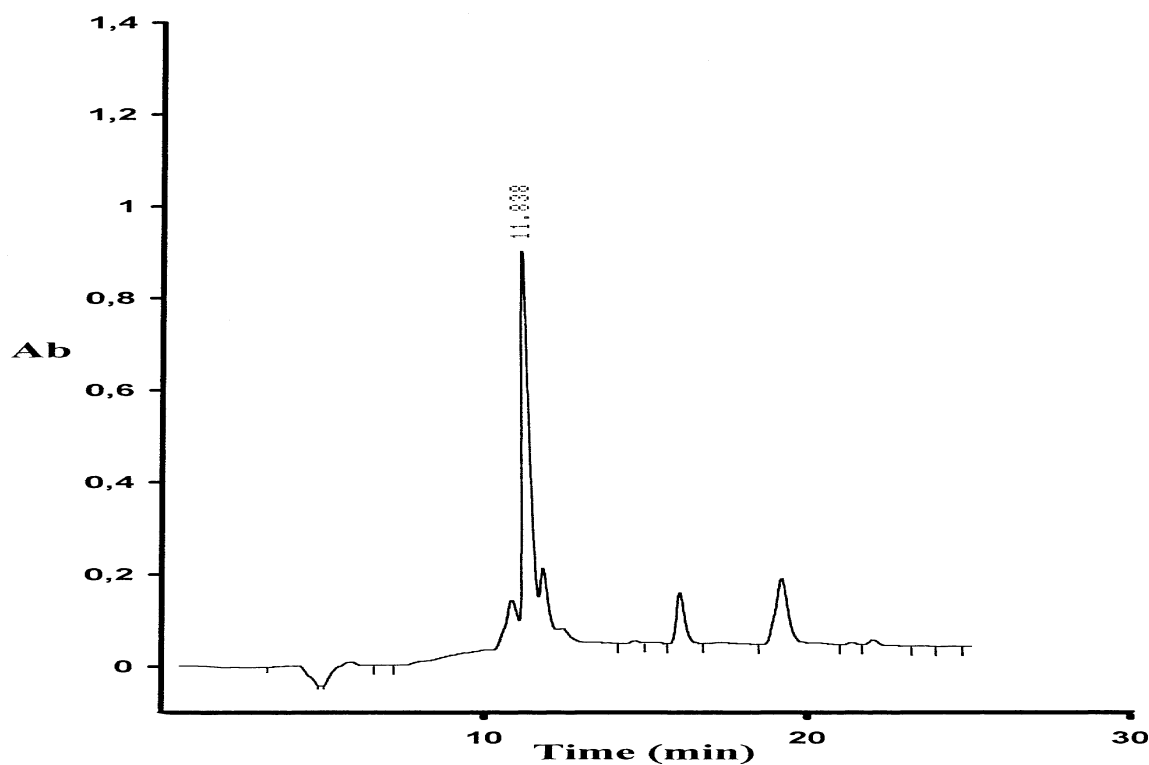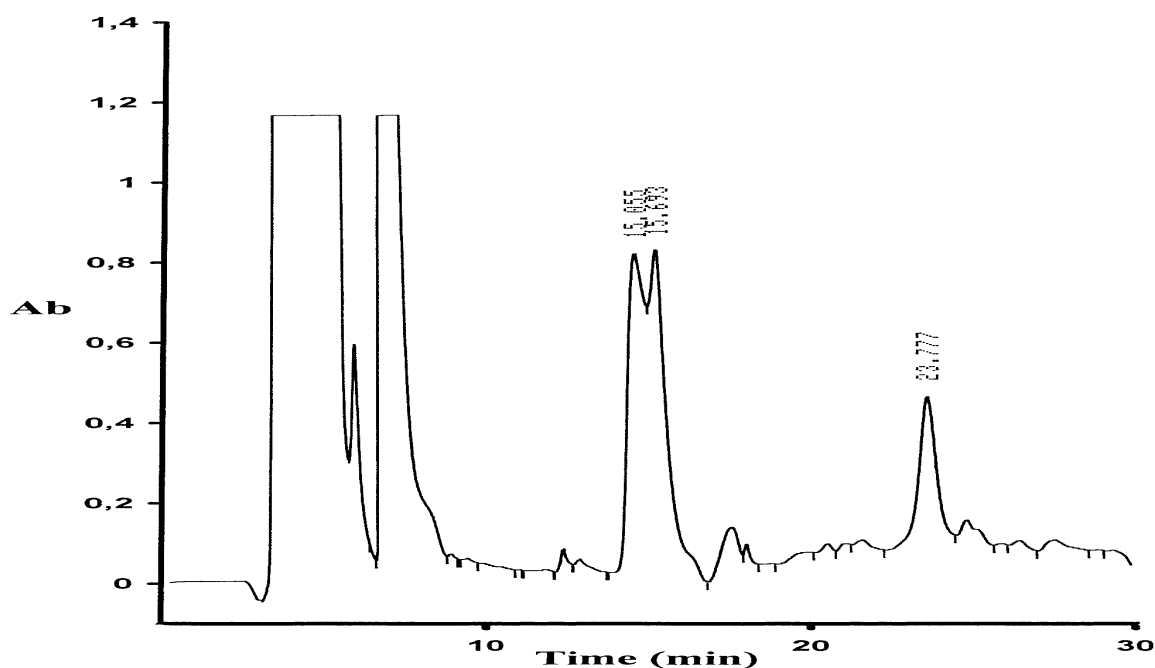f 150 μg crude peptide in 100 μl aqueous 10% TFA solution (the peak at 15.7 min is due to scavenger phenol from the cleavage mixture).
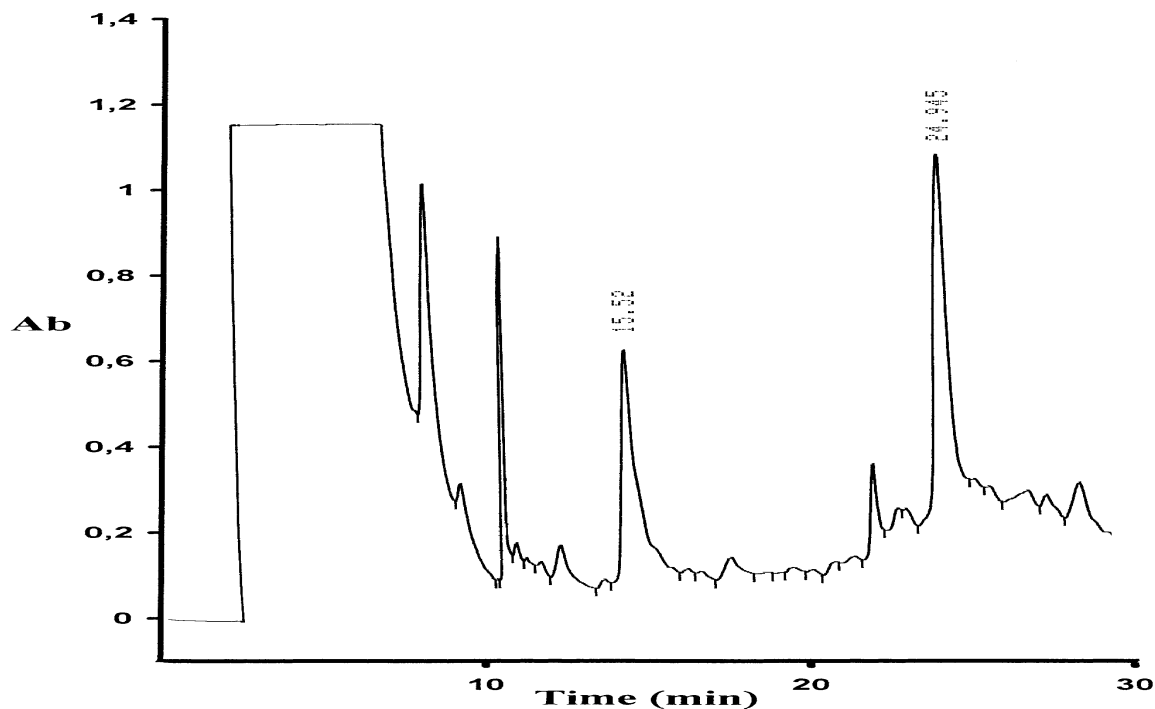

Figure 68. RP-HPLC analysis of crude oxidized [(N-Me) Ala^{25}, (N-Me) Leu^{27}] IAPP (in oxidized form) using gradient 1 on C$_{18}$ column, flow rate 2 ml /min and detection at 214 nm. Injection of 2 mg crude peptide in 2 ml 3 M Gdn HCl in aqueous 0.1 M NH$_4$HCO$_3$ solution (the peak at 15.5 min is due to scavenger phenol from the cleavage mixture).
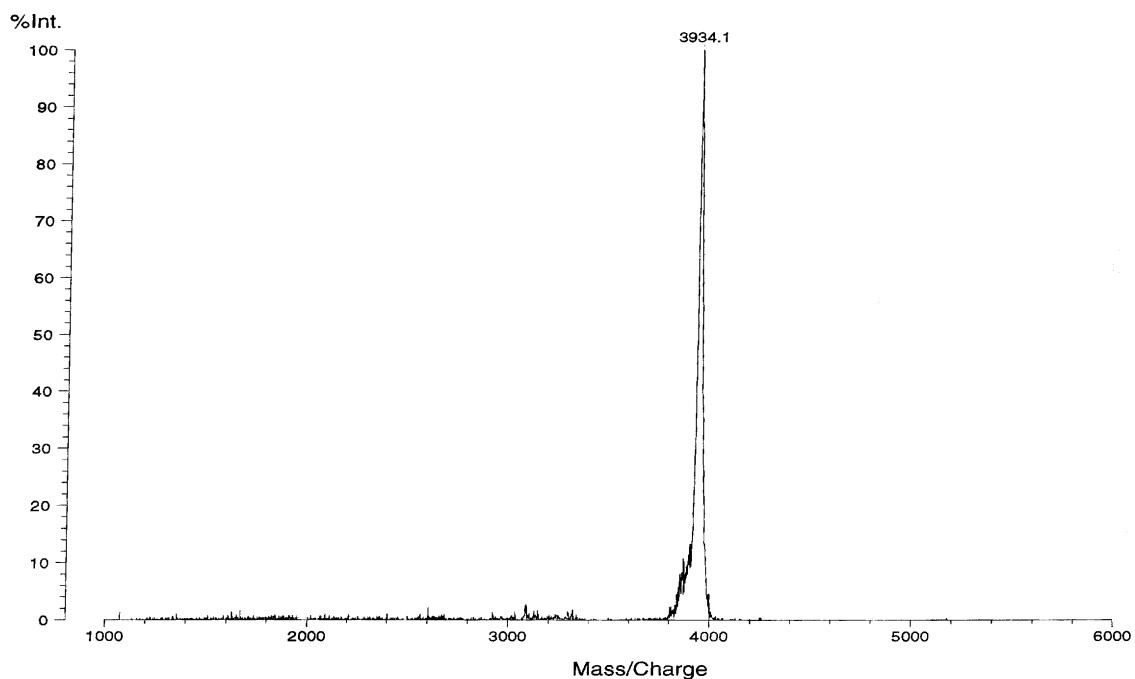
Figure 69. MALDI-MS of HPLC purified peak at 24.9 min (see Figure 68) from crude [(N-Me) Ala^{25}, (N-Me) Leu^{27}] IAPP.
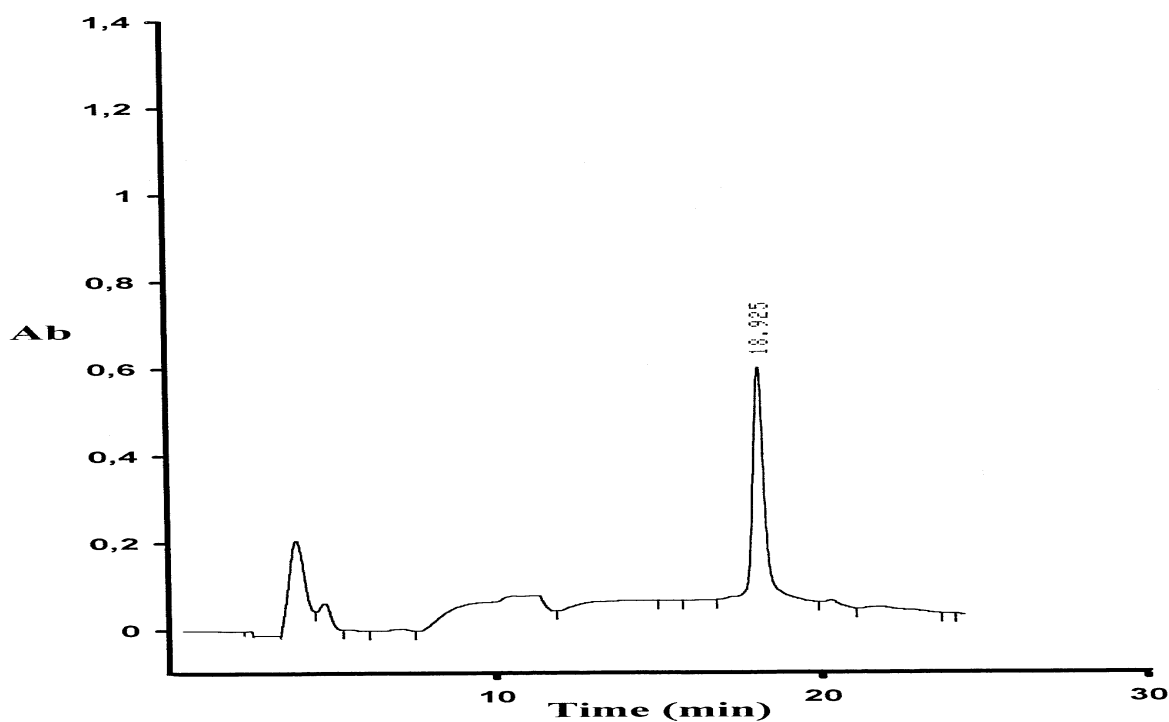

Figure 70. RP-HPLC of pure [(N-Me) Ala^{25}, (N-Me) Leu^{27}] IAPP (in oxidized form) using gradient 2 on C$_{18}$ column, flow rate 2 ml / min and detection at 214 nm. Injection of 10 µg pure peptide in 100 µl aqueous 100 mM HCl.

5.2.5 Synthesis of [(N-Me) Ile^{26}, (N-Me) Leu^{27}] IAPP [4]

The first synthetic attempt on Rink Amide MBHA resin (substitution level: 0.21 mmole Tyr / gr) aimed to study synthetic difficulties up to Ser^{19}. The synthesis up to residue Ser^{28} was performed as described before (see 5.2.1). (N-Me) Leu^{27} was coupled twice (4-fold excess) with TBTU (4-fold excess) and DIEA (6-fold excess) (2 x 75 min). Kaiser test indicated complete coupling. For the coupling of (N-Me) Ile^{26} 6-fold excess was used and longer coupling times were applied: the first coupling was 17 hrs at RT and the second coupling for 4 hrs at 50 °C then left for 17 hrs at RT. The coupling efficiency of (N-Me) Ile^{26} on (N-Me) Leu^{27} was 60 to 70% as estimated by cleavage and RP-HPLC analysis. The peptide resin Fmoc-[(N-Me) Ile^{26}, (N-Me) Leu^{27}] IAPP [26-37] was acetylated before proceeding. For the coupling of Ala^{25} 5-fold excess was used: first coupling for 6 hrs and the second coupling for 18 hrs at RT. A small aliquot of [(N-Me) Ile^{26}, (N-Me) Leu^{27}] IAPP [25-37] resin was cleaved with TFA / water (95/5) (2 hrs, RT) and the cleavage mixture was analysed by RP-HPLC. The RP-HPLC analysis (Figure 71) showed the presence of a peak at 11.3 min, corresponding to IAPP [28-37] and a broad peak at 15.2-15.6 min (the intended product was eluting at 15.6 min but the separation from the peptide without Ala at 15.2 min was difficult). In order to increase the coupling yield of Ala^{25} on (N-Me) Ile^{26} a third coupling of Ala (5-fold excess, 1 x 150 min) was performed followed by acetylation of the Fmoc-[(N-Me) Ile^{26}, (N-Me) Leu^{27}] IAPP [25-37] resin. Coupling of Gly^{24} (5-fold excess, 1 x 100, 1 x 180 min) was followed by Phe^{23} (5-fold excess, 1 x 100min, 1 x 11 hrs and 1 x 18 hrs). A small aliquot of [(N-Me) Ile^{26}, (N-Me) Leu^{27}] IAPP [23-37] resin was cleaved and analysed by RP-HPLC. According to the RP-HPLC analysis (Figure 72) three main products were formed: peak at 11.5 min, peak at 12.9 min and a broad peak at 17.4-17.7 min. The product at 12.9 min corresponding to [(N-Me) Leu^{27}] IAPP [27-37] was formed from bond cleavage during TFA deprotection between Ac-(N-Me) Ile^{26} and (N-Me) Leu^{27} . The peptide resin Fmoc-[(N-Me) Ile^{26}, (N-Me) Leu^{27}] IAPP [23-37] was acetylated before coupling the remaining amino acids: Asn^{22} (5-fold excess, 1 x 120 min, 1 x 140 min), Asn^{21} (5-fold excess, 1 x 120 min, 1 x 18 hours), Ser^{20} (5-fold excess, 1 x 70 min, 1 x 80 min) and finally Ser^{19} (5-fold excess, 1 x 70 min, 1 x 80 min). Cleavage of peptide resin and RP-HPLC analysis (Figure 73) showed that the expected product [(N-Me) Ile^{26}, (N-Me) Leu^{27}] IAPP [19-37] had a retention time of 16.5 min ([M+H]$^{+}$ expected: 1963.1, found: 1963.9) (Figure 74). The peak at 11.1 min corresponded to IAPP [28-37] ([M+H]$^{+}$ expected: 1029.0, found: 1031.0) and the peak at 12.5 min corresponded to [(N-Me)

Leu^{27}] IAPP [27-37] ([M+H]$^{+}$ expected: 1157.2, found: 1159.7). The synthesis was stopped due to the low yield with regard to [(N-Me) Ile^{26}, (N-Me) Leu^{27}] IAPP [19-37].

Figure 71. RP-HPLC analysis of crude [(N-Me) Ile^{26}, (N-Me) Leu^{27}] IAPP [25-37] (1st synthesis) using gradient 2 on C$_{18}$ column, flow rate 2 ml / min and detection at 214 nm. Injection of 30 µg crude peptide in 100 µl aqueous 10% TFA solution.

Figure 72. RP-HPLC analysis of crude [(N-Me) Ile[26], (N-Me) Leu[27]] IAPP [23-37] (1st synthesis) using gradient 2 on C_{18} column, flow rate 2 ml / min and detection at 214 nm. Injection of 30 µg crude peptide in 100 µl aqueous 10% TFA solution.
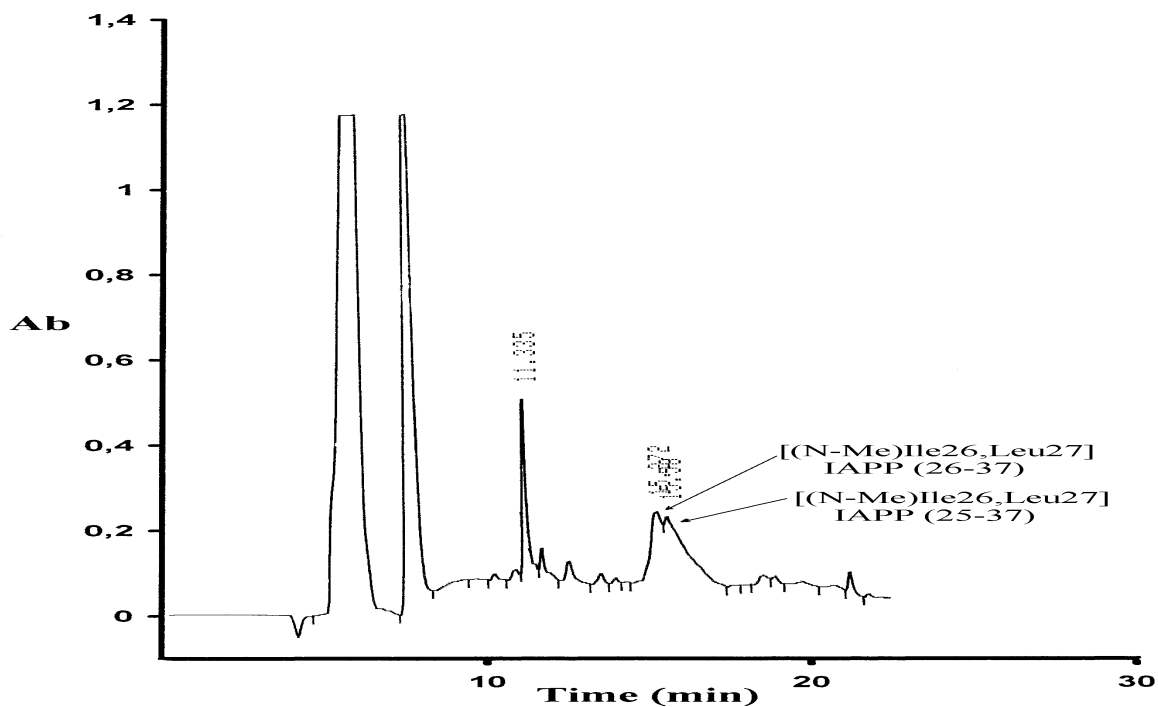

Figure 73. RP-HPLC analysis of crude [(N-Me) Ile[26], (N-Me) Leu[27]] IAPP [19-37] (1st synthesis) using gradient 2 on C_{18} column, flow rate 2 ml / min and detection at 214 nm. Injection of 2 mg crude peptide in 2 ml aqueous 10% AcOH solution.
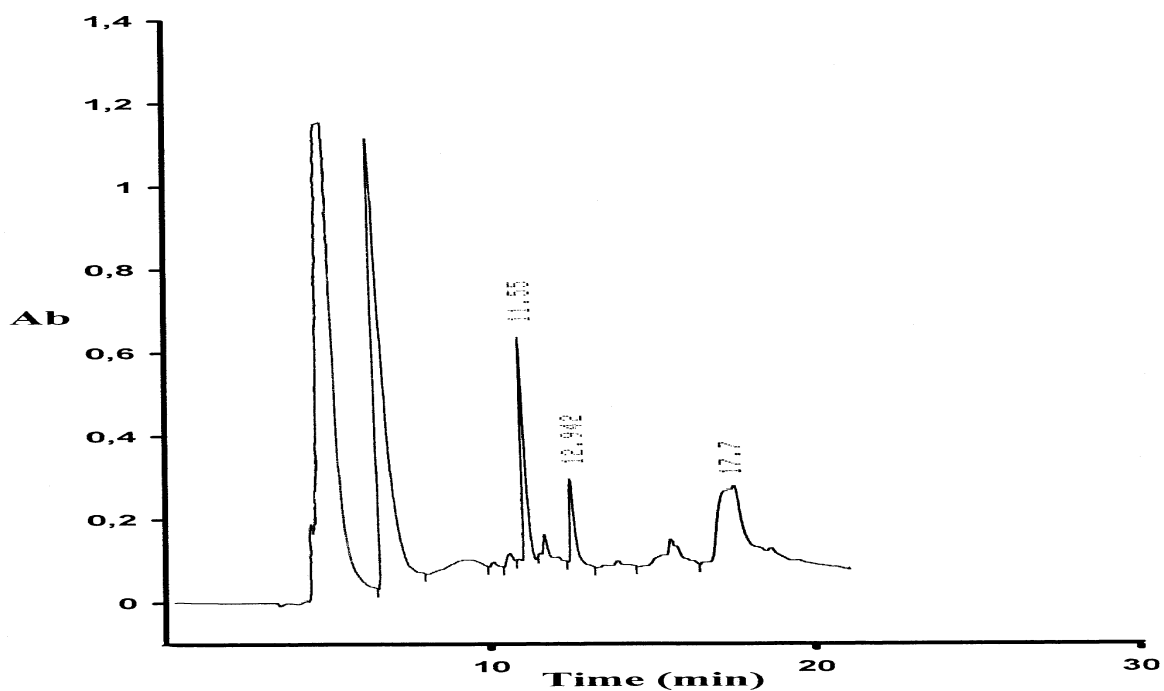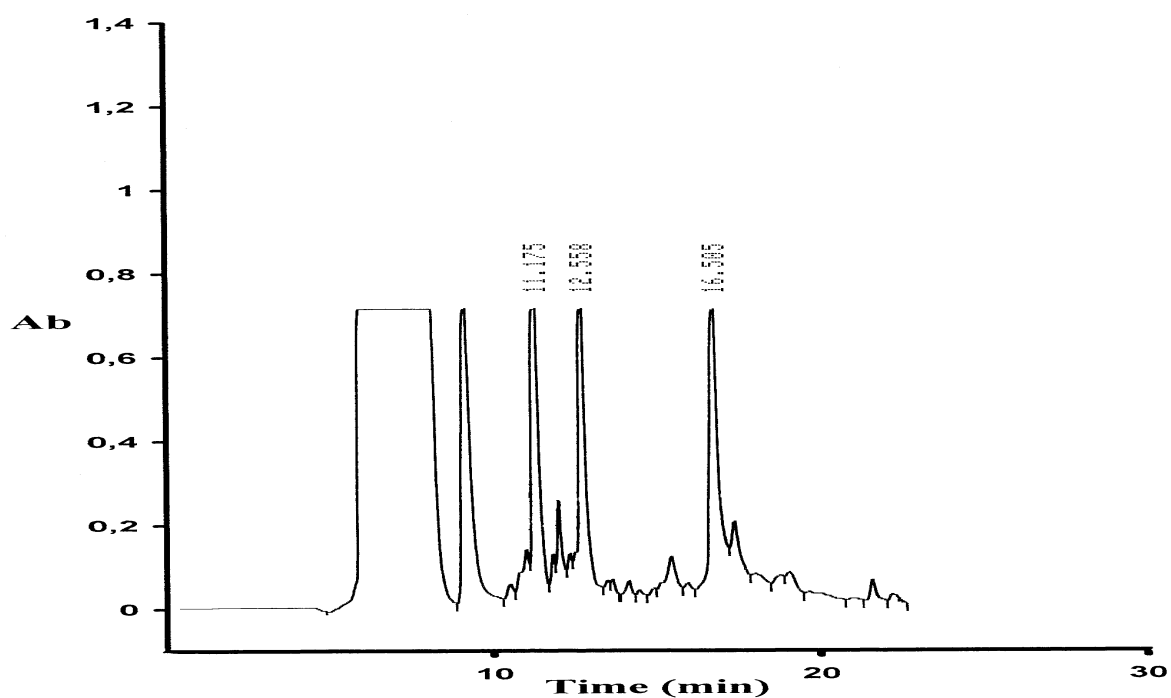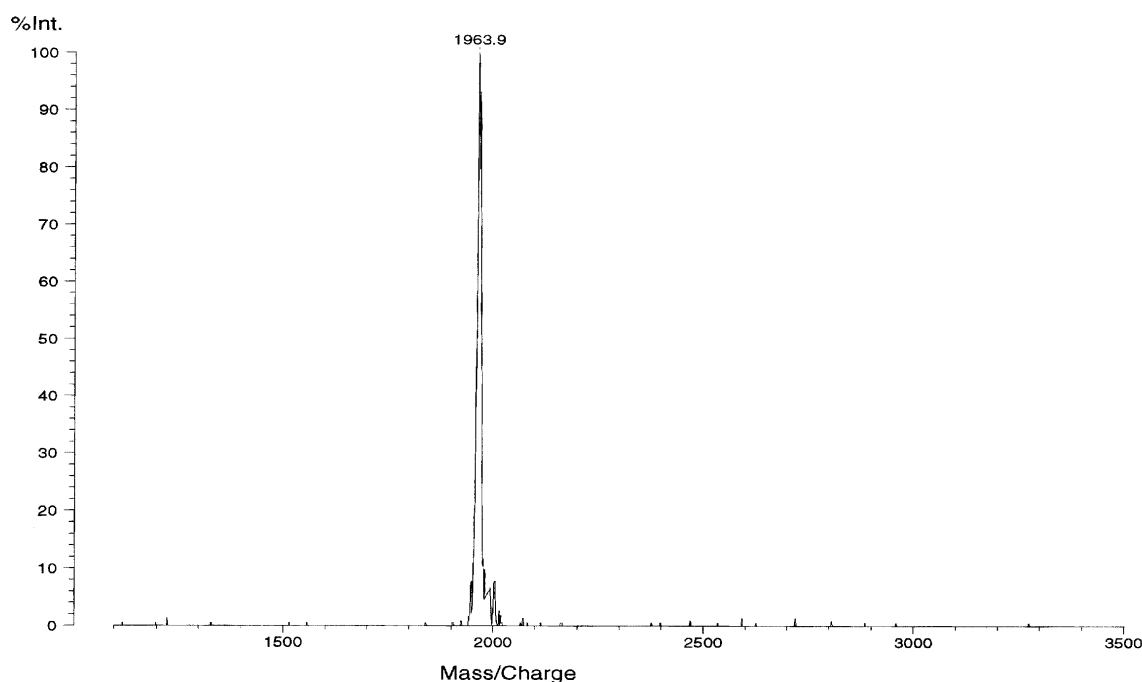
Figure 74. MALDI-MS of HPLC purified peak at 16.5 min (see Figure 73) from crude [(N-Me) Ile^{26}, (N-Me) Leu^{27}] IAPP [19-37] (1st synthesis).

Next, a second synthetic attempt was carried out on Rink amide MBHA resin (substitution level: 0.25 mmole Tyr /gr). Coupling of (N-Me) Leu^{27} was performed twice (4-fold excess, 1 x 95 min, 1 x 150 min). The next residue (N-Me) Ile^{26} was coupled four times to improve coupling yields: in the first three times 5-fold excess was applied (1 x 100 min, 1 x 16 hrs, 1 x 3 hrs respectively), whereas the fourth coupling 7-fold excess and performed with for 16 hrs at RT, followed by heating for 4 hrs at 40 °C and 20 hrs at RT. RP-HPLC analysis (Figure 75) of an aliquot showed: the peak at 15.0 min corresponded to the expected product [(N-Me) Ile^{26}, (N-Me) Leu^{27}] IAPP [26-37] and as indicated by the RP-HPLC profile the extended coupling of (N-Me) Ile^{26} on (N-Me) Leu^{27} lead to a coupling yield 80 to 90%. The peptide resin Fmoc-[(N-Me) Ile^{26}, (N-Me) Leu^{27}] IAPP [26-37] was acetylated and the next amino acid Ala^{25} was coupled twice: first coupling (6-fold excess) for 2 hrs at 40 °C and 23 hrs at RT and the second coupling (6-fold excess) for 3 hrs at 40 °C and 19 hrs at RT. RP-HPLC analysis (Figure 76) showed at least three main products: two of them were newly formed (peaks at 11.0 and 12.1 min, respectively), whereas the peak at 15.3 min had according to MALDI-MS a mass of 1286.3 corresponding to [(N-Me) Ile^{26}, (N-Me) Leu^{27}] IAPP [26-37] ([M+H]$^{+}$ expected: 1285.4) indicating that the Ala^{25} coupling to (N-Me) Ile^{26} did not work. Ala^{25} (6-fold excess) was recoupled for a third time. Conditions were: 3 hrs at 40 °C and 14

hrs at RT, followed by acetylation of the Fmoc-[(N-Me) Ile[26], (N-Me) Leu[27]] IAPP [25-37] resin. The remaining residues till Ser[19] were coupled twice using 5-fold excess amino acid for 90 min each coupling cycle. RP-HPLC analysis (Figure 77) of crude [(N-Me) Ile[26], (N-Me) Leu[27]] IAPP [19-37] showed the same three products as in the first synthesis, with the expected product [(N-Me) Ile[26], (N-Me) Leu[27]] IAPP [19-37] eluting at 16.5 min.

The peptide resin [(N-Me) Ile[26], (N-Me) Leu[27]] IAPP [19-37] from the second synthesis was used for further elongation. Residues from His[18] till Lys[1] were coupled twice (4-fold excess) with TBTU (4-fold excess) and DIEA (6-fold excess) for a coupling time of about 90 min except for Cys[7] and Cys[2] residues that were coupled twice with HOBt (4-fold excess) and DIC (4-fold excess) in DMF for 90 min. The peptide resin was cleaved in small amounts using reagent K (3 hrs, RT). The crude peptide after lyophilisation overnight was dissolved in 10% AcOH and analysed by RP- HPLC. According to the RP-HPLC analysis (Figure 78) the peak at 19.1 min was the expected product ([M+H]$^{+}$ expected: 3936.4, found: 3935.9), whereas the earlier eluting peaks at 11.3 min and 12.6 min were (as mentioned above) IAPP [28-37] and [(N-Me) Leu[27]] IAPP [27-37] respectively. Air oxidation (in the dark) was accomplished by dissolving crude peptide in aqueous 0.1 M NH_4HCO_3 containing 3 M Gdn HCl and after 2 hrs the solution was purified by RP-HPLC. The eluting peak at 19.3 min (Figure 79) was identified by MALDI-MS (Figure 80) to correspond to the expected product [(N-Me) Ile[26], (N-Me) Leu[27]] IAPP ([M+H]$^{+}$ expected: 3934.4, found: 3933.1). An analytical RP-HPLC of pure, oxidized [(N-Me) Ile[26], (N-Me) Leu[27]] IAPP is shown in Figure 81. The overall yield of the oxidized peptide with regard to the crude peptide was 5%.

Figure 75. RP-HPLC analysis of crude [(N-Me) Ile[26], (N-Me) Leu[27]] IAPP [26-37] (2nd synthesis) using gradient 2 on C_{18} column, flow rate 2 ml / min and detection at 214 nm. Injection of 40 µg crude peptide in 150 µl aqueous 10% TFA solution.
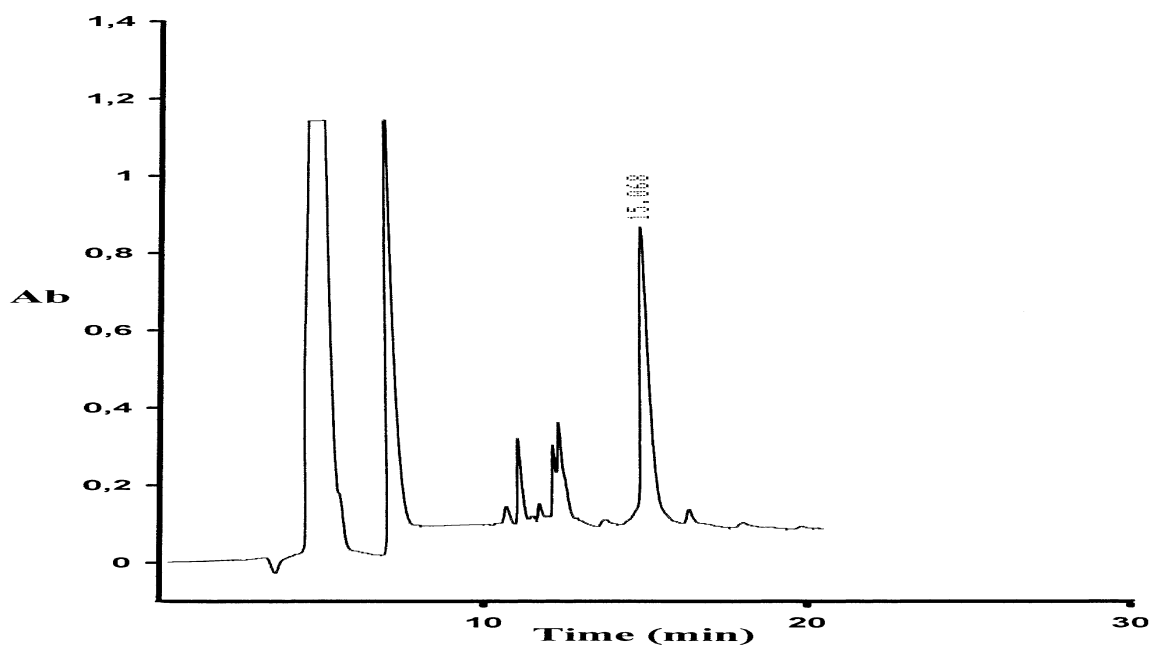

Figure 76. RP-HPLC analysis of crude [(N-Me) Ile[26], (N-Me) Leu[27]] IAPP [25-37] (2nd synthesis) using gradient 2 on C_{18} column, flow rate 2 ml / min and detection at 214 nm. Injection of 30 µg crude peptide in 150 µl aqueous 10% TFA solution.

Figure 77. RP-HPLC analysis of crude [(N-Me) Ile^{26}, (N-Me) Leu^{27}] IAPP [19-37] (2nd synthesis) using gradient 2 on C$_{18}$ column, flow rate 2 ml / min and detection at 214 nm. Injection of 30 μg crude peptide in 150 μl aqueous 10% TFA solution.

Figure 78. RP-HPLC analysis of crude [(N-Me) Ile^{26}, (N-Me) Leu^{27}] IAPP (2nd synthesis) (in reduced form) using gradient 2 on C$_{18}$ column, flow rate 2 ml / min and detection at 214 nm. Injection of 125 μg crude peptide in 50 μl aqueous 10% AcOH solution.
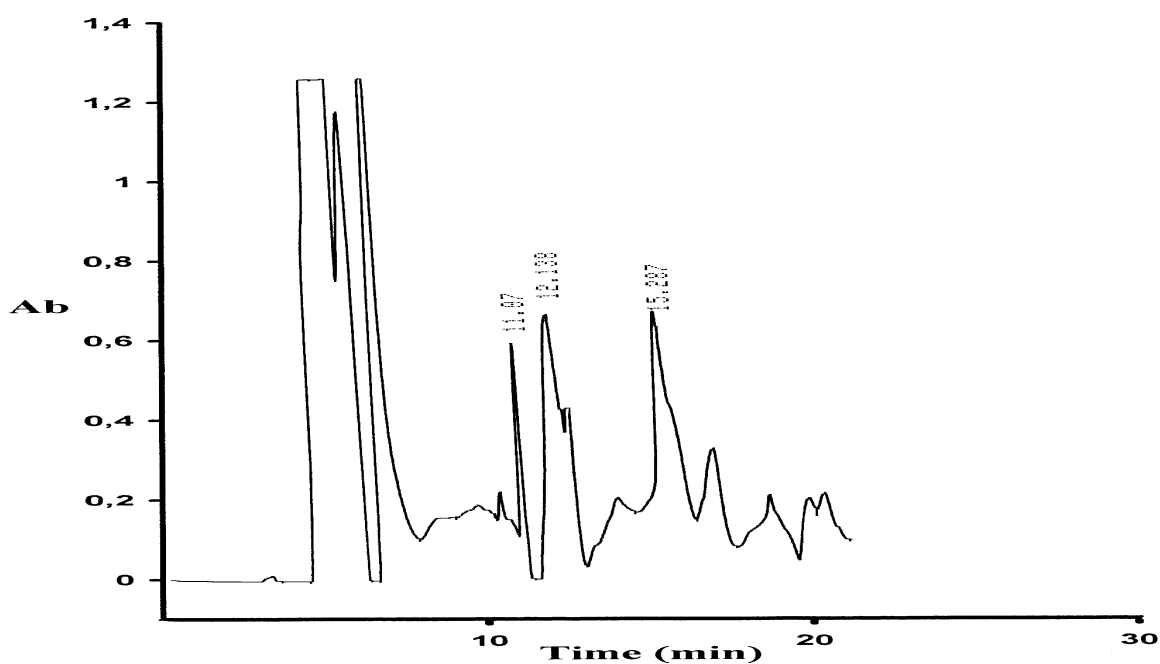
Figure 79. RP-HPLC analysis of crude oxidized [(N-Me) Ile^{26}, (N-Me) Leu^{27}] IAPP (2nd synthesis) (in oxidized form) using gradient 2 on C$_{18}$ column, flow rate 2 ml / min and detection at 214 nm. Injection of 300 μg crude peptide in 300 μl 3 M Gdn HCl in aqueous 0.1 M NH$_4$HCO$_3$ solution.

Figure 80. MALDI-MS of HPLC purified peak at 19.3 min (see Figure 79) from crude [(N-Me) Ile^{26}, (N-Me) Leu^{27}] IAPP.

Figure 81. RP-HPLC of pure [(N-Me) Ile^{26}, (N-Me) Leu^{27}] IAPP (in oxidized form) using gradient 2 on C$_{18}$ column, flow rate 2 ml / min and detection at 214 nm. Injection of 7 μg pure peptide in 100 μl aqueous 100 mM HCl.
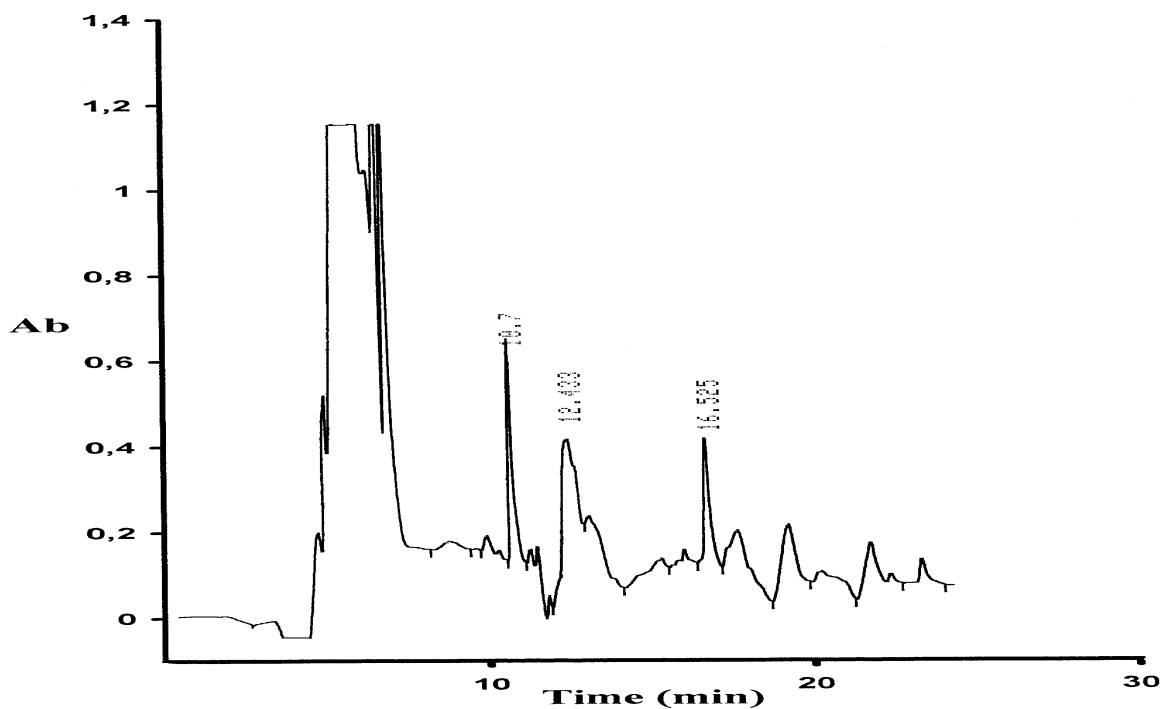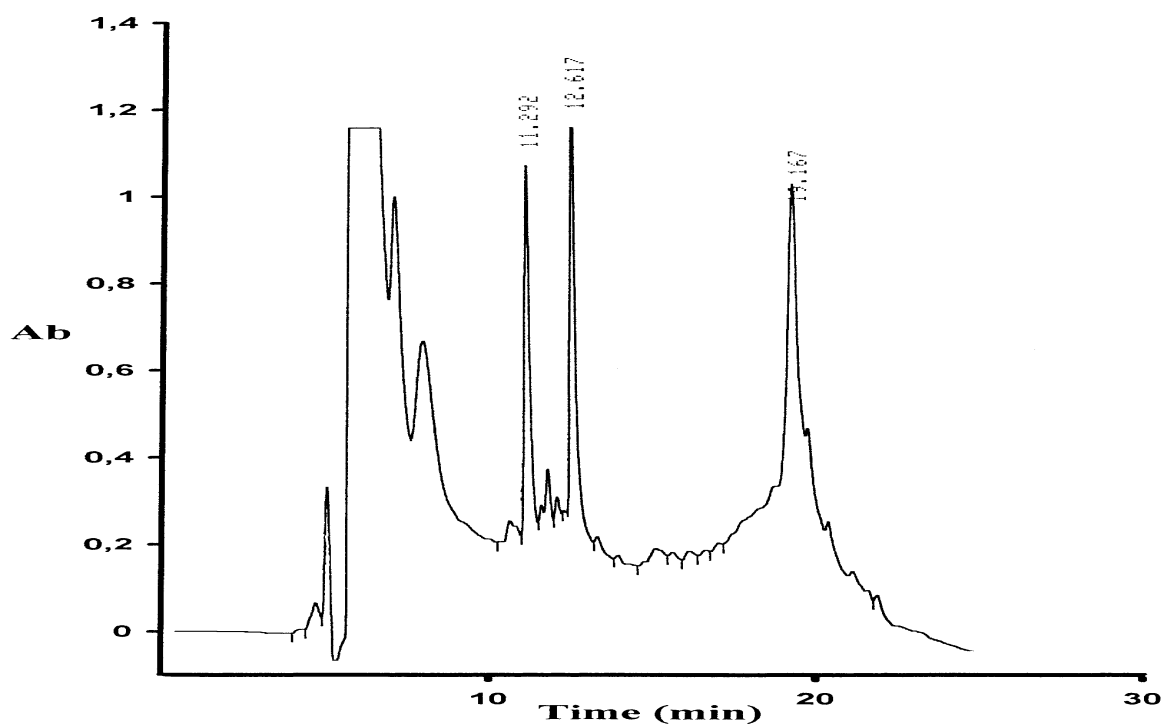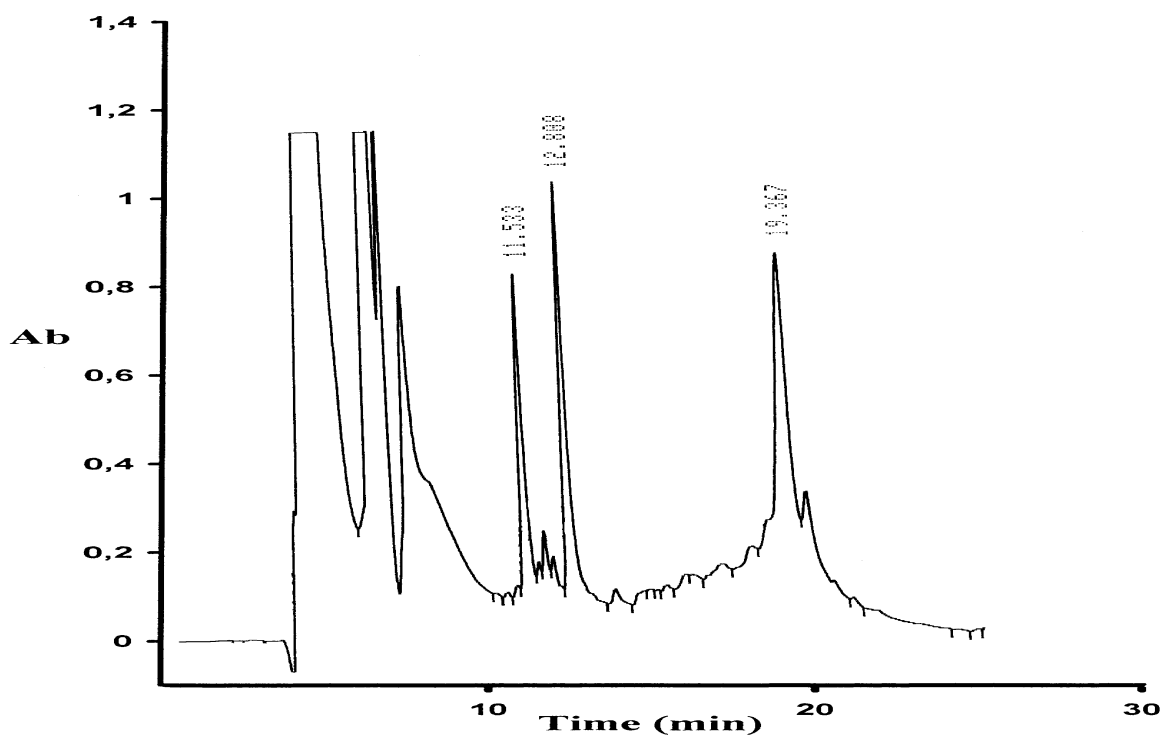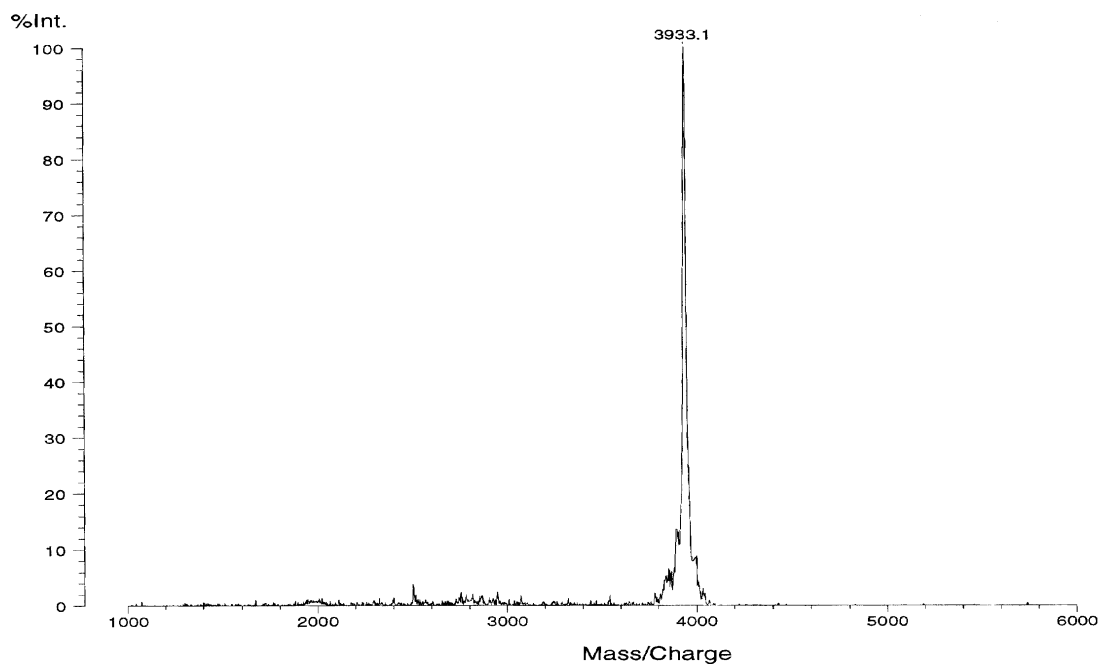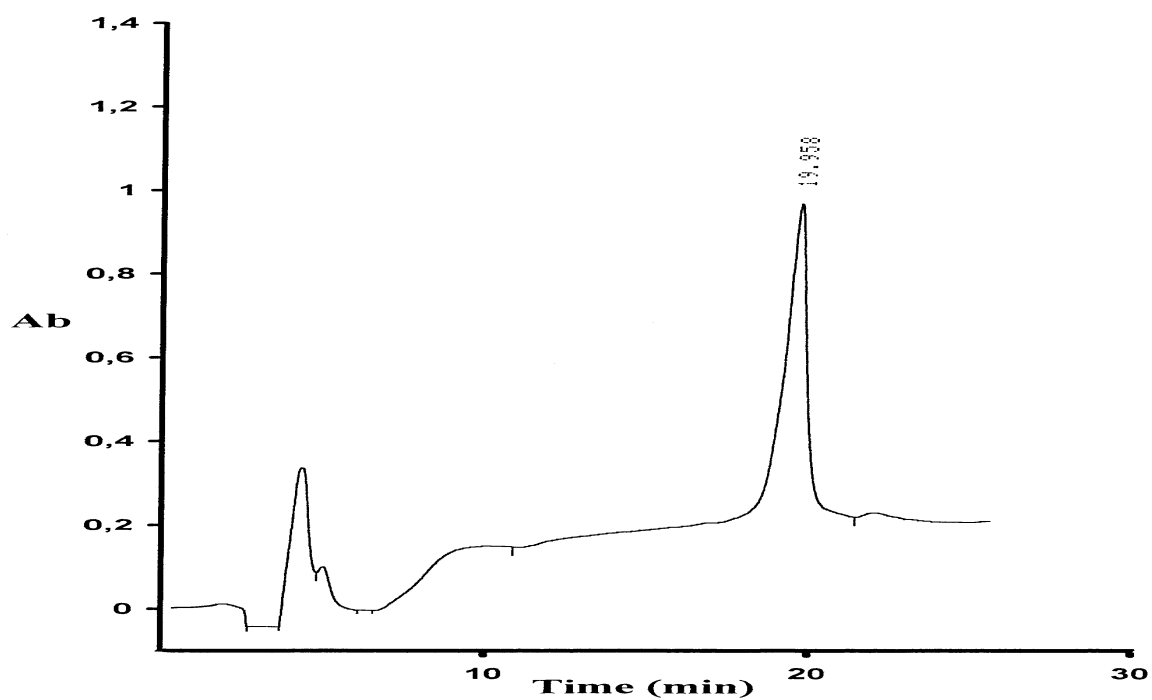
5.2.6 Synthesis of [(N-Me) Ala²⁵, (N-Me) Ile²⁶, (N-Me) Leu²⁷] IAPP [5]

The synthesis of an IAPP analogue with three consecutive N-methyl residues was a big challenge. In the first attempt, (N-Me) Leu²⁷ (6-fold excess, 2 x 75 min) was successfully coupled on Ser²⁸, as was judged by the RP-HPLC profile after cleavage of a small aliquot of peptide resin. As shown in Figure 82, the peak at 12.7 min was the peptide [(N-Me) Leu²⁷] IAPP [27-37]. For the coupling of (N-Me) Ile²⁶ 8-fold excess was used twice; the first coupling was performed for 17 hrs at RT, while the second one for 4 hrs at 50 °C and for 17 hours at RT. However, the RP-HPLC trace (Figure 83) indicated that the coupling of (N-Me) Ile²⁶ on (N-Me) Leu²⁷ was 60 to 70% complete. The peak at 15.2 min was the product [(N-Me) Ile²⁶, (N- Me) Leu²⁷] IAPP [26-37], whereas the peak at 12.7 min was [(N- Me) Leu²⁷] IAPP [27-37]. The peptide resin Fmoc-[(N-Me) Ile²⁶, (N- Me) Leu²⁷] IAPP [26-37] was acetylated and the synthesis was continued with one sixth of the peptide resin which was used for coupling (N-Me) Ala²⁵. This coupling (10-fold excess of AA) with 10-fold excess of TBTU was performed in a mixture of DMF / DCM / NMP (1:1:1), without adding DIEA for 24 hrs. Cleavage of an aliquot of [(N-Me) Ala²⁵, (N-Me) Ile²⁶, (N-Me) Leu²⁷] IAPP [25-37] resin and subsequent RP-HPLC separation (Figure 84) revealed that two main products were formed: one at 11.2 min corresponding to IAPP [28-37] due to incomplete coupling of (N-Me) Ile²⁶ to (N-Me) Leu²⁷ and cleavage of the amide bond between Ac-(N-Me) Leu²⁷ and Ser²⁸ during TFA deprotection (see 5.2.4), and one peak at 15.2 min corresponding to (N-Me) Ile²⁶, (N-Me) Leu²⁷] IAPP [26-37]. The peak at 15.2 min according to MALDI-MS had a mass of 1283.5 and indicated that the coupling of (N-Me) Ala²⁵ to (N-Me) Ile²⁶ without DIEA in the coupling mixture did not work at all.

In a second synthetic attempt, (N-Me) Leu²⁷ was coupled twice (4-fold excess, 1 x 70 min, 1 x 90 min). (N-Me) Ile²⁶ was coupled four times: two couplings were performed using 4-fold excess (1 x 80min, 1 x 85 min), a third coupling was performed using 8-fold excess for 7 hrs at 50 °C and for 15 hrs at RT, and the fourth one (4-fold excess) for 4 hrs at 60 °C. Cleavage of [(N-Me) Ile²⁶, (N-Me) Leu²⁷] IAPP [26-37] resin and RP-HPLC separation (Figure 85) showed that two main products were present: one peak at 12.5 min, corresponding to [(N-Me) Leu²⁷] IAPP [27-37], and one at 15. 1 min with a mass of 1284.6, corresponding to [(N-Me) Ile²⁶ , (N-Me) Leu²⁷] IAPP [26-37] ([M+H]⁺ expected:1285.4, found: 1284.6). Again, the coupling of (N-Me) Ile²⁶ on (N-Me) Leu²⁷ was 60 to 70% complete as judged by the RP-HPLC trace (Figure 85). The Fmoc-[(N-Me) Ile²⁶, (N- Me) Leu²⁷] IAPP [26-37] resin was acetylated before proceeding. (N-Me) Ala²⁵ was coupled twice (using the standard protocol

with TBTU / DIEA): the first coupling (8-fold excess) was performed for 90 min at 50 °C and for 5 hrs at RT, and the second coupling (4-fold excess) for 18 hrs at RT. Again, an aliquot of [(N-Me) Ala^{25}, (N-Me) Ile^{26}, (N-Me) Leu^{27}] IAPP [25-37] resin was cleaved and analysed by RP-HPLC. As shown in Figure 86, the peak at 11.3 min, corresponding to IAPP [28-37] was again present in great amount, whereas the broad peak at 15.2-15.6 min contained both the peptide without (N-Me) Ala^{25} (peak at 15.2 min) as identified by MALDI-MS ([M+H]$^{+}$ expected: 1285.4, found: 1285.4) (Figure 87) and the intended peptide [(N-Me) Ala^{25}, (N-Me) Ile^{26}, (N- Me) Leu^{27}] IAPP [25-37] (shoulder at 15.6 min) as confirmed by MALDI-MS ([M+H]$^{+}$ expected: 1371.5, found: 1368.0) (Figure 88).

Both synthetic attempts were aborted at this point due to the low yields of expected product. The data again confirmed that the formation of the truncated peptide IAPP [28-37] was taken place during the TFA / water cleavage of the acetylated peptide resin (see also 5.2.4). During the cleavage reaction (the acetylated fragment Ac-(N-Me) Leu^{27} IAPP [27-37] which is already present on the resin due to incomplete coupling of (N-Me) Ile^{26} to (N-Me) Leu^{27} and subsequent acetylation) the peptide bond between (N-Me) Leu^{27} and Ser^{28} breaks off with the release of Ac-(N-Me) Leu^{27}-OH (not detectable under the chromatographic conditions employed) and IAPP [28-37]. Additionally, the coupling of (N-Me) Ala^{25} on (N-Me) Ile^{26} was practically not possible (very low coupling yield) under the coupling conditions employed.
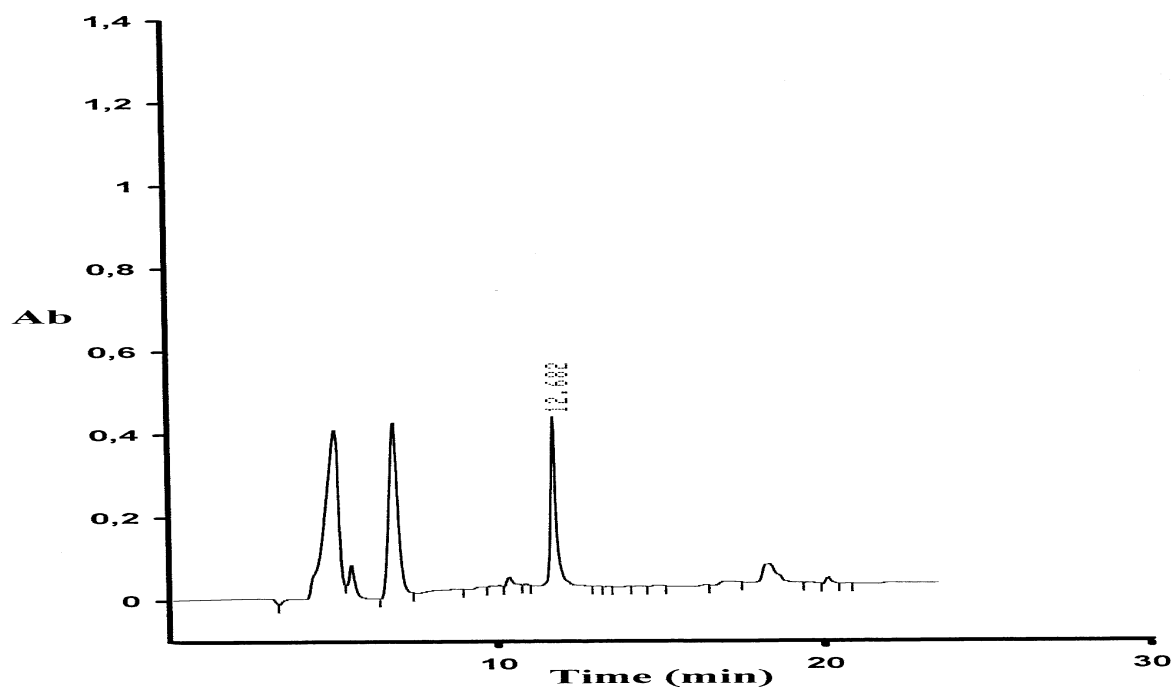
Figure 82. RP-HPLC analysis of crude [(N-Me) Leu^{27}] IAPP [27-37] (1st synthesis) using gradient 2 on C$_{18}$ column, flow rate 2 ml / min and detection at 214 nm. Injection of 40 μg crude peptide in 100 μl aqueous 10% TFA solution.
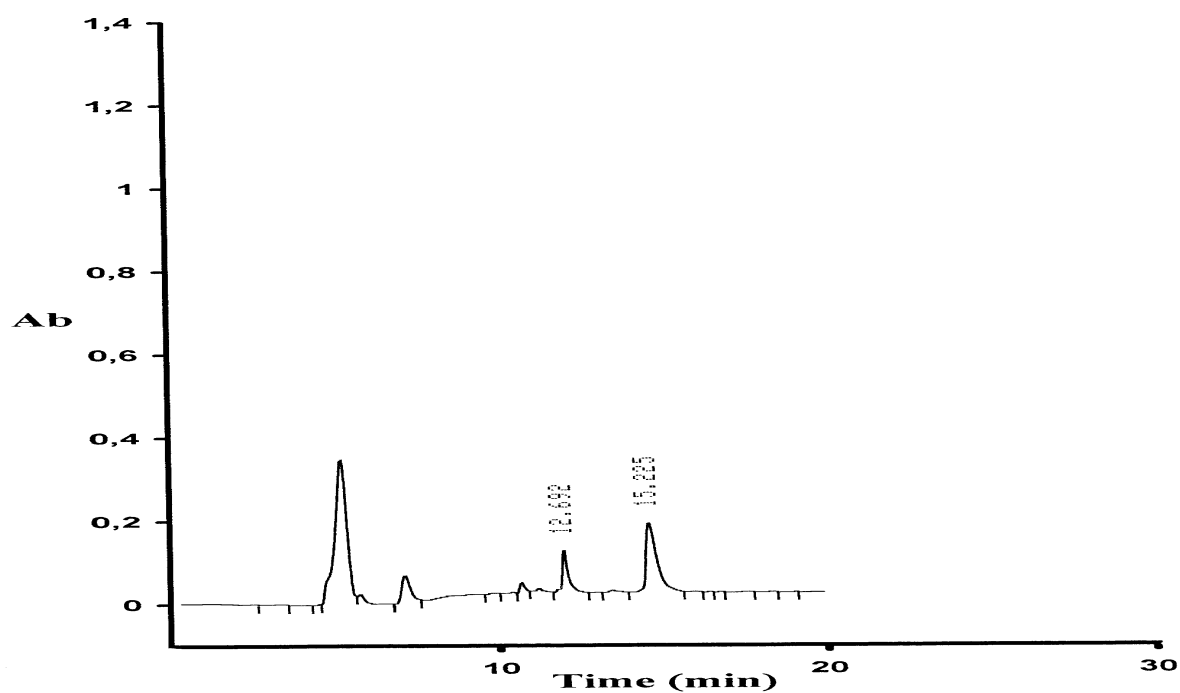
Figure 83. RP-HPLC analysis of crude [(N-Me) Ile^{26}, (N-Me) Leu^{27}] IAPP [26-37] (1st synthesis) using gradient 2 on C$_{18}$ column, flow rate 2 ml / min and detection at 214 nm. Injection of 40 μg crude peptide in 100 μl aqueous 10% TFA solution.
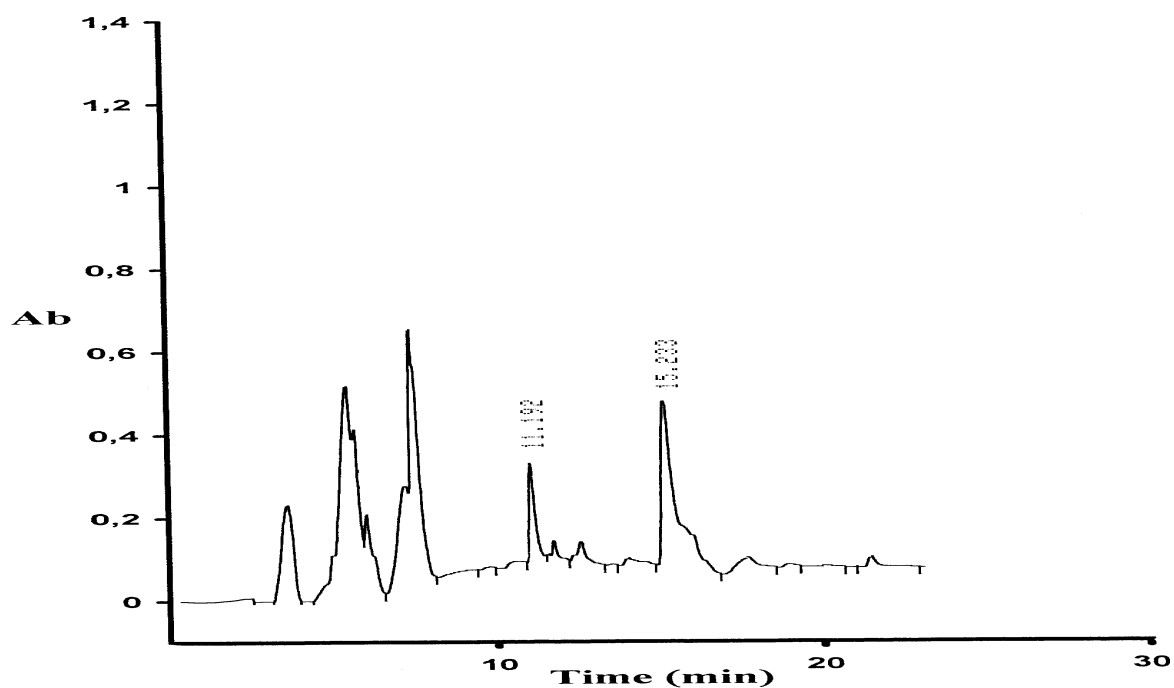
Figure 84. RP-HPLC analysis of crude [(N-Me) Ala^{25}, (N-Me) Ile^{26}, (N-Me) Leu^{27}] IAPP [25-37] (1st synthesis) using gradient 2 on C$_{18}$ column, flow rate 2 ml / min and detection at 214 nm. Injection of 40 µg crude peptide in 100 µl aqueous 10% TFA solution.
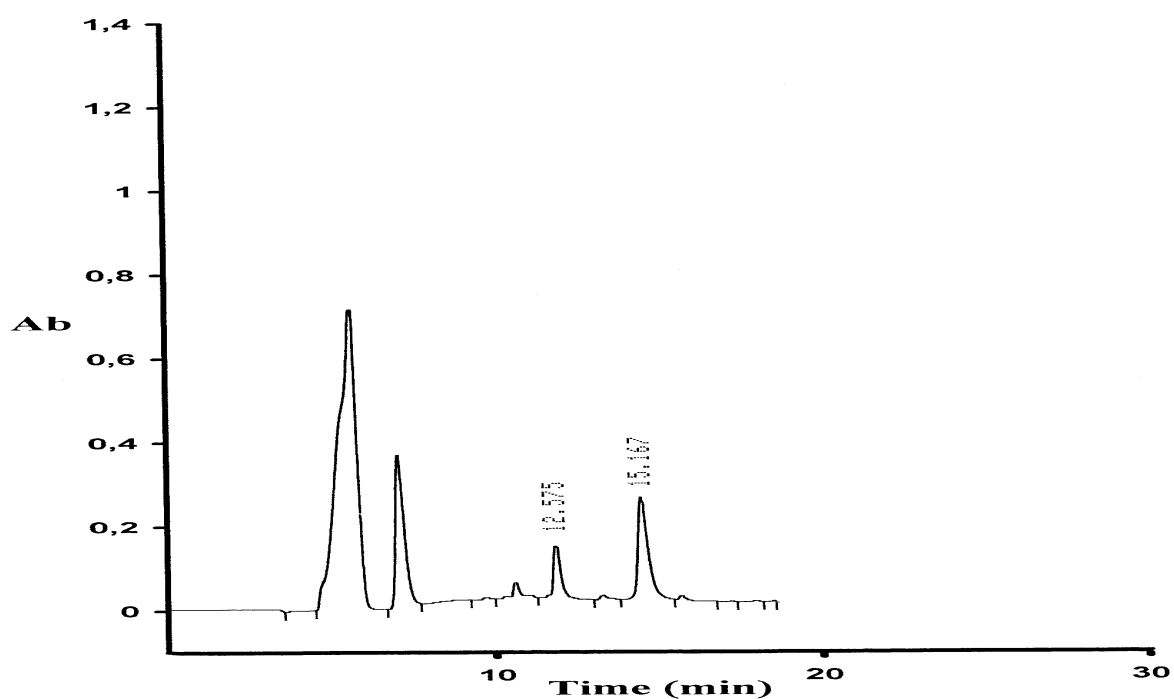
Figure 85. RP-HPLC analysis of crude [(N-Me) Ile^{26}, (N-Me) Leu^{27}] IAPP [26-37] (2nd synthesis) using gradient 2 on C$_{18}$ column, flow rate 2 ml / min and detection at 214 nm. Injection of 40 µg crude peptide in 100 µl aqueous 10% TFA solution.
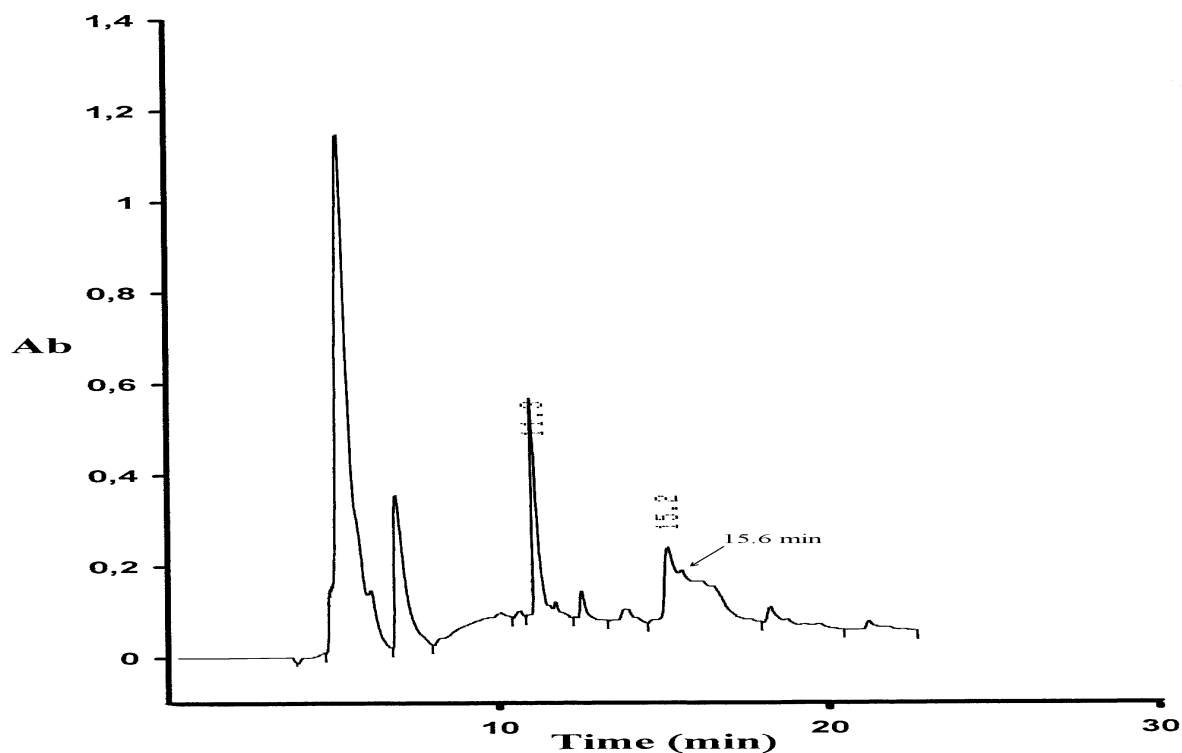
Figure 86. RP-HPLC analysis of crude [(N-Me) Ala^{25}, (N-Me) Ile^{26}, (N-Me) Leu^{27}] IAPP [25-37] (2nd synthesis) using gradient 2 on C$_{18}$ column, flow rate 2 ml / min and detection at 214 nm. Injection of 50 µg crude peptide in 100 µl aqueous 10% TFA solution.
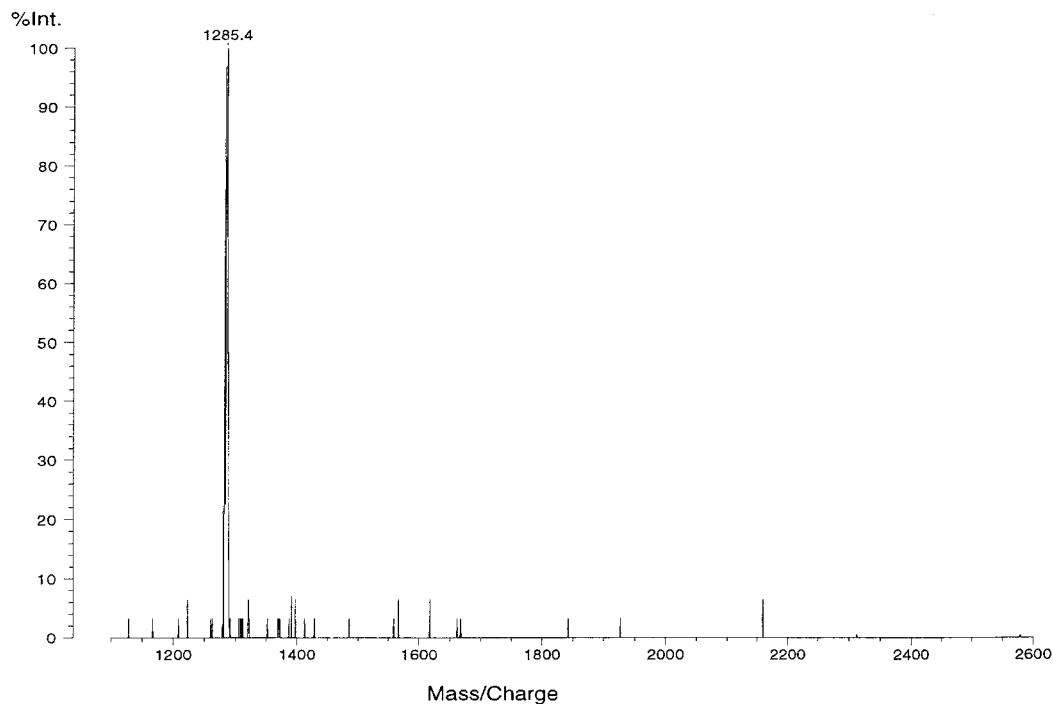
Figure 87. MALDI-MS of HPLC peak at 15.2 min (see Figure 86) from crude [(N-Me) Ala^{25}, (N-Me) Ile^{26}, (N-Me) Leu^{27}] IAPP [25-37].
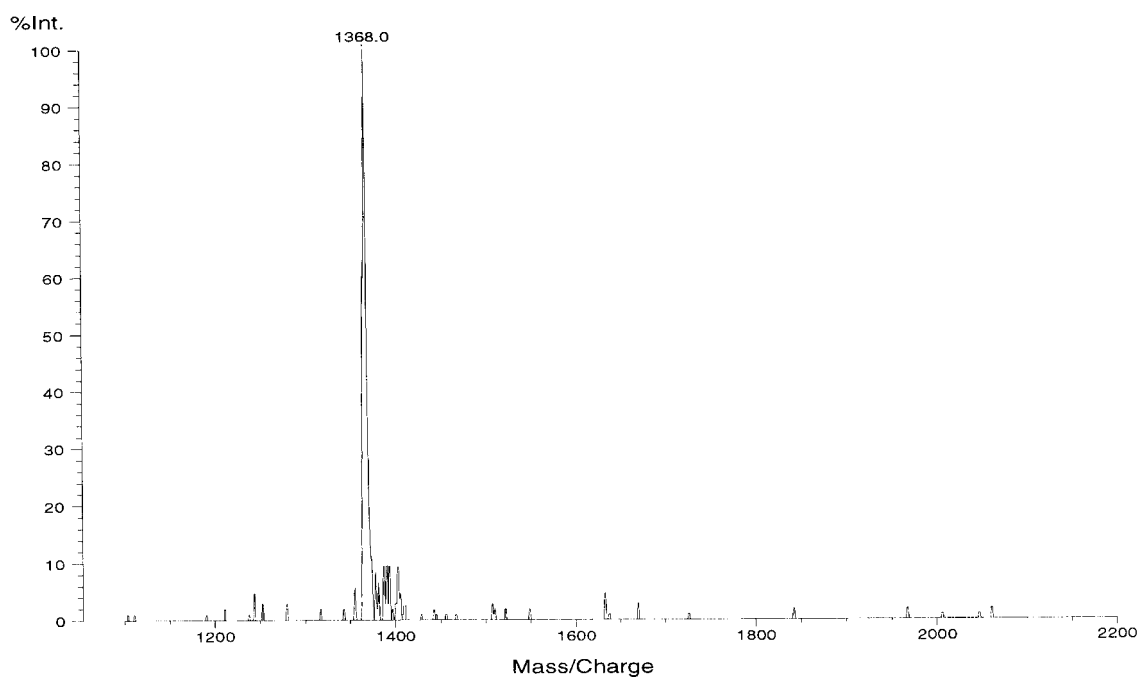
Figure 88. MALDI-MS of HPLC shoulder at ~15.6 min (see Figure 86) from crude [(N-Me) Ala^{25}, (N-Me) Ile^{26}, (N-Me) Leu^{27}] IAPP [25-37].

5.2.7 Synthesis of S20G-IAPP [6]

A large scale synthesis was to be performed and optimized at each step. Standard Fmoc-chemistry was applied and the resin used was Rink amide MBHA (2 gr, substitution level: 0.33 mmole Tyr / gr). Double couplings for each residue were applied following attachment of Tyr[37] to the resin. Couplings (4-fold excess) were performed by activation with TBTU (4-fold excess), neutralization with DIEA (6-fold excess) in DMF and coupling time 45 min each time. This protocol was followed till residue Leu[27], whereas in the difficult region Ile[26] to Gly[24] the second coupling was accomplished by activation using the more reactive coupling reagent 2-(1H-9 azabenzotriazole-1-yl)-1,1,3,3-tetramethyluronium hexafluorophosphate (HATU) (4-fold excess, 1 x 45 min). Moreover, for residues Ala[25] and Gly[24] the first coupling (with TBTU) was performed with 8-fold excess for 1 hr. Peptide resin was always acetylated after the couplings (as part of the protocol) in the region Ile[26] till Lys[1]. The coupling of Asn[22] also proved to be very difficult: even after two couplings (4-fold excess, TBTU) free amino groups were detected by the Kaiser test. Therefore, the coupling was repeated two more times (4-fold excess TBTU, 2 x 1 hr). The next residue Asn[21] was also coupled twice: the first coupling was performed with TBTU (4-fold excess, 1 x 45 min) and the second coupling with HATU (4-fold excess, 1 x 55 min). At this point, a small aliquot of IAPP [21-37] resin was cleaved and analysed by RP-HPLC according to our standard procedure. The peak eluting at 17.0 min (Figure 89) was identified by FAB-MS as the expected product IAPP [21-37] ([M+H]$^+$ expected: 1758.9, found: 1757.8).

Residues from Gly[20] till Leu[12] were coupled twice with TBTU (4-fold excess), followed by acetylation at each step. For residues Arg[11], Gln[10] and Thr[9] the second coupling was performed with HATU (4-fold excess), as, based on the experience from the previous syntheses, these residues were difficult to couple. Cys[7] and Cys[2] residues were coupled three times: the first two couplings with DIC (3-fold excess, 1 x 60 min, 1 x 45 min), whereas the third coupling with HATU / DIEA (1.5-fold excess each, 1 x 45 min), followed by acetylation of the resin. At the end of the synthesis the resin was cleaved in small amounts with reagent K (3 hrs, RT). The crude peptide was dissolved in 10% AcOH and was analysed by RP-HPLC. The peak at 23.8 min (Figure 90) was the expected peptide according to MALDI-MS. Air oxidation (in the dark) was performed in 6 M Gdn HCl in aqueous 0.1 M NH$_4$HCO$_3$ using the crude peptide. Oxidation usually required 2 hrs and the peptide was purified directly after oxidation to avoid aggregation according to our standard procedure. The peak at 24.2 min (Figure 91) which was identified by MALDI-MS (Figure 92) to be the intended peptide S20G-IAPP ([M+H]$^+$ expected: 3874.3, found: 3873.6) was collected, whereas the peak at 22.9 min was a deletion peptide corresponding according to

MALDI-MS to acetylated S20G IAPP [10-37] ([M+H]$^+$ expected: 3024.3, found: 3025.5) that may have formed due to incomplete coupling of Thr^9 to Gln^{10} and subsequent acetylation. An analytical HPLC of pure S20G-IAPP is shown in Figure 93. The yield of the oxidation / purification procedures with regard to the crude material was 6%.
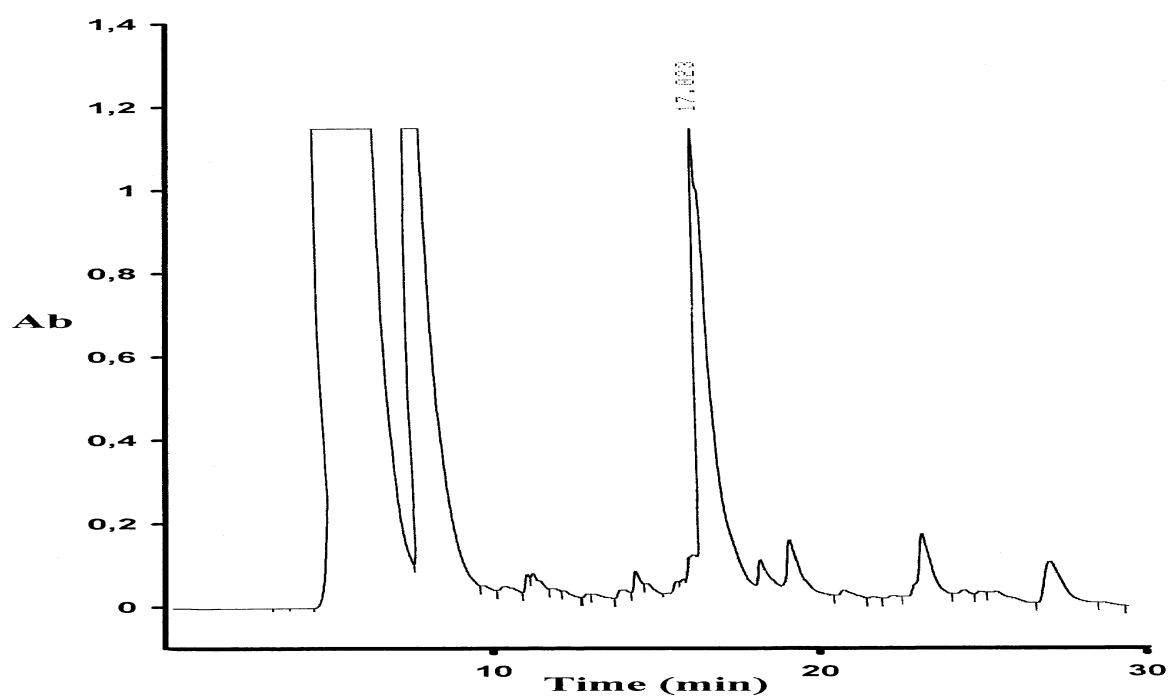

Figure 89. RP-HPLC analysis of crude IAPP [21-37] using gradient 2 on C$_{18}$ column, flow rate 2 ml / min and detection at 214 nm. Injection of 400 μg crude peptide in 500 μl aqueous 10% TFA solution.
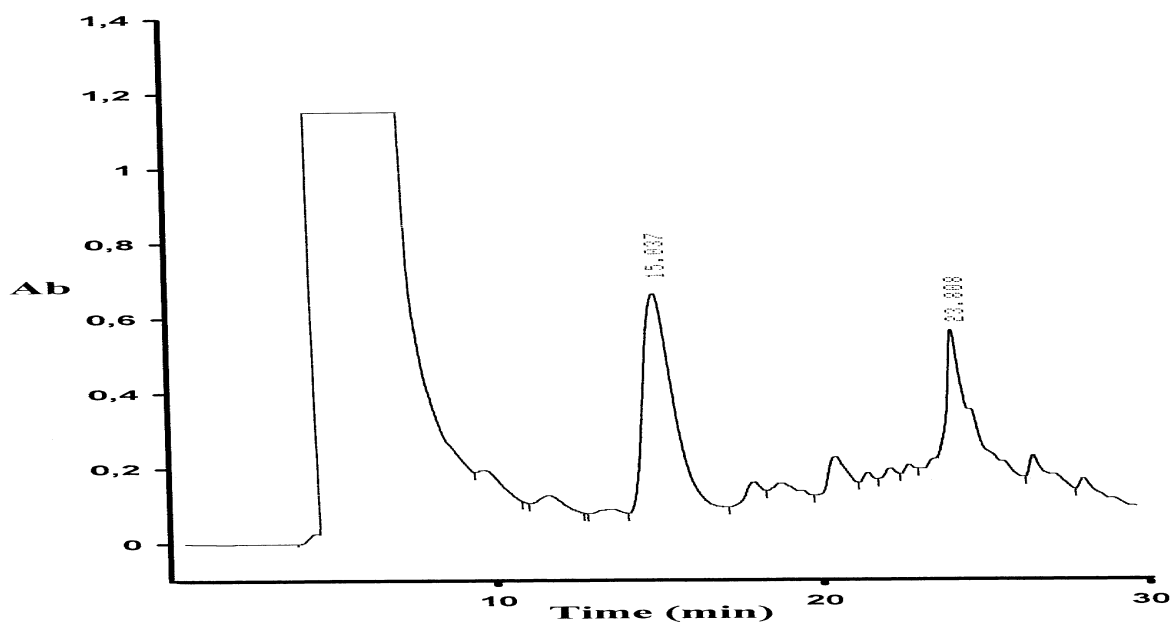
Figure 90. RP-HPLC analysis of crude S20G-IAPP (in reduced form) using gradient 1 on C_{18} column, flow rate 2 ml / min and detection at 214 nm. Injection of 500 µg crude peptide in 1 ml aqueous 10% AcOH solution (the peak at 15.0 min is due to scavenger phenol from the cleavage mixture).
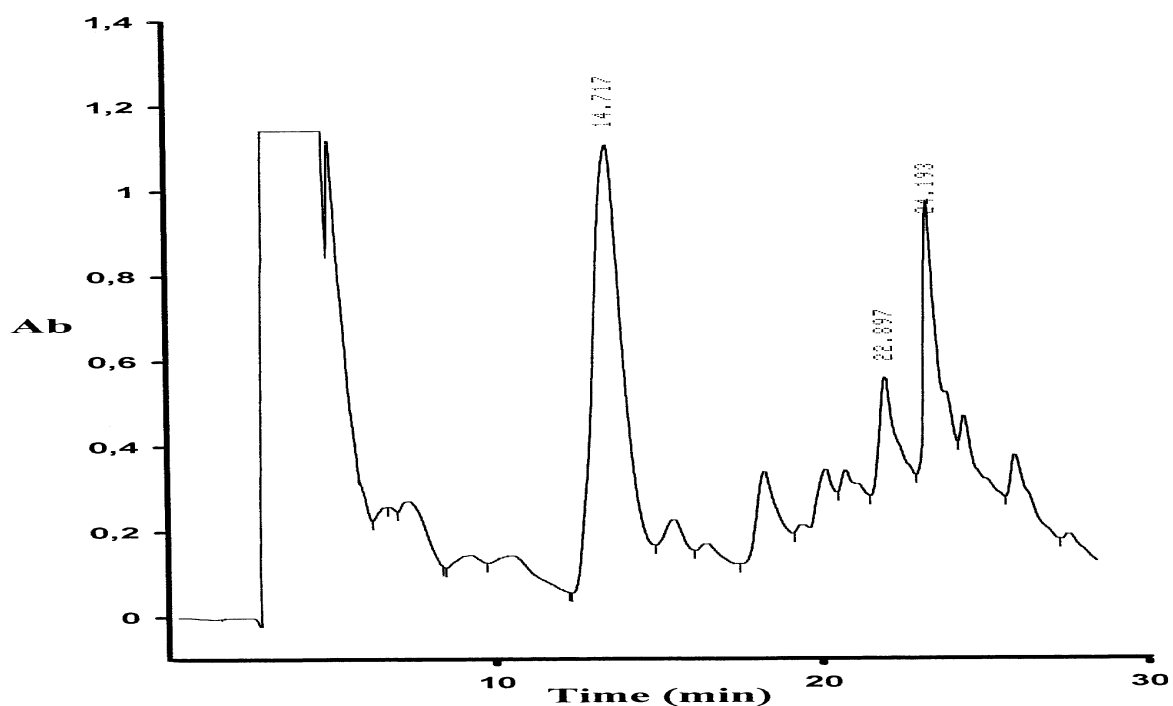
Figure 91. RP-HPLC analysis of crude S20G-IAPP (in oxidized form) using gradient 1 on C_{18} column, flow rate 2 ml / min and detection at 214 nm. Injection of 500 µg crude peptide in 500 µl 6 M Gdn HCl in aqueous 0.1 M NH_4HCO_3 solution after 4 hrs oxidation (the peak at 14.7 min is due to scavenger phenol from the cleavage mixture).
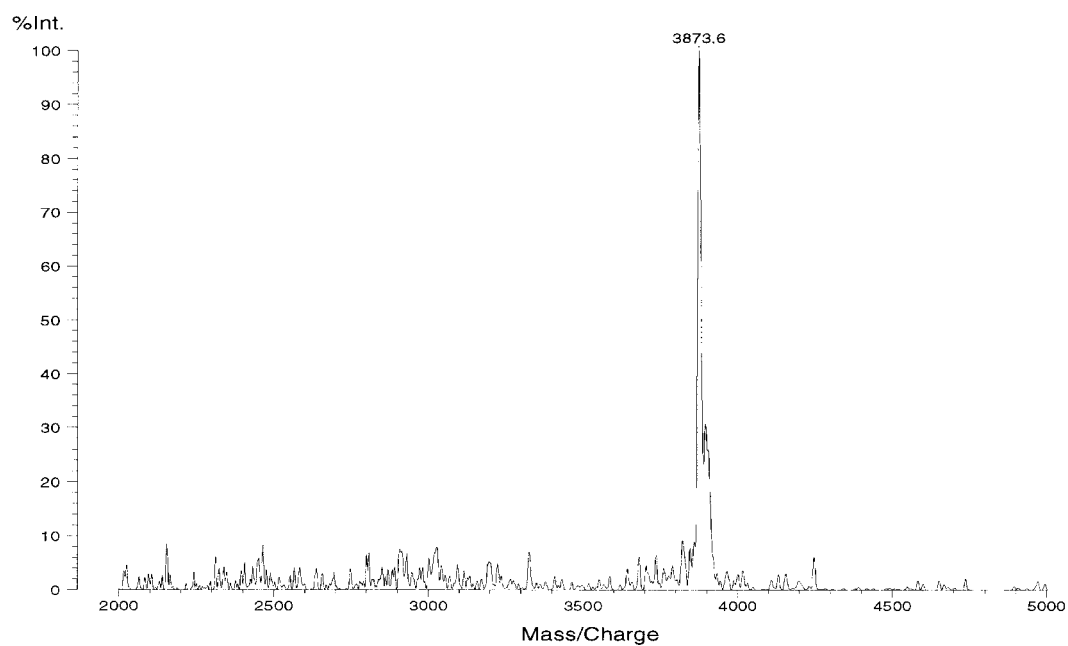
Figure 92. MALDI-MS of oxidized and HPLC purified peak at 24.2 min (see Figure 91) from crude S20G-IAPP.
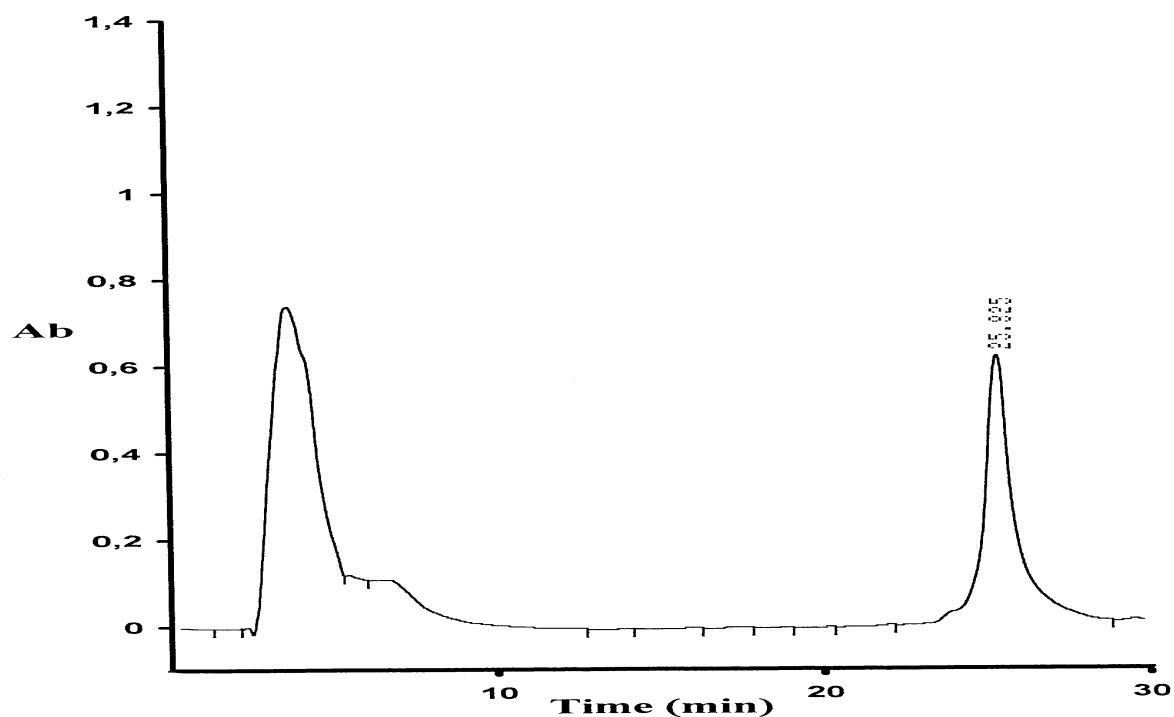
Figure 93. RP-HPLC of pure S20G-IAPP (in oxidized form) using gradient 1 on C_{18} column, flow rate 2 ml / min and detection at 214 nm. Injection of 60 µg pure peptide in 50 µl aqueous 6 M Gdn HCl.

5.2.8 FT-IR and cytotoxicity studies of IAPP and the IAPP analogue [2]

IAPP amyloid aggregates contain the peptide chains in a β-sheet conformation and have been found to be cytotoxic to a variety of cells [91]. To begin to investigate the effect of selective N-methylation on the β-sheet, amyloid formation and cytotoxicity potential of IAPP FT-IR spectroscopy was first performed. IAPP and analogue [2] were incubated under strong amyloidogenic conditions (high concentration of peptide) and FT-IR spectra were recorded. In Figure 94 the FT-IR spectra of the two peptides are shown: the native IAPP had a broad absorbance maximum at 1630 cm^{-1}, which is often assigned to β-sheet structure [92]. In contrast, in the spectrum of [2] the absorbance maximum was shifted at about 1660 cm^{-1}, indicating the presence of significant amounts of non-β structures. The differences in β-sheet forming potential between the two peptides strongly indicates that the N-methylation of the two residues Gly^{24} and Ile^{26} inhibited the β-sheet forming potential of IAPP and may thus have affected amyloidogenicity.
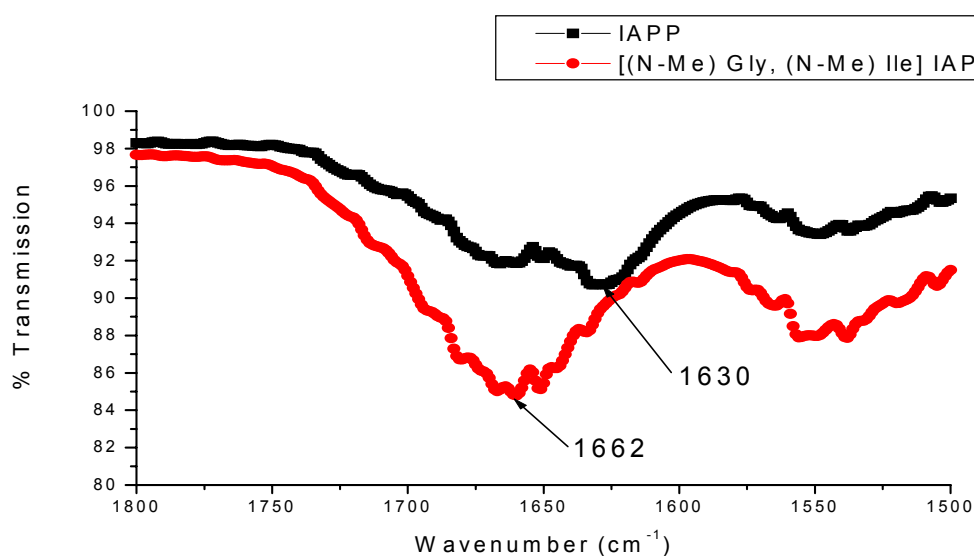
Figure 94. Effect of N-methylation on the secondary structure / β-sheet formation potential of the native IAPP sequence versus the IAPP analogue [2] as assessed by FT-IR of aged solutions. IAPP and [2] were incubated under strong amyloidogenic conditions as follows: IAPP or [2] was incubated at a concentration of 2.14 mM in 10% AcOH at RT for 4 days. Following neutralization with 10% NH$_4$OH peptide solutions were applied to a CaF$_2$ plate, air-dried and the spectra were recorded as described [86].

Cytotoxic effects of IAPP versus [2] were tested on the HTB14 human glioblastoma /astrocytoma cell line 24 hrs following application of the peptide onto the cells. The cytotoxic potential of aged IAPP was then compared to the one of aged [2] by using the MTT reduction assay [93].

Peptide cytotoxicities were tested at concentrations of 50 and 5 nM. The results of the cytotoxicity assay suggested (Figure 95) that the methylated IAPP analogue [2] was not cytotoxic, whereas IAPP was strongly cytotoxic.
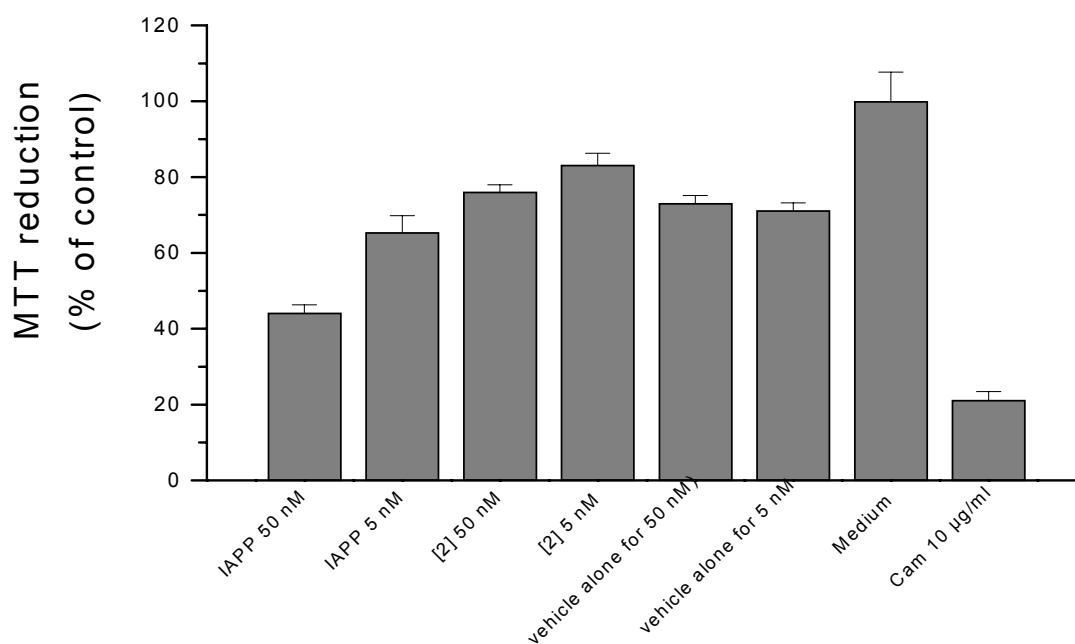
Figure 95. Cytotoxicity assay of IAPP and [2]. Data are percentages of control values (vehicle alone) and are the mean (± SD) of five determinations. Camptothecin (Cam 10 µg / ml) was used as a cell death inducing agent (positive control) [94]. HFIP (0.01% and 0.001%) was used as a control (vehicle alone) for the IAPP and analogue [2] concentrations of 50 and 5 nM, respectively [95].

Together, the results of the IR and cytotoxicity studies strongly suggested that N-methylation at Gly^{24} and Ile^{26} strongly affected the β-sheet formation potential of IAPP and inhibited its cytotoxicity.

6 Discussion

6.1 Discussion of the results of the bioactivity studies on the calcitonin analogues

In this work a number of hCt analogues were designed and synthesized to study the effect of conformational restriction of region [17-21] on receptor binding and activation using side chain lactam bridge. In these studies, covalently linking the side-chains of Asp[17] and Lys[21] or Asp[17] and Orn[21] was found to enhance the receptor binding affinities of these peptides compared to native hCt up to three times for receptor sites in T47D cells. These constrained analogues (analog 1 and CCcyclo) bound tightly to the receptors, suggesting that the constraints introduced into their structures might have stabilized their solution conformations prior to the receptor binding step. The enhanced binding affinities of these analogues were accompanied by equal or slightly enhanced increases of the adenylate cyclase activity, as expected for a direct ligand-receptor interaction [96]. Analogues that contained shorter ring size (DCcyclo and FCcyclo) than analog 1 and CCcyclo showed reduced receptor binding affinities and also their potencies to stimulate the production of cAMP were lowered. The 19-membered ring-containing analogues CCcyclo and GCcyclo were found thus to be the strongest Ct-receptor ligands, whereas the Glu[17] / Dab[21] lactam bridge of GCcyclo resulted in two-fold and three-fold reduced adenylate activation potency, compared to native hCt and CCcyclo, respectively. The biological importance of constraining the conformation via the lactam-bridge was highlighted in the case of CClinear where the complete absence of the bridge resulted in an extremely low ability to bind to the receptor and activate AC.
The topological features of region [17-21] for Ct bioactivity were further explored by studying the importance of the chirality of residues 18 and 19 (analogues of group 2). A β-turn conformation strongly depends on the nature and chirality of the amino acids at its corner positions and small changes can affect the type and stability of the turn. Inversement of chirality of residue Phe[19] by D-Phe[19] was expected to stabilize a type II β-turn conformation, whereas substituting Lys[18] by D-Lys[18] was expected to stabilize a type II′ β-turn [24]. The substitution Aib[18] for Lys[18] might retain the postulated type I β-turn [97]. The study of the non-bridged analogues [D-Phe[19]]hCt (OClinear) and [D-Lys[18]]hCt (NClinear) provided information about the effect of the substituents alone on hCt bioactivity. Although all analogues of group 2 had similar binding affinities to hCt, their ability to induce adenylate cyclase activation was up to three times less than hCt. The order of AC activation potency was: ACcyclo>ECcyclo>BCcyclo. This indicated that inversement of chirality of residues at positions 18 and 19 strongly affects the bioactivity of hCt. The non-bridged analogues

(OClinear and NClinear) showed lower receptor binding affinities and AC activation potencies than hCt. Together, it may be concluded that residues Lys[18], Phe[19] are important for the biological activity of hCt, and that the incorporation of the lactam bridge can partly compensate for the loss of bioactivity observed during the inversement of chirality at residues 18 and 19.

Next, the effect of introducing 'Asx-turn' inducing residues such as Pro / Ser at positions 18 and 19 was studied (analogues of group 3). From the analogues of this group only ICcyclo retained some binding affinity for the receptor, whereas the other analogues showed no receptor binding. This finding suggested that in ICcyclo the elimination of the side chain of Lys[18] might in small extent be tolerated, whereas in HCcyclo the elimination of the side chains of both Lys[18] and Phe[19] resulted in abolishment of receptor binding. The AC activation potencies were extremely low in accordance with the lack of receptor binding affinities for these peptides. From the results with cyclic and linear analogues it was supported that residues 18 and 19 are very important for bioactivity.

The importance of a putative H-bond between the carbonyl group at position 17 (Asp[17]) was studied next using analogues with (N^{α}-methyl) at Phe[19] (group 4) and a series of βeta peptides (group 5). The carbonyl group of the side chain of Asp[17] was postulated to participate in a hydrogen bond with the NH group of the Phe[19] residue [71]. Introduction of the N-methylated amino acid at the NH of Phe[19] position was expected to disrupt the putative H-bonding. In fact, both analogues QCcyclo and QClinear exhibited extremely weak binding affinities and AC activation potencies. In the βeta peptides, the distorted backbone had the same overall effect: no binding to receptor and no stimulation of the adenylate cyclase system.

Next, the functional role of the side-chain carbonyl group of Asn[17] was studied (group 6). In the non-bridged analogues [Dap[17]]hCt and [Dab[17]]hCt, the carbonyl group was eliminated while the rest of the molecule retained the same sequence as hCt. Both analogues showed weak binding affinities and AC activation potencies compared to native hCt, with the former analogue ([Dap[17]]hCt) being more active than the latter ([Dab[17]]hCt). Thus, the deletion of the carbonyl group of the side chain of Asn[17] resulted in reduced biological properties. It is interesting to note that the longer side chain of Dab[17] has a strong negative effect on bioactivity. This suggests that bioactivity may also be related to the exact position (topology) of the NH_2 group of the side chain of Asn[17].

The role of the proposed amphiphilic α-helical region [8-22] of Ct and its amino acid composition was evaluated in the peptides TCcyclo and TClinear (group 7). In these analogues the aromatic residues Tyr[12] and Phe[16,19] of the hydrophobic face of the potential

helix of hCt, were substituted by Leu[12,16,19] that are present in the sCt sequence [38]. In addition, Phe[22] was replaced by Tyr [98]. In all analogues, the incorporation of the lactam bridge resulted in increased receptor binding affinities and enhanced potencies in AC activation. Surprisingly, analogue TCcyclo exhibited a somewhat reduced binding affinity as compared to sCt and CCcyclo. However, its ability to activate AC was similar to sCt. The unbribged TClinear, bound to the receptor as strong as hCt and had a four times reduced AC activation potency as compared to hCt.

The results of the bicyclic analogues confirmed and strongly supported the working hypothesis suggested by Kapurniotu *et al.* [22] that a type I β turn/antiparallel β sheet centered around residues 18 and 19 play a crucial role in hCt bioactivity. Moreover, the importance of the side chain carbonyl at Asp[17] was significant as it was suggested for stabilizing the potential β turn/β sheet by hydrogen bonding to the NH group of Phe[19]. The importance of β turn conformations has often been attributed to the resulting surface exposure and clustering of side chains, which might be important pharmacophores and/or to the nucleation of folding into bioactive conformation [99]. However, the stabilization of the β turn/β sheet conformation alone may not be the only factor for hCt bioactivity, which depends on additional factors such as overall conformational flexibility, and the topology of the side chains of certain residues in the [17-21] region.

Overall the results suggested that the receptor binding affinity and the agonist potency of hCt may have determinants that are different from those of sCt. For sCt, it has been suggested that the binding of the central amphiphilic α-helical segment to the extracellular N-terminal receptor domain may be the major determinant of affinity to the hCt receptor [100]. Binding of an α-helical state may be less important for hCt since the underlying sequence shows a lesser propensity for helix formation [101]. Instead, the affinity of hCt for receptors may be determined by additional interactions involving the peptide sequences that was constrained by the bridge and/or the C-terminal segment that may be correctly oriented by the bridge for optimal receptor interaction.

6.2 Discussion of the syntheses and studies of the IAPP analogues

The SPPS of IAPP belongs to the difficult syntheses. This is due to the fact that IAPP is an amyloid forming peptide and has the potential of β-sheet formation and aggregation during synthesis [102]. In fact, the synthesis of IAPP proved to be a very difficult one. The HPLC profile indicated many by-products, the chromatographic purification was extensive and the final yield with regard to pure peptide was not satisfactory.

Since S20G-IAPP was reported to be more aggregation prone than IAPP its synthesis was expected to be more difficult than the IAPP one. Therefore an optimised protocol was applied: a) by utilization of HATU for the second coupling of residues Gly[24], Ala[25], Ile[26], Asn [21], Arg[11], Gln[10], and Thr[9] that were expected, based on the experience with IAPP, to be difficult to reach completeness and b) acetylation was performed after all (double) couplings in region between residues 26 and 2. In fact, the results showed that this synthetic protocol worked much better than the IAPP one. However, difficult couplings in the IAPP region [8-10] as well as with the Cys residues were still encountered.

The incorporation of (N-Me) residues into the β-sheet core IAPP region [20-29] was expected to cause even more synthetic difficulties The reason for this are sequence-related (hydrophobic amino acids in region [20-29]) and the steric hindrance caused by the (N-Me) residues [103]. N-methylation has been reported to allow formation of left-handed α-helical structures, to promote *cis-trans* isomerization of the peptide bond, to disrupt hydrogen bonding of the amide nitrogen, and to increase the hydrophobicity of the peptide [104]. On the other hand, the incorporation of (N-Me) moieties in crucial for β-sheet formation amide bonds was expected to suppress synthetic problems related to internal β-sheet formation and aggregation.

Peptide bond formation is generally not difficult when only the acid component of the coupling pair is N-methylated, and these reactions proceed well under standard coupling conditions, although one must be aware of the potential for racemization and diketopiperazine formation [105]. On the other hand, serious problems with coupling rates arise when the amine component or when both the amine and the acid components are N-methylated [106]. Low coupling rates in these cases can lead to extended reaction times, undesired side reactions, racemization or incomplete couplings that give rise to deletion sequences [107].

In the synthesis of [(N-Me) Phe[23], (N-Me) Ala[25]] IAPP [19-37] (part of analogue [1]), (N-Me) Ala[25] as well as Gly[24] were coupled without any difficulties. The second N-methylated residue (N-Me) Phe[23] was also coupled without significant difficulty, whereas the coupling of

Asn[22] to (N-Me) Phe[23] could not reach completion (60 to 70% completion according to HPLC analysis). To avoid formation of deletion sequences the peptide resin was acetylated after the couplings of AA 24 to 21. Cleavage and RP-HPLC analysis of [(N-Me) Phe[23], (N-Me) Ala[25]] IAPP [19-37] resin showed two main products: the intended peptide [(N-Me) Phe[23], (N-Me) Ala[25]] IAPP [19-37] and the deletion sequence [(N-Me) Ala[25]] IAPP [24-37]. Detailed HPLC and mass spectroscopic analysis of the synthesis products between residues 25-22 suggested that the truncated peptide formed due to peptide bond cleavage between (N-Me) Phe[23] and Gly[24] in the acetylated truncated peptide sequence Ac-[(N-Me) Phe[23], (N-Me) Ala[25]] IAPP [23-37]. This latter peptide sequence corresponded to about 35% of the total product and formed due to the incomplete coupling of Asn[22] to (N-Me) Phe[23] and the subsequent capping of the non-reacted amino groups of (N-Me) Phe[23] with Ac₂O. This finding was in accordance to previous findings that suggested that the presence of a N-methylated residue makes the amide bond C-terminal to this residue susceptible to TFA-mediated hydrolysis [15]. In this latter work, resin-bound Ac-(N-Me) PheSerLeuGly has been found to get readily hydrolysed during treatment of the peptide resin with TFA yielding the two products Ac-(N-Me) Phe and Ser-Leu-Gly (yield of hydrolysis: 76%).

During the synthesis of [(N-Me) Gly[24], (N-Me) Ile[26]] IAPP [19-37] (part of analogue [2]) the coupling of (N-Me) Ile[26] to Leu[27] could not reach completion (70 to 80% completion). In addition, the coupling of Ala[25] to (N-Me) Ile[26] was even more difficult and, although it was repeated five-times, it could not reach completion (60 to 70% completion). Acetylations were thus performed after the couplings of the above residues to avoid formation of deletion sequences. The second N-methyl residue (N-Me) Gly[24], however, was coupled without any difficulties and this was the case for the remaining residues until residue 19. Overall, the peptide resin was acetylated after the couplings of (N-Me) Ile[26], Ala[25], (N-Me) Gly[24] and Phe[23]. It was concluded that the major difficulties of the synthesis of [(N-Me) Gly[24], (N-Me) Ile[26]] IAPP [19-37] were due to the couplings of residues (N-Me) Ile[26] and Ala[25]. The yield in main product [(N-Me) Gly[24], (N-Me) Ile[26]] IAPP [19-37] was 50 to 55% with regard to the total functional groups of the resin. The truncated acetylated sequences represented 40 to 45% of the total product and it was observed that the acetylated sequence Ac-[(N-Me) Ile[26] IAPP [26-37] was also hydrolysed to a small extent during TFA treatment yielding the dipeptide Ac-(N-Me) Ile[26]-Leu[27]-OH and IAPP [28-37].

In the synthesis of [(N-Me) Ala[25], (N-Me) Leu[27]] IAPP [19-37] (part of analogue [3], the (N-Me) Leu[27] coupled efficiently. In contrast, the coupling of Ile[26] was difficult and could not reach completion (30 to 40% completion). This low coupling efficiency of Ile[26] to (N-Me)

Leu[27] could also be partly attributed to the relative "high loading" of the resin (0.5 mmole / gr) used for this synthesis as compared to the "low loading" resins (0.2-0.3 mmole / gr) used for the syntheses of the other N-methylated analogues in which the coupling efficiency was normally double (60 to 70% completion). The coupling of (N-Me) Ala[25] and Gly[24] proceeded without difficulty. The peptide resin was acetylated after the couplings of (N-Me) Leu[27], Ile[26], (N-Me) Ala[25] and Gly[24]. However, cleavage and RP-HPLC analysis of the [(N-Me) Ala[25], (N-Me) Leu[27]] IAPP [24-37] resin showed two main products were formed: the intended peptide [(N-Me) Ala[25], (N-Me) Leu[27]] IAPP [24-37] and the deletion sequence IAPP [28-37]. The finding that IAPP [28-37] was not acetylated, although the coupling of (N-Me) Leu[27] on [28-37] resin was followed by acetylation of free amine groups on the resin, indicated that IAPP [28-37] might have formed during TFA cleavage of the peptide from the resin. To investigate that issue the following study was done: Fmoc-(N-Me) Leu[27] was coupled to [28-37] resin and the resin was then subjected to Fmoc cleavage conditions. The H_2N-[27-37] resin was then acetylated with Ac_2O. The cleavage of the Ac-(N-Me) Leu[27] IAPP [27-37] resin with TFA / H_2O that was performed thereafter yielded only the peptide [28-37] and not Ac-(N-Me) Leu[27] IAPP [27-37]. This result clearly demonstrated that the amide bond between Ac-(N-Me) Leu[27] and Ser[28] in Ac-[(N-Me) Leu[27]] IAPP [27-37] resin is susceptible to cleavage by TFA / H_2O (95/5) and suggested that this was the side reaction that was observed during the synthesis.

Further in the synthesis of [3], the coupling of Phe[23] to Gly[24] could not reach completion (70 to 80% completion) although the Kaiser test was negative. The resin was not acetylated. The couplings of the following residues Asn[22], Asn[21], Ser[20] and Ser[19] did not cause any difficulties. Cleavage and RP-HPLC analysis of [(N-Me) Ala[25], (N-Me) Leu[27]] IAPP [19-37] resin showed three main products: the intended peptide [(N-Me) Ala[25], (N-Me) Leu[27]] IAPP [19-37] and the deletion sequences IAPP [28-37] (formed as mentioned above) and [(N-Me) Ala[25], (N-Me) Leu[27]] IAPP [24-37] that formed due to incomplete coupling of Phe[23] to Gly[24]. The yield of the main product [(N-Me) Ala[25], (N-Me) Leu[27]] IAPP [19-37] was 25 to 30% with regard to the total functional groups of the resin, whereas the truncated sequences IAPP [28-37] and [(N-Me) Ala[25], (N-Me) Leu[27]] IAPP [24-37] represented 60-65 and 10%, respectively, of the total functional groups of the resin.

In the 1st synthesis of [(N-Me) Ile[26], (N-Me) Leu[27]] IAPP [19-37] (part of analogue [4]), (N-Me) Leu[27] coupled efficiently. The coupling of (N-Me) Ile[26] to (N-Me) Leu[27] could not reach completion (60 to 70% completion). The peptide resin was, therefore, acetylated after the coupling of (N-Me) Ile[26]. Coupling of Ala[25] was also very difficult. Cleavage and RP-HPLC

analysis of [(N-Me) Ile^{26}, (N-Me) Leu^{27}] IAPP [25-37] resin showed three products: the intended peptide [(N-Me) Ile^{26}, (N-Me) Leu^{27}] IAPP [25-37], the peptide [(N-Me) Ile^{26}, (N-Me) Leu^{27}] IAPP [26-37] that formed due to the incomplete coupling of Ala^{25} to (N-Me) Ile^{26} (50 to 60% completion) and the deletion sequence IAPP [28-37] that formed by the peptide bond cleavage between Ac-(N-Me) Leu^{27} and Ser^{28}. The peptide resin was acetylated after the coupling of Ala^{25}. Coupling of residues Gly^{24}, Phe^{23}, Asn^{22}, Asn^{21}, Ser^{20} and Ser^{19} proceeded without difficulties. Cleavage and RP-HPLC analysis of [(N-Me) Ile^{26}, (N-Me) Leu^{27}] IAPP (19-37) resin showed three products: the intended peptide [(N-Me) Ile^{26}, (N-Me) Leu^{27}] IAPP [19-37], and the truncated sequences IAPP [28-37] and [(N-Me) Leu^{27}] IAPP [27-37] formed by peptide bond cleavage of Ac-(N-Me) Leu^{27} and Ser^{28} and Ac-(N-Me) Ile^{26} and (N-Me) Leu^{27}, respectively. The yield of the intended product [(N-Me) Ile^{26}, (N-Me) Leu^{27}] IAPP [19-37] was 40% with regard to the total functional groups of the resin, whereas the truncated sequences represented the remaining 60%.

The synthesis of [(N-Me) Ile^{26}, (N-Me) Leu^{27}] IAPP [19-37] was repeated. Following coupling of (N-Me) Leu^{27} the coupling (N-Me) Ile^{26} was performed several times using longer reaction times and increased temperatures. In this way the coupling of (N-Me) Ile^{26} to (N-Me) Leu^{27} was almost complete (80 to 90% completion). The peptide resin was acetylated after this coupling. The coupling of Ala^{25} to (N-Me) Ile^{26} was very difficult. Cleavage and RP-HPLC analysis of [(N-Me) Ile^{26}, (N-Me) Leu^{27}] IAPP [25-37] resin (before acetylation of non-reacted groups of (N-Me) Ile^{26}) showed four products: the intended peptide [(N-Me) Ile^{26}, (N-Me) Leu^{27}] IAPP [25-37], the peptide [(N-Me) Ile^{26}, (N-Me) Leu^{27}] IAPP [26-37] that formed due to the incomplete coupling of Ala^{25} to (N-Me) Ile^{26}, and the deletion sequences IAPP [28-37] and [(N-Me) Leu^{27}] IAPP [27-37]. The latter two deletion sequences could have formed via a partial cleavage from the resin of the dipeptide (N-Me) Ile^{26}- (N-Me) Leu^{27} (possible formation of a diketopiperazine) and via break up of the peptide bond between (N-Me) Ile^{26} and (N-Me) Leu^{27}. The peptide resin was acetylated after the coupling of Ala^{25}. Coupling of residues Gly^{24}, Phe^{23}, Asn^{22}, Asn^{21}, Ser^{20} and Ser^{19} proceeded without difficulties. Similarly to the results obtained by the 1st synthesis, cleavage and RP-HPLC analysis of [(N-Me) Ile^{26}, (N-Me) Leu^{27}] IAPP [19-37] resin showed three products: the intended peptide [(N-Me) Ile^{26}, (N-Me) Leu^{27}] IAPP [19-37], and the deletion sequences IAPP [28-37] and (N-Me) Leu^{27}] IAPP [27-37]. These results suggested that the incomplete coupling of Ala^{25} to (N-Me) Ile^{26} and the presence of consequtive N-methylated residues caused the observed side reactions. Moreover, the presence of the two consecutive N-methyl residues resulted in incomplete couplings and break up of peptide bonds C-terminal to the N-methylated residues.

The yield in the intended product [(N-Me) Ile^{26}, (N-Me) Leu^{27}] IAPP [19-37] was 30% with regard to the total functional groups of the resin, whereas the truncated sequences represented the remaining 70%.

In the synthesis of [(N-Me) Ala^{25}, (N-Me) Ile^{26}, (N-Me) Leu^{27}] IAPP [25-37], (analogue [5]) (N-Me) Leu^{27} coupled efficiently. The coupling of the (N-Me) Ile^{26}, however, was as expected a difficult one and could not reach completion (60 to 70% completion). Accordingly, the peptide resin Fmoc-[(N-Me) Ile^{26}, (N-Me) Leu^{27}] IAPP [26-37] was acetylated after this coupling. Coupling of the following N-methyl residue (N-Me) Ala^{25} was even more difficult. Cleavage and RP-HPLC analysis of [(N-Me) Ala^{25}, (N-Me) Ile^{26}, (N-Me) Leu^{27}] IAPP [25-37] resin showed, as expected, three products: the intended peptide [(N-Me) Ala^{25}, (N-Me) Ile^{26}, (N-Me) Leu^{27}] IAPP [25-37], and the deletion sequences [(N-Me) Ile^{26}, (N-Me) Leu^{27}] IAPP [26-37], that formed due to incomplete coupling of (N-Me) Ala^{25} to (N-Me) Ile^{26} and IAPP [28-37] that formed by peptide bond cleavage between and Ac-(N-Me) Leu^{27} and Ser^{28}. Two synthetic attempts were undertaken and both gave the main product only in very low yield (20-30% with regard to the total functional groups of the resin). Therefore, this synthesis was not continued any further.

Taken together, the results of the syntheses indicated that the peptide bond breaking observed during the TFA / H$_2$O mediated cleavage was primarily affected by the nature of the N-methylated residue and secondly by the exact position of the N-methyl residue in the sequence. (N-Me) Leu^{27} exhibited the greatest destabilizing effect on the peptide backbone. Although the coupling of this residue to Ser^{28} was complete in all cases, the presence of (N-Me) Leu^{27} resulted in poor couplings for the next two residues Ile^{26} and/or (N-Me) Ile^{26} and Ala^{25} or (N-Me) Ala^{25}. Acetylations performed in this region resulted in end capping of incomplete couplings but at the same time they rendered the peptide bond between the N-methylated and the following C-terminal residue acid labile leading thus to enhanced susceptibility towards acid hydrolysis. The same was true for (N-Me) Ile^{26} as well as for (N-Me) Phe^{23} whereas Ac-(N-Me) Ala^{25} or Ac-(N-Me) Gly^{24} did not cause any destabilization of the peptide bond C-terminal to them. In the latter cases, the smaller alkyl side-chain of Ala or the complete absence of side-chain in Gly as compared to the larger alkyl side-chains of Leu or Ile or the aromatic ring of Phe could account for the absence of any destabilizing effect on peptide bonds. These findings were in accordance with the findings of Urban *et. al.*[15] that the steric interactions of the alkyl side chains (larger versus smaller) and the inductive effect of the methyl group might be related to the stabilization of the proposed oxazolone intermediate of the peptide bond cleavage reaction, accounting thus for the differences in peptide bond

labilities between peptides containing (N-Me) Gly (this and Urban's work), (N-Me) Ala (this and Urban's work), (N-Me) Phe (this and Urban's work), (N-Me) Leu (this work), and (N-Me) Ile (this work). Thus, the nature of the residue on the N-terminal side of the N-methylated peptide strongly affects peptide bond lability.

In the N-methylated analogues [1]-[4], residues 1 to 18 did not cause any difficulties with the exception of residues in the IAPP region [7-10]. Difficulties with the coupling of these latter residues were also encountered during the synthesis of the native IAPP sequence. The main products of the synthesis of the N-methylated analogues were obtained in a quite good purity degree, which facilitated the oxidation and purification procedures. The overall yield for the pure N-methylated peptide in oxidized form was thus between 5 to 10% with regard to the initial substitution level of the resin.

N-methyl amino acids are present in several naturally occurring peptides exhibiting important biological properties, such as cyclosporines or dolastatins. It has been also established that the metabolic stability of biologically active peptides can be altered or enhanced by the introduction of N-methylated amino acid residues, which has become an important modification in peptide chemistry [108]. The difficulties with the couplings involving N-methyl amino acids have been addressed by several groups, and a number of specialized reagents and methods are now available to facilitate the coupling of N-methyl amino acids. As mentioned above, cyclosporine, an immunosuppressive cycloundecapeptide with seven N-methyl residues, is a formidable synthetic challenge and different groups have reported different methods of achieving this. In 1995, the first synthesis of a cyclosporin derivative by solid-phase methods, as compared to standard solution synthesis of the peptide, was reported [109]. The linear undecapeptide precursor was synthesized under SPPS conditions by use of the azabenzotriazole-based coupling reagents HATU and HOAt, which were effective for the coupling of the sterically hindered, N-methylated amino acids. It was shown that the synthesis of the peptide utilizing HOAt/DIC resulted in higher couplings yields compared to HATU-mediated couplings. In the year 2000, the synthesis of cyclosporin O (both in solution and solid-phase) using novel thiazolium-, immonium- and pyridinium-type coupling reagents was reported [110]. In this study, the peptide was successfully synthesized in 20-23% overall yield using the novel coupling reagents 2-bromo-3-ethyl-4-methyl thiazolium tetrafluoroborate (BEMT) and 2-bromo-1-ethyl pyridinium tetrafluoroborate (BEP) which were used for the fast coupling of the N-methylated amino acids with low epimerization and excellent coupling yields. Recently, the use of triphosgene as highly efficient reagent for the solid-phase synthesis of peptides containing N-alkylated amino acids has been reported [11, 111]. In one of

these reports the total SPPS of cyclosporin O was described. Synthesis was achieved in high purity and an overall yield of 15% utilizing trisphosgene as the activating agent for the coupling of the N-methylated amino acids. In addition, a comparative evaluation study of four different coupling methods showed that the better coupling yields were obtained with triphosgene (bis[trichloromethyl] carbonate, BTC), as compared to HOAt/DIC, or symmetrical anhydride method using DCC or tetramethylfluorformamidinium hexafluorophosphate (TFFH) method. The study concluded that in contrast to the liquid-phase synthesis of the cyclosporin analogue with all the intermediate purification steps, the approach on solid-phase synthesis utilizing the inexpensive activating reagent BTC was time- and cost-efficient for obtaining the peptide analogue in good yields and purity.

Finally, the findings that contrary to IAPP the N-methylated IAPP analogue [2] has reduced β-sheet forming potential and no cytotoxic properties suggested that N-methylation of selective residues in the amyloid core of IAPP (FGAIL) is, in principle, a suitable strategy to reduced or completely inhibit the amyloidogenic and cytotoxic potential of IAPP. N-methylation of protein contact sides is a well-known approach to inhibit protein self-association and has been also shown to inhibit Aβ(25-35) amyloid formation [112]. Kapurniotu *et al.* [93] have also shown that the short N-methylated IAPP sequences F(N-Me)GA(N-Me)IL, NF(N-Me)GA(N-Me)IL, SNNF(N-Me)GA(N-Me)IL, and SNNF(N-Me)GA(N-Me)ILSS were, contrary to their precursor sequences, highly soluble, unable to aggregate into β-sheet and amyloid fibrils and devoid of cytotoxicity. Together with these reports the results presented in this thesis on the IAPP analogue [2] also suggest that the rational N-methylation strategy [93] may be applicable to various amyloidogenic sequences as a general strategy to convert amyloidogenic and cytotoxic peptide sequences in non-amyloidogenic and non-cytotoxic ones with potential diagnostic or therapeutic applications.

7 Zusammenfassung

Konformationell eingeschränkte Analoga von nativ-vorkommenden bioaktiven Polypeptiden sind wichtige Werkzeuge, welche der Aufklärung von Strukturaktivitäts-Beziehungen dienen und beim Design und der Entwicklung von Leitstrukturen mit therapeutischen und diagnostischen Anwendungen Einsatz finden können.

In der hier vorgelegten Doktorarbeit wurden Konformationsrestriktionen auf zwei Polypeptide aus der Calcitonin-Gen-Peptid-Familie, das Calcium- und Knochenstoffwechsel-regulierende Hormon Calcitonin (Ct) und das Kohlenhydratmetabolismus-regulierende Hormon Islet Amyloid Polypeptid (IAPP) angwendet. Diese zwei, aus 32 bzw. 37 Aminosäure bestehenden, Polypeptide haben eine gemeinsame genetische Herkunft und weisen zum Teil eine Primärstrukturhomologie sowie überlappende Bioaktivitäten und Rezeptorkreuzreaktivitäten auf.

Das Peptidhormon Ct wird seit mehreren Jahren therapeutisch zur Behandlung von Osteoporose eingesetzt. Die niedrige Bioaktivität der beim Menschen vorkommenden Ct-Sequenz (hCt) führte jedoch dazu, dass hCt eine nur geringe medizinische Anwendung gefunden hat. Aufgrund seiner hohen Bioaktivität wird heutzutage hauptsächlich synthetisches Calcitonin aus Lachs (sCt) therapeutisch eingesetzt. Vor kurzem wurde gezeigt, dass die Einführung von i, $i+4$-Seitenkette-zu-Seitenkette-Lactamverbrückungen zwischen den Resten 17 und 21 von hCt zu Analoga mit stark erhöhter hypocalcämischer Aktivität *in vivo* führen kann (Kapurniotu *et al.*, *Eur. J. Biochem.* (1999)). Diese Arbeiten haben zur Entdeckung des hCt-Analogs cyclo[17,21]-[Asp[17], Orn[21]]hCt geführt, welches bis dato das potenteste bekannte hCt-Analog im Bezug auf die hypocalcämische Aktivität im Tiermodell *in vivo* ist. Es wurde darüber hinaus vorgeschlagen, dass die Bioaktivität vo hCt mit dem Vorhandensein bzw. der Stabilisierung eines β-Faltblatt-/β-Haarnadelschleifen-enthaltenden konformeren Zustands zwischen den Resten 17 und 21 zusammenhängen könnte.

Das Ziel des ersten Teils der hier vorgelegten Arbeit war es, eine detaillierte Auskunft über die Wirkung von Konformationsrestriktionen in der Region 17-21 von hCt auf die Rezeptorbindungsaffinität und die Aktivierung der Adenylatcyclase (AC) zu bekommen und dadurch möglicherweise strukturelle Eigenschaften identifizieren zu können, welche mit der Bioaktivität in Zusammenhang stehen könnten. Die spezifischen Fragestellungen, welchen nachgegangen wurde sind:

- der Effekt der Ringgröße der Lactambrücke und der verschiedenen Arten an β-Haarnadelschleifen-stabilisierenden Resten an den Positionen 18 und 19 auf Rezeptorbindungsaffinität und Adenylatcyclaseaktivierung,

- die Rolle einer potentiellen „Asx- Haarnadelschleifen"-Konformation in der Region 17-21,

- die H-Brückenbindungsfähigkeit der Aminogruppe von Phe[19] und der Seitenkette von Aminosäurerest 17 bei der Rezeptorbindungsaffinität und Adenylatcyclaseaktivierung,

- und letzlich der Effekt der Einführung bestimmter hydrophober Aminosäurereste aus der α-helikalen Region der sCt-Sequenz in die entsprechende Region des potenten hCt-Analogs cyclo[17,21]-[Asp[17], Orn[21]]hCt auf die Bioaktivität.

Im Hinblick auf diese Ziele wurden fünfundzwanzig hCt-Analoga designt, welche eine cyclische Konformationsrestriktion und/oder verschiedene Substituenten für Aminosäurereste in der Region 17 bis 20 enthalten, die aufgrund der Literatur für die Bioaktivität potenziell für wichtig gehalten werden konnten. Die Analoga wurden in guten Ausbeuten und guter Reinheit durch Festphasenpeptidsynthese (SPPS) mittels der Boc- und/oder der Fmoc-Strategie in Kombination mit speziellen Seitenkettenschutzstrategien für die Seitenkette-zu-Seitenketten-Cyclisierung am Harz hergestellt. Nach RP-HPLC-Reinigung und Charakterisierung mittels Massenspektometrie wurden die Ct-Rezeptorbindungsaffinitäten und Adenylatcyclaseaktivierungspotenziale der Analoga an der Brustcarcinom-Zelllinie T47D untersucht.

Die Untersuchungen mit den „Ringgröße"-Analoga zeigten, dass die 19-gliedrigen Analoga cyclo[17,21]-[Asp[17], Orn[21]]hCt und cyclo[17,21]-[Glu[17], Dab[21]]hCt zusammen mit dem 20-gliedrigen Analog cyclo[17,21]-[Asp[17], Lys[21]]hCt die höchsten Rezeptorbindungsaffinitäten verglichen zu den anderen Analoga aufweisen. Der Adenylatcyclaseaktivierungs-Assay zeigte, dass cyclo[17,21]-[Asp[17], Orn[21]]hCt der stärkste hCt-Agonist ist, während cyclo[17,21]-[Asp[17], Lys[21]]hCt ein zu hCt Ähnliches AC-Aktivierungspotenzial aufweist und cyclo[17,21]-[Glu[17], Dab[21]]hCt ein schwächeres AC-Aktivierungspotenzial als hCt zeigt. Die Rezeptorbindungsaffinitäten und AC-Aktivierungspotenziale waren jedoch signifikant reduziert beim 18-gliedrigen cyclo[17,21]-[Asp[17], Dab[21]]hCt und sehr schwach beim 17-gliedrigen Analog cyclo[17,21]-[Asp[17], Dap[21]]hCt. Interessanterweise wies [Asp[17], Orn[21]]hCt keine Rezeptorbindungsaffinität und ein nur sehr schwaches AC-Aktivierungspotenzial auf. Dies deutete darauf hin, dass die durch die Asp[17]- zu Orn[21]-Verbrückung induzierte Konformationsrestriktion in cyclo[17,21]-[Asp[17], Orn[21]]hCt mit seiner erhöhten Rezeptorbindungsaffinität und dem verstärkten AC-Aktivierungspotenzial zusammenhängt.

Die Untersuchungen mit verschiedenen Substitutionsanaloga von cyclo[17,21]-[Asp[17], Lys[21]]hCt und den entsprechenden linearen Kontrollpeptiden zeigten, dass das Umkehren der Chiralität der Aminosäurereste in den Positionen 18 und 19 oder das Ersetzen von Lys[18] durch einen Typ I-β-Haarnadelschleifen-stabilisierenden Rest (Aib) mit den Anforderungen an das cyclische Analog bzgl. seiner Rezeptorbindung kompatibel ist, während diese Substitutionen zu einer Reduktion des AC-Aktivierungspotenzials führten. In der hCt-Sequenz führten diese Substitutionen zu einer starken Abnahme von Rezeptorbindingsaffinität und AC-Aktivierungspotenzial.

Darüber hinaus zeigten die Untersuchungen mit verschiedenen Substitutionsanaloga von cyclo[17,21]-[Asp[17], Orn[21]]hCt, bei welchen die Reste 18 und 19 durch die "Asx-*turn*"-induzierenden Reste Pro und Ser ersetzt wurden, dass Lys[18] und Phe[19] sehr wichtig für die Rezeptorbindung und die AC-Aktivierung sind. Es stellte sich nämlich heraus, dass die obigen Substitutionen zu Analoga mit stark reduzierter Rezeptorbindung und stark reduziertem AC-Aktivierungspotenzial führen.

Die Untersuchungen mit den N-methylierten Phe[19]-Analoga von cyclo[17,21]-[Asp[17], Orn[21]]hCt deuten darauf hin, dass ein intaktes H-Brückenbildungspotenzial dieser Aminosäure für Rezeptorbindung und AC-Aktivierung sehr wichtig ist. Darüber hinaus, haben die Untersuchungen mit den beta-Analoga von cyclo[17,21]-[Asp[17], Orn[21]]hCt gezeigt, dass die Integrität des Peptidrückgrades zwischen den Resten 17 und 21 für die Rezeptorbindung und die AC-Aktivierung notwendig ist. Die Ergebnisse der Untersuchungen mit den hCt-Analoga, welche Dab oder Dap an der Stelle von Asn[17] hatten, weisen darauf hin, dass die Carbonyl- und auch die Aminofunktion der Asn-Seitenkette mit der Rezeptorbindung und der AC-Aktivierung stark zusammenhängen. Letzlich weisen die Untersuchungen zum Effekt der Einführung von hydrophoben Resten aus der helikalen Region von sCt in cyclo[17,21]-[Asp[17], Orn[21]]hCt oder [Asp[17], Orn[21]]hCt darauf hin, dass die Anwesenheit von Nle[8], Leu[12,16,19] und Tyr[22] zu einer starken Erhöhung des AC-Aktivierungspotenzials führt. Diese Substituenten allein führten auch zu einer starken Zunahme der Rezeptorbindungsaffinität von [Asp[17], Orn[21]]hCt und hatten keinen Einfluss auf die Affinität von cyclo[17,21]-[Asp[17], Orn[21]]hCt. Zusammenfassend haben die Ergebnisse der Untersuchungen mit allen hCt-Analoga gezeigt, dass die Region 17 bis 21 von hCt eine sehr wichtige Rolle für die biologische Aktivität dieses Hormons spielt, und dass kleine strukturelle Veränderungen in dieser Region die Rezeptorbindungsaffinität und das AC-Aktivierungspotenzial stark beeinflussen können. Dies deutet darauf hin, dass rational eingeführte strukturelle Veränderungen in der Region 17 bis

21 von hCt möglicherweise zu hochpotenten und somit therapeutisch interessanten hCt-Agonisten führen könnten.

Das zweite Mitglied der Calcitonin-Gen-Peptid-Familie, das Hormon IAPP, spielt eine wichtige Rolle bei der Pathogenese des Typ II Diabetes mellitus. Dies wird hauptsächlich auf Befunde zurückgeführt, wonach in den Bauchspeicheldrüsen von mehr als 95% der Typ II Diabetes-Patienten Amyloidaggregate bestehend aus IAPP gebildet werden, und dass solche Aggregate zelltoxische Eigenschaften aufweisen. Die Aufklärung des molekularen Mechanismus, der der β-Faltblattbildung von IAPP und den damit assoziierten Amyloidbildungs- und Zelltoxizitätspotenzialen dieses Moleküls zugrundeliegt, ist die Grundvoraussetzung für das Verständnis der molekularen Grundlagen dieser Krankheit und die Entwicklung von therapeutischen Strategien. Es wurde kürzlich vorgeschlagen, dass die Strategie der Konformationsrestriktion von kurzen β-Faltblatt-bildenden, amyloidogenen und zytotoxischen Peptidsequenzen mittels der strukturbasierten Einführung von N-Methylresten in bestimmte ausgewählte Amidbindungen eine geeignete Strategie für das Aufklären von Struktur-Amyloidogenese-Zytotoxizitäs-Beziehungen solcher Sequenzen und für die Umwandlung von amyloidogenen Peptidsequenzen in nicht-amyloidogene und nicht-zytotoxische Sequenzen ist.

Der zweite Teil dieser Doktorarbeit beschreibt detailliert die Festphasenpeptidsynthesen der (humanen) IAPP-Peptidsequenz, welche aufgrund der amyloidogenen Moleküleigenschaften mehr als komplex sind. Auch die hoch-amyloidogene IAPP-Mutante S20G-IAPP, für die pathophysiologische Relevanz vermutet wird, sowie fünf, mittels N-Methylierung von Amidbindungen, konformationell-eingeschränkte IAPP-Analoga wurden in dieser Arbeit synthetisiert und dargestellt. Darüber hinaus umfasst dieser Teil der Arbeit die Ergebnisse erster Untersuchungen an einem der N-methylierten Analog zum Effekt der N-Methylierung auf das β-Faltblattbildungspotenzial und die Zelltoxizität von IAPP.

Die SPPS von IAPP, S20G-IAPP, und der N-methylierten IAPP-Analoga stellte sich als eine sehr schwierige Aufgabe heraus. Dies war auf die Anwesenheit verschiedenener sterisch gehinderter und zur Aggregation neigender Aminosäurereste in der IAPP-Sequenz sowie auch auf Synthese-inhärente Probleme, welche mit der sterischen Hinderung von Kupplungen und der Labilität von Peptidbindungen in N-methylierten Sequenzen zusammenhängen, zurückzuführen. Da die SPPS von IAPP das Produkt in niedriger Ausbeute lieferte, wurde für die Synthese der Mutante S20G-IAPP ein entsprechend optimiertes synthetisches Protokoll verwendet. Letzteres führte in guter Ausbeute zu einem –nach RP-HPLC-Reinugung- reinen S20G-IAPP. Während der Synthese der N-methylierten Analoga [(N-Me) Phe[23], (N-Me)

Ala^{25}] IAPP [1], [(N-Me) Gly^{24}, (N-Me) Ile^{26}] IAPP [2], [(N-Me)Ala^{25}, (N-Me) Leu^{27}] IAPP [3] und [(N-Me) Ile^{26}, (N-Me) Leu^{27}] IAPP [4] erwiesen sich jedoch verschiedene Kupplungen, bei welchen N-Methyl-Reste involviert waren, als unvollständig. Die nicht-gekoppelten Aminofunktionen der N-Methyl-Reste wurden daher anschließend mittels Acetylierung *gecapped*. Es stellte sich jedoch heraus, dass die Acetylierungen einiger N-methylierten Reste zu einer Anzahl an TFA-vermittelten Amidbindungsspaltungen geführt hatten. Die beobachteten Amidbindungsspaltungen lagen dabei zwischen Ac-(N-Me) Ile und Leu oder (N-Me) Leu, zwischen Ac-(N-Me) Phe und Gly und zwischen Ac-(N-Me) Leu und Ser. Die Nebenprodukte der obigen Synthesen wurden komplett charakterisiert und die auftretenden Nebenreaktionen somit komplett aufgeklärt. Die Untersuchungen zeigten auch, dass die obigen Peptidbindungen eine TFA-Labilität (unter den Bedingungen der TFA-mediierten Abspaltung des Peptids vom Anker) aufweisen, und zwar nur, wenn die N-methylierten Reste in acetylierter Form vorliegen. Somit fand diese Nebenreaktion bei den acetylierten Rumpfsequenzen bei der finalen TFA-Abspaltungsstufe am Ende der Synthese statt, wobei sich die gewünschten Volllängen-Peptidsequenzen *per se* unter den Bedingungen der Fmoc-Synthesestrategie als stabil erwiesen. Die Synthese des fünften IAPP Analogs ([(N-Me) Ala^{25}, (N-Me) Ile^{26}, (N-Me) Leu^{27}] IAPP [5]), welches drei aufeinanderfolgende, N-methylierte Reste enthalten sollte, wurde aufgrund der niedrigen Kupplungsausbeute von (N-Me) Ala^{25} on (N-Me) Ile^{26} nur bis zu diesem Schritt durchgeführt. Aus den Ergebnissen der Synthesen der IAPP-Analoga [1] – [4] lässt sich zusammenfassend schließen, dass die Ausbeuten der Synthesen aufgrund der unvollständigen Kupplungen niedrig waren, wobei insgesamt weniger Nebenprodukte im Vergleich zur IAPP-Synthese auftraten. Letzteres führte zu höheren Ausbeuten der RP-HPLC-Reinigungsprozesse der N-methylieren Analoga verglichen mit IAPP.

Letztlich wurde [(N-Me) Gly^{24}, (N-Me) Ile^{26}] IAPP [2] als Analogon ausgewählt, um die Wirkung der strukturbasierten N-Methylierung von Amidbindungen auf die β-Faltblatt- und Zytotoxizitätspotenziale von IAPP zu untersuchen. Diese Untersuchungen zeigten deutlich, dass die zwei N-Methyl-Reste an Gly^{24} und Ile^{26} zu einer starken Reduktion des β-Faltblattbildungspotenzials und zur kompletten Inhibition der Zytotoxizität von IAPP im *in vitro*-Modell der pankreatischen Zelllinie RIN5fm geführt hatten. Diese Ergebnisse wiesen darauf hin, dass es einen direkten Zusammenhang der Konformationsrestriktion, welche durch die strukturbasierten N-Methylierung von Amidbindungen erzielt wurde, mit dem Amyloidbildungspotenzial und der Zytotoxizität von IAPP gibt.

Zusammenfassend haben die Ergebnisse dieser Arbeit gezeigt, dass die Restriktion der konformationellen Flexibilität von bioaktiven Polypeptiden mittlerer Länge wichtige Auskunft über ihre Struktur-Aktivitäts-Beziehungen liefern kann und zum Design von potenten Agonisten (wie hCt-Analoga) oder zu Abkömmlingen der nativ vorkommenden Polypeptidsequenz mit komplett veränderten biophysikalischen Eigenschaften (wie IAPP-Analoga) führen kann. Auch lässt sich aus den erzielten Ergebnissen ableiten, dass diese Strategie auch auf weitere Polypeptide, wie z.B. weitere amyloidogene Polypeptide oder Polypeptide größerer Länge übertragbar sein sollte. Diese Arbeit hat auch gezeigt, dass die SPPS von N-methylierten und zur Aggregation neigenden Polypeptidsequenzen noch immer ein anspruchsvolles Ziel für den Synthetiker ist, wobei in der vorgelegten Doktorarbeit wichtige Ansätze zur Optimierung solcher Synthesen erarbeitet wurden.

8 References

[1]   Synthesis Notes, Novabiochem catalog **1999**, pp 3-5.

[2]   K. C. Pugh, E. J. York, J. M. Stewart, Int. J. Peptide Protein Res. **1992**, 40, 208-213.

[3]   G. B. Fields, C. G. J. Fields, Am. Chem. Soc. **1991**, 113, 4202-4207.

[4]   L. Miranda, P. F. Alewood, Proc. Natl. Acad. Sci. USA. **1999**, Vol. 96, 1181-1186.

[5]   J. P. Tam, Y. A. Lu, J Am. Chem. Soc. **1995**, 117, 12058-12063.

[6]   F. Albericio, M. Cases, J. Alsina, S. A. Triolo, L. A. Carpino, S. A. Kates, Tetrahedron Letters **1997**, 38, 4853-4856.

[7]   J. R. Spencer, V. V. Antonenko, N. G. J. Delaet, M. Goodman, Int. J. Peptide Protein Res. **1992**, 40, 282-293.

[8]   M. Schnölzer, P. Alewood, A. Jones, D. Alewood, S. B. H. Kent, Int. J. Peptide Protein Res. **1992**, 40, 180-193.

[9]   L. Andersson, L. Blomberg, L. Lepsa, B. Nilson, M. Verlander, Biopolymers **2000**, Vol. 55, 227-250.

[10]   T. Wöhr, F. Wahl, A. Nefzi, B. Rohwedder, T. Sato, X. Sun, M. J. Mutter, Am. Chem. Soc. **1996**, 118, 9218-9227.

[11]   B. Thern, J. Rudolph, G. Jung, Angew. Chem. **2002**, 114, 2401-2403.

[12]   M. Bodansky, In: Peptide Chemistry, 2nd Ed., Springer-Verlag: Berlin, **1993**, pp 106-107.

[13]   C. Chiva, M. Vilaseca, E. Giralt, F. Albericio, Peptide Sci. **1999**, 5, 131-140.

[14]   G. Barany, F. Albericio, J Am. Chem. Soc. **1985**, 107, 4936-4942.

[15]   J. Urban, T., Vaisar, R., Shen, M. Lee, Int. J. Peptide Protein Res. **1996**, 47, 182-189.

[16]   P. Y. Chou, G. D. Fasman, Adv. Enzymol. **1978**, 47, 45-148.

[17]   J. Rizo, L. M.Gierasch, Annu. Rev. Biochem. **1992**, 61, 387-418.

[18]   A. F. Spatola, A. L. Rockwell, L. M. Gierasch, Biopolymers **1983**, 24, 137-155.

[19]   G. R. Marshall, In: Intra-science chemistry reports, ed. N. Kharasch, Gordon & Breach, **1971**, pp 305-316.

[20]   A. Aubry, M. Marraud, Biopolymers **1989**, 28, 109-122.

[21]   A M. Felix, E. P. Heimer, C. T. Wang, T. J. Lambros, A. Fournier, T. F. Mowles, S. Maines, R. M. Campbell, B. B. Wegrzynski, V. Toome, D. C. Fry, V. S. Madison, Int. J. Peptide Protein Res. **1988**, 32, 441-454.

[22]   A. Kapurniotu, J. W. Taylor, J. Med. Chem. **1995**, 38, 836-847.

[23]   H. R. Marepalli, O. Antohli, J. M. Becker, F. J. Naider, J Am Chem Soc **1996**, 118, 6531-6539.

[24]   G. D. Rose, L. M. Gierasch, J. A. Smith, Adv. Protein Chem. **1985**, 37, 1-109.

[25] E. T. Kaiser, F. J. Kezdy, Proc. Natl. Acad. Sci.USA **1983**, 80, 1137-1143.

[26] V. J. Hruby, Life Sci. **1982**, 31, 189-199.

[27] H. Kessler, In: Trends in Drug Research, ed. V.Claassen, Amsterdam: Elsevier Sci. Publ., **1990**, pp 73-84.

[28] E. J. Milner-White, Trends Pharmacol. Sci., **1989**, 10, 70-74.

[29] S. J. Wimalawansa, Critical Reviews in Neurobiology **1997**, 11 (2&3), 167-239.

[30] P. C. Braga, Agents Actions **1994**, 41, 121-131.

[31] M. Azria, In: The Calcitonins: Physiology and Pharmacology, ed. M. Azria, Karger: Basel, **1989**, pp 133-143.

[32] R. M. Epand, R. F. Epand, R. C. Orlowski, J. K. Seyler, R. L. Colescott, Biochemistry **1986**, 25, 1964-1968.

[33] R. M. Epand, R. F. Epand, R. C. Orlowski, J. Pept. Res. **1985**, 25, 105-111.

[34] J. P. Meyer, J. T. Pelton, J. Hoflack, V. Saudek, Biopolymers **1991**, 31, 233-241.

[35] P. M. Sexton, D. M. Findlay, T. J. Martin, Curr. Med. Chem. **1999**, 6, 1067-1093.

[36] A. Motta, M. A. Castiglione Morelli, N. Goud, P. A. Temussi, Biochemistry **1989**, 28, 7996-8002.

[37] A. Motta, P. A. Temussi, E. Wünsch, G. A. Bovermann, Biochemistry **1991**, 30, 2364-2371.

[38] R. Maier, B. Kamber, B. Riniker, W. Rittel, Clin. Endicrinol. **1976**, 5, 327-332.

[39] S. Houssami, D. M. Findlay, C. L. Brady, D. E. Myers, T. J. Martin, P. M. Sexton, Endocrinology **1994**, 135, 183-190.

[40] A. H. Gorn, H. Y. Lin, M. Yamin, P. E. Auron, M. R. Flannery, D. R. Tapp, C. A. Manning, H. F. Loddish, S. M. Krane, S. R. Goldring, J. Clin. Invest. **1992**, 90, 1726-1735.

[41] E. E. Moore, R. E. Kuestner, S. D. Stroop, F. J. Grant, S. L. Matthewes, C. L. Brady, P. M. Sexton, D. M. Findlay, Mol. Endocrinol. **1995**, 9, 959-968.

[42] S. D. Stroop, H. Nakamuta, R. E. Kuestner, E. E. Moore, R. M. Epand, Endocrinology **1996**, 137, 4752-4756.

[43] J. W. Taylor, Biopolymers **2002**, 66, 49-75.

[44] T. J. Rink, K. Beaumont, J. Koda, A. Young, TIPS **1993**, 14, 113-118.

[45] M. K. Badman, K. I. Shennan, J. L. Jermany, K. Doherty, A. Clark, FEBS Let. **1996**, 378, 227-231.

[46] B. J. Edwards, J. E. Morley, Life Sci. **1992**, 51, 1899-1912.

[47] P. Degano, R. A. Silvestre, M. Salas, E. Peiro, J. Marco, J. Regul. Pept. **1993**, 43, 91-96.

[48]   D. Poyner, TIPS **1995**,16, 424-428.

[49]   S. Gebre-Medhin, C. Olofsson, H. Mulder, Diabetologia **2000**, 43, 687-695.

[50]   G. G. Glenner, D. Eanes, C. Wiley, Biochem. Biophys. Res. Commun. **1988**, 155, 608-
         614.

[51]   P. Westermark, U. Engström, K. Johnson, G. T. Westermark, C. Betsholz, Proc. Natl.
         Acad. Sci. USA **1990**, 87, 5036-5040.

[52]   J. S. Richardson, Adv. Protein Chem. **1981**, 34, 167-339.

[53]   T. T. Ashburn, P. T. Jr. Lansbury, J. Am. Chem. Soc. **1993**, 115, 11012-11013.

[54]   P. Westermark, C. Wernstedt, E. Wilander, D. W. Hayden, T. D. O'Brien, K. H. Johnson,
         Proc. Natl. Acad. Sci. USA **1987**, 84, 3881-3885.

[55]   M. Sunde, C. Blake, Adv. Protein Chem. **1997**, 50, 129-159.

[56]   C. M. Dobson, TIBS **1999**, 24, 329-332.

[57]   J. D. Harper, P. T. Jr. Lansbury, Annu. Rev. Biochem. **1997**, 66, 385-407.

[58]   P. T. Jr. Lansbury, B. Caughy, Chem. Biol. **1995**, 2, 1-5.

[59]   R. Kayed, J. Bernhagen, N. Greenfield, K. Sweimeh, H. Brunner, W. Voelter, A.
         Kapurniotu, J. Mol. Biol. **1999**, 287, 781-796.

[60]   J. M. Stewart, J. D. Young, In: Solid phase peptide synthesis, Pierce Chemical Company,
         Rockford, **1984**, pp 23.

[61]   T. Kaiser, G. J. Nicholson, H. J. Kohlbau, W. Voelter, Tetrahedron Leters **1996**, 37,1187-
         1190.

[62]   M. Bodansky, In: Peptide Chemistry, 2nd Ed., Springer-Verlag: Berlin, **1993**, pp 125-128.

[63]   E. Kaiser, R. L. Colescott, C.D., Bossinger, P.I. Cook, Anal. Biochem. **1970**, 34, 595-598.

[64]   J. D. Fontenot, J. M. Ball, M. A. Miller, C. M. David, R. C. Montelaro, Pept. Res. **1991**,
         4, 19-25.

[65]   J. M. Stewart, J. D. Young, In: Solid phase peptide synthesis, Pierce Chemical Company,
         Rockford, **1984**, pp 38-39.

[66]   M. A. Mitchell, T. A. Runge, W. R. Mathews, A. K. Ichhpurani, N. K. Harn, P. J.
         Dobrowolski, F. M. Eckenrode, Int. J. Pept. Protein Res. **1990**, 36, 350-355.

[67]   D. S. King, C. G. Fields, G. B. Fields, Int. J. Pept. Protein Res. **1990**, 36, 255-266

[68]   Synthesis Notes, Novabiochem catalog **1999**, pp 52.

[69]   S. Moore, D. H. Spackman, W. H. Stein, Anal. Chemistry **1958**, 30, 1185-1190.

[70]   G. R. Moe, E. T. Kaiser, Biochemistry **1985**, 24, 1971-1976.

[71]   A. Kapurniotu, R. Kayed, J. W. Taylor, W. Voelter, Eur. J. Biochem. **1999**, 265, 606-618.

[72] A. Abbadi, M. Mcharfi, A. Aubry, S. Premilat, G. Boussard, M. Marraud, J. Am. Chem. Soc. **1991**, 113, 2729-2735.

[73] A. Kazantzis, M. Waldner, J. W. Taylor, A. Kapurniotu, Eur. J. Biochem. **2002**, 269, 780-791.

[74] A. Abbadi, G. Boussard, M. Marraud, Int. J. Biol. Macromol. **1986**, 8, 252-255.

[75] R. M. Epand, R. F. Epand, R. C. Orlowski, E. Flanigan, G. L. Stahl, Biophys. Chem. **1985**, 23, 39-48.

[76] T. J. Lukas, M. B. Prystowsky, B. W. Erickson, Proc. Natl. Acad. Sci. USA **1981**, 78, 2791-2795.

[77] J. M. Stewart, J. D. Young, In: Solid phase peptide synthesis, Pierce Chemical Company, Rockford, **1984**, pp 28-29.

[78] J. Blake, C. H. Li, J. Am. Chem. Soc. **1968**, 90, 5882-5884.

[79] A. Grauer, F. Raue, H. H. Reinel, H. G. Schneider, J. Schroth, A. Kabay, P. Brügger, R. Ziegler, Bone and Mineral **1992**, 17, 65-74.

[80] H. Y. Lin, T. L. Harris, M. S. Flannery, A. Aruffo, E. H. Kaji, A. Gorn, J. Kolakowski, H. F. Lodish, S. R. Goldring, Science **1991**, 254, 1022-1024.

[81] P. B. Chock, S. G. Rhee, E. R. Stadtman, Annu. Rev. Biochem. **1980**, 49, 813-843.

[82] E. Blind, F. Raue, P. Kienle, J. Schroth, A. Grauer, A. Kabay, P. Brügger, R. Ziegler, Analytical Biochemistry **1993**, 212, 91-97.

[83] cAMP Biotrak EIA documentation, Amersham Pharmacia Biotech **1999**, pp 9.

[84] T. T. Ashburn, M. Auger, P. T. Lansbury, J. Am. Chem. Soc. **1992**, 114, 790-791.

[85] J. M. Griffiths, T. T. Ashburn, M. Auger, P. Costa, R. G. Griffin, P. T. Lansbury, J. Am. Chem. Soc. **1995**, 117, 3539-3546.

[86] K. Tenidis, M. Waldner, J. Bernhagen, W. Fischle, M. Bergmann, M. Weber, M.-L. Merkle, W. Voelter, H. Brunner, A. Kapurniotu, J. Mol. Biol. **2000**, 295, 1055-1071.

[87] A. Kapurniotu, A. Schmauder, K. Tenidis, J. Mol. Biol. **2002**, 315, 39-350.

[88] S. Y. Ko, R. M. Wenger, Helv. Chim. Acta **1997**, 80, 695-705.

[89] J. R. Spencer, N. G. J. Delaet, A. Palmer, V. V. Antonenko, M. Goodman, J. Org. Chem. **1993**, 58, 1635-1638.

[90] Z. Ma, G. T. Westermark, S. Sakagashira, T. Sanke, A. Gustavson, H. Sakamoto, U. Engström, K. Nanjo, P. Westermark, Amyloid: J. Protein Folding Disord. **2001**, 8, 242-249.

[91] A. Kapurniotu, Biopolymers (Peptide Science) **2001**, 60, 438-459.

[92] S. Krimm, J. Bandekar, Advan. Protein Chem. **1986**, 38, 181-364.

[93]   M. S. Shearman, C. I. Ragan, L. L. Iversen, Proc. Natl. Acad. Sci. USA **1994**, 91, 1470-1474.

[94]   Z. Darzynkiewicz, S. Bruno, G. Del Bino, F. Traganos, Ann NY Acad Sci **1996**, 803, 93-100.

[95]   A. Kapurniotu, J. Bernhagen, N. Greenfield, Y. Al-Abed, S. Teichberg, R. W. Frank, W. Voelter, R. Bucala, Eur. J. Biochem. **1998**, 251, 208-216.

[96]   J. W. Taylor, Q. K. Jin, M. Sbacchi, L. Wang, P. Belfiore, M. Garnier, A. Kazantzis, A. Kapurniotu, P. F. Zaratin, M. A. Scheideler, J. Med. Chem. **2002**, 45, 1108-1121.

[97]   J. R. Cann, R. E. London, C. Unkefer, R. J. Vavrek, J. M. Stewart, J. Pept. Res. **1987**, 29, 486-496.

[98]   R. Maier, B. Kamber, B. Riniker, W. Rittel, Horm. Metab. Res. **1975**, 7, 511-514.

[99]   P. E. Wright, H. J. Dyson, R. A. Lerner, Biochemistry **1988**, 27, 7167-7175.

[100]   G. Siligardi, B. Samori, S. Melandri, M. Visconti, A. F. Drake, Eur. J. Biochem. **1994**, 221, 1117-1125.

[101]   H. Nakamuta, R. C. Orlowski, R. M. Epand, Endocrinology **1990**, 127, 163-169.

[102]   M. R. Nilsson, L. L. Nguygen, D. P. Raleigh, Analytical Biochemistry **2001**, 288, 76-82.

[103]   S. C. Miller, T. S. Scanlan, J. Am. Chem. Soc. **1997**, 119, 2301-2302.

[104]   P. Manavalan, F. A. Momany, Biopolymers **1980**, 19, 1943-1973.

[105]   B. Castro, J. R. Dormoy, G. Evan, C. Selve, Tetrahedron Lett. **1975**, 16, 1219-1222.

[106]   J. Coste, E. Frerot, P. Jouin, B. Castro, Tetrahedron Lett. **1991**, 32, 1967-1970.

[107]   Y. Angell, C. Garci-Echeveria, D. Rich, Tetrahedron Lett. **1994**, 35, 5981-5984.

[108]   P. Li, J. C. Xu, Tetrahedron Lett., **1999**, 40, 8301-8304.

[109]   Y. M. Angell, T. L. Thomas, G. R. Flentke, D. H. Rich, J. Am. Chem. Soc. **1995**, 117, 7279-7280.

[110]   P. Li, J. C. Xu, J. Org. Chem. **2000**, 65, 2951-2958.

[111]   B. Thern, J. Rudolph, G. Jung, Tetrahedron Letters **2002**, 43, 5013-5016.

[112]   E. Hughes, R. M. Burke, A. J. Doig, J. Biol. Chem. **2000**, 275, 25109-25115.

During my studies, I was instructed by the following academic teachers:

N. Argyropoulos, J. Bernhagen, G. Georgatsos, C. Johnson, A. Kapurniotu, A. Makris, C. Petrakis, W. Voelter.

Lebenslauf

Vorname:	Athanasios
Name:	Kazantzis
Geburtstag:	11/02/1971
Geburtsort:	Volos-Magnesia
Staatsangehörigkeit:	Griechisch

Oktober 1976 - Juni 1982	Grundschule Volos
Oktober 1982 - Juni 1988	Mehrzweigiges Lyzeum Nea Ionia/Volos
Juli 1988	Abitur

Oktober 1988 - Juni 1994	Aristoteles-Universität Thessaloniki
Juli 1994	Diplom-Chemie

Oktober 1996 - Juni 1997	*Mediterranean Agronomic Institute* in Chania / Kreta
Juli 1997	Diplom der *Specialized Post-Graduate Studies in Natural Products*

November 1997 - April 1999	*Mediterranean Agronomic Institute* in Chania / Kreta
Juli 2000	Master of Science (MSc) in *Natural Products*

Oktober 1999 – Dezember 2003	Anfertigung der Dissertation mit dem Titel „Festphasensynthesen und Untersuchungen von konformationell-eingeschränkten Analoga der Calcitonin-Gen-Peptid-Superfamilien-Polypeptide Calcitonin (Ct) und Islet Amyloid Polypeptid (IAPP)" am Physiologisch-chemischen Institut der Universität Tübingen (1999 – 2002) und Institut für Biochemie des Uniklinikums der RWTH Aachen (2002 – 2003).